Institut für Theoretische Physik I
Universität Stuttgart
Pfaffenwaldring 57
70550 Stuttgart

Fluctuation theorems in closed modular quantum systems: local effective dynamics

Von der Fakultät Mathematik und Physik der Universität Stuttgart zur Erlangung der Würde eines Doktors der Naturwissenschaften (Dr. rer. nat.) genehmigte Abhandlung

Vorgelegt von

Jens Teifel

aus Heilbronn

Hauptberichter:	Prof. Dr. Günter Mahler
Mitberichter:	Prof. Dr. Ulrich Weiß
Tag der mündlichen Prüfung:	27. Juli 2010

Institut für Theoretische Physik der Universität Stuttgart

2010

(Dissertation Universität Stuttgart)

Danksagung

Im Folgenden möchte ich mich bei mehreren Personen bedanken, die mit Rat und Unterstützung diese Arbeit maßgeblich beeinflusst haben.

Zu allererst möchte ich mich bei Herrn Prof. Dr. G. Mahler für die Unterstützung in den letzten Jahren bedanken, für das stetige Interesse am Fortschritt dieser Arbeit und für die interessanten und stets hilfreichen Diskussionen.

Herrn Prof. Dr. U. Weiß danke ich herzlich für die Übernahme des Mitberichts.

Für die Übernahme des Prüfungsvorsitzes möchte ich mich bei Herrn Prof. Dr. C. Bechinger bedanken.

Für die zahlreichen interessanten Diskussionen, auch jenseits der Physik, möchte ich mich bei meinen gegenwärtigen wie auch ehemaligen Kollegen, M. Henrich, T. Jahnke, A. Kettler, S. Lanéry, K. Rambach, F. Rempp, H. Schröder, P. Vidal, G. Waldherr, H. Weimer und M. Youssef bedanken.

Ferner allen Institutsmitgliedern für die freundliche Atmosphäre.

Ganz besonders danke ich meinen Eltern Helga und Fritz Teifel für Ihre vielfältige Unterstützung und Hilfe.

Ich danke Anette Häusser für Ihre immerwährende Unterstützung und für alles, was hier in Kürze nicht geschrieben werden kann.

Contents

1. Introduction

Thermodynamics has originally been developed as a phenomenological theory in order to describe the behavior of macroscopic systems. This theory focused on the stationary state the system would evolve into for long enough observation times (equilibrium state) as well as processes, during which the system resides in - or at least very close to - such equilibrium states. With great success, thermodynamics enabled physicists to describe processes like, e. g., heat conduction and heat engines. Remarkably, the laws of thermodynamics do not depend on the details of the microscopic constituents the macroscopic system is composed of [26]. Despite of the fact that the detailed dynamics for the large numbers of components of the system are practically unsolvable, in general, the macroscopic behavior of the system might be described quite easily by thermodynamics. Therefore one often aims at a thermodynamic description for large systems.

However, for processes driving the system far away from its equilibrium state the laws of thermodynamics do either only give boundaries on thermodynamic variables in terms of inequalities or do not apply at all, in general. Such processes are often encountered in nature or in technical applications, where one aims at maximizing power output rather than efficiency for heat engines, e. g.. Therefore, the discovery of several fluctuation theorems in the 90's of the 20th century, which make statements about thermodynamic variables for systems which are not in equilibrium, has triggered new interesting studies on thermodynamic processes [19]. A prominent example is the Jarzynski relation [6]: It relates the work performed during a process driving the system arbitrarily far away from equilibrium with the free energy difference between two equilibrium states. The fluctuating quantity therein is the work being performed during single process realizations.

Although originally developed to describe large systems, thermodynamic relations can also apply to very small systems consisting of few particles only. Indeed, a new access to deriving thermodynamic properties from the underlying dynamics is concerned with relatively small systems [44]. In contrast to classical approaches by Boltzmann (H-theorem), e. g., it is based on quantum mechanics, only. As nano-scale structures often show a behavior which cannot be explained by classical mechanics, it is of interest to examine if their dynamics can be described by thermodynamic relations, as the detailed description

by quantum mechanics is very challenging even for small systems due to the fast growing Hilbert space dimension.

When discussing non-equilibrium phenomena in quantum systems from a thermodynamical point of view, as for the Jarzynski relation, the key concepts of heat and work have to be defined. Here, we use the definition given in [33] in order to investigate quantum versions of the Jarzynski relation. We focus on modular closed quantum systems, investigating whether local effective observables of a sub-part of interest fulfill the Jarzynski relation. Our approach is different from the various quantum generalizations of the Jarzynski relation with respect to the process realization: So far, only situations have been studied where the process is realized by an external, classical driver, described by an explicitly time-dependent Hamiltonian (c. f. Chap. 2). In contrast to these studies, this work is basically concerned with situations where the Hamiltonian of the compound system is time-independent. However, the local effective Hamiltonian of the system under consideration might be time-dependent, of course.

Eventually, non-equilibrium processes and fluctuation theorems might contribute to a better understanding of the origin and applicability range of thermodynamic relations [19]. E. g., idealized models which perfectly explain experimental results for quasistatic processes may become problematic in non-equilibrium situations. On the other hand, the Jarzynski relation can be easily shown to fulfill the 2nd law of thermodynamics. Also, the generalized definitions of heat and work as well as the Jarzynski relation can shed new light on the discussion of cyclic processes which are realized by partially non-equilibrium process steps.

Part I.

External control

2. Fluctuation theorems

When describing processes in standard thermodynamics it is usually required that these processes are performed quasistatically, the system being arbitrarily close to a thermal equilibrium state throughout the process. For this condition to be fulfilled, the process velocity has to be sufficiently small. In nature, however, one often faces relatively fast processes invalidating the assumptions made in standard thermodynamics. Therefore, for describing non-equilibrium processes the discovery of fluctuation theorems (FTs) in the last decade of the past century [13, 14, 23] has been very important. FTs are closely connected to non-equilibrium work relations which can be seen as special cases of FTs, cf. [21, 39, 77], e. g.. In this manuscript we focus on the Jarzynski relation [6] as it has a relatively clear conceptual meaning and interpretation.

2.1. Jarzynski relation

The Jarzynski relation (JR), formulated in 1996 [6], has given rise to many studies in the field of thermodynamics far from thermal equilibrium with focus on fluctuation theorems [4, 21, 59, 71, 72, 75, 77], e. g.. Also, scenarios where the JR fails to give the correct free energy estimate have been studied and discussed [2, 45, 49–51, 56, 57]. The JR relates the work ΔW performed on a non-equilibrium process with the free energy difference of two equilibrium states. The initial state of the system of interest is required to be a thermal state. Then, the free energy difference can be recovered from

$$\overline{\mathrm{e}^{-\beta\Delta W}} = \mathrm{e}^{-\beta\Delta F}. \tag{2.1}$$

Here, β refers to the inverse initial temperature of the system, ΔW to the work for a *single* process realization, ΔF to the free energy difference of two isothermal states corresponding to the initial and final Hamiltonians, respectively. The average on the left-hand side is taken over many process realizations. Note, that the actual final state does not have to be thermal at all.

The JR has been tested experimentally for pulling dynamics of single molecule RNA strands [48], e. g., and similar experiments [35, 37].

2.2. Quantum Jarzynski relation

Soon after the JR was formulated, a quantum version of the JR for closed quantum systems was shown to hold by Mukamel [68]. There, the identification of work seems straightforward as the total energy change can be understood as being work. As for classical mechanics, many studies on quantum fluctuation theorems have been performed [10, 11, 32, 46, 52, 61, 62, 65, 66, 73, 80]. They are concerned with different setups and local dynamics of the quantum system under consideration. Meanwhile, an experimental test has been suggested [34]. The following subsections can be found in [53].

2.2.1. Generalized fluctuation theorem and the Jarzynski estimator

A quantum thermodynamic process is typically controlled by some external (mechanical) parameter $\gamma(t)$ [38], which modifies the respective Hamiltonian $\hat{H}(\gamma)$ and thus its eigenstates $|\varphi_n(\gamma)\rangle$ and spectrum $E_n(\gamma)$, here and in the following assumed to be discrete. The parameter γ may be compared, e. g, with the box volume for a classical gas. For a complete process description there must be at least one additional thermal control parameter constituting a two-dimensional control plane. On this control plane we can then impose additional constraints defining specific processes.

We distinguish, inter alia, isotherms (temperature $T = \text{const}$) and isentropes (entropy $S = \text{const}$). According to the first law the infinitesimal change of the internal energy $E(\gamma) = \mathrm{Tr}\left\{\hat{\rho}\hat{H}(\gamma)\right\}$ can be decomposed as $\mathrm{d}E = đW + đQ$ where $đQ$ is the heat and

$$đW = \left(\frac{\partial E}{\partial \gamma}\right)_s \mathrm{d}\gamma \tag{2.2}$$

the work by the effective force $f = \left(\frac{\partial E}{\partial \gamma}\right)_s$. If we restrict ourselves to (thermodynamically) adiabatic processes, $đQ = 0$, we can identify $đW$ supplied by the driving system with its effect on the driven system, $\mathrm{d}E$.

For the finite process considered here it is assumed now that we can measure the energy change $\Delta E_{fi} = E_f(\gamma_t) - E_i(\gamma_0)$, where $E_i(\gamma_0)$ is the initial eigenenergy, $E_f(\gamma_t)$ the final eigenenergy of the individual system described by $\hat{H}(\gamma)$. Here, ΔE_{fi} is a stochastic variable representing measurement-induced fluctuations. This random variable replaces the concept of trajectories usually envisioned for classical models. Its ensemble average is ΔE. ΔE_{fi} is the stochastic variable of choice here, because

- it is related to a well-defined quantum measurement scheme,
- it directly enters the quantum Jarzynski relation (see below),
- the alternative use of the externally supplied ΔW_{fi} would be problematic (even in the case of an otherwise closed quantum system) as long as the energetic impact due to the two projective measurements on the quantum system cannot be neglected (cf. [78]).

Most if not all theoretical papers on such driven quantum systems depend on this idea [34, 68].

In the Jarzynski scenario one is interested in the free energy difference ΔF between two isothermal states, which can be inferred from the distribution of work during an arbitrary process.

After the process under consideration has been completed at time t, the pertinent expectation value (cf. [68]) reads

$$\overline{\mathrm{e}^{-\beta\Delta E_{fi}}} = \sum_{fi} \mathrm{e}^{-\beta[E_f(t)-E_i(0)]} K_{fi}(t)\varrho_{ii}(0), \tag{2.3}$$

where $\beta = \frac{1}{k_B T}$ denotes the reciprocal temperature, k_B the Boltzmann constant and $K_{fi}(t)$ is the conditional probability of finding the system at time t in the energy-eigenstate $|f(t)\rangle$ if the system had been found initially in the energy-eigenstate $|i(0)\rangle$. As the indices i, f refer to different basis sets we have, in general, $K_{fi} \neq K_{if}$. Using for $\varrho_{ii}(0)$ the canonical state

$$\varrho_{ii}(0) = \frac{1}{Z_0}\mathrm{e}^{-\beta E_i(0)}, \tag{2.4}$$

one immediately gets

$$\overline{\mathrm{e}^{-\beta\Delta E_{fi}}} = \frac{1}{Z_0}\sum_{fi} \mathrm{e}^{-\beta E_f(t)} K_{fi}(t). \tag{2.5}$$

Here, Z_0 is the partition sum at time $t = 0$. Using the definition

$$s(f) \equiv \sum_i K_{fi}(t) \tag{2.6}$$

we can rewrite Eq. (2.5) as

$$\overline{\mathrm{e}^{-\beta\Delta E_{fi}}} = \frac{1}{Z_0}\sum_{f} \mathrm{e}^{-\beta E_f(t)} s(f) = \frac{Z_t}{Z_0}\overline{s}, \tag{2.7}$$

where Z_t is the partition sum for the canonical state corresponding to the final Hamiltonian $\hat{H}(t)$ and the initial temperature T, and $\overline{s}(t)$ is the thermal average,

$$\overline{s}(t) = \frac{1}{Z_t} \sum_f \mathrm{e}^{-\beta E_f(t)} s(f) \equiv \mathrm{e}^{-\lambda(\beta)\beta}. \tag{2.8}$$

In general, $\lambda(\beta)$ depends on all the details of the process. Note that we have

$$\lambda(\beta) = -\frac{1}{\beta} \ln \overline{s}. \tag{2.9}$$

With $\frac{Z_t}{Z_0} = \mathrm{e}^{-\beta \Delta F}$ and Eq. (2.8) we get for Eq. (2.7)

$$\overline{\mathrm{e}^{-\beta \Delta E_{fi}}} = \mathrm{e}^{-\beta \Delta F} \mathrm{e}^{-\lambda(\beta)\beta}. \tag{2.10}$$

Solving for the desired free energy change we end up with

$$\Delta F = -\frac{1}{\beta} \ln \left(\overline{\mathrm{e}^{-\beta \Delta E_{fi}}} \right) - \lambda(\beta) \tag{2.11}$$

as a generalized fluctuation theorem. The Jarzynski estimator

$$\Delta F^{\mathrm{JR}} = -\frac{1}{\beta} \ln \left(\overline{\mathrm{e}^{-\beta \Delta E_{fi}}} \right), \tag{2.12}$$

thus fundamentally deviates from the real free energy change ΔF by

$$\Delta F^{\mathrm{JR}} - \Delta F = \lambda(\beta), \quad \Delta^{\mathrm{JR}}_{\mathrm{rel}} \equiv \left| \frac{\lambda(\beta)}{\Delta F} \right| \tag{2.13}$$

The last ratio will be used as a measure for the relative deviation of the Jarzynski estimator from the correct free energy change. For $\lambda(\beta) = 0$ (i. e. the Jarzynski estimator is applicable) the function $s(f)$ has to be independent of f.

For $s(f)$ dependent on f the *universality* of the Jarzynski relation is lost: The fluctuations responsible for ΔF^{JR} are not only controlled by ΔF but depend on more details of the model as expressed by $\lambda(\beta)$.

A simple example refers to a system coupled to a heat bath of temperature β. Note that here we have $\Delta E_{fi} \neq \Delta W_{fi}$. Using, nevertheless, two-time energy measurements, where the final energy measurement is carried out after relaxation of the system back to a thermal state with the same final temperature as before, then leads to $s(f) = \frac{N}{Z_t} e^{-\beta E_f(t)}$ with N being the dimension of the system's Hilbert space. Substituting this into Eq. (2.5) gives $\overline{e^{-\beta \Delta E_{fi}}} = \frac{N}{Z_t Z_0} \sum_f e^{-2\beta E_f(t)}$, which is, in general, not equal to $\frac{Z_t}{Z_0}$.

2.2.2. Isentropic process: unitary transformation

In an experiment, the direct approach of determining the free energy difference ΔF between two isothermal states via measuring the work performed during an isothermal process might not be feasible. Possibly, the process cannot be performed isothermal at all or the process has to be performed that slow that the duration of the measurement is too long to be sensible. In these situations the JR (cf. Eq. (2.1)) is of obvious practical use.

For an estimation of ΔF the isothermal process from γ_0 to γ_t, say, will now be substituted by an isentrope (no bath coupling) with the same control parameter change. Typically, the state reached after the first step will be far from equilibrium. This step might be performed arbitrarily fast.

The Schrödinger dynamics generated by a time-dependent Hamiltonian $\hat{H}(t)$ is given by

$$|\Psi(t)\rangle = \hat{U}(t)\,|\Psi(0)\rangle \tag{2.14}$$

with

$$\hat{U}(t) = \hat{T}\exp\left[-\frac{\mathrm{i}}{\hbar}\int_0^t \hat{H}(t_1)\mathrm{d}t_1\right], \tag{2.15}$$

$\hat{T}$ being the time-ordering operator.

Let $|i(0)\rangle$ be a complete basis for $|\Psi(0)\rangle$, i. e.

$$\langle\Psi(0)|\Psi(0)\rangle = \sum_i |\,\langle i(0)|\Psi(0)\rangle\,|^2 = 1. \tag{2.16}$$

For the considered process to be unitary it has to be possible to map the complete set of eigenfunctions at any time t bijectively onto the complete set of initial eigenfunctions $|i(0)\rangle$,

$$|\Psi(t)\rangle = \sum_i |i(0)\rangle\,\langle i(0)|\Psi(t)\rangle\,, \tag{2.17}$$

i. e. the state $|\Psi(t)\rangle$ has to be expandable into the original basis. Then it immediately follows that $\hat{U}(t)\hat{U}^\dagger(t) = \hat{1}$, i. e. $\hat{U}(t)$ is unitary so that with

$$\langle f(t)|\,\hat{U}(t)\,|i(0)\rangle = U_{fi}(t), \quad K_{fi}(t) = |U_{fi}(t)|^2 \tag{2.18}$$

one finds

$$s(f) = \sum_i K_{fi}(t) = 1. \tag{2.19}$$

As a consequence $\lambda = 0$, the Jarzynski estimator works. The isentropic process (possibly non-adiabatic in the quantum mechanical sense) is conventionally associated with work [5]. In particular, for an instantaneous change ($t \to 0^+$), the expansion of $U(t)$, Eq. (2.15), gives $\hat{U}(t) \to \hat{1}$ and thus [55] (sudden approximation)

$$K_{fi}(0^+) = |\langle f(0^+)|i(0)\rangle|^2. \tag{2.20}$$

Unitary evolution thus implies that the Jarzynski relation holds; does non-unitarity necessarily lead to a violation of this relation? This question will be taken up in the next chapter.

3. Non-unitary processes

In this chapter we will discuss several causes for non-unitary dynamics of quantum systems. For open quantum systems it is well known that the dynamics cannot be described by a unitary time-evolution operator, generally. In the following section we discuss an other source of non-unitarity in detail, which is characterized by non-matching Hilbert spaces corresponding to the initial and final Hamiltonian. The last section is concerned also with non-matching Hilbert spaces, the source for the change of dimension of Hilbert space, however, being quite different. The following section can also be found in EPJ B **75** [53].

3.1. Boundary switching processes

In classical thermodynamics one is often interested in processes which alter a given boundary condition or constraint on a system, e. g. the volume of a cylinder. Such a process will henceforth be called boundary switching process. A microscopic model of a gas confined in a cylinder would include the atoms and molecules of the cylinder enforcing an effective potential on the gas inside (cf. also [44]). Requiring the cylinder to be ideally isolated naturally leads to an effective potential of infinite height in a microscopic description. However, from a physical point of view, such a potential should be considered an *idealization*. For quasi-static processes, this microscopic description works perfectly. However, one should be careful when investigating processes far from equilibrium where high process velocities are encountered. There, the idealized picture involving infinitely high potentials might be problematic.

3.1.1. Non-unitarity from mechanical control

The eigenfunctions $|\psi\rangle$ of some one-dimensional one-particle Hamiltonian

$$\hat{H}(\gamma) \equiv -\frac{\hbar^2}{2M}\frac{\partial^2}{\partial x^2} + \hat{V}(x,\gamma) \tag{3.1}$$

solve (for fixed γ) the time-independent Schrödinger equation,

$$\hat{H}(\gamma)\,|\psi_n(\gamma)\rangle = E_n(\gamma)\,|\psi_n(\gamma)\rangle\,. \tag{3.2}$$

We consider two examples, both implying non-unitarity transformations.

Boundary switching process (BSP)

Here, the potential well under movements of one wall of the well is considered:

$$\hat{V}_1(x, L(t)) \equiv \begin{cases} \infty & x < 0 \\ 0 & 0 \leq x \leq L(t) \\ \infty & x \leq L(t) \end{cases} \tag{3.3}$$

with $L_0 \leq L(t) \leq L_1$. Parameters are L_1 and $r \equiv \frac{L_1}{L_0}$, $r \geq 1$ characterizes the process ratio.

The eigenfunctions of the potential well of different widths (i. e. different constraints) are not defined on the same Hilbert space, eigenfunctions of the broader well cannot be expanded into those of the smaller one leading to non-unitary evolution when varying the width of the well.

In particular we get for the instantaneous expansion of the well from L_0 to L_1 using $K_{fi}(0^+) = |\langle f(0^+)|i(0)\rangle|^2$ (cf. Eq. (2.20))

$$s(f, r) = \sum_i K_{fi}(0^+) = \frac{1}{r} - \frac{\sin(\frac{2f\pi}{r})}{2f\pi}. \tag{3.4}$$

The deviation from the Jarzynski estimator $\lambda(r, \beta) = -\ln \overline{s(f, r)}$ is zero only for $r = 1$, a trivial case.

Note that $s(f, r)$ is also dependent on the process velocity and therefore the Jarzynski estimator does depend on the process details. In the case of an adiabatic process (in the quantum mechanical sense) one obtains $K_{fi} = \delta_{fi}$ and the Jarzynski estimator gives the correct result. However, in the Jarzynski relation scenario one is usually interested in fast, far from equilibrium processes. Therefore, we will focus on instantaneous changes hereafter.

The relative error of the Jarzynski relation, Eq. (2.13), is shown in Fig. 3.1 as a function of r and β and more detailed for the process ratio $r = 1.31$ as a function of β in Fig. 3.2. This error is unacceptable for $r > 1$ and $\beta \leq 1$. Errors above 10% may easily occur.

Here and in the following, all energies are in units of $E_u = \frac{2}{\pi^2} E_1^\infty$, where E_1^∞ denotes the energy of the ground state in the narrow well with width L_0: $E_n^\infty = \frac{\hbar^2}{2M} \left(\frac{n\pi}{L_0}\right)^2$. The unit of β is E_u^{-1}.

Partition switching process (PSP)

Alternatively, we consider a one-dimensional model related to the classical scenario where an ideal gas confined on a specific side of a bipartite cylinder

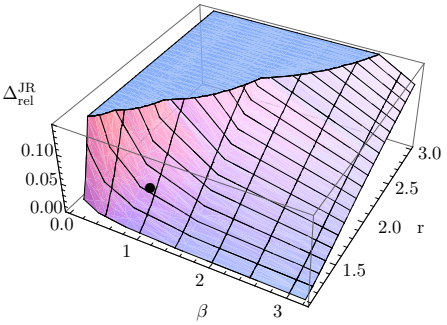

Figure 3.1.: Relative error $\Delta_{\mathrm{rel}}^{\mathrm{JR}}$ of the Jarzynski estimator for BSP as a function of the inverse initial temperature β and the process ratio $r \geq 1$. The dot indicates the more closely investigated parameter window.

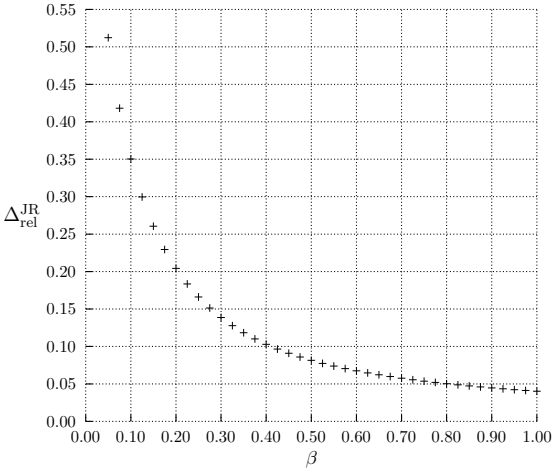

Figure 3.2.: Relative error $\Delta_{\mathrm{rel}}^{\mathrm{JR}}$ of the Jarzynski estimator for BSP versus the inverse temperature β for $r = 1.31$.

expands into the other, initially evacuated compartment, after opening an initially closed stopcock.

Introducing a thin but impenetrable partition by adding a potential step of infinite height and vanishing width into the standard potential well (cf. Eq. (3.3) with $L(t) = L_1$) at arbitrary position $0 < x_w < L_1$, one has for the potential $\hat{V}_2(x, x_w) = \hat{V}_1(x, L_1) + V_w\delta(x - x_w)$, with $\delta(x - x_w)$ being the Dirac delta-distribution. This model gives a deviation of the Jarzynski estimator for instantaneous removal of the partition:

Let the particle be initially prepared in a canonical state. Additionally requiring the particle to start on a specific side of the partition is not considered a canonical state in the sense of Eq. (2.4) (cf. [8]). The probability of observing the particle on either side of the partition is unequal zero, but the partition introduces an additional boundary condition at $x = x_w$. The eigenfunctions of this very well, $|i_w(0)\rangle$, are required to vanish at the position of the partition for $V_w \to \infty$. For finite but non-vanishing V_w all eigenfunctions have a local minimum at $x = x_w$. Therefore the eigenfunctions are restricted and we have (cf. Eqs. (2.19,2.20))

$$s(f, x_w) = \sum_i |\langle f(0^+)|i_w(0)\rangle|^2 \neq 1 \tag{3.5}$$

leading to a violation of the Jarzynski relation (s depends on f, in general). Here, $|f(0^+)\rangle$ denote the eigenfunctions of the well as in Eq. (3.3) with $L(t) = L_1$.

This additional restriction obviously leads to a change of Hilbert space when removing the partition and accordingly to non-unitary dynamics.

In the special case where the partition with $V_w \to \infty$ is located at $x_w = \frac{1}{2}L_1$, one has two totally decoupled potential wells featuring the same width. Straightforward calculations lead to

$$K_{fi}(t) = \frac{4\left[f\cos(f\pi)\sin(2i\pi) - 2i\cos(2i\pi)\sin(f\pi)\right]^2}{(f^2 - 4i^2)\pi^2}, \tag{3.6}$$

which immediately gives

$$s(f, \frac{1}{2}L_1) = \begin{cases} 1 & \text{if } f \text{ is even} \\ 0 & \text{if } f \text{ is odd.} \end{cases} \tag{3.7}$$

The f-dependence of s invalidates the Jarzynski estimator. Note that the failure of the Jarzynski relation should not come as a surprise, as the reversed process for BSP and PSP, respectively, would inevitably lead to a loss of probability.

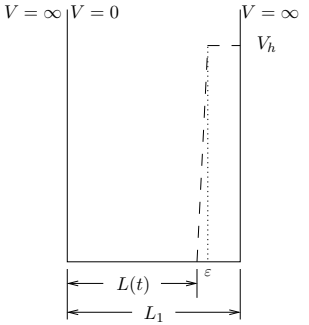

Figure 3.3.: A potential well with a width varying between L_0 and L_1 may be approximated by a fixed potential well of width L_1 amended by a potential step of height V_h. This step is introduced at $x = L(t)$, with a steep, but finite gradient within L and $L + \varepsilon$. $L(t)$ will be taken to be controlled externally, $L_0 \leq L(t) \leq L_1 - \varepsilon$.

3.1.2. Extended model space

In what follows we introduce a class of potentials characterized by an additional (phenomenological) parameter. This is done in such a way that for any finite value of this parameter the potential still leads to a unitary process.

Quasi-boundary switching process (QBSP)

The failure of the Jarzynski relation for BSP (cf. Sec. 3.1.1) is a definite mathematical consequence. However, one may generalize this model such that the BSP would represent some asymptotic limit only.

For this purpose we consider the one-dimensional potential well as depicted in Fig. 3.3. For the Hamilton operator (3.1) we thus choose the potential

$$\hat{V}_3(x, L(t)) = \begin{cases} \infty & x < 0 \\ 0 & a < x < L(t) \\ \frac{1}{\varepsilon} V_h [x - L(t)] & L(t) < x < L(t) + \varepsilon \\ V_h & L(t) + \varepsilon < x < L_1 \\ \infty & x > L_1 \end{cases} \tag{3.8}$$

with $L_0 \leq L(t) \leq L_1 - \varepsilon$, $\varepsilon \ll L_0$.

The eigenfunctions have to fulfill the boundary conditions

$$\psi_n(0) = 0 = \psi_n(L_1), \tag{3.9}$$

and the continuity conditions

$$\psi_n(L(t)-\epsilon) \stackrel{!}{=} \psi_n(L(t)+\epsilon),\ \left.\frac{\partial\psi_n(x)}{\partial x}\right|_{L(t)-\epsilon} \stackrel{!}{=} \left.\frac{\partial\psi_n(x)}{\partial x}\right|_{L(t)+\epsilon} \tag{3.10}$$

in the limit of ϵ going to zero.

In addition to L_1, r of the box model (3.3) there is now an additional characteristic parameter V_h for the height of the potential step at position $L(t)$. Small V_h means *soft* barrier; with increasing V_h the barrier becomes more and more rigid. For V_h finite the step has a steep but finite slope. The potential is thus continuous, which will be of use now:

The considered model system can be mapped onto Eqs. (A.1-A.4) constituting the theorem of expansion (see Appendix). In doing so we identify $(\alpha_1, \alpha_2) = (1, 0)$, $(\gamma_1, \gamma_2) = (1, 0)$, $p(x) = 1$, $w(x) = \frac{2ME}{\hbar^2}$ and $q(x) = -\frac{2MV(x)}{\hbar^2}$. All these functions are continuous, $p(x)$ also differentiable and $w(x)$ also positive. The functions we want to expand are eigenfunctions of the well with a different width of the step potential, thus being of course piecewise continuously differentiable in $J = [a, b] = [0, L_1]$ and with $\nu(a) = \nu(b) = 0$. Also, they can be chosen to be real-valued.

Since all requirements are met it is clear that we can expand any eigenfunction of the potential $\hat{V}$ with $L(t) = L_0$ into the complete set of eigenfunctions of the potential with arbitrary $L(t)$, leading to a unitary time-evolution of the system. Therefore, the Jarzynski relation is fulfilled for a process which varies the position $L(t)$. Of course this also applies to the limiting case of sudden changes of $L(t)$.

Quasi partition switching process (QPSP)

In a similar way also the partition switching process PSP (cf. Sec. 3.1.1) can be generalized: we replace the partition, which is of the form of Dirac's delta distribution $\delta(x - x_w)$, with the Gaussian,

$$\delta_a(x - x_w) = \frac{1}{a\sqrt{\pi}} \mathrm{e}^{-(x-x_w)^2/a^2} \tag{3.11}$$

which approaches the delta distribution for $a \to 0$. Moreover we require the prefactor V_w to stay finite (it may be arbitrarily large, though). The initial state where the particle is confined on a specific side of the finite potential inside the well can - in the strict sense - not be considered an equilibrium state due to a finite tunneling probability through the finite potential. For this model class the Jarzynski estimator works (as long as $a > 0$) for the free energy change since its eigenfunctions can serve as a complete basis for the eigenfunctions of the standard potential well with width L_1.

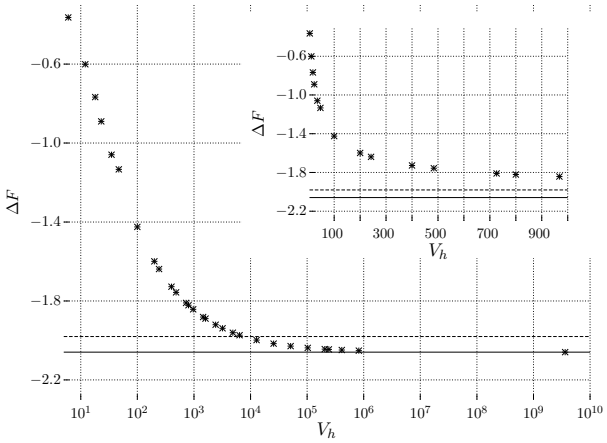

Figure 3.4.: Exact free energy change $\Delta F^{\mathrm{QBSP}} = \Delta F^{\mathrm{QBSP}}_{\mathrm{JR}}$ versus V_h. The exact $\Delta F^{\mathrm{BSP}}_{\beta=1}$ is indicated by the solid horizontal line. The prediction of the JR for BSP, $\Delta F^{\mathrm{BSP}}_{\mathrm{JR}}$, is indicated by the dashed horizontal line. The inset shows the behavior for small V_h; $\beta = 1$, $r = 1.31$.

Comparison of QBSP with BSP

In this section numerical results for ΔF for both, the QBSP and the BSP are presented and compared to each other, based on an initial narrow potential well of width $L(0) = \frac{L_1}{r}$. Then, the potential step is removed instantaneously for the QBSP. For the BSP we instantaneously dilate the potential well to its new width $L = L_1$. ΔF^{QBSP} obviously depends on the potential rigidity parameter V_h. According to Fig. 3.4 a very rigid barrier would have to be chosen to obtain $\Delta F^{\mathrm{QBSP}}_{\beta=1} \approx \Delta F^{\mathrm{BSP}}_{\beta=1}$. Note, however, that $\Delta F^{\mathrm{BSP}}_{\mathrm{JR}} \neq \Delta F^{\mathrm{QBSP}}_{\mathrm{JR}}$ even for very large V_h. In this sense, the QBSP cannot be used to model the BSP - and vice versa - with respect to the Jarzynski relation for instantaneous processes. (For slow, quasi-static processes, though, we find $\Delta F^{\mathrm{BSP}}_{\mathrm{JR}} = \Delta F^{\mathrm{QBSP}}_{\mathrm{JR}} = \Delta F$).

The free energy change for BSP, $\Delta F^{\mathrm{BSP}}_{\beta=1}$, can easily be calculated and we find $\Delta F^{\mathrm{BSP}}_{\beta=1} \approx -2.06$ for $r = 1.31$. On the other hand, the Jarzynski estimator for BSP would give $\Delta F^{\mathrm{BSP}}_{\mathrm{JR}} \approx -1.98$ which deviates from the true free energy change of this BSP, i. e. $\Delta^{\mathrm{JR}}_{\mathrm{rel}} \approx 0.04$. This error rapidly increases for increasing r (cf. Fig. 3.1); unfortunately, increasing r also implies significantly increasing numerical effort. This is why we restrict ourselves to comparatively small r.

Now, although fulfilled (for QBSP) the practical use of the Jarzynski relation may be limited due to rare events as will be investigated more closely in the following section.

3.1.3. Simulation of measurement series for QBSP

We have seen that the Jarzynski estimator generally works for unitary models. Its practical applicability, however, rests upon the amount of statistical data available. The work distribution $P(\Delta E)$ allows us to analyze experimental procedures aimed at a test of the Jarzynski estimator, in particular for models with large V_h.

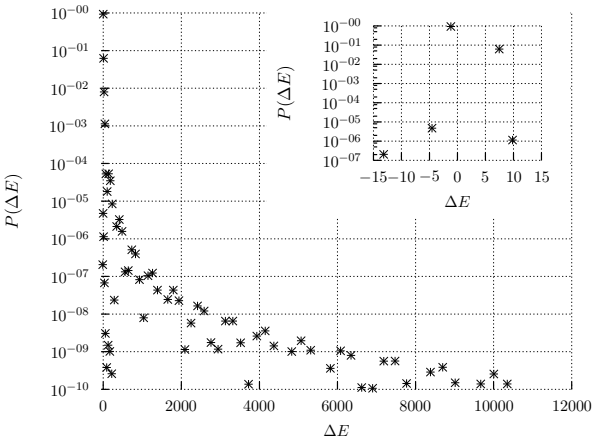

Figure 3.5.: Work distribution for QBSP for $\beta = 1$, $r = 1.31$ and $V_h = 46.9$: Probability P to observe work ΔE in units E_1. Mind the logarithmic scale of the y-axis. Probabilities smaller than 10^{-10} are omitted. The inset shows the region of the work distribution around $\Delta E = 0$.

Direct strategy

Studying $P(\Delta E)$ for the QBSP (cf. Fig 3.5), it becomes obvious that there are a lot of transitions which occur with almost vanishing probability. Therefore, in an experiment, these transitions will most likely never be observed. The question is, whether these transitions will make a significant difference for the average of ΔE or of $\mathrm{e}^{-\beta\Delta E}$. If so it would be necessary to perform the process extremely often to get a reliable estimate. The effect of rare events on

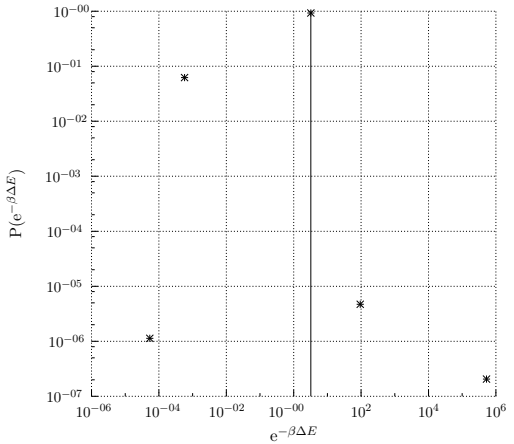

Figure 3.6.: Probability distribution $\mathrm{P}(\mathrm{e}^{-\beta\Delta E})$ for QBSP for $\beta = 1$ and $V_h = 46.9$ as in Fig. 3.5. The mean $\overline{\mathrm{e}^{-\beta\Delta E}}$ is indicated by the vertical line. The x- and y-axis are scaled logarithmically.

the convergence of exponentially weighted values has already been considered in [9], e. g. If the number of experiments one has to perform becomes too large to be feasible, we will call the Jarzynski relation practically not applicable.

A closer look reveals the true nature of the problem for experimental confirmation of the Jarzynski relation, here. The large number of transitions with large positive values for ΔE, cf. Fig. 3.5, have almost no influence on the average of $\mathrm{e}^{-\beta\Delta E}$ while the unlikely events with large negative work values are important to get a good estimate. This can be seen quite clearly in Fig. 3.6, where the probability $P(\mathrm{e}^{-\beta\Delta E})$ is depicted. The large deviation, which corresponds to a transition from $n = 2$ ($L(t = 0)$) to the ground state ($n = 1$) for $L(t) = L_1$ with $\Delta E \approx -13.2$, is responsible for the Jarzynski estimator to approach the actual free energy change so slowly. The lower the temperature, corresponding to larger β, the more crucial the large deviation becomes.

Note that using the true distribution from Fig. 3.5 or Fig. 3.6 to calculate the Jarzynski estimator, we find $\Delta_{\mathrm{rel}}^{\mathrm{JR}} \leq 10^{-8}$, the finite value being due to numerical errors. We thus expect for a typical measurement series to find the following feature: Calculating the average of $\mathrm{e}^{-\beta\Delta E}$ after each additional repetition, $\lambda_{\mathrm{exp}}(\beta) = \Delta F^{\mathrm{JR}} - \Delta F$ will be non-zero and stay almost constant even for a large number of repetitions. We introduce the relative simulated (i. e. "observed") error $\delta_{\mathrm{rel}}^{\mathrm{JR}} \equiv \frac{\lambda_{\mathrm{exp}}(\beta)}{\Delta F}$. Only when routinely observing the

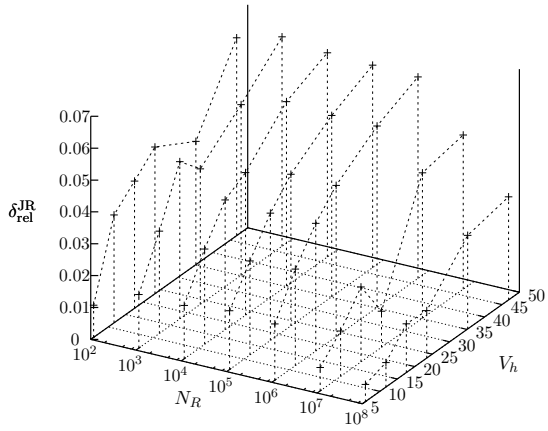

Figure 3.7.: Simulated relative error of the Jarzynski estimator, $\delta_{\mathrm{rel}}^{\mathrm{JR}}$, for QBSP for different numbers of measurements, N_R, and different potential heights V_h. In general, the higher V_h the more measurements are necessary to get a good estimate for ΔF. Parameters are $r = 1.31$, $\beta = 1$.

highly unlikely event of $\Delta E \approx -13.2$, the estimator will improve significantly.

This expectation is confirmed when we study the applicability of the Jarzynski relation dependent on the height V_h of the switching potential. To this end, we simulate the outcome of an experiment performed on the system. The resulting work distribution will be used to determine $\overline{\mathrm{e}^{-\beta\Delta E}}$. This simulation is done for various repetition numbers N_R. The relative error dependent on V_h and N_R is depicted in Fig. 3.7.

The resulting plateau behavior is unfortunate and could easily make the experimenter believe to have already obtained full convergence. The higher V_h, the larger N_R for reaching the Jarzynski estimator within a given error bar. Even for relatively low V_h, i. e. $V_h = 46.9E_u \approx 10E_1^{\infty}$, about $N_R \approx 10^8$ repetitions of the experiment would be necessary to get the error $\delta_{\mathrm{rel}}^{\mathrm{JR}}$ down to approximately 3.2%. The efforts get even more demanding for higher V_h. For very large V_h the Jarzynski relation is practically not applicable, even though still mathematically correct, i. e. it cannot be used to predict free energy changes. This scenario is superficially reminiscent of *algorithmic hardness* [24] and may thus be called experimentally hard.

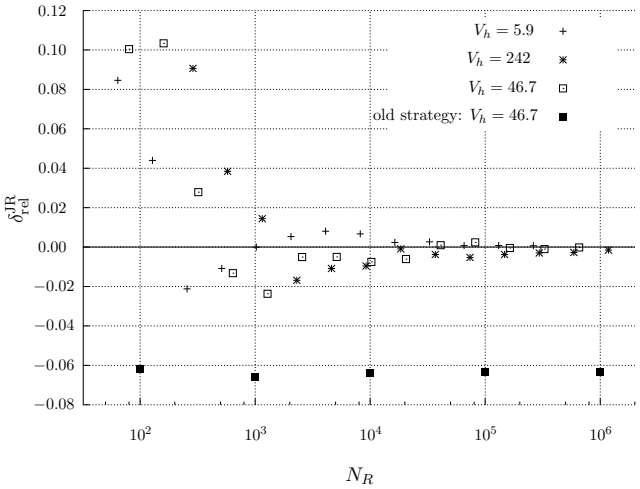

Figure 3.8.: Improved strategy: Relative error of the simulated Jarzynski estimator for QBSP as a function of numbers of measurements, N_R^{tot}. Here, $N_R = 2N_R^i$ for $V_h = 5.9$, $N_R = 5N_R^i$ for $V_h = 46.7$ and $N_R = 9N_R^i$ for $V_h = 242$, respectively, where N_R^i are the number of repetitions per state explored. The relative error of the old strategy for $V_h = 46.7$ is also shown. Parameters are $r = 1.31$, $\beta = 1$.

Improved strategy

One may wonder whether the blow-up of experimental efforts could be avoided using other measurement strategies. In a classical context improved strategies have already been discussed reducing the dissipation of work during the process, e. g., by altering the equations of motion in computational thermodynamics [69] or by using optimal work protocols [74].

Here, the origin of the fluctuations described by the Jarzynski relation is two-fold: i) the thermal indeterminacy as described by the initial canonical state, and ii) the quantum non-adiabaticity described by the conditional probabilities $K_{fi}(t)$, in either case followed up by quantum measurements. In the quasi-static limit only the thermal uncertainty survives; in the scenario considered below only the quantum features remain.

One reason for the small probability of observing the transition from $n = 2$ to the ground state is due to the (assumed) low temperature and the resulting small initial occupation probability of the excited states. But one could instead prepare the system in different initial energy-eigenstates, then perform the process and measure the energy at the end of the process. This would correspond to measuring the conditional probability $K_{fi}(t)$ (cf. Sec. (2.2.1)) rather than $P(\Delta E)$. Of course, the number of initial eigenstates $n^{\min}$ as well as the number of measurements for each of these initial states necessary to get a reliable Jarzynski estimator, N_R^i, depends on the initial temperature, V_h, r and the system parameters of the particle and are generally unknown. Fig. 3.8 shows $\delta_{\text{rel}}^{\text{JR}}$ with $V_h = 5.9 \approx 1E_1^\infty$ for this measurement strategy. (Note that contrary to Eq. (2.13) we took into account the relative sign, here.) The system was prepared initially in any one of the 2 lowest energy-eigenstates, $n^{\min} = 2$. The total number of repetitions $N_R = 2N_R^i$ necessary to get a reliable estimator is $N_R \approx 10^5$ and therefore this method would significantly improve the use of the Jarzynski estimator. Here, N_R^i denotes the number of repeated measurements after initially preparing the system in the energy-eigenstate $|\varphi_i(V_h)\rangle$. A further advantage of this method is the possibility to test whether $s(f) = 1$ is already independent of f using Eq. (2.6) on the pertinent subspace. If this relation does not hold the experimenter knows that the Jarzynski estimator will fail to give the correct result.

For higher V_h, i. e. a more rigid barrier, this strategy requires slightly more measurements N_R as also shown in Fig. 3.8 for $V_h = 242 \approx 50E_1^\infty$. Here, the system had to be prepared initially in the lowest 9 energy-eigenstates since measuring fewer states does not give a good estimator even for arbitrarily large numbers of measurements. A total of $N_R \approx 10^6$ measurements are necessary to give a good estimate for ΔF. Generally, the higher V_h the more initial states have to be taken into account. A closer study shows that the number

of initial states necessary to get a good estimator, $n^{\min}$ scales with V_h as $n^{\min} \approx \sqrt{V_h}$, thus N_R increases slowly with V_h.

Therefore, for large V_h, this new measurement strategy also seems to fail (for reasonable numbers N_R) to give the correct result for the free energy change, i. e. $\delta_{\mathrm{rel}}^{\mathrm{JR}}$ stays finite. Moreover, $n^{\min}$ depends strongly on the initial β chosen. For higher temperature $n^{\min}$ gets larger. But, at least, there is apparently no plateau behavior and the consistency of data can be tested as described above.

3.1.4. Conclusion

Interactions with the environment are the fundamental source of noise in both classical and quantum systems [58]. In the quantum domain the *Jarzynski scenario* differs in several respects from that in the classical domain:

i) The dynamical strategy is based on the comparison between initial and final energy measurement instead of considering trajectories [48]. These energy differences of the total system constitute the work ΔW as a random variable.

ii) Ensemble averages define the mean energy change as well as the Jarzynski estimator, ΔF^{JR}.

iii) The Jarzynski estimator does not necessarily give the correct mean free energy change ΔF: Fundamental deviations, $\Delta_{\mathrm{rel}}^{\mathrm{JR}}$, are due to non-unitary transformations resulting from the type of mechanical control (e. g. boundary switching processes BSP).

iv) Even if the Jarzynski estimator works, though, (like for QBSP) its practical applicability may be limited due to statistical errors, $\delta_{\mathrm{rel}}^{\mathrm{JR}}$.

v) "Bad statistics" become dominant for QBSP with increasing rigidity of the potential.

vi) Optimization of the measurement strategy is possible. Here, we have proposed an alternative strategy, which is based on the preparation of a set of pure initial states allowing to directly determine the conditional probability K_{fi}.

Also, the PSP and QPSP can shed new light on the Gibbsian paradox [20], as only for PSP a mixing entropy for identical particles is to be expected for a true thermal initial state. For QPSP, all particles can be found on both sides of the partition for the initial state, already.

3.2. Partially thermalized initial states

As we have seen in the previous section, non-matching Hilbert spaces can lead to a violation of the JR. Here, we consider situations where the initial condition for the applicability of the JR is violated: We now start in a state characterized by partial equilibrium. One may argue that a violation of the JR would not come as a surprise if the initial condition is violated. However, consider, e. g., a macro-molecule. Perfect thermalization would mean that all degrees of freedom feature a thermal distribution with the same inverse temperature β. This would mean a thermal center of mass motion, thermal fundamental vibrations and rotations, thermal electronic state as well as thermal electron and nuclear spin states. Especially as the latter have relaxation times up to several hours or even days, it might be problematic to enforce them all being thermal. Of course, as the energy scales of the different contributions are largely separated, one may argue that even the exponentially weighting used in the JR does surely not lead to serious deviations of the JR from the correct free energy estimate.

However, there might exist situations in which such small deviations from perfect thermalization might indeed influence the accuracy of the JR. E. g., from molecular physics it is well known that the nuclear spin state of the nuclei forming the molecule can influence the rotational motion of that very molecule [28]. For instance, there exist two different configurations of the hydrogen molecule H_2: One, where the nuclear spins of the hydrogen nuclei are parallel ($I = 1$), called o-H_2 (short for ortho-hydrogen), and one where they are anti-parallel ($I = 0$), named p-H_2 (short for para-hydrogen). At room temperature, they should be found equally probable[1]. As the electronic ground state of the hydrogen molecule, ${}^1\Sigma_g^+$, has positive parity (for details we refer to [28]) the combined wave function of spin and rotation have to feature negative parity (we discuss only the vibrational ground state, here. Even at room temperature a thermal distribution would almost only feature the vibrionic ground state). Thus, p-H_2 assumes rotational states with $J = 0, 2, 4 \ldots$, while o-H_2 can only assume $J = 1, 3, 5, \ldots$. As the energy difference between the rotational ground state $J = 0$ and the first excited state $J = 1$ is given by $E_{J=1} - E_{J=0} \approx 175\,\mathrm{K}$ in terms of k_B, we find that at low temperatures almost only p-H_2 should be present. As the conversion between p-H_2 and o-H_2 is quite slow (inter-conversion between singlet and triplet spin states), one could easily end up in a non-thermal state.

Now, imagine a situation at low temperature where only p-H_2 is present

[1] Strictly speaking, one expects a ratio of $\frac{\mathrm{p-H_2}}{\mathrm{o-H_2}} = \frac{1}{3}$ due to statistical weighting (degeneracy).

(at $T = 10\,\mathrm{K}$ only about one molecule out of a million would be in the ortho-state, e. g.). If, due to the working protocol a transition into the ortho-state was fairly probable, the accessible Hilbert space would have to grow larger compared to the initial one where only the para-state was present.

4. Composite quantum systems

Here, we briefly discuss two different classes of approaches to generalized quantum Jarzynski relations (QJRs) (Secs. 4.1 and 4.2). Then, in Sec. 4.3 we introduce the concept of bilocal measurements as a quantum generalization of the JR. In Sec. 4.4 we discuss necessary concepts for generalizing the JR to closed quantum systems, which will then be studied in detail in Chap. 5.

4.1. Reinterpretation

The first class of generalizations uses the fact that for unitary dynamics the QJR holds [68]. One member of this class has been discussed in [11]: If the system under consideration is coupled to some environment, then the dynamics for the compound system including the environment is unitary. The compound system is closed apart from some external work source. If the combined system starts in a canonical state it is possible to formulate the JR for this system. Now, re-interpreting the occurring observables, i. e. the work performed during the process and the free energy difference, it is possible - under appropriate restrictions - to get a QJR with respect to the system only.

An illustrative, very simplified example refers to a quantum system coupled to a classical bath. For this bath we require that it does solely exchange heat with its surroundings, $\Delta W_B = 0$, and that it is sufficiently large so that $\Delta F_B = 0$. Moreover, if it is coupled weakly to the quantum system and therefore $\Delta Q_S = -\Delta Q_B$, then,

$$\overline{\mathrm{e}^{-\beta W}} = \overline{\mathrm{e}^{-\beta \Delta E_{\mathrm{tot}}}} = \overline{\mathrm{e}^{-\beta(\Delta W_S + \Delta Q_S + \Delta Q_B)}} = \overline{\mathrm{e}^{-\beta \Delta W_S}} = \mathrm{e}^{-\beta \Delta F_{\mathrm{tot}}}. \tag{4.1}$$

If the coupling is weak enough to justify the approximation $F = F_S + F_B$, then we arrive at

$$\overline{\mathrm{e}^{-\beta \Delta W_S}} = \mathrm{e}^{-\beta(\Delta F_S + \Delta F_B)} = \mathrm{e}^{-\beta \Delta F_S}, \tag{4.2}$$

which is the local JR for the system, only. The drawback of this approach is that the initial conditions are not easily generalizable as the compound system has to start in a canonical state.

For situations, where only parts of a composite quantum system are in thermal equilibrium, while the compound system is not, a different approach might be more promising.

4.2. Local dynamics

Another approach to generalized QJRs is to consider a quantum system in thermal equilibrium, coupled to another system, which we will call environment, henceforth. Then, by investigating the local dynamics of the system one may try to formulate a QJR (cf. [61], e. g.). The initial state of the compound system fulfills

$$\mathrm{Tr}_{\mathsf{env}}\left[\hat{\varrho}(0)\right] = \frac{\mathrm{e}^{-\beta\hat{H}_{\mathsf{sys}}}}{Z_{\mathsf{sys}}}. \tag{4.3}$$

In most cases, one would additionally require a factorizing initial state, $\hat{\varrho}(0) = \hat{\varrho}_{\mathsf{sys}}(0) \otimes \hat{\varrho}_{\mathsf{env}}(0)$, where the physical setting would involve that a thermalized state, now decoupled from the bath, is coupled to some environment.

An illustrative, but very restrictive example, refers to a quantum system in microcanonical contact with an environment. Microcanonical contact means that the environment is a purely dephasing one, no energy is exchanged between this environment and the system (cf. [44]). The following commutator relations for the interaction Hamiltonian, $\hat{H}_{\mathsf{se}}$, are required to hold,

$$\left[\hat{H}_{\mathsf{se}}, \hat{H}_s(t)\right] = 0, \quad \left[\hat{H}_{\mathsf{se}}, \hat{H}_{\mathsf{env}}\right] = 0, \tag{4.4}$$

where $\hat{H}_s(t)$ and $\hat{H}_{\mathsf{env}}$ denote the system and environmental Hamiltonian, respectively. Note that the system Hamiltonian is explicitly time-dependent due to external driving. As the system does not exchange energy with the environment, its energy change is solely due to the driver, thus

$$\overline{\mathrm{e}^{-\beta\Delta W_{fi}}} = \overline{\mathrm{e}^{-\beta\Delta W_{fi}+\Delta Q_{fi}}} = \overline{\mathrm{e}^{-\beta\Delta E_{fi}}}, \tag{4.5}$$

where we have used that the driver constitutes a perfect work source, thus $\Delta Q = 0$. Now, following the line of proof from Mukamel for unitary dynamics (cf. [68]),

$$\overline{\mathrm{e}^{-\beta\Delta E_{fi}}} = \sum_{fi} \mathrm{e}^{-\beta(E_f - E_i)} K_{fi}(t) \left[\varrho_{\mathsf{sys}}(0)\right]_{ii} = \frac{1}{Z_{\mathsf{sys}}(0)} \sum_{fi} \mathrm{e}^{-\beta E_f} K_{fi}(t), \tag{4.6}$$

where we have used that the system starts in a canonical state. The conditional probability, $K_{fi}(t)$ has already been introduced in Eq. (2.3),

$$K_{fi}(t) = \mathrm{Tr}_{\mathsf{sys}} \left\{ |f\rangle\langle f| \, \hat{\varrho}^t_{\mathsf{sys}}(i) \right\}, \tag{4.7}$$

where $\hat{\varrho}^t_{\mathsf{sys}}(i)$ denotes the density operator of the system after the process duration t for the case where the initial measurement lead to a projection onto energy-eigenstate $|i\rangle$.

Using the fact that the total system evolves unitarily, we find

$$K_{fi}(t) = \mathrm{Tr}_{\mathsf{sys,env}} \left\{ (|f\rangle\langle f| \otimes \hat{1}_{\mathsf{env}}) \hat{U}_t (|i\rangle\langle i| \otimes \hat{\varrho}^0_{\mathsf{env}}[M:i]) \hat{U}_t^\dagger \right\}, \tag{4.8}$$

where the argument $M : i$ of $\hat{\varrho}_{\mathsf{env}}$ denotes the fact that the density operator of the environment changes, in general, due to the projective measurement of the system for non-factorizing initial states. Now, if we additionally require a factorizing initial state and the environment to start in a diagonal state in its energy-eigenbasis, we find

$$\sum_i K_{fi}(t) = \mathrm{Tr}_{\mathsf{sys,env}} \left\{ (|f\rangle\langle f| \otimes \hat{1}_{\mathsf{env}}) \hat{U}_t (\hat{1}_{\mathsf{sys}} \otimes \hat{\varrho}^0_{\mathsf{env}}) \hat{U}_t^\dagger \right\} = 1, \tag{4.9}$$

where we have used that $\hat{U}_t \hat{U}_t^\dagger = \hat{1}$ and $[\hat{U}_t, \hat{\varrho}^0_{\mathsf{env}}] = 0$, as well as the completeness relation $\sum_i |i\rangle\langle i| = \hat{1}_{\mathsf{sys}}$. Substituting this into Eq. (4.6), we get

$$\overline{\mathrm{e}^{-\beta \Delta W_{fi}}} = \frac{Z_{\mathsf{sys}}(t)}{Z_{\mathsf{sys}}(0)}, \tag{4.10}$$

which is the local Jarzynski relation for the system only.

4.3. Bilocal Energy Fluctuation Theorem

Here, we want to consider a bipartite system, where both systems are initially in local thermal equilibrium. Then, we measure both systems projectively at the beginning and the end of a process, which is realized by an external driver, acting only locally on one part of the system. As above, we will call the part coupled to the external driver the *system* and the other the *environment*. The two-time measurements give two stochastic variables, $\Delta E^{\mathsf{sys}}_{fi}$ and $\Delta E^{\mathsf{env}}_{f'i'}$ for the system and the environment, respectively. In the following, we will call the exponentially weighted average,

$$\overline{\mathrm{e}^{-\beta_{\mathsf{sys}} \Delta E^{\mathsf{sys}}_{fi}} \mathrm{e}^{-\beta_{\mathsf{env}} \Delta E^{\mathsf{env}}_{f'i'}}}, \tag{4.11}$$

bilocal EFT due to the similarity (two-time energy measurements) to EFT. Note that if both systems start with the same inverse temperature β without any interaction, then bilocal EFT and EFT coincide. In the following, we will discuss two measurement strategies: First, the measurements are performed simultaneously, second, we deal with time-ordered measurements.

4.3.1. Simultaneous Measurements

Here, we assume that we can measure the system and the environment simultaneously. Suppose the system (local states $|n\rangle$) and the environment (local states $|n'\rangle$) start in a factorizing state,

$$\hat{\rho}^0 = \hat{\rho}^0_{\mathsf{sys}} \otimes \hat{\rho}^0_{\mathsf{env}} \text{ with } \hat{\rho}^0_{\mathsf{sys}} = \frac{\mathrm{e}^{-\beta_{\mathsf{sys}}\hat{H}_{\mathsf{sys}}}}{Z^0_{\mathsf{sys}}} \text{ and } \hat{\rho}^0_{\mathsf{env}} = \frac{\mathrm{e}^{-\beta_{\mathsf{env}}\hat{H}_{\mathsf{env}}}}{Z^0_{\mathsf{env}}}. \tag{4.12}$$

The local Hamiltonians fulfill

$$\hat{H}_{\mathsf{sys}}|n\rangle = E^{\mathsf{sys}}_n |n\rangle \text{ and } \hat{H}_{\mathsf{env}}|n'\rangle = E^{\mathsf{env}}_{n'}|n'\rangle . \tag{4.13}$$

The complete Hamiltonian reads $\hat{H} \equiv \hat{H}^t_{\mathsf{sys}} \otimes \hat{1}_{\mathsf{env}} + \hat{1}_{\mathsf{sys}} \otimes \hat{H}_{\mathsf{env}} + \hat{H}_{\mathsf{se}}$, thus the system is initially in a partial equilibrium state. Now, we measure both parts initially. We then find for the bilocal EFT

$$\overline{\mathrm{e}^{-\beta_{\mathsf{sys}}\Delta E_{\mathsf{sys}}}\mathrm{e}^{-\beta_{\mathsf{env}}\Delta E_{\mathsf{env}}}} = \sum_{ff',ii'} \mathrm{e}^{-\beta_{\mathsf{sys}}(E_f - E_i)}\mathrm{e}^{-\beta_{\mathsf{env}}(E_{f'} - E_{i'})} K_{ff',ii'} p(ii'), \tag{4.14}$$

with $p(ii')$ being the probability of finding the compound system in the initial state $|i\rangle \otimes |i'\rangle$. As we have required the system to start in a product state, the probabilities of the two subsystems are independent of each other and thus we find

$$p(ii') = q^{\mathsf{sys}}_i(0) \cdot q^{\mathsf{env}}_{i'}(0) = \frac{\mathrm{e}^{-\beta_{\mathsf{sys}}E^{\mathsf{sys}}_i}\mathrm{e}^{-\beta_{\mathsf{env}}E^{\mathsf{env}}_{i'}}}{Z^0_{\mathsf{sys}} Z^0_{\mathsf{env}}}. \tag{4.15}$$

Note, that we have assumed that the final energy-eigenstates in Eq. (4.14), $E_{f'}$ of the environment do not depend on the state of the system. Otherwise, the effective energy of the environment might depend on the state of the system measured, invalidating the following calculations. Here, $K_{ff',ii'}$ is the natural generalization of the conditional probability (cf. Sec. 2.2.1), given by

$$K_{ff',ii'} = \mathrm{Tr}\left\{|ff'\rangle\langle ff'|\, \hat{\rho}^t_{ii'}\right\} \tag{4.16}$$

with $|n\rangle \otimes |n'\rangle = |nn'\rangle$ and

$$\hat{\rho}^t_{ii'} = \hat{U}_t\, |ii'\rangle\langle ii'|\, \hat{U}^\dagger_t, \tag{4.17}$$

the density operator at time t after the two simultaneously performed initial measurements at $t = 0$. With this we immediately have

$$\sum_{ii'} K_{ff',ii'} = 1, \tag{4.18}$$

in analogy to Sec. 2.2.1. Substituting this sum rule and Eq. (4.15) into Eq. (4.14), we get

$$\overline{\mathrm{e}^{-\beta_{\mathsf{sys}}\Delta E_{\mathsf{sys}}}\mathrm{e}^{-\beta_{\mathsf{env}}\Delta E_{\mathsf{env}}}} = \frac{Z^t_{\mathsf{sys}} Z^t_{\mathsf{env}}}{Z^0_{\mathsf{sys}} Z^0_{\mathsf{env}}} = \mathrm{e}^{-\beta_{\mathsf{sys}}\Delta F_{\mathsf{sys}}}\mathrm{e}^{-\beta_{\mathsf{env}}\Delta F_{\mathsf{env}}}. \tag{4.19}$$

Now, we are interested in the effect of initial correlations,

$$\hat{\rho}^0 = \hat{\rho}^0_{\mathsf{sys}} \otimes \hat{\rho}^0_{\mathsf{env}} + \hat{C}^0_{\mathsf{se}}. \tag{4.20}$$

Then, we have for the initial probability $p(ii')$,

$$\begin{aligned} p(ii') &= \mathrm{Tr}\left\{\hat{P}_{ii'}\hat{\rho}^0\right\} = \mathrm{Tr}\left\{|ii'\rangle\langle ii'|\left(\hat{\rho}^0_{\mathsf{sys}} \otimes \hat{\rho}^0_{\mathsf{env}} + \hat{C}^0_{\mathsf{se}}\right)\right\} \\ &= q_i^{\mathsf{sys}}(0) \cdot q_{i'}^{\mathsf{env}}(0) + \langle ii'|\,\hat{C}^0_{\mathsf{se}}\,|ii'\rangle = \frac{\mathrm{e}^{-\beta_{\mathsf{sys}}E_i^{\mathsf{sys}}} e^{-\beta_{\mathsf{env}}E_{i'}^{\mathsf{env}}}}{Z^0_{\mathsf{sys}} Z^0_{\mathsf{env}}} + \langle ii'|\,\hat{C}^0_{\mathsf{se}}\,|ii'\rangle\,. \end{aligned} \tag{4.21}$$

Here, Eq. (4.17) remains valid due to

$$\begin{aligned} \hat{\rho}^0[M : ii'] &= \frac{\hat{P}_{ii'}\left(\hat{\rho}^0_{\mathsf{sys}} \otimes \hat{\rho}^0_{\mathsf{env}} + \hat{C}^0_{\mathsf{se}}\right)\hat{P}_{ii'}}{\mathrm{Tr}\left\{|ii'\rangle\langle ii'|\left(\hat{\rho}^0_{\mathsf{sys}} \otimes \hat{\rho}^0_{\mathsf{env}} + \hat{C}^0_{\mathsf{se}}\right)\right\}} \\ &= \frac{\left(q_i^{\mathsf{sys}}(0)q_{i'}^{\mathsf{env}}(0) + \langle ii'|\,\hat{C}^0_{\mathsf{se}}\,|ii'\rangle\right)|ii'\rangle\langle ii'|}{q_i^{\mathsf{sys}}(0)q_{i'}^{\mathsf{env}}(0) + \langle ii'|\,\hat{C}^0_{\mathsf{se}}\,|ii'\rangle} = |ii'\rangle\langle ii'|\,. \end{aligned} \tag{4.22}$$

Thus, sum rule Eq. (4.18) does also hold if initial correlations were present. Substituting this sum rule and Eq. (4.21) into Eq. (4.14) gives Eq. (4.19) for the first addend of Eq. (4.21), plus an additional addend involving the correlation term. Thus, although system and environment are in local equilibrium states we find a deviation from Eq. (4.19) which can be understood in detail when considering time-ordered measurements, as discussed in the subsequent section.

4.3.2. Time-ordered Measurements

Above, we have explicitly assumed that we perform the measurements simultaneously. This might be somewhat tricky in an experiment, therefore let us suppose that we measure the energy of the two subsystems within a very short time interval, in a definite order, but not simultaneously. Since initial correlations above let the bilocal EFT fail, one may wonder why this did not occur for final correlations.

In the following we will first measure the system and then the environment. We start with a factorizing state, which immediately gives

$$p(ii') = q_i^{\mathsf{sys}}(0) \cdot q_{i'}^{\mathsf{env}}(0). \tag{4.23}$$

Therefore, if the sum rule holds for the conditional probability $K_{ff',ii'}$ then bilocal EFT should estimate the free energy change correctly[1].

Now, we investigate $K_{ff',ii'}$. We do so by first determining the probability $p(f;ii')$ to find the system in the state $|f\rangle$ at the end of the process if it has initially been measured in the eigenstate $|ii'\rangle$, and then, second, the probability to measure immediately *afterwards* the environment in the state $|f'\rangle$. For the first measurement we find

$$p(f;ii') = \mathrm{Tr}\left\{\left(|f\rangle\langle f| \otimes 1_{\mathsf{env}}\right)\hat{\rho}_{ii'}^t\right\} = \mathrm{Tr}_{\mathsf{sys}}\left\{|f\rangle\langle f|\,\hat{\rho}_{\mathsf{sys},ii'}^t\right\} = q_f^{\mathsf{sys}}(t). \tag{4.24}$$

The subsequent measurement on the environment after the system has been measured in state $|f\rangle$ yields

$$\begin{aligned} p(f';f,ii') &= \mathrm{Tr}\left\{\left(\hat{1}_{\mathsf{sys}} \otimes |f'\rangle\langle f'|\right)\hat{\rho}^t[M:f,ii']\right\} \\ &= \mathrm{Tr}\left\{\left(\hat{1}_{\mathsf{sys}} \otimes |f'\rangle\langle f'|\right)\left(|f\rangle\langle f| \otimes \hat{\rho}_{\mathsf{env}}^t + \hat{P}_f\hat{C}_{\mathsf{se}}^t\hat{P}_f\frac{1}{q_f^{\mathsf{sys}}(t)}\right)\right\} \\ &= q_{f'}^{\mathsf{env}}(t) + \xi_{ff'} \end{aligned} \tag{4.25}$$

with

$$\xi_{ff'} = \mathrm{Tr}\left\{\left(\hat{P}_f \otimes \hat{P}_{f'}\right)\hat{C}_{\mathsf{se}}^t\frac{1}{q_f^{\mathsf{sys}}(t)}\right\}. \tag{4.26}$$

Now, the crucial quantity for the proof of the bilocal EFT is the sum rule

$$\sum_{ii'} K_{ff',ii'} = \sum_{ii'} p(f;ii')p(f';f,ii'), \tag{4.27}$$

[1] As above, the effective energy of the environment is supposed to be independent of the state of the system.

given by

$$\begin{aligned}
\sum_{ii'} q_f^{\mathsf{sys}}(t)\left(q_{f'}^{\mathsf{env}}(t)+\xi_{ff'}\right) &= \sum_{ii'} q_f^{\mathsf{sys}}(t) q_{f'}^{\mathsf{env}}(t) + \sum_{ii'} q_f^{\mathsf{sys}}(t)\xi_{ff'} \\
&= \sum_{ii'} \mathrm{Tr}_{\mathsf{sys}}\left\{\hat{P}_f \hat{\rho}_{\mathsf{sys}}^t\right\} \mathrm{Tr}_{\mathsf{env}}\left\{\hat{P}_{f'} \hat{\rho}_{\mathsf{env}}^t\right\} + \dots \\
&\quad \dots + \sum_{ii'} \mathrm{Tr}\left\{\left(\hat{P}_f \otimes \hat{P}_{f'}\right) \hat{C}_{\mathsf{se}}^t \frac{1}{q_f^{\mathsf{sys}}(t)}\right\} q_f^{\mathsf{sys}}(t) \\
&= \sum_{ii'} \mathrm{Tr}\left\{\hat{P}_f \rho_{\mathsf{sys}}^t \otimes \hat{P}_{f'} \hat{\rho}_{\mathsf{env}}^t + \left(\hat{P}_f \otimes \hat{P}_{f'}\right) \hat{C}_{\mathsf{se}}^t\right\} \\
&= \sum_{ii'} \mathrm{Tr}\left\{\left(\hat{P}_f \otimes \hat{P}_{f'}\right)\left(\hat{\rho}_{\mathsf{sys}}^t \otimes \hat{\rho}_{\mathsf{env}}^t + \hat{C}_{\mathsf{se}}^t\right)\right\} \\
&= \sum_{ii'} \mathrm{Tr}\left\{\left(\hat{P}_f \otimes \hat{P}_{f'}\right)\left(\hat{U}^t \left|ii'\right\rangle\!\left\langle ii'\right| \hat{U}^{t^\dagger}\right)\right\} = 1.
\end{aligned} \tag{4.28}$$

Here, we have used that $\mathrm{Tr}\left\{\hat{A}_{\mathsf{sys}} \otimes \hat{A}_{\mathsf{env}}\right\} = \mathrm{Tr}_{\mathsf{sys}}\left\{\hat{A}_{\mathsf{sys}}\right\} \mathrm{Tr}_{\mathsf{env}}\left\{\hat{A}_{\mathsf{env}}\right\}$ for operators $\hat{A}$ acting on the respective parts of the total Hilbert space. Thus, the bilocal EFT gives, indeed, the correct estimate of the free energy change.

As above, it is easy to show that the JR generally fails if initial correlations are present. We will investigate this case now, where

$$\hat{\rho}^0 = \hat{\rho}_{\mathsf{sys}}^0 \otimes \hat{\rho}_{\mathsf{env}}^0 + \hat{C}_{\mathsf{se}}^0 \text{ with } \hat{\rho}_{\mathsf{sys}}^0 = \frac{\mathrm{e}^{-\beta_{\mathsf{sys}} \hat{H}_{\mathsf{sys}}}}{Z_0^{\mathsf{sys}}} \text{ and } \hat{\rho}_{\mathsf{env}}^0 = \frac{\mathrm{e}^{-\beta_{\mathsf{env}} \hat{H}_{\mathsf{env}}}}{Z_0^{\mathsf{env}}}. \tag{4.29}$$

Apparently, there arises a problem with the additional addend, because initial time-ordered measurements lead to

$$p(i) = \mathrm{Tr}\left\{\left(\hat{P}_i \otimes \hat{1}_{\mathsf{env}}\right) \hat{\rho}^0\right\} = \mathrm{Tr}_{\mathsf{sys}}\left\{\hat{P}_i \hat{\rho}_{\mathsf{sys}}^0\right\} = q_i^{\mathsf{sys}}(0) = \frac{\mathrm{e}^{-\beta_{\mathsf{sys}} E_i^{\mathsf{sys}}}}{Z_0^{\mathsf{sys}}}, \tag{4.30}$$

and for the subsequent measurement on the environment,

$$\begin{aligned} p(i';i) &= \mathrm{Tr}\left\{\left(\hat{1}_{\mathsf{sys}}\otimes\hat{P}_{i'}\right)\hat{\rho}^0[M:i]\right\} \\ &= \mathrm{Tr}\left\{\left(\hat{1}_{\mathsf{sys}}\otimes\hat{P}_{i'}\right)|i\rangle\langle i|\otimes\left(\hat{\rho}^0_{\mathsf{env}}+\langle i|\,\hat{C}^0_{\mathsf{se}}\,|i\rangle\,\frac{1}{q_i^{\mathsf{sys}}(0)}\right)\right\} \\ &= \mathrm{Tr}\left\{\left(\hat{P}_i\otimes\hat{P}_{i'}\right)\hat{1}_{\mathsf{sys}}\otimes\hat{\rho}^0_{\mathsf{env}}+\left(\hat{P}_i\otimes\hat{P}_{i'}\right)\hat{C}^0_{\mathsf{se}}\frac{1}{q_i^{\mathsf{sys}}(0)}\right\} \\ &= q^{\mathsf{env}}_{i'}(0)+\xi_{ii'} = \frac{\mathrm{e}^{-\beta E^{\mathsf{env}}_{i'}}}{Z_0^{\mathsf{env}}}+\xi_{ii'}. \end{aligned} \tag{4.31}$$

$$\implies\quad p(ii') = p(i';i)p(i) = \frac{\mathrm{e}^{-\beta_{\mathsf{sys}}E^{\mathsf{sys}}_i}\mathrm{e}^{-\beta_{\mathsf{env}}E^{\mathsf{env}}_{i'}}}{Z_0^{\mathsf{sys}}Z_0^{\mathsf{env}}}+\langle ii'|\,\hat{C}^0_{\mathsf{se}}\,|ii'\rangle\,. \tag{4.32}$$

The initial state of the system after both measurements is

$$\begin{aligned} \hat{\rho}^0[M:ii'] &= \frac{\hat{P}_{i'}\left[|i\rangle\langle i|\otimes\left(\hat{\rho}^0_{\mathsf{env}}+\langle i|\,\hat{C}^0_{\mathsf{se}}\,|i\rangle\,\frac{1}{q_i^{\mathsf{sys}}(0)}\right)\right]\hat{P}_{i'}}{\mathrm{Tr}_{\mathsf{env}}\left\{\hat{P}_{i'}\left[\hat{\rho}^0_{\mathsf{env}}+\langle i|\,\hat{C}^0_{\mathsf{se}}\,|i\rangle\,\frac{1}{q_i^{\mathsf{sys}}(0)}\right]\right\}} \\ &= \frac{\left\{q^{\mathsf{env}}_{i'}(0)+\langle ii'|\,\hat{C}^0_{\mathsf{se}}\,|ii'\rangle\,\frac{1}{q_i^{\mathsf{sys}}(0)}\right\}|ii'\rangle\langle ii'|}{q^{\mathsf{env}}_{i'}(0)+\langle ii'|\,\hat{C}^0_{\mathsf{se}}\,|ii'\rangle\,\frac{1}{q_i^{\mathsf{sys}}(0)}} = |ii'\rangle\langle ii'|\,, \end{aligned} \tag{4.33}$$

thus we can use the same reasoning as above to find

$$\overline{e^{-\beta_{\mathsf{sys}}\Delta E_{\mathsf{sys}}-\beta_{\mathsf{env}}\Delta E_{\mathsf{env}}}} = \frac{Z_t^{\mathsf{sys}}Z_t^{\mathsf{env}}}{Z_0^{\mathsf{sys}}Z_0^{\mathsf{env}}}+\delta_{\mathsf{corr}} \tag{4.34}$$

with

$$\delta_{\mathsf{corr}} = \sum_{ff',ii'} e^{-\beta_{\mathsf{sys}}E^{\mathsf{sys}}_f}e^{-\beta_{\mathsf{env}}(E^{\mathsf{sys}}_{f'}-E^{\mathsf{sys}}_{i'})}q^{\mathsf{sys}}_f(t)\left(q^{\mathsf{env}}_{f'}(t)+\xi_{ff'}\right)\xi_{ii'}, \tag{4.35}$$

where $\xi_{ii'}$ is defined analogously to $\xi_{ff'}$, cf. Eq. (4.26),

$$\xi_{ii'} = \langle ii'|\,\hat{C}^0_{\mathsf{se}}\,|ii'\rangle\,[q_i^{\mathsf{sys}}(0)]^{-1}\,. \tag{4.36}$$

Due to the additional addend, bilocal EFT fails, in general. It can be easily seen that for a factorizing initial state with $\hat{C}^0_{\mathsf{se}} = 0$ we have $\xi_{ii'} = 0$ and thus $\delta_{\mathsf{corr}} = 0$, reducing Eq. (4.34) to the result of the previous section. Here, it becomes obvious why bilocal EFT generally fails if the initial state is not

factorizing: When the environment is being measured, the probability distribution of the environment differs from that expected for a canonical state due to the additional correlation addend.

Thus, the environment effectively starts in a *non*-canonical state due to measurement induced co-jumps. For such initial states it is not surprising that bilocal EFT fails. Note that interchanging the order of measurement does not avoid this problem, because after first measuring the environment, the system is subsequently found in an effectively non-canonical state.

Note, that bilocal EFT is connected to Crooks' idea of determining the work performed onto the system by correcting the total energy change of the system by the heat flow into the environment [22]. If we take the latter for a heat bath, which is weakly coupled to the system, we expect that the compound state is factorizing. The system and the bath are supposed to start in thermal equilibrium, $\beta_{\mathsf{sys}} = \beta_{\mathsf{env}} \equiv \beta$. Moreover, for the bath we require $\Delta E^{\mathsf{env}}_{f'i'} = \Delta Q^{\mathsf{env}}_{f'i'}$, as only heat flows to the bath. Moreover, the bath is considered to be large so that $Z^{\mathsf{env}}_0 = Z^{\mathsf{env}}_t$. Using these relations, bilocal EFT can be rewritten to give

$$\overline{\mathrm{e}^{-\beta(\Delta E^{\mathsf{sys}}_{fi} + \Delta E^{\mathsf{env}}_{f'i'})}} = \overline{\mathrm{e}^{-\beta(\Delta E^{\mathsf{sys}}_{fi} + \Delta Q^{\mathsf{env}}_{f'i'})}} = \frac{Z^t_{\mathsf{sys}}}{Z^0_{\mathsf{sys}}} = \mathrm{e}^{-\beta \Delta F_{\mathsf{sys}}}, \tag{4.37}$$

which is exactly the idea of Crooks: Measure the energy difference of the system, correct this by the heat flow into the environment and get the equilibrium free energy difference of the bare system by averaging over all trajectories. The trajectories are here substituted by two-time energy measurements.

4.4. Closed quantum systems

Most papers on generalizations of the Jarzynski relation have so far been concerned with externally controlled quantum systems coupled to a macroscopic environment, usually taken for a perfect heat bath. The external driver is also supposed to be a classical one.

However, it is interesting to extend the JR to situations, where only quantum systems are involved, acting as well as drivers and environment. At first glance it might seem somehow surprising that it could be possible to find extensions of the JR in closed quantum systems, but since it is well-known that we can expect thermodynamic behavior of closed quantum systems with an appropriate embedding (cf., e. g. [44]), then why should it not be possible to investigate non-equilibrium fluctuation theorems, also.

Before we can discuss this approach in detail, however, the problem of how to define work and heat in quantum systems has to be investigated. For

the JR it is indispensable to decide whether an energy exchange between the system of interest and its surroundings has to be understood as work or heat, respectively. Here, we will use LEMBAS (**L**ocal **e**ffective **m**easurement **bas**is) in order to distinguish between work and heat [33]. Since this will be essential for our understanding of effective quantum JR, a short introduction to LEMBAS will be given in the first chapter of the following part.

Part II.

Closed quantum systems

5. LEMBAS: Heat and work

In order to investigate the quantum Jarzynski relation for closed quantum systems, we rely on a separation between heat and work within an energy flow. In 2008, LEMBAS [33] was introduced defining local effective energies with respect to a measurement basis. Using the 1st law of thermodynamics, the effective energy flow is then split into heat and work. LEMBAS can be used for quantum systems irrespective of their size and applies even to non-equilibrium situations. It has been formulated for bipartite systems only. Here, we want to investigate situations where several quantum systems are coupled to each other. Then, one has to be careful how the compound system can consistently be partitioned.

For our purpose, the measurement basis will be chosen to coincide with the bare local Hamiltonians of the respective quantum systems if not stated otherwise. The process on the system of interest might be enforced by an external driver or may be a consequence of the local effective dynamics arising from the surroundings of the system. Quite general, it might also be a combination of these two effects. The measurement basis initially chosen will not be changed for the final measurement. The following section is a short overview over LEMBAS [33].

5.1. Heat and work exchange between quantum sub-systems

Here, we will give a short summary of the LEMBAS principle with strict focus on the definitions and general ideas needed for the remainder of this thesis (for details cf. [33]). We consider a bipartite system given by the following Hamiltonian,

$$\hat{H} \equiv \hat{H}_{\mathsf{sys}} + \hat{H}_{\mathsf{env}} + \hat{H}_{\mathsf{se}}. \tag{5.1}$$

As mentioned above, the measurement basis is chosen to coincide with the eigenbasis of the bare local Hamiltonian, $\hat{H}_{\mathsf{sys}}$, say. The effective dynamics of the system is given by

$$\dot{\hat{\rho}}_{\mathsf{sys}} = -\mathrm{i}[\hat{H}_{\mathsf{sys}} + \hat{H}^{\mathsf{eff}}_{\mathsf{sys}}, \hat{\rho}_{\mathsf{sys}}] + \mathcal{L}_{\mathsf{inc}}(\hat{\rho}), \tag{5.2}$$

with the effective Hamiltonian

$$\hat{H}^{\mathsf{eff}}_{\mathsf{sys}} = \mathrm{Tr}\left(\hat{H}_{\mathsf{se}}\hat{1}_{\mathsf{sys}} \otimes \hat{\rho}_{\mathsf{env}}\right). \tag{5.3}$$

Now, the effective Hamiltonian is split into two parts according to

$$\hat{H}^{\mathsf{eff}}_{\mathsf{sys}} = \hat{H}^{\mathsf{eff},1}_{\mathsf{sys}} + \hat{H}^{\mathsf{eff},2}_{\mathsf{sys}}, \text{ with } [\hat{H}_{\mathsf{sys}}, \hat{H}^{\mathsf{eff},1}_{\mathsf{sys}}] = 0,\ [\hat{H}_{\mathsf{sys}}, \hat{H}^{\mathsf{eff},2}_{\mathsf{sys}}] \neq 0. \tag{5.4}$$

The part of the effective Hamiltonian, $\hat{H}^{\mathsf{eff},1}$, which commutes with the local bare Hamiltonian and thus the measurement basis, has to be taken into account for the local effective energy, giving

$$\hat{H}'_{\mathsf{sys}} = \hat{H}_{\mathsf{sys}} + \hat{H}^{\mathsf{eff},1}_{\mathsf{sys}}. \tag{5.5}$$

Therefore from this point of view, the effective internal energy is given by

$$U_{\mathsf{sys}} \equiv \mathrm{Tr}\left(\hat{H}'_{\mathsf{sys}}\hat{\rho}_{\mathsf{sys}}\right). \tag{5.6}$$

The general idea is now as follows: Energy exchange accompanied by a change of the local von-Neumann entropy is considered to be heat, whereas energy exchange without changing the von-Neumann entropy is considered to be work. Investigating the total differential of the local effective internal energy using the local dynamics, Eq. (5.2), one then gets

$$đW_{\mathsf{sys}} = \mathrm{Tr}\left\{\dot{\hat{H}}^{\mathsf{eff},1}_{\mathsf{sys}}\hat{\rho}_{\mathsf{sys}} - \mathrm{i}[\hat{H}'_{\mathsf{sys}}, \hat{H}^{\mathsf{eff},2}_{\mathsf{sys}}]\hat{\rho}_{\mathsf{sys}}\right\}\mathrm{d}t \tag{5.7}$$

$$đQ_{\mathsf{sys}} = -\mathrm{i}\,\mathrm{Tr}\left\{(\hat{H}'_{\mathsf{sys}} \otimes \hat{1}_{\mathsf{env}})[\hat{H}_{\mathsf{se}}, \hat{C}_{\mathsf{se}}]\right\}\mathrm{d}t. \tag{5.8}$$

Here, the correlation operator is defined as above,

$$\hat{C}_{\mathsf{se}} = \hat{\rho} - \hat{\rho}_{\mathsf{sys}} \otimes \hat{\rho}_{\mathsf{env}}. \tag{5.9}$$

With these definitions we can now look for quantum systems which act as work or heat sources for other quantum systems. The functionality will not only depend on the system itself but also on the interaction between the respective systems. Also, the functionality of a quantum system may depend on its surroundings.

For further reference, we will split the work into three addends:

$$đW^{(1)}_{\mathsf{sys}}(t) = \mathrm{Tr}\left\{\dot{\hat{H}}^{\mathsf{eff},1}_{\mathsf{sys}}(t)\hat{\rho}_{\mathsf{sys}}(t)\right\}\mathrm{d}t, \tag{5.10}$$

$$đW^{(2)}_{\mathsf{sys}}(t) = -\mathrm{i}\,\mathrm{Tr}\left\{[\hat{H}_{\mathsf{sys}}, \hat{H}^{\mathsf{eff},2}_{\mathsf{sys}}(t)]\hat{\rho}_{\mathsf{sys}}(t)\right\}\mathrm{d}t, \tag{5.11}$$

$$đW^{(3)}_{\mathsf{sys}}(t) = -\mathrm{i}\,\mathrm{Tr}\left\{[\hat{H}^{\mathsf{eff},1}_{\mathsf{sys}}, \hat{H}^{\mathsf{eff},2}_{\mathsf{sys}}(t)]\hat{\rho}_{\mathsf{sys}}(t)\right\}\mathrm{d}t. \tag{5.12}$$

Similarly, we will consider the following two addends for the heat

$$đQ^{(1)}_{\mathsf{sys}}(t) = -\mathrm{i}\,\mathrm{Tr}\left\{(\hat{H}_{\mathsf{sys}} \otimes \hat{1}_{\mathsf{env}})[\hat{H}_{\mathsf{se}}, \hat{C}_{\mathsf{se}}(t)]\right\} \mathrm{d}t, \tag{5.13}$$

$$đQ^{(2)}_{\mathsf{sys}}(t) = -\mathrm{i}\,\mathrm{Tr}\left\{(\hat{H}^{\mathsf{eff},1}_{\mathsf{sys}}(t) \otimes \hat{1}_{\mathsf{env}})[\hat{H}_{\mathsf{se}}, \hat{C}_{\mathsf{se}}(t)]\right\} \mathrm{d}t. \tag{5.14}$$

5.2. Perfect driver

If we want to generalize the JR to closed quantum systems without an external work source, we need a quantum system, which effectively acts as a work source on the system of interest. The system acting as a work source will be called a driver. For our purpose, a perfect driver should fulfill the following conditions:

1. When the driver is coupled to a system, the system should only receive work from the driver, $đQ_{\mathsf{sys}} = 0$.
2. The work protocol enforced by the driver should be independent of the state of the system (SID, *state-independent driving*) [1].
3. The work flow out of the driver should reach the system without any losses, $đW_{\mathsf{dr}} = đW_{\mathsf{sys}}$.
4. The driver itself should also receive only work, $đQ_{\mathsf{dr}} = 0$.

Note, that point 3 and 4 are not trivial since the separation of energy into heat and work might be non-symmetric for both systems. This can be easily understood especially for non-symmetric interactions and non-factorizing states or non-negligible interaction energy. For our purpose we might relax condition 2 a bit: We are mostly interested in an independent driving protocol with respect to the effective Hamiltonian of the driven system, especially in $\hat{H}^{\mathsf{eff},1}_{\mathsf{sys}}$. An effectively driving system already investigated in [31] will be studied with focus on fluctuation theorems in Chap. 6. Chap. 7 will deal with a different driving system, which comes closer to being a perfect driver and more suitable for numerically complex investigations.

5.3. Perfect heat source

For our purpose, we define a perfect heat source as follows:

1. The energy flow from the heat source should be solely heat.

[1] Note, that the effect of the driver may well depend on the state of the driver itself.

2. The energy flow out of the source should only be heat.

3. The heat should be exchanged without any losses, thus we should have that $đQ_{\mathsf{sys}} = đQ_{\mathsf{env}}$.

Note, that these requirements are less restrictive than for a perfect heat bath, where one usually requires that the system relaxes to a thermal state of definite temperature.

An example for a perfect heat source will be studied in Chap. 8.

5.3.1. Thermalizing environments

For the quantum model involving thermalization, cf. Chap. 14, we will be interested in quantum environments which enforce a thermal state of the system of interest. There have already been several studies concerning such setups, cf. [43, 44]. A LEMBAS study of such a typical setup reveals that the coupling via complex Gaussian distributed random hermitian matrices gives rise to both work and heat flows (cf. 5.3.2). This would lead to difficulties when discussing JR and EFT for a quantum system coupled to such a thermalizing environment, as it is usually preferable to have one work source only, which moreover should be clearly separated from the environment.

From our studies on the perfect heat source, cf. Chap. 8, one can already guess that a different kind of coupling would lead to pure heat flow for a special class of system states. Closely related studies to [43] use a slightly different interaction [42]. Under a related but different point of view [60], there has also been discussed a coupling similar to the one we use in Chap. 8 that seems indeed promising for our purpose. In the following, we will numerically discuss two examples.

5.3.2. Numerical study of thermalizing environments

We investigate a spin coupled to an environment (cf. Fig. 14.1 without the driver),

$$\hat{H} \equiv \frac{\omega_{\mathrm{sp}}}{2}\hat{\sigma}_z \otimes \hat{1}_{\mathsf{env}} + \hat{1}_{\mathsf{sys}} \otimes \sum_{i=0}^{2}\sum_{j=1}^{N_j}(E_i^{\mathsf{env}} + \varepsilon_j)\,|\phi(i,j)\rangle\langle\phi(i,j)| + \hat{H}_{\mathsf{se}}. \quad (5.15)$$

Here, E_i^{env} denote the energy of a j-fold degenerate energy-eigenstate $|\phi(i,j)\rangle$, and $\varepsilon_j \ll E_i^{\mathsf{env}}$ small randomly chosen additional energy addends, lifting degeneracy. Thus, the environment is modeled as three energy bands[2] which

[2] by bands we mean an accumulation of densely spaced energy levels.

are separated by an energy difference resonant to the splitting of the spin, $\omega_{\mathrm{sp}} = 1$, thus $E^{\mathsf{env}}_{i+1} - E^{\mathsf{env}}_{i} = 1$. For this setup it is known that a total of about $N = 200$ states of the environment give already nice results with respect to thermalization for suitable couplings $\hat{H}_{\mathsf{se}}$ [43]. As the numerical effort grows rapidly with N while thermalization does not improve significantly, we choose the total number of environment states to $N \approx 200$. The number of levels in the three energy bands are chosen such that we expect a final inverse temperature of the spin $\beta^{\mathsf{goal}}_{\mathsf{sp}} = 1.75$ (for details on the degeneracy structure of the environment and the respective expected temperature cf. [44] and [43]). For our numerics, we prepare the spin in the ground state and the environment in the middle energy band, distributed equally over the almost degenerate energy levels. Then, we solve the Schrödinger equation by exact diagonalization.

We choose two different couplings $\hat{H}_{\mathsf{se}}$, one of which should lead to pure heat exchange between the spin and the environment, as generally expected from a thermalizing environment.

Random coupling on total Hilbert space

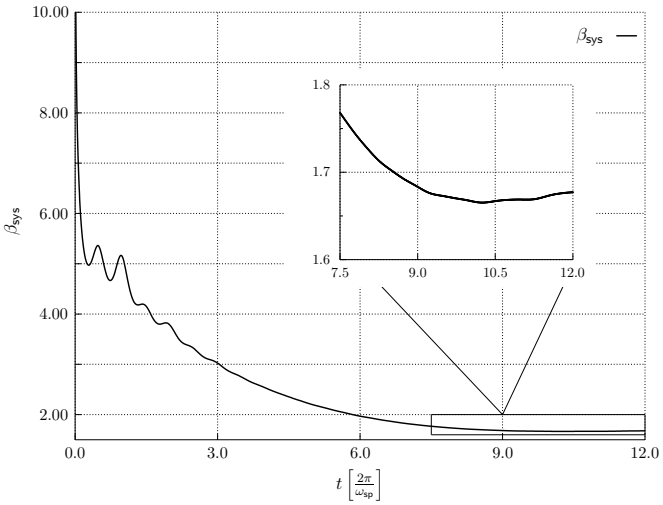

Figure 5.1.: Inverse temperature of the spin (system), β_{sys}, over time t. The inset shows the region between $t = 7.5$ and $t = 12.0$.

We start by choosing $\hat{H}_{\mathsf{se}} = \hat{G}$ in Eq. (5.15), with $\hat{G}$ being a complex Gaussian distributed Hermitian matrix with zero mean [43]. The spin is prepared in the ground state, initially. Fig. 5.1 shows the inverse temperature of the

system. As can be seen, the system does not relax to $\beta_{\mathsf{sp}}^{\mathsf{goal}}$, but rather to an inverse temperature of about 1.67. This is due to the fact that we have relatively few energy levels in the environment. The energy flow, separated into heat and work, can be found in Figs. 5.2 and 5.3, respectively. The environment thus acts as a combination of both heat and work source. Moreover, neither the heat nor the work adds up to zero. The closer to thermalization, the less energy is being exchanged. Even though most of the exchanged energy is attributed to heat, according to LEMBAS, we have a non-negligible portion of energy of about 10% of the total energy being transfered as work between the systems. Thus, none of our conditions on a perfect heat source are strictly fulfilled, here.

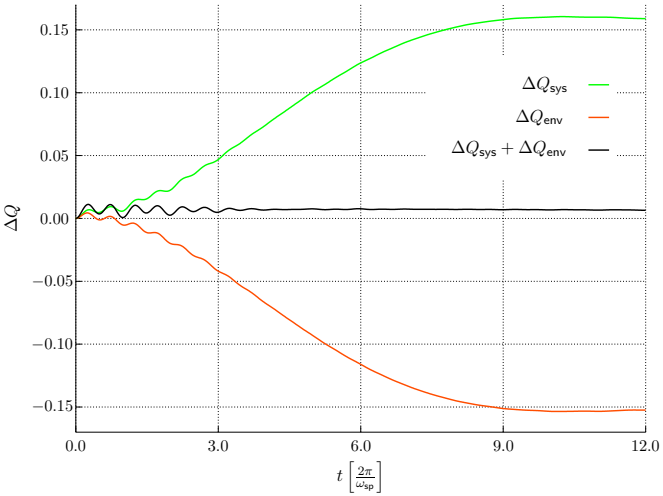

Figure 5.2.: Heat flows into system, ΔQ_{sys}, and into the environment, ΔQ_{env}, as well as $\Delta Q_{\mathsf{sys}} + \Delta Q_{\mathsf{env}}$ over time t.

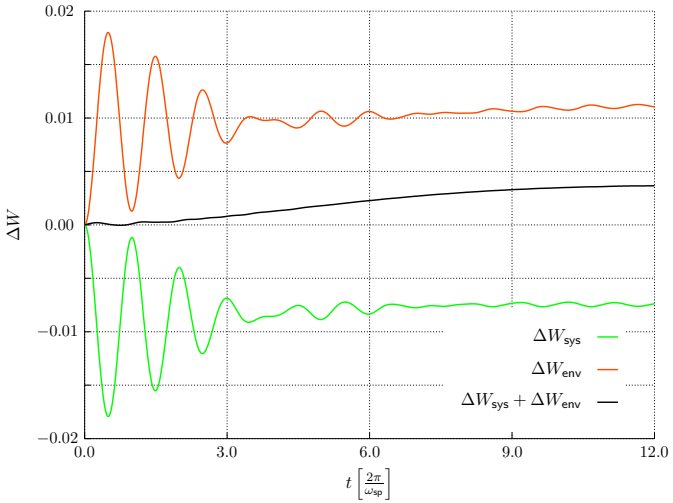

Figure 5.3.: Work exchange between system, ΔW_{sys}, and environment, ΔW_{env}, as well as $\Delta W_{\mathsf{sys}} + \Delta W_{\mathsf{env}}$ over time t.

Random coupling on environmental Hilbert space

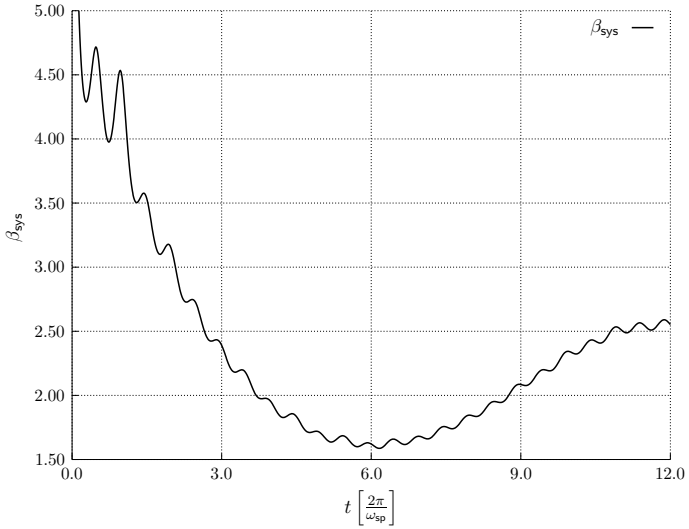

Figure 5.4.: Inverse temperature of the system, β_{sys}, over time t.

Now, we take the same model as in the previous paragraph, given by Eq. (5.15). Here, we consider a different coupling, $\hat{H}_{\mathsf{se}} = \hat{\sigma}_x \otimes \hat{G}$, with a Gaussian random Hermitian operator on the Hilbert space of the environment, $\hat{G}$. We use the same method as before in order to *normalize* the random matrix. Fig. 5.4 shows that with this parameter set, the relaxation takes longer than for the coupling discussed in the previous section. Therefore, when we want to use this coupling, we have to either increase the coupling strength, the size of the environment or let the system evolve for a longer time. The heat flows do not compensate each other as for the coupling discussed in the previous section (cf. Fig. 5.5) and the absolute of the total heat flows are approximately the same. As expected, Fig. 5.6 shows that the total work exchange is negligibly small, of about the same order as the numerical accuracy. Therefore, although condition 3 is not fulfilled, the other two conditions of a perfect heat source are.

Therefore, if we want to discuss a thermalizing environment as a perfect heat source, we have to choose the coupling carefully.

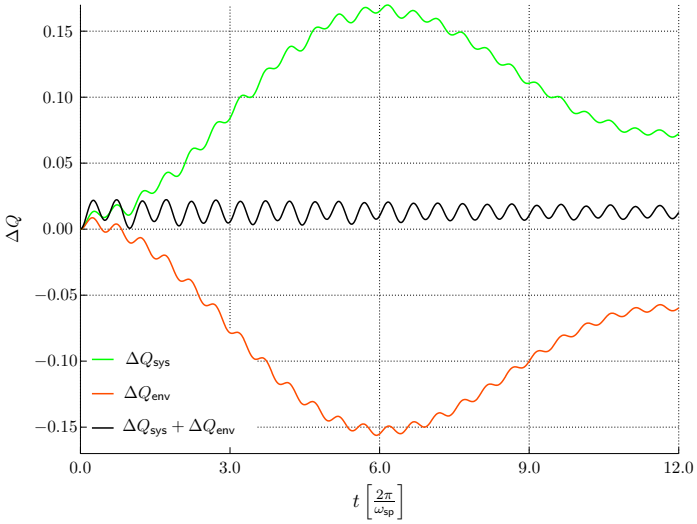

Figure 5.5.: Heat flows ΔQ_{sys} and ΔQ_{env} as well as $\Delta Q_{\mathsf{sys}} + \Delta Q_{\mathsf{env}}$ over t.

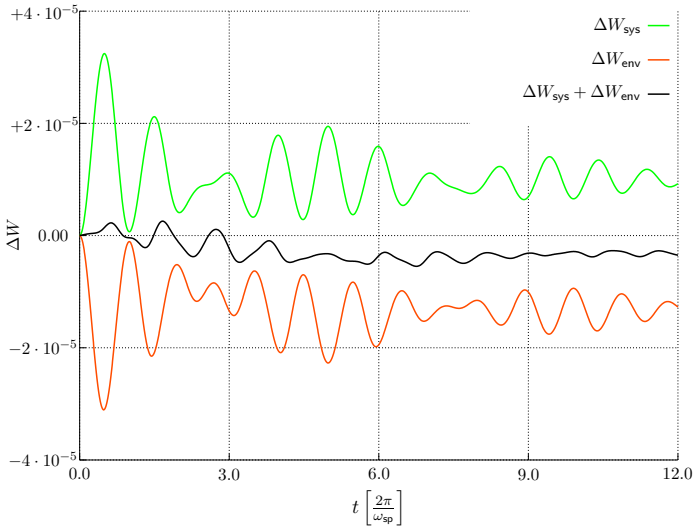

Figure 5.6.: Work exchange ΔW_{sys} and ΔW_{env} as well as $\Delta W_{\mathsf{sys}} + \Delta W_{\mathsf{env}}$ over t.

6. Spin-Oscillator model (SOM): Work

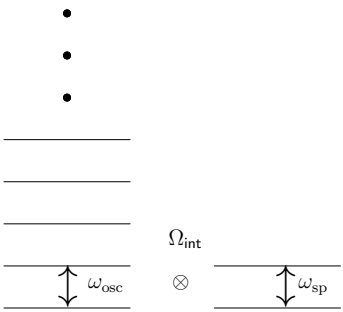

Figure 6.1.: Spin oscillator model: SOM. A spin with Zeeman-splitting ω_{sp} is coupled to a harmonic oscillator (frequency ω_{osc}) with coupling strength Ω_{int}. The dots indicate that the spectrum of the oscillator is unbounded.

In [31] it is shown, that a harmonic oscillator prepared in a coherent state $|\alpha\rangle\langle\alpha|$, coupled to a spin in an adequate way, can be considered an effective driving system. This model has been called SOM (*spin oscillator model*), cf. Fig. 6.1. Here, we are interested whether the oscillator of SOM can be considered as a perfect driver also in the sense of conditions 1-4 (Sec. 5.2).

Focusing on a special class of interactions, z-SOM, where z refers to the following distinct coupling, (cf. [31]), the Hamiltonian reads,

$$\hat{H}_{\mathsf{SOM}} \equiv \frac{\omega_{\mathrm{sp}}}{2}\hat{\sigma}_z \otimes \hat{1}_{\mathsf{osc}} + \hat{1}_{\mathsf{sp}} \otimes \omega_{\mathrm{osc}}(\hat{a}^\dagger\hat{a} + \frac{1}{2}\hat{1}_{\mathsf{osc}}) + \Omega_{\mathrm{int}}\hat{\sigma}_z \otimes \hat{X}. \tag{6.1}$$

The eigenstates of the local Hamiltonian of the spin, $\hat{H}_{\mathsf{sp}}$, are $|0\rangle$ and $|1\rangle$ with the respective eigenvalues $\mp\frac{\omega_{\mathrm{sp}}}{2}$. The local Hamiltonian of the oscillator will be denoted by $\hat{H}_{\mathsf{osc}}$, and the interaction Hamiltonian by $\hat{H}_{\mathsf{int}}$.

6.1. Effective description of the spin

We start by investigating the spin. The local measurement basis is chosen to coincide with the bare Hamiltonian of the spin, $\hat{H}_{\mathsf{sp}}$. Then we find for the effective Hamiltonian

$$\hat{H}^{\mathsf{eff}}_{\mathsf{sp}}(t) = \mathrm{Tr}_{\mathsf{env}}\left\{\Omega_{\mathrm{int}}\hat{\sigma}_z \otimes \hat{X}[1_{\mathsf{sys}} \otimes \hat{\rho}_{\mathsf{env}}(t)]\right\} = \Omega_{\mathrm{int}}\hat{\sigma}_z \mathrm{Tr}_{\mathsf{env}}\left\{\hat{X}\hat{\rho}_{\mathsf{env}}(t)\right\}. \quad (6.2)$$

Obviously, $[\hat{H}^{\mathsf{eff}}_{\mathsf{sp}}(t), \hat{H}_{\mathsf{sp}}] = 0$ and therefore we have

$$\hat{H}^{\mathsf{eff},1}_{\mathsf{sp}}(t) = \hat{H}^{\mathsf{eff}}_{\mathsf{sp}}(t) \;\text{ as }\; \hat{H}^{\mathsf{eff},2}_{\mathsf{sp}}(t) = 0. \quad (6.3)$$

Moreover, we immediately find

$$\hat{H}'_{\mathsf{sp}}(t) = \hat{H}_{\mathsf{sp}} + \hat{H}^{\mathsf{eff}}_{\mathsf{sp}}(t) = \frac{\omega_{\mathrm{sp}}}{2}\hat{\sigma}_z + \Omega_{\mathrm{int}}\hat{\sigma}_z\langle\hat{X}\rangle_{\hat{\rho}_{\mathsf{env}}(t)}, \quad (6.4)$$

with $\langle\hat{X}\rangle_{\hat{\rho}_{\mathsf{env}}(t)} = \mathrm{Tr}_{\mathsf{env}}\left\{\hat{X}\hat{\rho}_{\mathsf{env}}(t)\right\}$ denoting the expectation value of the position operator of the oscillator at time t.

First we determine the heat flow into the spin (cf. Eq. (5.8))

$$\begin{aligned} đQ_{\mathsf{sp}} &= -\mathrm{i}\,\mathrm{Tr}\left\{\hat{H}'_{\mathsf{sp}}(t)[\hat{H}_{\mathsf{int}}, \hat{C}_{\mathsf{sposc}}(t)]\right\}\mathrm{d}t \\ &= -\mathrm{i}\,\mathrm{Tr}\left\{\left(\frac{\omega_{\mathrm{sp}}}{2} + \Omega_{\mathrm{int}}\langle\hat{X}\rangle_{\hat{\rho}_{\mathsf{env}}(t)}\right)\hat{\sigma}_z[\Omega_{\mathrm{int}}\hat{\sigma}_z \otimes \hat{X}, \hat{C}_{\mathsf{sposc}}(t)]\right\}\mathrm{d}t \\ &= 0, \end{aligned} \quad (6.5)$$

where we have used the cyclic property of the trace and the fact that trivially $[\hat{\sigma}_z, \hat{\sigma}_z] = 0$. More general, we note that here we have $[\hat{H}'_{\mathsf{sp}}(t), \hat{H}_{\mathsf{int}}] = 0$. From this we can infer that condition 1 from Sec. 5.2 on a perfect work source is fulfilled.

Second, we calculate the work performed on the spin. From Eq. (5.7) we get

$$đW_{\mathsf{sp}} = \mathrm{Tr}\left\{\dot{\hat{H}}^{\mathsf{eff},1}_{\mathsf{sp}}(t)\hat{\rho}_{\mathsf{sp}}(t) - \mathrm{i}[\hat{H}'_{\mathsf{sys}}(t), \hat{H}^{\mathsf{eff},2}_{\mathsf{sp}}(t)]\hat{\rho}_{\mathsf{sp}}(t)\right\}\mathrm{d}t. \quad (6.6)$$

The second addend vanishes due to $\hat{H}^{\mathsf{eff},2}_{\mathsf{sp}}(t) = 0$, and by using Eq. (6.2),

$$\begin{aligned} đW_{\mathsf{sp}} &= \Omega_{\mathrm{int}}\frac{\mathrm{d}}{\mathrm{d}t}\left(\langle\hat{X}\rangle_{\hat{\rho}_{\mathsf{env}}(t)}\right)\mathrm{Tr}\left\{\hat{\sigma}_z\hat{\rho}_{\mathsf{sp}}(t)\right\}\mathrm{d}t \\ &= \Omega_{\mathrm{int}}\langle\hat{\sigma}_z\rangle_{\hat{\rho}_{\mathsf{sp}}(t)}\frac{\mathrm{d}}{\mathrm{d}t}\langle\hat{X}\rangle_{\hat{\rho}_{\mathsf{env}}(t)}. \end{aligned} \quad (6.7)$$

6.2. Effective description of the oscillator

In order to check the other conditions, we investigate the driver. The effective Hamiltonian reads

$$\hat{H}^{\mathsf{eff}}_{\mathsf{osc}}(t) = \mathrm{Tr}_{\mathsf{sp}}\left\{\hat{H}_{\mathsf{int}}\left(\hat{\rho}_{\mathsf{sp}}(t)\otimes\hat{1}_{\mathsf{osc}}\right)\right\} = \Omega_{\mathrm{int}}\hat{X}\,\mathrm{Tr}_{\mathsf{sp}}\left\{\hat{\sigma}_z\hat{\rho}_{\mathsf{sp}}(t)\right\}. \tag{6.8}$$

As we have $[\hat{H}_{\mathsf{osc}}, \hat{H}^{\mathsf{eff}}_{\mathsf{osc}}] \neq 0$ as long as $\mathrm{Tr}_{\mathsf{sp}}\{\hat{\sigma}_z\hat{\rho}_{\mathsf{sp}}(t)\} \neq 0$, we find

$$\hat{H}^{\mathsf{eff},1}_{\mathsf{osc}}(t) = 0 \;\text{ and }\; \hat{H}^{\mathsf{eff},2}_{\mathsf{osc}} = \hat{H}^{\mathsf{eff}}_{\mathsf{osc}}(t) = \Omega_{\mathrm{int}}\hat{X}\langle\hat{\sigma}_z\rangle_{\hat{\rho}_{\mathsf{sp}}(t)}. \tag{6.9}$$

Thus, we immediately have

$$\hat{H}'_{\mathsf{osc}} = \hat{H}_{\mathsf{osc}}. \tag{6.10}$$

With this, we get for the heat flow

$$\begin{aligned} đQ_{\mathsf{osc}} &= \mathrm{Tr}\left\{\hat{H}_{\mathsf{osc}}[\hat{H}_{\mathsf{int}}, \hat{C}_{\mathsf{sposc}}(t)]\right\}\mathrm{d}t \\ &= \omega_{\mathrm{osc}}\Omega_{\mathrm{int}}\,\mathrm{Tr}\left\{(\hat{a}^\dagger\hat{a}\otimes\hat{1}_{\mathsf{osc}})[\hat{\sigma}_z\otimes\hat{X}, \hat{C}_{\mathsf{sposc}}(t)]\right\} \neq 0, \end{aligned} \tag{6.11}$$

in general. Here, we have used that $\hat{1}_{\mathsf{osc}}$ trivially commutes with any operator and that $\hat{X}\hat{C}_{\mathsf{sposc}}$ is a bounded operator which allows the use of the cyclic property of the trace. Thus, condition 4 is violated, generally. However, as we are interested in the JR later on, we can assume that the spin has initially been measured, thus the spin is initially in an energy-eigenstate after the projective measurement. For the purity one has according to [31],

$$P_{\mathsf{osc}}(t) \propto c^2 + (1-c)^2 + 2c(1-c), \tag{6.12}$$

with c being the probability that the spin, initially in a diagonal state in the energy-eigenbasis, is in the ground state. From this, we can immediately infer that for our case, where $c = 1$ or $c = 0$ after the measurement, that

$$P_{\mathsf{osc}}(t) = 1 \;\forall\; t. \tag{6.13}$$

As the von-Neumann entropy remains zero for the oscillator, we know that for these two initial states, the heat flow into the oscillator vanishes.

This can be understood easily when considering the dynamics for the special initial state. The oscillator and the spin after the measurement both start in a pure state. The spin remains in a pure state throughout the dynamics as $\hat{U}(t) = \mathrm{e}^{-\mathrm{i}\hat{H}_{\mathsf{SOM}}t}$ and $[\hat{U}(t), \hat{\rho}_{\mathsf{sys}}(M:i)] = 0$. As both subsystems start in a

pure state, so does the compound system. Moreover, the compound system evolves unitarily, thus it does remain in a pure state. So, at any time the compound system and the spin are in a pure state from which necessarily follows that the oscillator is in a pure state, too [25]. Thus, the above result does not come as a surprise.

Next, we turn to the work performed by the oscillator. We find

$$đW_{\mathsf{osc}} = -\mathrm{i}\,\mathrm{Tr}\left\{[\hat{H}_{\mathsf{osc}}, \hat{H}^{\mathsf{eff}}_{\mathsf{osc}}(t)]\hat{\rho}_{\mathsf{osc}}(t)\right\}\mathrm{d}t, \tag{6.14}$$

where we have used that from $\hat{H}^{\mathsf{eff},1}_{\mathsf{osc}}(t) = 0\ \forall\ t$ directly follows that the first addend of Eq. (5.7) vanishes and that $\hat{H}^{\mathsf{eff},2}_{\mathsf{osc}}(t) = \hat{H}^{\mathsf{eff}}_{\mathsf{osc}}(t)$. Using Eq. (6.8) we find

$$đW_{\mathsf{osc}} = -\mathrm{i}\Omega_{\mathrm{int}}\,\mathrm{Tr}\left\{[\hat{H}_{\mathsf{osc}}, \hat{X}]\hat{\rho}_{\mathsf{osc}}(t)\right\}\langle\hat{\sigma}_z\rangle_{\hat{\rho}_{\mathsf{sp}}(t)}\mathrm{d}t. \tag{6.15}$$

We note that $[\hat{H}_{\mathsf{int}}, \hat{X}] \propto [\hat{X}, \hat{X}] = 0$ and that trivially $[\hat{H}_{\mathsf{sp}}, \hat{X}] = 0$, as they are acting on different subspaces of the total Hilbert space. We can thus rewrite the expression for the work as

$$đW_{\mathsf{osc}} = -\mathrm{i}\Omega_{\mathrm{int}}\,\mathrm{Tr}\left\{[\hat{H}_{\mathsf{osc}} + \hat{H}_{\mathsf{int}} + \hat{H}_{\mathsf{sp}}, \hat{X}]\hat{\rho}_{\mathsf{osc}}(t)\right\}\langle\hat{\sigma}_z\rangle_{\hat{\rho}_{\mathsf{sp}}(t)}\mathrm{d}t. \tag{6.16}$$

As $\hat{X}\hat{\rho}_{\mathsf{osc}}(t)$ as well as $\hat{\rho}_{\mathsf{osc}}$ alone are bounded operators, we can use the cyclic property of the trace to get

$$\begin{aligned} đW_{\mathsf{osc}} &= -\mathrm{i}\Omega_{\mathrm{int}}\,\mathrm{Tr}\left\{[\hat{\rho}_{\mathsf{osc}}(t), \hat{H}_{\mathsf{SOM}}]\hat{X}\right\}\langle\hat{\sigma}_z\rangle_{\hat{\rho}_{\mathsf{sp}}(t)}\mathrm{d}t \\ &= -\Omega_{\mathrm{int}}\,\mathrm{Tr}\left\{\dot{\hat{\rho}}_{\mathsf{osc}}(t)\hat{X}\right\}\langle\hat{\sigma}_z\rangle_{\hat{\rho}_{\mathsf{sp}}(t)}\mathrm{d}t \\ &= -\Omega_{\mathrm{int}}\langle\hat{\sigma}_z\rangle_{\hat{\rho}_{\mathsf{sp}}(t)}\frac{\mathrm{d}}{\mathrm{d}t}\langle\hat{X}\rangle_{\hat{\rho}_{\mathsf{osc}}(t)}\mathrm{d}t. \end{aligned} \tag{6.17}$$

In the first step we have used the von-Neumann equation. Comparison with Eq. (6.7) gives

$$đW_{\mathsf{osc}} = -đW_{\mathsf{sp}}, \tag{6.18}$$

so that condition 3, Sec. 5.2, is satisfied.

Since the equations of motion of the oscillator depend on the state of the spin, and as the effective splitting of the spin is directly controlled by the state of the oscillator, we do *not* expect state-independent driving. Indeed, an analytical treatment of SOM shows that the peak-to-peak amplitude of the effective splitting depends on the system parameters and especially on the

initial state of the spin (cf. [31], Sec. VI and appendix C). In summary, we have shown analytically that conditions 1 and 3 hold, whereas condition 4 only holds for the discussed initial states. According to [31] condition 2, Sec. 5.2, fails.

However, the state-dependency of the driver can be influenced by a proper choice of parameters. For large α and mass m of the oscillator, the state-dependency is reduced, while the effect of the oscillator as a work source is almost not influenced if one keeps the ratio $\frac{|\alpha|^2}{m}$ constant (for details, cf. [31]). However, increasing α leads to higher numerical effort, since one has to take more levels of the oscillator into account to keep the error from the cut-off of the spectrum of the oscillator small.

6.3. Numerics

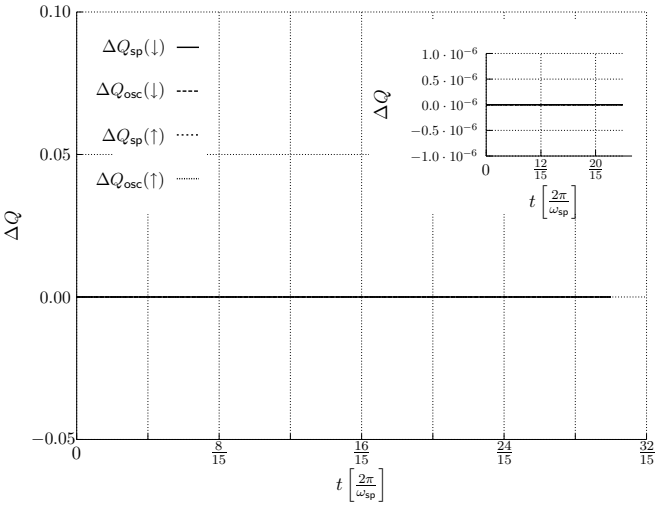

Figure 6.2.: ΔQ_{sys} and ΔQ_{dr} for both, $\hat{\rho}^0_{\mathsf{sys}} = |\downarrow\rangle\langle\downarrow|$ and $\hat{\rho}^0_{\mathsf{sys}} = |\uparrow\rangle\langle\uparrow|$. The heat flows vanish during all process times t considered.

Here, we present numerical results for the system described in the preceding sections. We start by preparing the oscillator in a coherent and the spin in a thermal state, respectively. Then, the spin is projected into an energy-eigenstate with the corresponding probability. We choose $\omega_{\mathrm{osc}} = \omega_{\mathrm{sp}} = 1$, $\Omega_{\mathrm{int}} = -0.2$, $m = 45$, $\alpha = 3$ and the inverse temperature of the spin

$\beta_{\mathsf{sp}}^{\mathsf{eff}} = 0.85$. In the following, the spin will be called system and the oscillator driver, respectively. Note that the system temperature is given with respect to $\hat{H}'_{\mathsf{sys}}(0)$. For the initial state of the system after the measurement we will use the short-hand notation $\downarrow$ and $\uparrow$ if the system has been projected into the ground state or the excited one, respectively.

The heat flow into the system and the driver can be found in Fig. 6.2 for both, $\hat{\rho}_{\mathsf{sys}}^0 = |\downarrow\rangle\langle\downarrow|$ and $\hat{\rho}_{\mathsf{sys}}^0 = |\uparrow\rangle\langle\uparrow|$. Note that the heat flow is zero at any time t. The larger scale for the y-axis was chosen for better comparison with the work exchange, the scale of the inset was chosen in order to show that the heat flows do indeed vanish within numerical accuracy. This confirms the findings from Secs. 6.1 and 6.2 for the heat flows. Thus we have numerically confirmed that conditions 1 and 4 are fulfilled. This result remains valid for arbitrarily long process times.

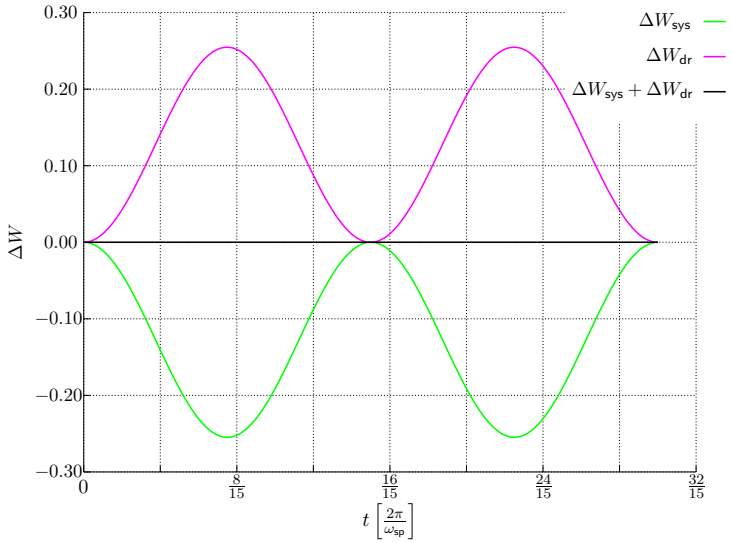

Figure 6.3.: ΔW_{sys} and ΔW_{dr} as well as their sum (black line) for $\hat{\rho}_{\mathsf{sys}}^0 = |\downarrow\rangle\langle\downarrow|$ over process time t.

Next, we turn to the work exerted on the system. The results for $\hat{\rho}_{\mathsf{sys}}^0 = |\downarrow\rangle\langle\downarrow|$ and $\hat{\rho}_{\mathsf{sys}}^0 = |\uparrow\rangle\langle\uparrow|$ can be found in Figs. 6.3 and 6.4, respectively. The direction of work exchange depends on the initial state of the system. If the system has been projected into the ground state, the oscillator receives energy from the spin, thus the spin works on the oscillator and vice versa for the excited state. Moreover, these two figures suggest that we have, indeed,

a perfect work transfer as it seems that the work performed by the driver is completely absorbed by the system. This impression is indeed confirmed by the sum $\Delta W_{\mathsf{sys}} + \Delta W_{\mathsf{osc}}$ (black line in Figs. 6.3 and 6.4). Within numerical accuracy this sum vanishes, confirming our discussion at the end of Sec. 6.2. Thus, condition 3 is verified numerically.

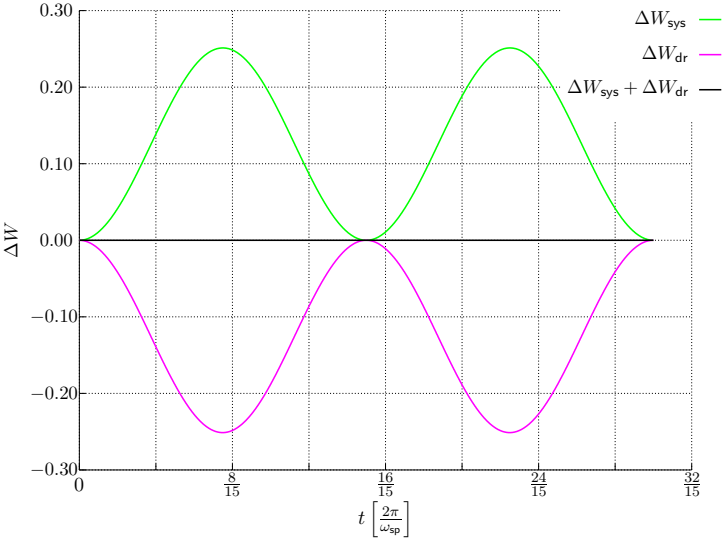

Figure 6.4.: ΔW_{sys} and ΔW_{dr} as well as their sum (black line) for $\hat{\rho}^0_{\mathsf{sys}} = |\uparrow\rangle\langle\uparrow|$ over process time t.

Next, we turn to the state-dependency of the driver. Here, we are especially interested in the effective Hamiltonian of the system, more precisely in $\hat{H}'_{\mathsf{sys}}(t)$. This effective Hamiltonian does generally depend on the state of the driver, whose state is also influenced by the state of the system itself. The back-action may lead to state-dependent driving, which we do indeed expect according to our discussion in Sec. 6.2. As we are interested in the JR, we do not consider the effective Hamiltonian of the system directly, but the effective partition sum, given by

$$Z^{\mathsf{eff}}_{\mathsf{sys}} = \mathrm{Tr}\left\{ \mathrm{e}^{-\beta^{\mathsf{eff}}_{\mathsf{sys}} \hat{H}'_{\mathsf{sys}}} \right\}. \tag{6.19}$$

In Fig. 6.5 the effective partition sum is depicted for two different initial states. It is obvious that both cases nearly coincide which shows that we have almost no state-dependent driving, here. From the discussion at the end of Sec. 6.2, we know that state-dependent driving can be influenced by changing α and

m of the oscillator. Keeping the ratio $\frac{\alpha^2}{m}$ constant, the actual driving of the oscillator should also not change. With the definition of the relative deviation of the partition sum for $\hat{\rho}^0_{\mathsf{sys}} = |\uparrow\rangle\langle\uparrow|$ from $\hat{\rho}^0_{\mathsf{sys}} = |\downarrow\rangle\langle\downarrow|$,

$$\delta_{\mathsf{rel}} Z^{\mathsf{eff}}_{\mathsf{sys}}[\uparrow;\downarrow] \equiv \frac{Z^{\mathsf{eff}}_{\mathsf{sys}}(\downarrow) - Z^{\mathsf{eff}}_{\mathsf{sys}}(\uparrow)}{Z^{\mathsf{eff}}_{\mathsf{sys}}(\downarrow)}, \tag{6.20}$$

where the argument of the partition sum refers to the initial state of the system. Fig. 6.6 shows the deviation for three different parameter sets for the oscillator. As expected, the relative deviation gets smaller the larger α and m, thus the state-dependency is reduced for larger oscillator masses m. For $m = 5$ the maximal relative deviation is about 1%, while for $m = 45$ it is less than 2‰.

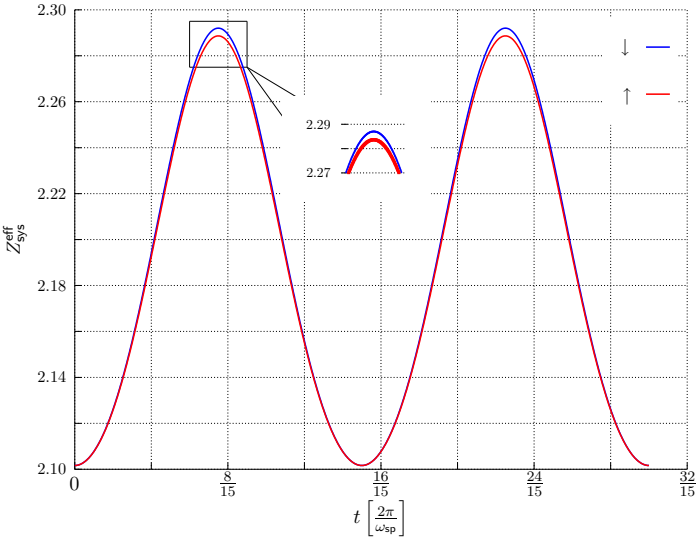

Figure 6.5.: Effective partition sum $Z^{\mathsf{eff}}_{\mathsf{sys}}(t)$ over t for $\hat{\rho}^0_{\mathsf{sys}} = |\downarrow\rangle\langle\downarrow|$ (blue line) and $\hat{\rho}^0_{\mathsf{sys}} = |\uparrow\rangle\langle\uparrow|$ (red line). The inset shows the region around $t = \frac{7}{15}\frac{2\pi}{\omega_{\mathrm{sp}}}$.

Note, that the parameters were chosen so that $\frac{\alpha^2}{m} = \frac{1}{5} = \text{const}$. Therefore, we expect that the driving effect is nearly the same for all three parameters. Within the deviation induced by the state-dependent driving, we actually find that the driving is indeed the same for all three parameter sets, as Fig. 6.7 for $\hat{\rho}_{\mathsf{sys}} = |\downarrow\rangle\langle\downarrow|$ confirms. Thus, we have found a way to reduce the state-dependency of the driving. However, as mentioned in Sec. 6.2, this comes at the cost of higher numerical effort: In order to keep the error from the cut-off

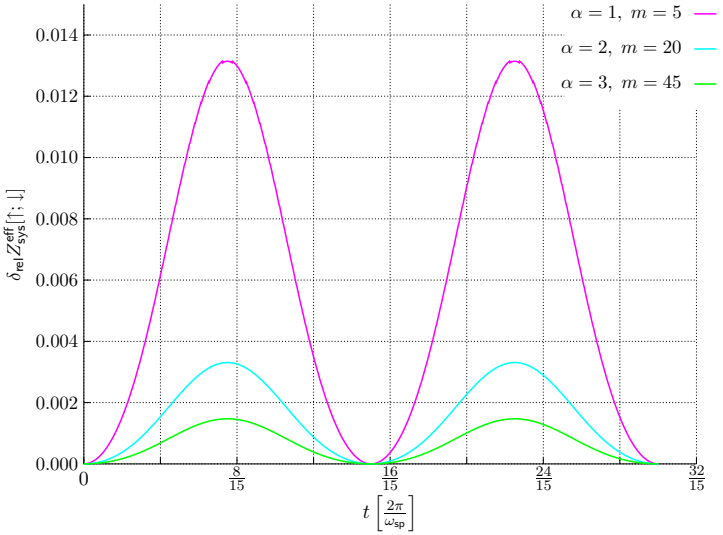

Figure 6.6.: Relative deviation of effective partition sum for three different parameter sets of the oscillator: $\alpha = 1,\ m = 5$ (magenta line), $\alpha = 2,\ m = 20$ (cyan line), $\alpha = 3,\ m = 45$ (green line)

of the spectrum of the oscillator approximately the same, one has to take more levels of the oscillator into account the larger α. Details on how the energy level, at which the cut-off was made, $N_{\mathsf{cut-off}}$, as well as the resulting dimension of the total Hilbert space (including the system), $\mathsf{dim}(\mathcal{H})$, are influenced by α (for given maximal cut-off error for initial state), are given in the table below:

α	$N_{\mathsf{cut-off}}$	$\mathsf{dim}(\mathcal{H})$
1	21	42
2	34	68
3	48	96

Thus, our numerics confirm that, according to LEMBAS, the oscillator effectively acts as a work source on the spin.

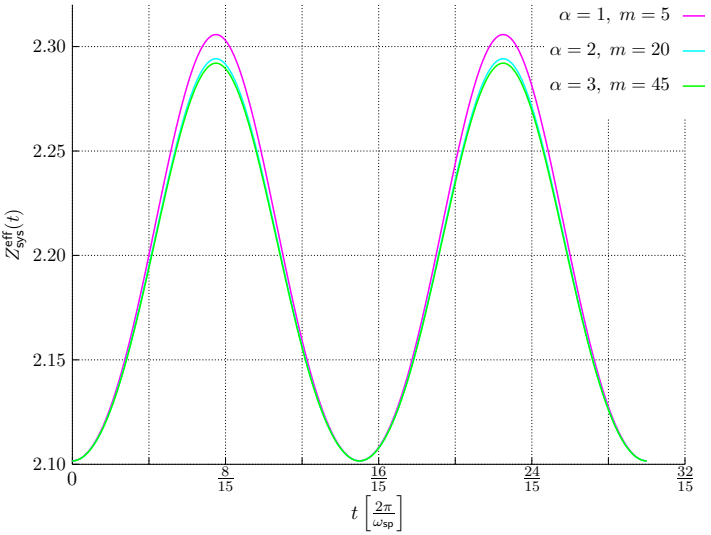

Figure 6.7.: $Z^{\mathsf{eff}}_{\mathsf{sys}}(t)$ for three different parameter sets of α and m for $\hat{\rho}_{\mathsf{sys}} = |\downarrow\rangle\langle\downarrow|$.

7. Bipartite three-spin model: Work

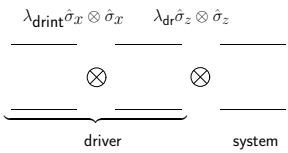

Figure 7.1.: Two spin driver: The two spins on the left can be considered as an effective driver for the third spin on the right-hand side, the system. Justification for this interpretation is given in the text.

We investigate a network of spins under a thermodynamic point of view. Here, we look for a driver built up of two-level systems only. In particular, we try to find an effectively driving system which comes closer to our definition of perfect than the oscillator (as we have seen in the previous section, the driving effect of the oscillator depends on the state of the system). Again, the driven system is taken to be a two-level system. We thus consider the following Hamiltonian (cf. Fig. 7.1),

$$\hat{H} \equiv \underbrace{\frac{\omega}{2}\left(\hat{\sigma}_z \otimes \hat{1}_{23} + \hat{1}_1 \otimes \hat{\sigma}_z \otimes \hat{1}_3\right) + \frac{\lambda_{\mathsf{drint}}}{2}\hat{\sigma}_x \otimes \hat{\sigma}_x \otimes \hat{1}_3}_{\equiv \hat{H}_{\mathsf{dr}}\text{: Hamiltonian of driver}} + \underbrace{\frac{\omega}{2}\hat{1}_{23} \otimes \hat{\sigma}_z}_{\equiv \hat{H}_{\mathsf{sys}}\text{: driven spin}} + \underbrace{\frac{\lambda_{\mathsf{dr}}}{2}\hat{1}_1 \otimes \hat{\sigma}_z \otimes \hat{\sigma}_z}_{\equiv \hat{H}_{\mathsf{drsys}}\text{: coupling driver}-\text{spin}} . \tag{7.1}$$

Here, the general idea is that the driver spins swap their energy periodically (cf. also Chap. 8) and since the effective splitting of the third spin, the system, is controlled by the occupation probability of the second spin, we expect a periodic driving behavior. In order to investigate this system more closely, we choose an operator basis representation (for a quite general overview over operator basis calculation we refer to [76]).

7.1. Operator basis

We use the following operator basis,

$$\mathfrak{B}_0 = \frac{1}{\sqrt{2}} \begin{pmatrix} 1 & 0 \\ 0 & 1 \end{pmatrix} = \frac{1}{\sqrt{2}} \hat{1} \tag{7.2}$$

$$\mathfrak{B}_1 = \frac{1}{\sqrt{2}} \begin{pmatrix} 0 & 1 \\ 1 & 0 \end{pmatrix} = \frac{1}{\sqrt{2}} \hat{\sigma}_x \tag{7.3}$$

$$\mathfrak{B}_2 = \frac{1}{\sqrt{2}} \begin{pmatrix} 0 & \mathrm{i} \\ -\mathrm{i} & 0 \end{pmatrix} = \frac{1}{\sqrt{2}} \hat{\sigma}_y \tag{7.4}$$

$$\mathfrak{B}_3 = \frac{1}{\sqrt{2}} \begin{pmatrix} -1 & 0 \\ 0 & 1 \end{pmatrix} = \frac{1}{\sqrt{2}} \hat{\sigma}_z, \tag{7.5}$$

which are renormalized Pauli spin operators. In the following, we will use the abbreviation $\eta \equiv \frac{1}{\sqrt{2}}$. From this we can easily infer the following identities:

$$\mathrm{Tr}\left\{\mathfrak{B}_\mu \mathfrak{B}_\nu\right\} = \delta_{\mu\nu}, \tag{7.6}$$

$$\mathrm{Tr}\left\{\mathfrak{B}_\mu\right\} = \eta^{-1}\delta_{\mu 0}, \tag{7.7}$$

$$\mathfrak{B}_i \mathfrak{B}_j = \mathrm{i}\eta\varepsilon_{ijk}\mathfrak{B}_k + \eta\delta_{ij}\mathfrak{B}_0, \tag{7.8}$$

$$\mathfrak{B}_0 \mathfrak{B}_\mu = \mathfrak{B}_\mu \mathfrak{B}_0 = \eta\mathfrak{B}_\mu, \tag{7.9}$$

where Latin indices run from 1 to 3, and Greek indices run from 0 to 3. Here, ε denotes the totally antisymmetric Levi-Civita tensor (cf., e. g. [36]).

We can transform any suitable (defined on the same Hilbert space $\mathcal{H}$) operator A into the new basis set by

$$\hat{A}_{\mathfrak{B}} = \sum_{\mu,\mu'\mu''} \mathrm{Tr}\left\{\hat{A}\left(\mathfrak{B}_\mu \otimes \mathfrak{B}_{\mu'} \otimes \mathfrak{B}_{\mu''}\right)\right\} \mathfrak{B}_\mu \otimes \mathfrak{B}_{\mu'} \otimes \mathfrak{B}_{\mu''}, \tag{7.10}$$

where the coefficients of the operator basis representation of $\hat{A}$ are given by

$$\hat{A}_{\mathfrak{B}}^{\mu\mu'\mu''} = \mathrm{Tr}\left\{\hat{A}\left(\mathfrak{B}_\mu \otimes \mathfrak{B}_{\mu'} \otimes \mathfrak{B}_{\mu''}\right)\right\}. \tag{7.11}$$

Here and in the following we label any operator expressed in the operator basis by a subindex $\mathfrak{B}$.

7.2. Schrödinger dynamics in the operator basis

Now, we formulate the Liouville-von Neumann equation in the operator basis. To this end, we first express the Hamiltonian in the operator basis, giving

$$\hat{H}_{\mathfrak{B}} = \eta^{-1} \left[\omega \left(\mathfrak{B}_3 \otimes \mathfrak{B}_0 \otimes \mathfrak{B}_0 + \mathfrak{B}_0 \otimes \mathfrak{B}_3 \otimes \mathfrak{B}_0 + \mathfrak{B}_0 \otimes \mathfrak{B}_0 \otimes \mathfrak{B}_3\right) + \ldots \right.$$
$$\left. \ldots + \lambda_{\mathsf{drint}} \mathfrak{B}_1 \otimes \mathfrak{B}_1 \otimes \mathfrak{B}_0 + \lambda_{\mathsf{dr}} \mathfrak{B}_0 \otimes \mathfrak{B}_3 \otimes \mathfrak{B}_3\right]. \tag{7.12}$$

In the following we will also use the abbreviation

$$\hat{H}_{\mathfrak{B}}^{\mathsf{spins}} \equiv \eta^{-1} \omega \left(\mathfrak{B}_3 \otimes \mathfrak{B}_0 \otimes \mathfrak{B}_0 + \mathfrak{B}_0 \otimes \mathfrak{B}_3 \otimes \mathfrak{B}_0 + \mathfrak{B}_0 \otimes \mathfrak{B}_0 \otimes \mathfrak{B}_3\right). \tag{7.13}$$

We consider pure Schrödinger dynamics for the density operator. Expressed in the operator basis we get for the coefficient $\alpha\alpha'\alpha''$ (cf. [76]):

$$\begin{aligned} \frac{\partial}{\partial t} \hat{\rho}_{\mathfrak{B}}^{\alpha\alpha'\alpha''} &= \frac{\partial}{\partial t} \mathrm{Tr}\left\{\hat{\rho}_{\mathfrak{B}} \mathfrak{B}_\alpha \otimes \mathfrak{B}_{\alpha'} \otimes \mathfrak{B}_{\alpha''}\right\} \\ &= -\mathrm{i} \sum_{\mu\mu'\mu''} \mathrm{Tr}\left\{\hat{H}_{\mathfrak{B}} \left[\mathfrak{B}_\mu \otimes \mathfrak{B}_{\mu'} \otimes \mathfrak{B}_{\mu''}, \mathfrak{B}_\alpha \otimes \mathfrak{B}_{\alpha'} \otimes \mathfrak{B}_{\alpha''}\right]\right\} \hat{\rho}_{\mathfrak{B}}^{\mu\mu'\mu''}. \end{aligned} \tag{7.14}$$

We consider the addends separately. We use Eqs. (7.6-7.9) in order to determine the addends. Moreover, we use a self-written MATHEMATICA script which can transform between energy-eigenbasis, operator basis and can perform basic calculations in the operator basis. A short exemplary study of the first addend, $\hat{H}_{\mathfrak{B}}^{\mathsf{sp1}}$ can be found in the appendix B.1. The other addends can be computed analogously or by using the aforementioned MATHEMATICA script. With this, we get for the spins

$$\begin{aligned} &\mathrm{Tr}\left\{\hat{H}_{\mathfrak{B}}^{\mathsf{spins}} \left[\mathfrak{B}_\mu \otimes \mathfrak{B}_{\mu'} \otimes \mathfrak{B}_{\mu''}, \mathfrak{B}_\alpha \otimes \mathfrak{B}_{\alpha'} \otimes \mathfrak{B}_{\alpha''}\right]\right\} \\ &\quad = \mathrm{i}\omega \left(\varepsilon_{3mn}\delta_{na}\delta_{\mu'\alpha'}\delta_{\mu''\alpha''} + \varepsilon_{3m'n'}\delta_{n'a'}\delta_{\mu\alpha}\delta_{\mu''\alpha''} + \varepsilon_{3m''n''}\delta_{n''a''}\delta_{\mu\alpha}\delta_{\mu'\alpha'}\right). \end{aligned} \tag{7.15}$$

For the internal coupling of the driver, $\hat{H}_{\mathsf{drint}} = \frac{\lambda_{\mathsf{drint}}}{2} \hat{\sigma}_x \otimes \hat{\sigma}_x$, we obtain

$$\begin{aligned} &\mathrm{Tr}\left\{\hat{H}_{\mathfrak{B}}^{\mathsf{drint}} \left[\mathfrak{B}_\mu \otimes \mathfrak{B}_{\mu'} \otimes \mathfrak{B}_{\mu''}, \mathfrak{B}_\alpha \otimes \mathfrak{B}_{\alpha'} \otimes \mathfrak{B}_{\alpha''}\right]\right\} \\ &\quad = -\mathrm{i}\lambda_{\mathsf{drint}}\delta_{\mu''\alpha''} \left(\delta_{\alpha'0}\delta_{m'1}\varepsilon_{1am} + \delta_{\alpha'1}\delta_{\mu'0}\varepsilon_{1am} + \delta_{\alpha 0}\delta_{m1}\varepsilon_{1a'm'} + \delta_{\alpha 1}\delta_{\mu 0}\varepsilon_{1a'm'}\right). \end{aligned} \tag{7.16}$$

Finally, we find for the coupling of the driver to the system spin:

$$\begin{aligned}&\mathrm{Tr}\left\{\hat{H}^{\mathsf{dr}}_{\mathfrak{B}}\left[\mathfrak{B}_{\mu}\otimes\mathfrak{B}_{\mu'}\otimes\mathfrak{B}_{\mu''},\mathfrak{B}_{\alpha}\otimes\mathfrak{B}_{\alpha'}\otimes\mathfrak{B}_{\alpha''}\right]\right\}\\&\quad=\mathrm{i}\lambda_{\mathsf{dr}}\delta_{\mu\alpha}\left[\varepsilon_{3m''n''}\delta_{n''a''}(\delta_{a'3}\delta_{\mu'0}+\delta_{\alpha'0}\delta_{m'3})+\varepsilon_{3m''a''}\delta_{n''a''}(\delta_{a''3}\delta_{\mu''0}+\delta_{\alpha''0}\delta_{m''3})\right].\end{aligned}\tag{7.17}$$

Inserting these three addends into the Schrödinger equation, Eq. (7.14), gives

$$\begin{aligned}\frac{\partial}{\partial t}\rho^{\alpha\alpha'\alpha''}_{\mathfrak{B}}=&\omega(\varrho_{1\alpha'\alpha''}\delta_{a2}-\varrho_{2\alpha'\alpha''}\delta_{a1}+\varrho_{\alpha1\alpha''}\delta_{a'2}-\varrho_{\alpha2\alpha''}\delta_{a'1}+\varrho_{\alpha\alpha'1}\delta_{a''2}-\varrho_{\alpha\alpha'2}\delta_{a''1}\\&-\lambda_{\mathsf{drint}}\left[\delta_{\alpha'0}(\delta_{a2}\varrho_{31\alpha''}-\delta_{a3}\varrho_{21\alpha''})-\delta_{a'3}(\delta_{\alpha0}\varrho_{12\alpha''}+\delta_{a1}\varrho_{02\alpha''})+\dots\right.\\&\qquad\left.\dots+\delta_{a'2}(\delta_{\alpha0}\varrho_{13\alpha''}+\delta_{a1}\varrho_{03\alpha''})+\delta_{a'1}(\delta_{a2}\varrho_{30\alpha''}-\delta_{a3}\varrho_{20\alpha''})\right]\\&+\lambda_{\mathsf{dr}}\left[\delta_{a''2}(\delta_{a'3}\varrho_{\alpha01}+\delta_{\alpha'0}\varrho_{\alpha31})-\delta_{a''1}(\delta_{a'3}\varrho_{\alpha02}+\delta_{\alpha'0}\varrho_{\alpha32})+\dots\right.\\&\qquad\left.\dots+\delta_{a'2}(\delta_{a''3}\varrho_{\alpha10}+\delta_{\alpha''0}\varrho_{\alpha13})-\delta_{a'1}(\delta_{a''3}\varrho_{\alpha20}+\delta_{\alpha''0}\varrho_{\alpha23})\right].\end{aligned}\tag{7.18}$$

For the sake of simplicity, we have introduced $\rho^{\alpha\alpha'\alpha''}_{\mathfrak{B}}\equiv\varrho_{\alpha\alpha'\alpha''}$ in order not to overload the labelling. This is unproblematic, here, since the three indices clearly show that the coefficients of the density operator refer to the operator basis and not to the energy-eigenbasis.

The equations of motion above give a set of 64 coupled ODEs. As the normalization of the density operator has to be guaranteed, we check whether our equations of motion do conserve this quantity:

$$\frac{\partial}{\partial t}\mathrm{Tr}\left\{\hat{\rho}_{\mathfrak{B}}(t)\right\}=\frac{\partial}{\partial t}\varrho_{000}(t)\overset{(7.18)}{=}0.\tag{7.19}$$

As necessary, the norm (probability conservation) is constant throughout the process.

7.3. Identifying independent subgroups of coefficients

For the system considered, here, we can identify two subgroups of independent dynamics. We find with the help of the MATHEMATICA script

$$\dot{\varrho}^t_{31\alpha''} = -\omega(\varrho^t_{32\alpha''} + \varrho^t_{31\alpha''}\delta_{a''1} - \varrho^t_{311}\delta_{a''2}) + \lambda_{\mathsf{drint}}\varrho^t_{20\alpha''} - \lambda_{\mathsf{dr}}(\varrho^t_{320}\delta_{a''3} + \varrho^t_{323}\delta_{\alpha''0}) \tag{7.20}$$

$$\dot{\varrho}^t_{20\alpha''} = \omega(\varrho^t_{10\alpha''} - \varrho^t_{202}\delta_{a''1} + \varrho^t_{201}\delta_{a''2}) + \lambda_{\mathsf{drint}}\varrho^t_{31\alpha''} + \lambda_{\mathsf{dr}}(\varrho^t_{231}\delta_{a''2} - \varrho^t_{232}\delta_{a''1}) \tag{7.21}$$

$$\dot{\varrho}^t_{32\alpha''} = \omega(\varrho^t_{31\alpha''} - \varrho^t_{322}\delta_{a''1} + \varrho^t_{321}\delta_{a''2}) + \lambda_{\mathsf{dr}}(\varrho^t_{313}\delta_{\alpha''0} + \varrho^t_{310}\delta_{a''3}) \tag{7.22}$$

$$\dot{\varrho}_{10\alpha''} = -\omega(\varrho^t_{20\alpha''} + \varrho^t_{102}\delta_{a''1} - \varrho^t_{101}\delta_{a''2}) + \lambda_{\mathsf{dr}}(-\varrho^t_{132}\delta_{a''1} + \varrho^t_{131}\delta_{a''2}) \tag{7.23}$$

$$\dot{\varrho}^t_{23\alpha''} = \omega(\varrho^t_{13\alpha''} - \varrho^t_{232}\delta_{a''1} + \varrho^t_{231}\delta_{a''2}) + \lambda_{\mathsf{dr}}(-\varrho^t_{202}\delta_{a''1} + \varrho^t_{201}\delta_{a''2}) \tag{7.24}$$

$$\dot{\rho}^t_{13\alpha''} = -\omega(\varrho^t_{23\alpha''} + \varrho^t_{132}\delta_{a''1} - \varrho^t_{131}\delta_{a''2}) + \lambda_{\mathsf{drint}}\varrho^t_{02\alpha''} + \lambda_{\mathsf{dr}}(\varrho^t_{101}\delta_{a''2} - \varrho^t_{102}\delta_{a''1}) \tag{7.25}$$

$$\dot{\rho}^t_{02\alpha''} = \omega(\varrho^t_{01\alpha''} - \varrho^t_{022}\delta_{a''1} + \varrho^t_{021}\delta_{a''2}) - \lambda_{\mathsf{drint}}\varrho^t_{13\alpha''} + \lambda_{\mathsf{dr}}(\varrho^t_{010}\delta_{a''3} + \varrho^t_{013}\delta_{\alpha''0}) \tag{7.26}$$

$$\dot{\varrho}^t_{01\alpha''} = \omega(-\varrho_{02\alpha''} - \varrho_{012}\delta_{a''1} + \varrho_{011}\delta_{a''2}) - \lambda_{\mathsf{dr}}(\varrho^t_{023}\delta_{\alpha''0} + \varrho^t_{020}\delta_{a''3}). \tag{7.27}$$

As can be easily seen, these 8×4 equations for the coefficients of the density operator form a closed subset of all 64 equations. This subgroup $\mathbb{S}_{\mathsf{off}}$ consists of 32 density operator coefficients,

$$\mathbb{S}_{\mathsf{off}} \equiv \{\varrho^t_{01\alpha''}, \varrho^t_{02\alpha''}, \varrho^t_{10\alpha''}, \varrho^t_{20\alpha''}, \varrho^t_{13\alpha''}, \varrho^t_{31\alpha''}, \varrho^t_{23\alpha''}, \varrho^t_{32\alpha''}\}. \tag{7.28}$$

For the other subgroup, $\mathbb{S}_{\mathsf{pdg}}$, we get

$$\dot{\varrho}^t_{21\alpha''} = \omega(\varrho^t_{11\alpha''} - \varrho^t_{22\alpha''} - \varrho^t_{212}\delta_{a''1} + \varrho^t_{211}\delta_{a''2}) - \dots$$
$$\dots - \lambda_{\mathsf{drint}}\varrho^t_{30\alpha''} - \lambda_{\mathsf{dr}}(\varrho^t_{220}\delta_{a''3} + \varrho^t_{223}\delta_{\alpha''0}) \tag{7.29}$$
$$\dot{\varrho}^t_{30\alpha''} = \omega(-\varrho^t_{302}\delta_{a''1} + \varrho^t_{301}\delta_{a''2}) + \lambda_{\mathsf{drint}}\rho_{21\alpha''} + \lambda_{\mathsf{dr}}(\varrho^t_{331}\delta_{a''2} - \varrho^t_{332}\delta_{a''1}) \tag{7.30}$$
$$\dot{\varrho}^t_{11\alpha''} = \omega(-\varrho^t_{12\alpha''} - \varrho^t_{21\alpha''} - \varrho^t_{112}\delta_{a''1} + \varrho^t_{111}\delta_{a''2}) - \lambda_{\mathsf{dr}}(\varrho^t_{123}\delta_{\alpha''0} + \varrho^t_{120}\delta_{a''3}) \tag{7.31}$$
$$\dot{\varrho}^t_{22\alpha''} = \omega(\varrho^t_{12\alpha''} + \varrho^t_{21\alpha''} - \varrho^t_{222}\delta_{a''1} + \varrho^t_{221}\delta_{a''2}) + \lambda_{\mathsf{dr}}(\varrho^t_{213}\delta_{\alpha''0} + \varrho^t_{210}\delta_{a''3}) \tag{7.32}$$
$$\dot{\varrho}^t_{33\alpha''} = \omega(-\varrho^t_{332}\delta_{a''1} + \varrho^t_{331}\delta_{a''2}) + \lambda_{\mathsf{dr}}(-\varrho^t_{302}\delta_{a''1} + \varrho^t_{301}\delta_{a''2}) \tag{7.33}$$
$$\dot{\varrho}^t_{12\alpha''} = \omega(\varrho^t_{11\alpha''} - \varrho^t_{22\alpha''} - \varrho^t_{122}\delta_{a''1} + \varrho^t_{121}\delta_{a''2}) - \dots$$
$$\dots - \lambda_{\mathsf{drint}}\varrho^t_{03\alpha''} + \lambda_{\mathsf{dr}}(\varrho^t_{110}\delta_{a''3} + \varrho^t_{113}\delta_{\alpha''0}) \tag{7.34}$$
$$\dot{\varrho}^t_{03\alpha''} = \omega(-\varrho^t_{032}\delta_{a''1} + \varrho^t_{031}\delta_{a''2}) + \lambda_{\mathsf{drint}}\varrho^t_{12\alpha''} + \lambda_{\mathsf{dr}}(\varrho^t_{001}\delta_{a''2} - \varrho^t_{002}\delta_{a''1}) \tag{7.35}$$
$$\dot{\rho}_{00\alpha''} = \omega(-\varrho^t_{002}\delta_{a''1} + \varrho^t_{001}\delta_{a''2}) + \lambda_{\mathsf{dr}}(-\varrho^t_{032}\delta_{a''1} + \varrho^t_{031}\delta_{a''2}) \tag{7.36}$$

From these equations of motion we readily infer that

$$\dot{\rho}^t_{000} = 0 \text{ from Eq. (7.36) with } \alpha'' = 0 \tag{7.37}$$
$$\dot{\rho}^t_{003} = 0 \text{ from Eq. (7.36) with } \alpha'' = 3 \tag{7.38}$$
$$\dot{\rho}^t_{330} = 0 \text{ from Eq. (7.33) with } \alpha'' = 0 \tag{7.39}$$
$$\dot{\rho}^t_{333} = 0 \text{ from Eq. (7.33) with } \alpha'' = 3 \tag{7.40}$$

The first relation has already been discussed as the conservation of normalization. These relations hold irrespective of the initial state of the system. The last three equations show that we have three constants of motion which can be interpreted physically: All of them are connected with the magnetization, where Eq. (7.38) corresponds to the magnetization of the system spin, Eq. (7.39) to the magnetization of the driver (both spins combined) and Eq. (7.40) to the total magnetization.

As we are interested in the JR, we will start in a special initial state, as the system spin has been measured initially. For the couplings given, we will then expect that the state of the system spin does not change. Therefore, we investigate the dynamics of the system more closely. As the system spin is given by

$$\dot{\rho}^{\mathsf{sp3}}_{\mathfrak{B}}(t) = \eta^{-2}\sum_{\mu''}\dot{\varrho}_{00\mu''}(t)\mathfrak{B}_{\mu''}, \tag{7.41}$$

we already know that only two addends are non-vanishing according to Eqs. (7.37) and (7.38). For the remaining addends we get from Eq. (7.36) with $\alpha'' = 1$ and $\alpha'' = 2$, respectively,

$$\dot{\varrho}^t_{001} = -\omega\varrho_{002} - \lambda_{\mathsf{dr}}\varrho_{032} \tag{7.42}$$
$$\dot{\varrho}^t_{002} = \omega\varrho_{001} + \lambda_{\mathsf{dr}}\varrho_{031}. \tag{7.43}$$

Thus, for general initial states we could have dynamics. From Eqs. (7.35) we obtain for $\alpha'' = 1$ and $\alpha'' = 2$

$$\dot{\varrho}^t_{031} = -\omega\varrho^t_{032} + \lambda_{\mathsf{drint}}\varrho^t_{121} - \varrho^t_{002} \tag{7.44}$$
$$\dot{\varrho}^t_{032} = \omega\varrho^t_{031} + \lambda_{\mathsf{drint}}\varrho^t_{122} + \lambda_{\mathsf{dr}}\varrho^t_{001}. \tag{7.45}$$

Now, using Eqs. (7.34) with $\alpha'' = 1$ and $\alpha'' = 2$ we get

$$\dot{\varrho}^t_{121} = \omega(\varrho^t_{111} - \varrho^t_{221} - \varrho^t_{122}) - \lambda_{\mathsf{drint}}\varrho^t_{031} \tag{7.46}$$
$$\dot{\varrho}^t_{122} = \omega(\varrho^t_{112} - \varrho^t_{222} - \varrho^t_{121}) - \lambda_{\mathsf{drint}}\varrho^t_{032}. \tag{7.47}$$

Investigating the new addends with Eqs. (7.31) and (7.32) we get

$$\dot{\varrho}^t_{111} = \omega(-\varrho^t_{121} - \varrho^t_{211} - \varrho^t_{112}) \tag{7.48}$$
$$\dot{\varrho}^t_{112} = \omega(-\varrho^t_{122} - \varrho^t_{212} + \varrho^t_{111}) \tag{7.49}$$
$$\dot{\varrho}^t_{221} = \omega(\varrho^t_{121} + \varrho^t_{211} - \varrho^t_{222}) \tag{7.50}$$
$$\dot{\varrho}^t_{222} = \omega(\varrho^t_{122} + \varrho^t_{212} + \varrho^t_{221}). \tag{7.51}$$

The additional addends not investigated yet are obtained from Eqs. (7.29),

$$\dot{\varrho}^t_{211} = \omega(\varrho^t_{111} - \varrho^t_{221} - \varrho^t_{212}) - \lambda_{\mathsf{drint}}\varrho^t_{301} \tag{7.52}$$
$$\dot{\varrho}^t_{212} = \omega(\varrho^t_{112} - \varrho^t_{222} + \varrho^t_{211}) - \lambda_{\mathsf{drint}}\varrho^t_{302}. \tag{7.53}$$

Again, this gives two new addends whose dynamics are given by Eq. (7.30),

$$\dot{\varrho}^t_{301} = -\omega\varrho^t_{302} + \lambda_{\mathsf{drint}}\varrho^t_{211} - \lambda_{\mathsf{dr}}\varrho^t_{332} \tag{7.54}$$
$$\dot{\varrho}^t_{302} = +\omega\varrho^t_{301} + \lambda_{\mathsf{drint}}\varrho^t_{212} + \lambda_{\mathsf{dr}}\varrho^t_{331}. \tag{7.55}$$

Finally, we have by Eqs. (7.33) that

$$\dot{\varrho}^t_{331} = -\omega\varrho^t_{332} - \lambda_{\mathsf{dr}}\varrho^t_{302} \tag{7.56}$$
$$\dot{\varrho}^t_{332} = +\omega\varrho^t_{331} + \lambda_{\mathsf{dr}}\varrho^t_{301} \tag{7.57}$$

Thus, our expectation for the dynamics of the system spin has led to our finding of a subgroup $\mathbb{S}_{\mathsf{mnd}}$ of $\mathbb{S}_{\mathsf{pdg}}$. The latter is therefore split into two halves with 16 elements each, where the subgroup $\mathbb{S}_{\mathsf{mnd}}$ is given by its elements

$$\mathcal{R}^t_{\mathsf{mnd}} = \{\mathcal{R}^t_{\mathsf{pdg}} \in \mathbb{S}_{\mathsf{pdg}} |\ \alpha'' = 1, 2\}. \tag{7.58}$$

For the special initial state where the system has been measured, all elements of the subgroup $\mathbb{S}_{\mathsf{mnd}}$ vanish at any time t. Thus, we have only a set of 16 ODEs left to solve which form the subgroup $\mathbb{S}_{\mathsf{mdg}} = \mathbb{S}_{\mathsf{pdg}} \setminus \mathbb{S}_{\mathsf{mnd}}$. As the four conserved quantities from Eqs. (7.37)-(7.40) are all elements of $\mathbb{S}_{\mathsf{mdg}}$, we are only left with a set of 12 coupled differential equations to solve.

7.4. Initial state

As we have already briefly discussed, we are mostly interested in initial states where the system spin has been measured, thus being prepared in an energy-eigenstate through the measurement. Therefore, we will now consider special initial states of the following form:

$$\hat{\rho}(0) = |2\rangle\langle 2| \otimes |1\rangle\langle 1| \otimes \hat{\rho}_D(0), \tag{7.59}$$

thus, a factorizing state where the driver is prepared in a compound state for which one spin is up and the other down (here, we have chosen spin 1 up, w. l. o. g.) in order to ensure effective driving dynamics. The system spin usually starts in a diagonal state, which is slightly more general than the states discussed above and corresponds to the canonical state before the initial measurement has been performed. Then, we find

$$\begin{aligned}\hat{\rho}_{\mathfrak{B}}(0) = &\sum_{\mu,\mu',\mu''} \mathrm{Tr}\left\{\hat{\rho}(0)\mathfrak{B}_\mu \otimes \mathfrak{B}_{\mu'} \otimes \mathfrak{B}_{\mu''}\right\} \mathfrak{B}_\mu \otimes \mathfrak{B}_{\mu'} \otimes \mathfrak{B}_{\mu''} \\ =&\eta^3 \left(\mathfrak{B}_0 \otimes \mathfrak{B}_0 \otimes \mathfrak{B}_0 + \chi\mathfrak{B}_0 \otimes \mathfrak{B}_0 \otimes \mathfrak{B}_3 - \mathfrak{B}_0 \otimes \mathfrak{B}_3 \otimes \mathfrak{B}_0 + \ldots\right. \\ &\ldots + \mathfrak{B}_3 \otimes \mathfrak{B}_0 \otimes \mathfrak{B}_0 - \mathfrak{B}_3 \otimes \mathfrak{B}_3 \otimes \mathfrak{B}_0 + \chi\mathfrak{B}_3 \otimes \mathfrak{B}_0 \otimes \mathfrak{B}_3 - \ldots \\ &\left.\ldots - \chi\mathfrak{B}_0 \otimes \mathfrak{B}_3 \otimes \mathfrak{B}_3 - \chi\mathfrak{B}_3 \otimes \mathfrak{B}_3 \otimes \mathfrak{B}_3\right),\end{aligned} \tag{7.60}$$

where we have introduced $\chi = 1 - 2c$ with $c \equiv \langle 1|\,\rho_D\,|1\rangle$ being the initial occupation probability of the ground state of the system spin. Thus, if the spin has been measured in the ground or excited state we have $c = 1 \implies \chi = -1$ and $c = 0 \implies \chi = +1$, respectively. For a thermal state, where $\frac{1}{2} \leq c \leq 1$, we find $\chi \in [-1, 0]$.

7.5. Effective description of the system

First, we start with investigating the energy flows of the system in terms of LEMBAS. To this end, we have a look at the effective Hamiltonian of the system spin,

$$H_{\mathsf{sys}}^{\mathsf{eff}}(t) = \mathrm{Tr}_{\mathsf{dr}}\left\{\hat{H}_{\mathsf{drsys}}\hat{\rho}_{\mathsf{dr}}^{t}\otimes\hat{1}_{\mathsf{sys}}\right\}. \tag{7.61}$$

Taking into account that

$$\hat{\rho}_{\mathsf{dr}}^{t}\otimes\hat{1}_{\mathsf{sys}} = \eta^{-1}\hat{\rho}_{\mathfrak{B},\mathsf{dr}}^{t}\otimes\mathfrak{B}_0 = \eta^{-2}\sum_{\mu\mu'}\varrho_{\mu\mu'0}^{t}\mathfrak{B}_\mu\otimes\mathfrak{B}_{\mu'}\otimes\mathfrak{B}_0, \tag{7.62}$$

we get in the operator basis

$$\begin{aligned}\hat{H}_{\mathfrak{B},\mathsf{sys}}^{\mathsf{eff}}(t) &\overset{(7.12)}{=} \eta^{-1}\sum_{\mu\mu'}\lambda_{\mathsf{dr}}\mathrm{Tr}_{\mathsf{dr}}\left\{(\mathfrak{B}_0\otimes\mathfrak{B}_3\otimes\mathfrak{B}_3)(\mathfrak{B}_\mu\otimes\mathfrak{B}_{\mu'}\otimes\mathfrak{B}_0)\right\}\varrho_{\mu\mu'0}^{t}\eta^{-2}\\ &= \eta^{-3}\lambda_{\mathsf{dr}}\sum_{\mu\mu'}\underbrace{\mathrm{Tr}\left\{\mathfrak{B}_0\mathfrak{B}_\mu\right\}}_{\delta_{0\mu}}\underbrace{\mathrm{Tr}\left\{\mathfrak{B}_3\mathfrak{B}_{\mu'}\right\}}_{\delta_{3\mu'}}\underbrace{\mathfrak{B}_3\mathfrak{B}_0}_{\eta\mathfrak{B}_3}\varrho_{\mu\mu'0}^{t}\\ &= \eta^{-2}\lambda_{\mathsf{dr}}\varrho_{030}^{t}\mathfrak{B}_3.\end{aligned} \tag{7.63}$$

Using the extension of this local operator on the total Hilbert space, $\hat{H}_{\mathfrak{B},\mathsf{sys}}^{\mathsf{eff}}(t) = \eta^{-4}\lambda_{\mathsf{dr}}\varrho_{030}^{t}\mathfrak{B}_0\otimes\mathfrak{B}_0\otimes\mathfrak{B}_3$, we can easily infer that we have $\left[\hat{H}_{\mathfrak{B},\mathsf{sys}}^{\mathsf{eff}}(t),\hat{H}_{\mathfrak{B},\mathsf{sys}}\right] = 0\;\forall\,t$, which gives $\hat{H}_{\mathfrak{B},\mathsf{sys}}^{\mathsf{eff},2}(t) = 0$ and thus $\hat{H}_{\mathfrak{B},\mathsf{sys}}^{\mathsf{eff}}(t) = \hat{H}_{\mathfrak{B},\mathsf{sys}}^{\mathsf{eff},1}(t)$.

7.5.1. Work on system

Having determined the effective Hamiltonian of the system, we now turn to calculate the work performed on the system by the effective dynamics. In order to simplify the expressions, we consider the three addends introduced above separately. We find

$$\hat{H}_{\mathfrak{B},\mathsf{sys}}^{\mathsf{eff},2} \overset{(7.63)}{=} 0 \implies đW_{\mathsf{sys}}^{(2)} \overset{(5.11)}{=} 0 \overset{(5.12)}{=} đW_{\mathsf{sys}}^{(3)}. \tag{7.64}$$

Thus, we are only left with the first contribution, which gives

$$\begin{aligned}đW_{\mathsf{sys}}^{(1)} = đW_{\mathsf{sys}} &= \mathrm{Tr}\left\{\frac{\mathrm{d}}{\mathrm{d}t}\left(\hat{H}_{\mathfrak{B},\mathsf{sys}}^{\mathsf{eff},1}\right)\hat{\rho}_{\mathfrak{B},\mathsf{sys}}\right\}\mathrm{d}t\\ &= \eta^{-2}\sum_{\mu''}\mathrm{Tr}\left\{\eta^{-2}\lambda_{\mathsf{dr}}\dot{\varrho}_{030}^{t}\mathfrak{B}_3\mathfrak{B}_{\mu''}\right\}\varrho_{00\mu''}^{t}\mathrm{d}t,\end{aligned} \tag{7.65}$$

where we have used

$$\hat{\rho}_{\mathfrak{B},\mathsf{sys}} = \sum_{\mu\mu'\mu''} \mathrm{Tr}_{12}\left\{\varrho_{\mu\mu'\mu''}\mathfrak{B}_\mu \otimes \mathfrak{B}_{\mu'} \otimes \mathfrak{B}_{\mu''}\right\} = \eta^{-2}\sum_{\mu''}\varrho^t_{00\mu''}\mathfrak{B}_{\mu''}. \tag{7.66}$$

Substituting Eq. (7.35) with $\alpha'' = 0$ for $\dot{\varrho}^t_{030}$ and using $\mathrm{Tr}\{\mathfrak{B}_3\mathfrak{B}_{\mu''}\} = \delta_{3\mu''}$, we get

$$\begin{aligned} đW_{\mathsf{sys}} &= \eta^{-4}\lambda_{\mathsf{dr}}\varrho^t_{003}\lambda_{\mathsf{drint}}\varrho^t_{120}\mathrm{d}t \\ &= \eta^{-4}\lambda_{\mathsf{dr}}\lambda_{\mathsf{drint}}\varrho^0_{003}\varrho^t_{120}\mathrm{d}t, \end{aligned} \tag{7.67}$$

where we have also used that $\dot{\varrho}^t_{003} = 0$.

7.5.2. Heat flow into system

As the coupling of the system spin with its surroundings is given by

$$\hat{H}_{\mathfrak{B},\mathsf{drsys}} = \eta^{-1}\lambda_{\mathsf{dr}}\mathfrak{B}_0 \otimes \mathfrak{B}_3 \otimes \mathfrak{B}_3 \tag{7.68}$$

and since we have

$$\hat{H}_{\mathfrak{B},\mathsf{sys}} + \hat{H}^{\mathsf{eff},1}_{\mathfrak{B},\mathsf{sys}} = \eta^{-1}\omega\mathfrak{B}_0 \otimes \mathfrak{B}_0 \otimes \mathfrak{B}_3 + \eta^{-3}\lambda_{\mathsf{dr}}\varrho^t_{030}\mathfrak{B}_0 \otimes \mathfrak{B}_0 \otimes \mathfrak{B}_3 = \hat{H}'_{\mathfrak{B},\mathsf{sys}}, \tag{7.69}$$

we can immediately infer that

$$\left[\hat{H}'_{\mathfrak{B},\mathsf{sys}}, \hat{H}_{\mathfrak{B},\mathsf{drsys}}\right] = 0. \tag{7.70}$$

Using the cyclic property of the trace then yields

$$đQ_{\mathsf{sys}}(t) = 0 \;\forall\; t. \tag{7.71}$$

Thus, only work is performed on the spin, which immediately gives that condition 1, Sec. 5.2, is fulfilled.

7.6. Effective description of driver

Now, we commence with a LEMBAS treatment of the driver. Again, we start with determination of the effective Hamiltonian for the driver,

$$\hat{H}^{\mathsf{eff}}_{\mathsf{dr}}(t) = \mathrm{Tr}_{\mathsf{sys}}\left\{\hat{H}_{\mathsf{drsys}}(\hat{1}_{\mathsf{dr}} \otimes \hat{\rho}_{\mathsf{sys}})\right\}, \tag{7.72}$$

which reads in the operator basis

$$\hat{H}^{\mathsf{eff}}_{\mathfrak{B},\mathsf{dr}}(t) \overset{(7.12)}{=} \eta^{-1}\sum_{\mu''}\mathrm{Tr}_{\mathsf{sys}}\left\{\lambda_{\mathsf{dr}}(\mathfrak{B}_0\otimes\mathfrak{B}_3\otimes\mathfrak{B}_3)(\mathfrak{B}_0\otimes\mathfrak{B}_0\otimes\mathfrak{B}_{\mu''})\right\}\varrho^t_{00\mu''}\eta^{-4}$$

$$= \eta^{-5}\lambda_{\mathsf{dr}}\sum_{\mu''}\underbrace{\mathfrak{B}_0\mathfrak{B}_0}_{\eta\mathfrak{B}_0}\otimes\underbrace{\mathfrak{B}_3\mathfrak{B}_0}_{\eta\mathfrak{B}_3}\underbrace{\mathrm{Tr}\left\{\mathfrak{B}_3\mathfrak{B}_{\mu''}\right\}}_{\delta_{3\mu''}}\varrho^t_{00\mu''} \tag{7.73}$$

$$= \eta^{-3}\lambda_{\mathsf{dr}}\varrho^t_{003}\mathfrak{B}_0\otimes\mathfrak{B}_3. \tag{7.74}$$

First, we note that according to Eq. (7.38) we have that the effective Hamiltonian is time-independent as $\varrho^t_{003} = \varrho^0_{003}$. This holds irrespective of the initial state. The extension on the total Hilbert space of the effective Hamiltonian gives $\eta^{-4}\lambda_{\mathsf{dr}}\varrho^0_{003}\mathfrak{B}_0\otimes\mathfrak{B}_3\otimes\mathfrak{B}_0$. We can easily infer that

$$\left[\hat{H}^{\mathsf{eff}}_{\mathfrak{B},\mathsf{dr}}(t),\hat{H}_{\mathsf{dr}}\right]\neq 0, \tag{7.75}$$

in general. Only if we would have $\lambda_{\mathsf{drint}} = 0$ the equality above would hold and we would have vanishing $H^{\mathsf{eff},2}_{\mathfrak{B},\mathsf{dr}}$. As this case would lead to no dynamics at all for the special initial state we will require $\lambda_{\mathsf{drint}}\neq 0$ throughout the remainder of this thesis. Now, the task is to identify $\dot{H}^{\mathsf{eff},1}_{\mathfrak{B},\mathsf{dr}}$ and $\dot{H}^{\mathsf{eff},2}_{\mathfrak{B},\mathsf{dr}}$. To this end, we diagonalize $\hat{H}_{\mathfrak{B},\mathsf{dr}}$, by means of

$$\hat{H}^{D}_{\mathfrak{B},\mathsf{dr}} = T\hat{H}_{\mathfrak{B},\mathsf{dr}}T^{-1}, \tag{7.76}$$

where $\hat{H}^{D}_{\mathfrak{B},\mathsf{dr}}$ is a diagonal matrix, T and T^{-1} the transformation matrix and its inverse. The transformation matrix contains the eigenvectors of the operator given in a basis set. With the help of MATHEMATICA we get the eigenvectors and thus the transformation matrix T. We use this transformation on $\hat{H}^{\mathsf{eff}}_{\mathfrak{B},\mathsf{dr}}(t)$,

$$\tilde{\hat{H}}^{\mathsf{eff}}_{\mathfrak{B},\mathsf{dr}} = T\hat{H}^{\mathsf{eff}}_{\mathfrak{B},\mathsf{dr}}(t)T^{-1} = \tilde{\hat{H}}^{\mathsf{eff}}_{\mathfrak{B},\mathsf{dr}}(D) + \tilde{\hat{H}}^{\mathsf{eff}}_{\mathfrak{B},\mathsf{dr}}(nD), \tag{7.77}$$

where $\tilde{\hat{H}}^{\mathsf{eff}}_{\mathfrak{B},\mathsf{dr}}(D)$ is a diagonal matrix containing the diagonal of $\tilde{\hat{H}}^{\mathsf{eff}}_{\mathfrak{B},\mathsf{dr}}$ and $\tilde{\hat{H}}^{\mathsf{eff}}_{\mathfrak{B},\mathsf{dr}}(nD)$ then contains only the off-diagonal elements. Since $\tilde{\hat{H}}^{\mathsf{eff}}_{\mathfrak{B},\mathsf{dr}}(D)$ obviously commutes with $\hat{H}^{D}_{\mathfrak{B},\mathsf{dr}}$ (which is also diagonal in this transformed basis), we choose this part as $\tilde{\hat{H}}^{\mathsf{eff},1}_{\mathfrak{B},\mathsf{dr}}$ and the other as $\tilde{\hat{H}}^{\mathsf{eff},2}_{\mathfrak{B},\mathsf{dr}}$, respectively. Transforming back into the original basis then yields

$$\hat{H}^{\mathsf{eff},1}_{\mathfrak{B},\mathsf{dr}} = T^{-1}\tilde{\hat{H}}^{\mathsf{eff}}_{\mathfrak{B},\mathsf{dr}}(D)T, \tag{7.78}$$

$$\hat{H}^{\mathsf{eff},2}_{\mathfrak{B},\mathsf{dr}} = T^{-1}\tilde{\hat{H}}^{\mathsf{eff}}_{\mathfrak{B},\mathsf{dr}}(nD)T. \tag{7.79}$$

Performing these steps in MATHEMATICA, we get:

$$\hat{H}^{\mathsf{eff},1}_{\mathfrak{B},\mathsf{dr}} = 2N\xi\omega^2(\mathfrak{B}_0\otimes\mathfrak{B}_3+\mathfrak{B}_3\otimes\mathfrak{B}_0)+N\xi\lambda_{\mathsf{drint}}\omega(\mathfrak{B}_1\otimes\mathfrak{B}_1-\mathfrak{B}_2\otimes\mathfrak{B}_2) \tag{7.80}$$

$$\hat{H}^{\mathsf{eff},2}_{\mathfrak{B},\mathsf{dr}} = -N\xi\lambda_{\mathsf{drint}}\omega(\mathfrak{B}_1\otimes\mathfrak{B}_1-\mathfrak{B}_2\otimes\mathfrak{B}_2)+N\xi(\lambda^2_{\mathsf{drint}}+2\omega^2)(\mathfrak{B}_0\otimes\mathfrak{B}_3) - 2N\xi\omega^2(\mathfrak{B}_3\otimes B_0) \tag{7.81}$$

with $\xi\equiv\eta^{-4}\lambda_{\mathsf{dr}}\rho^0_{003}$ and $N\equiv\frac{1}{\lambda^2_{\mathsf{drint}}+4\omega^2}$. Three short consistency checks readily yield $\hat{H}^{\mathsf{eff},1}_{\mathfrak{B},\mathsf{dr}}+\hat{H}^{\mathsf{eff},2}_{\mathfrak{B},\mathsf{dr}}=\hat{H}^{\mathsf{eff}}_{\mathfrak{B},\mathsf{dr}}(t)$, $\left[\hat{H}_{\mathfrak{B},\mathsf{dr}},\hat{H}^{\mathsf{eff},1}_{\mathfrak{B},\mathsf{dr}}\right]=0$, as well as $\left[\hat{H}_{\mathfrak{B},\mathsf{dr}},\hat{H}^{\mathsf{eff},2}_{\mathfrak{B},\mathsf{dr}}\right]\neq 0$. Note, that both, $\hat{H}^{\mathsf{eff},1}_{\mathfrak{B},\mathsf{dr}}$ as well as $\hat{H}^{\mathsf{eff},2}_{\mathfrak{B},\mathsf{dr}}$ are time-independent.

7.6.1. Work performed by driver

Here, we want to quantify the work performed by the driver. For the driver to be perfect, this work should equal the amount of work received by the system.

The first addend is directly found to be zero due to

$$\frac{\mathrm{d}}{\mathrm{d}t}\hat{H}^{\mathsf{eff},1}_{\mathfrak{B},\mathsf{dr}}=0 \implies đW^{(1)}_{\mathfrak{B},\mathsf{dr}}=0, \tag{7.82}$$

according to Eq. (7.74) with $\dot{\rho}^t_{003}=0$.

Next, we use that $\left[\hat{H}_{\mathfrak{B},\mathsf{dr}},\hat{H}^{\mathsf{eff},2}_{\mathfrak{B},\mathsf{dr}}\right]=\left[\hat{H}_{\mathfrak{B},\mathsf{dr}},\hat{H}^{\mathsf{eff}}_{\mathfrak{B},\mathsf{dr}}(t)\right]$ as $\left[\hat{H}_{\mathfrak{B},\mathsf{dr}},\hat{H}^{\mathsf{eff},1}_{\mathfrak{B},\mathsf{dr}}\right]=0$, which then gives in Eq. (5.11)

$$\begin{aligned} đW^{(2)}_{\mathsf{dr}} &= -\mathrm{i}\mathrm{Tr}\left\{\left[\omega(\mathfrak{B}_3\otimes\mathfrak{B}_0+\mathfrak{B}_0\otimes\mathfrak{B}_3)+\lambda_{\mathsf{drint}}\mathfrak{B}_1\otimes\mathfrak{B}_1,\eta^{-3}\lambda_{\mathsf{dr}}\varrho^t_{003}\mathfrak{B}_0\otimes\mathfrak{B}_3\right]\hat{\rho}_{\mathfrak{B},\mathsf{dr}}\right\}\\ &= -\mathrm{i}\eta^{-3}\lambda_{\mathsf{drint}}\lambda_{\mathsf{dr}}\varrho^t_{003}\mathrm{Tr}\left\{[\mathfrak{B}_1\otimes\mathfrak{B}_1,\mathfrak{B}_0\otimes\mathfrak{B}_3]\,\hat{\rho}_{\mathfrak{B},\mathsf{dr}}\right\}\mathrm{d}t\\ &= -\mathrm{i}\eta^{-2}\lambda_{\mathsf{drint}}\lambda_{\mathsf{dr}}\varrho^t_{003}\mathrm{Tr}\left\{\mathfrak{B}_1\otimes[\mathfrak{B}_1,\mathfrak{B}_3]\,\hat{\rho}_{\mathfrak{B},\mathsf{dr}}\right\}\mathrm{d}t, \end{aligned} \tag{7.83}$$

where we have used that the first two addends vanish and that $\mathfrak{B}_1\mathfrak{B}_0=\mathfrak{B}_0\mathfrak{B}_1=\eta\mathfrak{B}_1$. For the commutator we get

$$[\mathfrak{B}_1,\mathfrak{B}_3]=-\mathrm{i}\eta\mathfrak{B}_2-\mathrm{i}\eta\mathfrak{B}_2=-2\mathrm{i}\eta\mathfrak{B}_2=-\mathrm{i}\eta^{-1}\mathfrak{B}_2. \tag{7.84}$$

Substituting

$$\hat{\rho}^t_{\mathfrak{B},\mathsf{dr}}=\mathrm{Tr}_{\mathsf{sys}}\left\{\sum_{\mu\mu'\mu''}\rho^t_{\mu\mu'\mu''}\mathfrak{B}_\mu\otimes\mathfrak{B}_{\mu'}\otimes\mathfrak{B}_{\mu''}\right\}=\eta^{-1}\sum_{\mu\mu'}\varrho^t_{\mu\mu'0}\mathfrak{B}_\mu\otimes\mathfrak{B}_{\mu'} \tag{7.85}$$

and the commutator relation, Eq. (7.84), into Eq. (7.83) gives

$$\begin{aligned} đW_{\mathsf{dr}}^{(2)} &= -\mathrm{i}\eta^{-2}\lambda_{\mathsf{drint}}\lambda_{\mathsf{dr}}\varrho_{003}^{t}(-\mathrm{i})\eta^{-1}\eta^{-1}\sum_{\mu\mu'}\mathrm{Tr}\left\{(\mathfrak{B}_1\otimes\mathfrak{B}_2)(\mathfrak{B}_\mu\otimes\mathfrak{B}_{\mu'})\right\}\varrho_{\mu\mu'0}^{t} \\ &= -\eta^{-4}\lambda_{\mathsf{drint}}\lambda_{\mathsf{dr}}\varrho_{003}^{0}\varrho_{120}^{t} \overset{(7.67)}{=} -đW_{\mathsf{sys}}. \end{aligned} \tag{7.86}$$

Thus, if the remaining contribution to the work vanishes, we have that the work into the spin equals the work delivered by the driver. The opposite sign is due to the convention that energy flow out of the system is counted negatively, energy flow into the system positively. Therefore, the work done **by** the driver (negative for the driver) equals the work done **on** the system (positive). With no other energy flows, this would be the perfect work exchange. Next, let us consider $đW_{\mathsf{dr}}^{(3)}$. To this end, we first have a look at $\left[\hat{H}_{\mathfrak{B},\mathsf{dr}}^{\mathsf{eff},1},\hat{H}_{\mathfrak{B},\mathsf{dr}}^{\mathsf{eff},2}\right]$. After a lengthy but straightforward calculation by using MATHEMATICA we get

$$\left[\hat{H}_{\mathfrak{B},\mathsf{dr}}^{\mathsf{eff},1},\hat{H}_{\mathfrak{B},\mathsf{dr}}^{\mathsf{eff},2}\right] = -\frac{2\mathrm{i}\lambda_{\mathsf{drint}}\eta^{-6}\lambda_{\mathsf{dr}}^{2}(\varrho_{003}^{0})^{2}\omega}{2\lambda_{\mathsf{drint}}^{2}+8\omega^{2}}\left(\mathfrak{B}_1\otimes\mathfrak{B}_2+\mathfrak{B}_2\otimes\mathfrak{B}_1\right). \tag{7.87}$$

Substituting this into Eq. (5.12), we get

$$\begin{aligned} đW_{\mathsf{dr}}^{(3)} &= -\frac{\eta^{-6}\lambda_{\mathsf{drint}}\lambda_{\mathsf{dr}}^{2}(\rho_{003}^{0})^{2}\omega}{\lambda_{\mathsf{drint}}^{2}+4\omega^{2}}\sum_{\mu\mu'}\mathrm{Tr}\left\{\left(\mathfrak{B}_1\otimes\mathfrak{B}_2+\mathfrak{B}_2\otimes\mathfrak{B}_1\right)(\mathfrak{B}_\mu\otimes\mathfrak{B}_{\mu'})\right\}\varrho_{\mu\mu'0}^{t}\eta^{-1} \\ &= -\frac{\eta^{-7}\lambda_{\mathsf{drint}}\lambda_{\mathsf{dr}}^{2}(\varrho_{003}^{0})^{2}\omega}{\lambda_{\mathsf{drint}}^{2}+4\omega^{2}}\left(\varrho_{120}^{t}+\varrho_{210}^{t}\right)\mathrm{d}t. \end{aligned} \tag{7.88}$$

Therefore, condition 3 seems not to be fulfilled. A closer study of the dynamics is necessary in order to decide whether the dynamics is such that this addend really vanishes. Before investigating the dynamics closer, we first have a look at the heat flow.

7.6.2. Heat flow into driver

We start with $đQ_{\mathsf{dr}}^{(1)}$, giving

$$đQ_{\mathsf{dr}}^{(1)} = -\mathrm{i}\mathrm{Tr}\left\{\hat{H}_{\mathfrak{B},\mathsf{dr}}\left[\hat{H}_{\mathfrak{B},\mathsf{drsys}},\hat{C}_{\mathfrak{B},\mathsf{drsys}}\right]\right\}\mathrm{d}t, \tag{7.89}$$

with the correlations between driver and system given by

$$\begin{aligned} \hat{C}_{\mathfrak{B},\mathsf{drsys}} &= \hat{\rho}_{\mathfrak{B}}-\hat{\rho}_{\mathfrak{B},\mathsf{dr}}\otimes\hat{\rho}_{\mathfrak{B},\mathsf{sys}} \\ &= \sum_{\mu\mu'\mu''}\left(\varrho_{\mu\mu'\mu''}^{t}-\varrho_{\mu\mu'0}^{t}\varrho_{00\mu''}^{t}\eta^{-3}\right)\mathfrak{B}_\mu\otimes\mathfrak{B}_{\mu'}\otimes\mathfrak{B}_{\mu''}. \end{aligned} \tag{7.90}$$

By using the cyclic property of the trace we get

$$\begin{aligned}
đQ^{(1)}_{\mathsf{dr}} &= -\mathrm{i}\mathrm{Tr}\left\{\left[\hat{H}_{\mathfrak{B},\mathsf{dr}},\hat{H}_{\mathfrak{B},\mathsf{drsys}}\right]\hat{C}_{\mathfrak{B},\mathsf{drsys}}\right\}\mathrm{d}t \\
&= -\mathrm{i}\eta^{-2}\lambda_{\mathsf{drint}}\mathrm{Tr}\left\{\left[\mathfrak{B}_1\otimes\mathfrak{B}_1\otimes\mathfrak{B}_0,\lambda_{\mathsf{dr}}\mathfrak{B}_0\otimes\mathfrak{B}_3\otimes\mathfrak{B}_3\right]\hat{C}_{\mathfrak{B},\mathsf{drsys}}\right\}\mathrm{d}t \\
&= -\mathrm{i}\lambda_{\mathsf{drint}}\lambda_{\mathsf{dr}}\mathrm{Tr}\left\{\left(\mathfrak{B}_1\otimes[\mathfrak{B}_1,\mathfrak{B}_3]\otimes\mathfrak{B}_3\right)\hat{C}_{\mathfrak{B},\mathsf{drsys}}\right\}\mathrm{d}t, \qquad (7.91)
\end{aligned}$$

where we have used that $\hat{H}_{\mathfrak{B},\mathsf{dr}}$ partially commutes with $\hat{H}_{\mathfrak{B},\mathsf{drsys}}$. From above we already know that $[\mathfrak{B}_1,\mathfrak{B}_3]=-\mathrm{i}\eta^{-1}\mathfrak{B}_2$, thus we get

$$\begin{aligned}
đQ^{(1)}_{\mathsf{dr}} &= -\eta^{-1}\lambda_{\mathsf{drint}}\lambda_{\mathsf{dr}}\mathrm{Tr}\left\{\left(\mathfrak{B}_1\otimes\mathfrak{B}_2\otimes\mathfrak{B}_3\right)\hat{C}_{\mathfrak{B},\mathsf{drsys}}\right\}\mathrm{d}t \\
&= -\eta^{-1}\lambda_{\mathsf{drint}}\lambda_{\mathsf{dr}}\left(\varrho^t_{123}-\varrho^t_{120}\varrho^t_{003}\eta^{-3}\right)\mathrm{d}t, \qquad (7.92)
\end{aligned}$$

where we used Eq. (7.90) in the last step. Finally, we turn to $đQ^{(2)}_{\mathsf{dr}}$. Similarly to above, we find using the cyclic property of the trace

$$\begin{aligned}
đQ^{(2)}_{\mathsf{dr}} &= -\mathrm{i}\mathrm{Tr}\left\{\left[\hat{H}^{\mathsf{eff},1}_{\mathfrak{B},\mathsf{dr}},\hat{H}_{\mathsf{drsys}}\right]\hat{C}_{\mathfrak{B},\mathsf{drsys}}\right\}\mathrm{d}t \\
&= -\frac{\eta^{-1}\lambda_{\mathsf{dr}}\lambda_{\mathsf{drint}}\omega\xi}{\lambda^2_{\mathsf{drint}}+4\omega^2}\mathrm{Tr}\left\{\left(\mathfrak{B}_1\otimes\mathfrak{B}_2\otimes\mathfrak{B}_3+\mathfrak{B}_2\otimes\mathfrak{B}_1\otimes\mathfrak{B}_3\right)\hat{C}_{\mathfrak{B},\mathsf{drsys}}\right\}\mathrm{d}t \\
&= -\frac{\eta^{-4}\lambda^2_{\mathsf{dr}}\lambda_{\mathsf{drint}}\omega\varrho^0_{003}}{\lambda^2_{\mathsf{drint}}+4\omega^2}\left(\varrho^t_{123}-\varrho^t_{120}\varrho^0_{003}\eta^{-3}+\varrho^t_{213}-\varrho^t_{210}\varrho^0_{003}\eta^{-3}\right)\mathrm{d}t. \qquad (7.93)
\end{aligned}$$

Thus, in general, it seems as if the driver might receive heat and an additional work contribution from the system spin. Therefore, we now have a closer look at the dynamics of the compound system.

7.6.3. Detailed investigation of dynamics

In order to solve the equations of motion, we investigate the dynamics in the operator basis. There, we have already found the equations of motion for the 64 coefficients, with the according subdynamics. As only coefficients of the subgroup $\mathbb{S}_{\mathsf{mdg}}$ occur in the equations for heat and work, we only consider its 12 elements. In oder to write the equations of motion in a convenient way, we introduce a vector containing all twelve coefficients,

$$\vec{\rho}(t)=\left(\varrho^t_{030},\varrho^t_{033},\varrho^t_{110},\varrho^t_{113},\varrho^t_{120},\varrho^t_{123},\varrho^t_{210},\varrho^t_{213},\varrho^t_{220},\varrho^t_{223},\varrho^t_{300},\varrho^t_{303}\right)^T. \qquad (7.94)$$

Then, the equations of motion can be written as a matrix-vector multiplication,

$$\dot{\vec{\rho}}(t) = \mathcal{A}\vec{\rho}(t), \tag{7.95}$$

with $\mathcal{A}$ being time-independent as we have only time-independent coefficients, here (constant interactions).

The formal solution can be given easily,

$$\vec{\rho}(t) = \mathrm{e}^{\mathcal{A}t}\vec{\rho}(0). \tag{7.96}$$

In order to compute the matrix exponential $\mathrm{e}^{\mathcal{A}t}$, we diagonalize $\mathcal{A}$. Turning to our actual problem we find that $\mathcal{A}$ is a real-valued skew-symmetric matrix. Therefore, it is a normal matrix as it commutes with its transpose,

$$\mathcal{A}\mathcal{A}^T = \mathcal{A}\,(-\mathcal{A}) = -\mathcal{A}\mathcal{A} = \mathcal{A}^T\mathcal{A}. \tag{7.97}$$

Since it is a normal matrix the spectral theorem applies and we know that it is indeed diagonalizable with a unitary matrix $\mathcal{T}$. Moreover, we know that for even-dimensional skew-symmetric matrices, the eigenvalues λ all come in pairs $\pm\lambda$, and since $\mathcal{A}$ is real-valued, the non-zero eigenvalues are pure imaginary. In our case, we find that we have a four-fold degeneracy of the eigenvalue 0. If MATHEMATICA was able to give orthonormalized eigenvectors the solution would be fairly simple, cf. B.2.

It turns out that the diagonalization is not quite easy for the general case. The problem is to find orthonormal eigenvectors. For the analytic expressions, here, MATHEMATICA is not able to give a set of orthogonalized eigenvectors. Therefore, we consider non-orthogonal basis vectors, which are well-studied due to their importance in crystal theory, e. g.. Details on how the set of ODEs can be solved are given in App. B.3.

For the matrix exponential, we get with the abbreviations $\lambda_{\mathsf{drint}}^2 + \lambda_{\mathsf{dr}}^2 \equiv l_1^2$ and $\lambda_{\mathsf{drint}}^2 + \lambda_{\mathsf{dr}}^2 \pm 4\lambda_{\mathsf{dr}}\omega + 4\omega^2 \equiv l_\pm^2$,

$$\begin{aligned}\mathrm{e}^{\tilde{A}t} = \mathsf{diag}\Big\{&1, 1, 1, 1, \exp(-\mathrm{i}l_1 t), \exp(-\mathrm{i}l_1 t), \exp(+\mathrm{i}l_1 t), \exp(+\mathrm{i}l_1 t), \dots \\ &\exp(-\mathrm{i}l_+ t), \exp(+\mathrm{i}l_+ t), \exp(-\mathrm{i}l_- t), \exp(+\mathrm{i}l_- t)\Big\}.\end{aligned} \tag{7.98}$$

Unfortunately, the general solutions for the coefficients are quite complex and therefore not very insightful. For the special initial state, however, the solutions are relatively simple. As we are interested in the coefficients appearing

in our expressions for heat and work, respectively, we constrict ourselves to these coefficients for the specific initial state. For this we obtain

$$\varrho^t_{120} = -\frac{\mathrm{i}\lambda_{\mathsf{drint}}\left(\mathrm{e}^{\mathrm{i}l_1 t} - \mathrm{e}^{-\mathrm{i}l_1 t}\right)}{4\sqrt{2}l_1} = \frac{\lambda_{\mathsf{drint}}}{2\sqrt{2}l_1}\sin(l_1 t), \tag{7.99}$$

$$\varrho^t_{210} = \frac{\mathrm{i}\lambda_{\mathsf{drint}}\left(\mathrm{e}^{\mathrm{i}l_1 t} - \mathrm{e}^{-\mathrm{i}l_1 t} +\right)}{4\sqrt{2}l_1} = -\varrho^t_{120}, \tag{7.100}$$

$$\varrho^t_{123} = -\frac{\mathrm{i}\lambda_{\mathsf{drint}}\left(\mathrm{e}^{\mathrm{i}l_1 t} - \mathrm{e}^{-\mathrm{i}l_1 t}\right)}{4\sqrt{2}l_1}\chi = \varrho^t_{120}\chi, \tag{7.101}$$

$$\varrho^t_{213} = \frac{\mathrm{i}\lambda_{\mathsf{drint}}\left(\mathrm{e}^{\mathrm{i}l_1 t} - \mathrm{e}^{-\mathrm{i}l_1 t}\right)}{4\sqrt{2}l_1}\chi = -\varrho^t_{123} = \varrho^t_{210}\chi\left(= -\varrho^t_{120}\chi\right). \tag{7.102}$$

We are specially interested in the non-vanishing addends of work and heat for the driver. We start with $đW^{(3)}_{\mathsf{dr}}$, and with our solutions for the special initial state we immediately find that according to Eq. (7.100)

$$\varrho^t_{120} + \varrho^t_{210} = 0. \tag{7.103}$$

Thus, we have that $đW^{(3)}_{\mathsf{dr}} = 0$. Moreover, with $\varrho^t_{003} = \chi\eta^3$, we have for $đQ_{\mathsf{dr}}$,

$$đQ^{(1)}_{\mathsf{dr}} = \eta^{-1}\lambda_{\mathsf{drint}}\lambda_{\mathsf{dr}}\left(\varrho^t_{123} - \varrho^t_{120}\chi\right)\mathrm{d}t = 0 \tag{7.104}$$

as follows directly from Eq. (7.101). Using again that $\varrho^t_{003} = \chi\eta^3$ we have from Eq. (7.93)

$$đQ^{(2)}_{\mathsf{dr}} \propto \underbrace{\varrho^t_{123} - \varrho^t_{120}\chi}_{=0} + \underbrace{\varrho^t_{213} - \varrho^t_{210}\chi}_{=0} = 0, \tag{7.105}$$

where we have used Eqs. (7.101) and (7.102), respectively.

Thus, we end up with $đQ_{\mathsf{dr}} = 0$ and $đW_{\mathsf{dr}} = -đW_{\mathsf{sys}}$, validating conditions 4 and 3 on a perfect driver, Sec. 5.2, respectively. In order to confirm that we have state-independent driving, it is sufficient for our purpose, that the effective Hamiltonian of the system evolves independent of the initially measured state. Thus, we have a look at $\hat{H}^{\mathsf{eff},1}_{\mathfrak{B},\mathsf{sys}}$, given by Eq. 7.63. The time-dependency is solely due to

$$\varrho^t_{030} = \frac{\lambda^2_{\mathsf{dr}} + \lambda^2_{\mathsf{drint}}\cos(l_1 t)}{\sqrt{2l_1}}, \tag{7.106}$$

which is independent of χ and therefore, independent of the initial state of the system (restricting ourselves to diagonal states, initially). Thus, for our

purpose condition 2 is also fulfilled. The two-spin driver can thus act as a perfect work source for the considered initial states.

Moreover, for the two-spin driver we are able to obtain analytical results for the work being performed onto the system, as the solutions for the coefficients connected to work exchange can be integrated easily (cf. Eqs. (7.99)-(7.102)).

7.7. Numerics

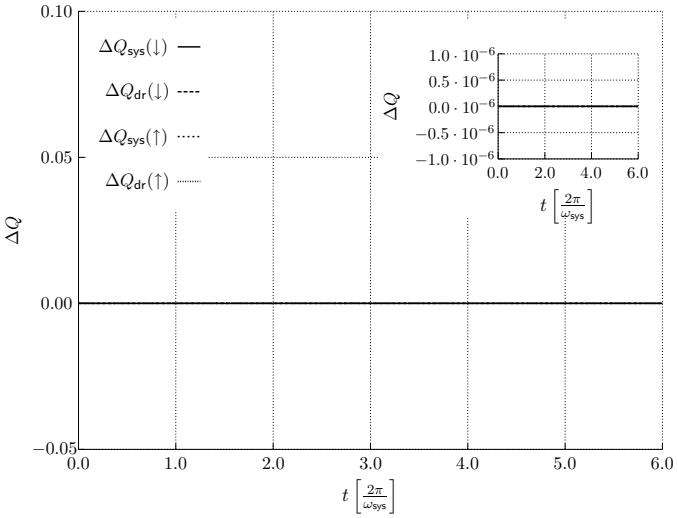

Figure 7.2.: Heat flow into spin, ΔQ_{sys}, and driver, ΔQ_{dr}, for $\hat{\rho}^0_{\mathsf{sys}} = |\downarrow\rangle\langle\downarrow|$ and $\hat{\rho}^0_{\mathsf{sys}} = |\uparrow\rangle\langle\uparrow|$, respectively, over process time t.

Here, we numerically test the analytical findings from the previous section. We start by numerically investigating the heat and work exchange between driver and system. We choose $\omega = 1$, $\lambda_{\mathsf{drint}} = 0.2$, $\lambda_{\mathsf{dr}} = 0.2$ and $\beta_{\mathsf{sys}} = 1.5$. The driver starts in pure factorizing state, $\hat{\rho}^0_{\mathsf{dr}} = |\uparrow\downarrow\rangle\langle\uparrow\downarrow|$. Note that here the inverse temperature of the system, β_{sys}, refers to the bare local temperature.

Fig. 7.2 shows both heat flows, ΔQ_{sys} and ΔQ_{dr} for the initial measurement projecting the system in the ground state and the excited one, respectively. The scale was chosen for better comparison with the work exchange, while the inset allows to confirm that the heat flows really vanish within numerical accuracy. Our analytical findings of Secs. 7.5.2 and 7.6.3 are in perfect agreement with the numerics.

For the work exchange between system and driver, we find that the direction of the energy flow depends on the initial state the system was measured in, cf. Figs. 7.3 and 7.4, for $\hat{\rho}^0_{\mathsf{sys}} = |{\downarrow}\rangle\langle{\downarrow}|$ and $\hat{\rho}^0_{\mathsf{sys}} = |{\uparrow}\rangle\langle{\uparrow}|$, respectively. In the first case the driver extracts work from the system while in the second one, the driver exerts work onto the system. This is quite analogous to Sec. 6.3. Also, it looks like the work exchange between system and driver is perfect in the sense that the energy is transfered without losses as found in the analytical study (cf. Sec. 7.6.3).

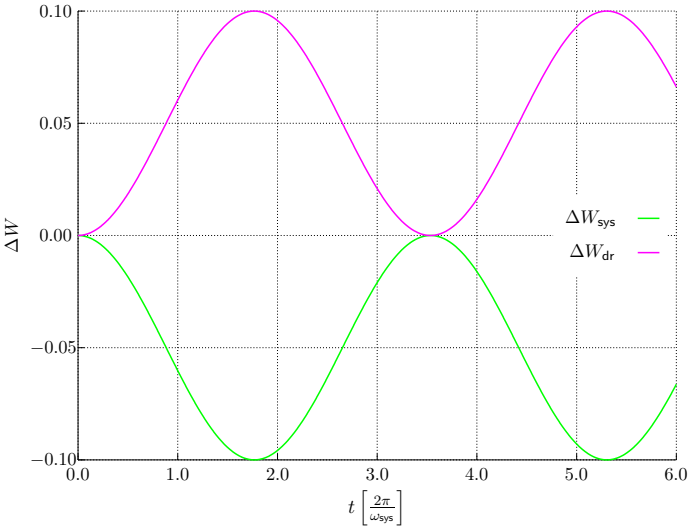

Figure 7.3.: Work exerted onto the system, ΔW_{sys} by the driver, ΔW_{dr} for $\hat{\rho}^0_{\mathsf{sys}} = |{\downarrow}\rangle\langle{\downarrow}|$ over process time t.

A closer investigation, however, yields that the work exchange given by our numerics is not perfect, cf. Fig. 7.5. The finite error should be due to numerical accuracy, as we have to integrate the work exchange for several times t, approximating the integral by a series of rectangles. Thus, the error may add up, explaining the relatively large difference between the work flows. We can easily check this assumption by comparing the analytic solutions for the work exchange, $\Delta W^{\mathsf{ana}}_{\mathsf{sys}}$ and $\Delta W^{\mathsf{ana}}_{\mathsf{dr}}$ with the numerical solutions. We find that $\Delta W^{\mathsf{ana}}_{\mathsf{sys}} = \Delta W_{\mathsf{sys}}$ within numerical accuracy, but $\Delta W^{\mathsf{ana}}_{\mathsf{dr}} \neq \Delta W_{\mathsf{dr}}$. From Fig. 7.6 we can infer that, indeed, the numerical error from the integration, $\delta W^{\mathsf{ana}}_{\mathsf{dr}} \equiv \Delta W^{\mathsf{ana}}_{\mathsf{dr}} - \Delta W^{\mathsf{num}}_{\mathsf{dr}}$, is responsible for the misfit of energy flows, as the difference between the numerical and the analytical solution equals the difference of energy flows into the system and the driver.

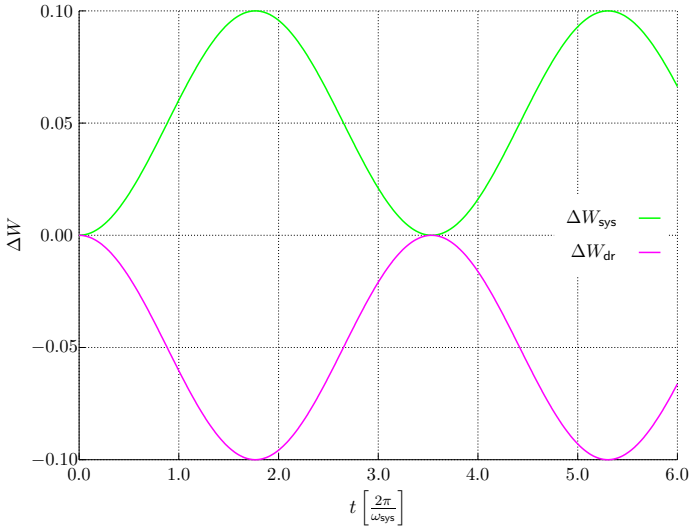

Figure 7.4.: Work exerted onto the system, ΔW_{sys} by the driver, ΔW_{dr} for $\hat{\rho}^0_{\mathsf{sys}} = |\uparrow\rangle\langle\uparrow|$ over process time t.

For further studies, it is important to keep this error on an acceptable level. On the one hand, the error should not exceed a certain threshold, on the other hand the numerical effort, rising approximately linearly with the number of time steps calculated, has to be tolerable. Fig. 7.7 shows the relative deviation δW_{dr} for $\hat{\rho}^0_{\mathsf{sys}} = |\downarrow\rangle\langle\downarrow|$ for different numbers of integration steps, N_{step}. As can be seen, a moderate number of $N_{\mathsf{step}} \approx 1000$ gives already quite good results.

Last, we check the state-dependency of the driver. We proceed analogously to Sec. 6.3, investigating the effective partition sum of the system. As Fig. 7.8 shows, the evolution of the partition sum does not depend on the initial state of the system as both curves, for $\hat{\rho}^0_{\mathsf{sys}} = |\downarrow\rangle\langle\downarrow|$ and $\hat{\rho}^0_{\mathsf{sys}} = |\uparrow\rangle\langle\uparrow|$ coincide. The small inset shows the relative deviation $\delta_{\mathsf{rel}} Z^{\mathsf{eff}}_{\mathsf{sys}}[\uparrow;\downarrow]$, cf. Eq. (6.20). Thus, we have state-independent driving as required by condition 3.

The numerical results are in perfect agreement with the analytical findings of the preceding sections.

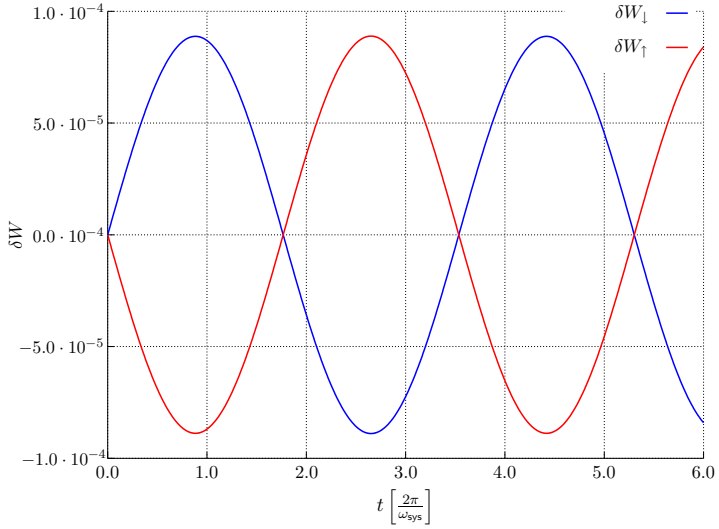

Figure 7.5.: $\delta W = \Delta W_{\mathsf{sys}} + \Delta W_{\mathsf{dr}}$ for $\hat{\rho}^0_{\mathsf{sys}} = |{\downarrow}\rangle\langle{\downarrow}|$ (blue line) and $\hat{\rho}^0_{\mathsf{sys}} = |{\uparrow}\rangle\langle{\uparrow}|$ (red line) over process time t.

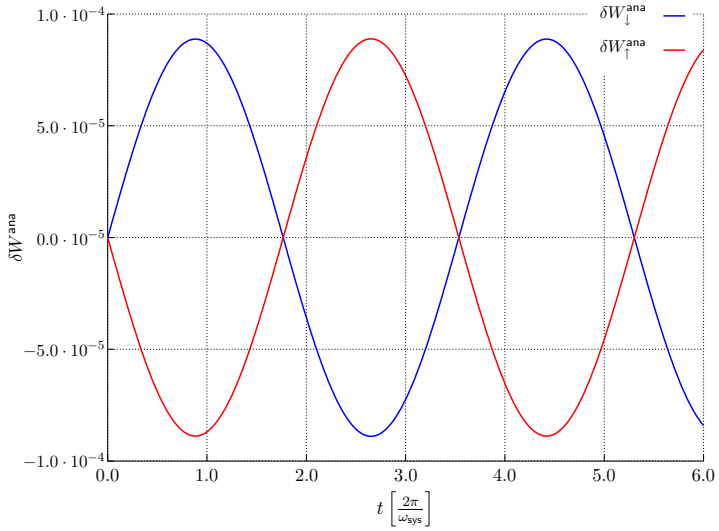

Figure 7.6.: Deviation of numerical from analytical result, $\delta W^{\mathsf{ana}}_{\mathsf{dr}}$, for $\hat{\rho}^0_{\mathsf{sys}} = |{\downarrow}\rangle\langle{\downarrow}|$ (blue line) and $\hat{\rho}^0_{\mathsf{sys}} = |{\uparrow}\rangle\langle{\uparrow}|$ (red line) over time t.

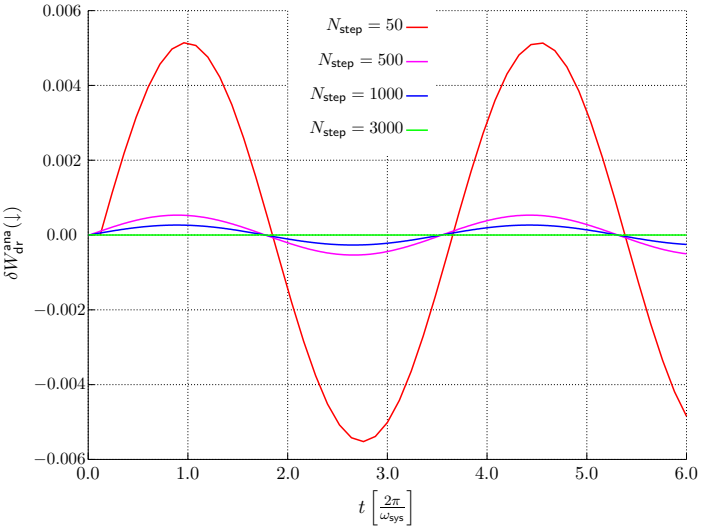

Figure 7.7.: Deviation of numerical result from analytical prediction, $\delta W_{\mathsf{dr}}^{\mathsf{ana}}$, for $\hat{\rho}_{\mathsf{sys}}^{0} = |\downarrow\rangle\langle\downarrow|$ for different numbers of integration steps, N_{step}.

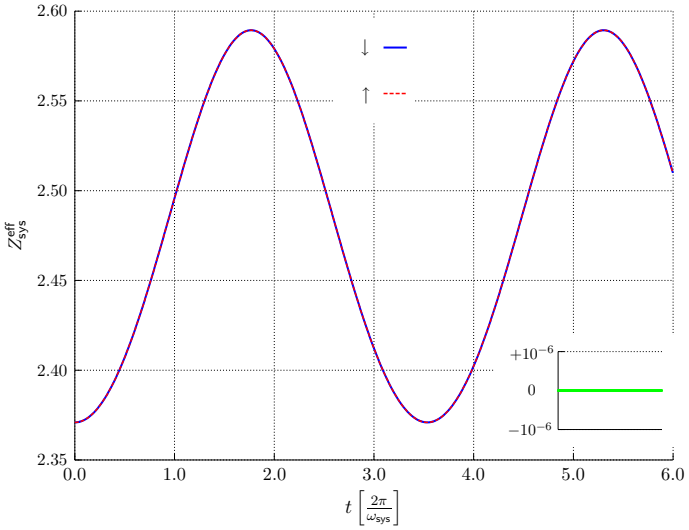

Figure 7.8.: Effective partition sum of the system, $Z_{\mathsf{sys}}^{\mathsf{eff}}(t)$, for $\hat{\rho}_{\mathsf{sys}}^{0} = |\downarrow\rangle\langle\downarrow|$ (blue line) and $\hat{\rho}_{\mathsf{sys}}^{0} = |\uparrow\rangle\langle\uparrow|$ (red dashed line). The inset shows the relative deviation of both partition sums, $\delta_{\mathsf{rel}} Z_{\mathsf{sys}}^{\mathsf{eff}}[\uparrow;\downarrow]$.

8. Two-spin model: Heat

In this chapter, we present a simple example for an "environment" that acts as a perfect heat source in the sense of Sec. 5.3. The compound closed system consists of two coupled spins, here. It might be surprising that it could be possible as well as feasible to consider a single spin as an "environment" which exchanges heat with another spin. One may argue that thermodynamic variables make no sense in such a setting. However, using LEMBAS we are able to discuss heat and work exchange for two spins and we will see that this distinction can indeed be helpful (and therefore sensible) for an intuitive understanding of the results for the JR and the fluctuation estimators introduced in Chap. 9.

8.1. Single spin as heat source

We consider two coupled spins with the following Hamiltonian,

$$\hat{H} \equiv \hat{H}_{\mathsf{sys}} + \hat{H}_{\mathsf{env}} + \frac{\lambda_{\mathsf{env}}}{2}\hat{\sigma}_x \otimes \hat{\sigma}_x, \tag{8.1}$$

with $\hat{H}_{\mathsf{sys}} = \frac{\omega_{\mathsf{sys}}}{2}\hat{\sigma}_z$ and $\hat{H}_{\mathsf{env}} = \frac{\omega_{\mathsf{env}}}{2}\hat{\sigma}_z$. As for the driver, we use the operator basis introduced in Chap. 7, Sec. 7.1, Eqs. (7.5). In this operator basis, the Hamiltonian reads

$$\hat{H}_{\mathfrak{B}} = \omega_{\mathsf{sys}}\mathfrak{B}_3 \otimes \mathfrak{B}_0 + \omega_{\mathsf{env}}\mathfrak{B}_0 \otimes \mathfrak{B}_3 + \lambda_{\mathsf{env}}\mathfrak{B}_1 \otimes \mathfrak{B}_1. \tag{8.2}$$

Now, we proceed as for the perfect driver. We start by investigating the system, first, and then turn to the environment. (Here both are interchangeable.)

8.1.1. Local effective description of the system

The effective Hamiltonian of the system, $\hat{H}^{\mathsf{eff}}_{\mathsf{sys}}$, is given by

$$\begin{aligned}\hat{H}^{\mathsf{eff}}_{\mathfrak{B},\mathsf{sys}}(t) &= \eta^{-1}\lambda_{\mathsf{env}} \sum_{\mu} \mathrm{Tr}_{\mathsf{env}}\{(\mathfrak{B}_1 \otimes \mathfrak{B}_1)(\mathfrak{B}_0 \otimes \mathfrak{B}_{\mu'})\}\varrho^t_{0\mu'} \\ &= \lambda_{\mathsf{env}}\varrho^t_{01}\mathfrak{B}_1. \end{aligned} \tag{8.3}$$

Obviously, we have $\hat{H}^{\mathsf{eff},1}_{\mathfrak{B},\mathsf{sys}} = 0$ and $\hat{H}^{\mathsf{eff},2}_{\mathfrak{B},\mathsf{sys}} = \hat{H}^{\mathsf{eff}}_{\mathfrak{B},\mathsf{sys}}(t)$. With this we find according to Eqs. (5.10) to (5.12) for the work performed onto the system $đW^{(1)}_{\mathsf{sys}} = 0$, $đW^{(3)}_{\mathsf{sys}} = 0$ and

$$\begin{aligned} đW_{\mathsf{sys}} = đW^{(2)}_{\mathsf{sys}} &= -\mathrm{i}\omega_{\mathsf{sys}}\lambda_{\mathsf{env}}\varrho^t_{01}\sum_\mu \mathrm{Tr}\left\{[\mathfrak{B}_3,\mathfrak{B}_1]\mathfrak{B}_\mu\right\}\varrho^t_{\mu 0}\mathrm{d}t \\ &= -\mathrm{i}\omega_{\mathsf{sys}}\lambda_{\mathsf{env}}\varrho^t_{01}\sum_\mu \mathrm{Tr}\left\{\mathrm{i}\mathfrak{B}_2\mathfrak{B}_\mu\right\}\varrho^t_{\mu 0}\mathrm{d}t \\ &= \omega_{\mathsf{sys}}\lambda_{\mathsf{env}}\varrho^t_{01}\varrho^t_{20}\mathrm{d}t. \end{aligned} \tag{8.4}$$

Thus, in general, the environment acts at least partially as an external driver onto the system.

Next, we turn to the heat flow into the system. From Eqs. (5.13) and (5.14), we have $đQ^{(2)}_{\mathsf{sys}} = 0$ and

$$\begin{aligned} đQ^{(1)}_{\mathsf{sys}} &= -\mathrm{i}\eta^{-1}\omega_{\mathsf{sys}}\lambda_{\mathsf{env}}\mathrm{Tr}\left\{\mathfrak{B}_3\otimes\mathfrak{B}_0[\mathfrak{B}_1\otimes\mathfrak{B}_1,\hat{C}_{\mathfrak{B},\mathsf{se}}]\right\}\mathrm{d}t \\ &= \omega_{\mathsf{sys}}\lambda_{\mathsf{env}}\mathrm{Tr}\left\{\mathfrak{B}_2\otimes\mathfrak{B}_1\hat{C}_{\mathfrak{B},\mathsf{se}}\right\}\mathrm{d}t. \end{aligned} \tag{8.5}$$

With the correlations in the operator basis, given by

$$\hat{C}_{\mathfrak{B},\mathsf{se}} = \sum_{\mu\mu'}\varrho^t_{\mu\mu'}\mathfrak{B}_\mu\otimes\mathfrak{B}_{\mu'} - \eta^{-2}\sum_{\mu\mu'}\varrho^t_{\mu 0}\varrho^t_{0\mu'}\mathfrak{B}_\mu\otimes\mathfrak{B}_{\mu'}, \tag{8.6}$$

we have

$$đQ^{(1)}_{\mathsf{sys}} = \omega_{\mathsf{sys}}\lambda_{\mathsf{env}}\left(\varrho^t_{21} - \eta^{-2}\varrho^t_{20}\varrho^t_{01}\right). \tag{8.7}$$

In order to determine the energy flows, we investigate the dynamics more closely. This study is closely related to the one for the perfect driver. Indeed, as only two spins are involved, here, it is much more easy to find the solutions.

We start by restricting ourselves to a special class of initial states given by

$$\hat{\rho}^0 = \hat{\rho}^D_{\mathsf{sys}}\otimes\hat{\rho}^D_{\mathsf{env}}, \tag{8.8}$$

which describes a factorizing state of two systems, both in a diagonal state in their respective energy-eigenbasis. The probability of the system being in its ground state is given by c_{sys}, the one for the environment by c_{env}. Then, we have for the initial coefficients in the operator basis

$$\begin{aligned} &\varrho^0_{00} = \eta^2,\ \varrho^0_{03} = \eta^2 - c_{\mathsf{env}},\ \varrho^0_{30} = \eta^2 - c_{\mathsf{sys}}, \\ &\varrho^0_{33} = \eta^2\left(-1+2c_{\mathsf{env}}\right)\left(-1+2c_{\mathsf{sys}}\right), \end{aligned} \tag{8.9}$$

while all other coefficients vanish. From this we can immediately identify 8 vanishing coefficients at any time t. Moreover, we have two constants of motion from the equations of motion, $\dot{\varrho}_{00}(t) = 0$ and $\dot{\varrho}_{33}(t) = 0$, which lead to $\varrho^t_{00} = \eta^2$ (norm conservation) and $\varrho^t_{33} = \eta^2\,(-1 + 2c_{\mathsf{env}})\,(-1 + 2c_{\mathsf{sys}})$, which is related to the total magnetization.

For the considered initial state we find that $\varrho^t_{20} = 0$ and $\varrho^t_{01} = 0$ at any time t, thus we have that $đW_{\mathsf{sys}} = 0$, cf. Eq. (8.4). Moreover, the heat flow simplifies to

$$đQ^{(1)}_{\mathsf{sys}} = \omega_{\mathsf{sys}}\lambda_{\mathsf{env}}\varrho^t_{21}\mathrm{d}t. \tag{8.10}$$

For the special class of initial states condition 1 on the perfect heat source, cf. Sec. 5.3, is fulfilled. Next, we turn to the source itself.

8.1.2. Effective description of the environment

Due to the symmetry of the total system and the coupling, the treatment of the environment is very similar to the one for the system. The effective Hamiltonian $\hat{H}^{\mathsf{eff}}_{\mathsf{env}}$ of the environment reads

$$\begin{aligned}\hat{H}^{\mathsf{eff}}_{\mathfrak{B},\mathsf{env}}(t) &= \eta^{-1}\lambda_{\mathsf{env}}\sum_{\mu}\mathrm{Tr}_{\mathsf{env}}\{(\mathfrak{B}_1\otimes\mathfrak{B}_1)(\mathfrak{B}_\mu\otimes\mathfrak{B}_3)\}\varrho^t_{\mu 0}\\ &= \lambda_{\mathsf{env}}\varrho^t_{10}\mathfrak{B}_1.\end{aligned} \tag{8.11}$$

Obviously, we have $\hat{H}^{\mathsf{eff},1}_{\mathfrak{B},\mathsf{env}} = 0$ and $\hat{H}^{\mathsf{eff},2}_{\mathfrak{B},\mathsf{env}} = \hat{H}^{\mathsf{eff}}_{\mathfrak{B},\mathsf{env}}(t)$. With this we find according to Eqs. (5.10) to (5.12) for the work performed on the environment $đW^{(1)}_{\mathsf{env}} = 0$, $đW^{(3)}_{\mathsf{env}} = 0$ and

$$\begin{aligned}đW_{\mathsf{env}} = đW^{(2)}_{\mathsf{env}} &= -\mathrm{i}\omega_{\mathsf{env}}\lambda_{\mathsf{env}}\varrho^t_{10}\sum_{\mu'}\mathrm{Tr}\left\{[\mathfrak{B}_3,\mathfrak{B}_1]\mathfrak{B}_{\mu'}\right\}\varrho^t_{0\mu'}\mathrm{d}t\\ &= \omega_{\mathsf{env}}\lambda_{\mathsf{env}}\varrho^t_{10}\varrho^t_{02}\mathrm{d}t.\end{aligned} \tag{8.12}$$

For the special class of initial states we have that $\varrho^t_{10} = 0$ and $\varrho^t_{02} = 0$ at any time t, thus $đW^{(2)}_{\mathsf{env}} = 0$. Condition 2 for a perfect heat source is therefore fulfilled. In order to check the last condition we investigate the heat flow according to LEMBAS. From Eqs. (5.13) and (5.14), we have $đQ^{(2)}_{\mathsf{env}} = 0$ and

$$\begin{aligned}đQ^{(1)}_{\mathsf{env}} &= -\mathrm{i}\eta^{-1}\omega_{\mathsf{env}}\lambda_{\mathsf{env}}\mathrm{Tr}\left\{\mathfrak{B}_0\otimes\mathfrak{B}_3[\mathfrak{B}_1\otimes\mathfrak{B}_1,\hat{C}_{\mathfrak{B},\mathsf{se}}]\right\}\mathrm{d}t\\ &= \omega_{\mathsf{env}}\lambda_{\mathsf{env}}\mathrm{Tr}\left\{\mathfrak{B}_1\otimes\mathfrak{B}_2\hat{C}_{\mathfrak{B},\mathsf{se}}\right\}\mathrm{d}t.\end{aligned} \tag{8.13}$$

Using Eq.(8.6) gives

$$đQ^{(1)}_{\mathsf{env}} = \omega_{\mathsf{env}}\lambda_{\mathsf{env}}\left(\varrho^t_{12} - \eta^{-2}\varrho^t_{10}\varrho^t_{02}\right)\mathrm{d}t. \tag{8.14}$$

As we know the second addend to vanish, we end up with

$$đQ^{(1)}_{\mathsf{env}} = \omega_{\mathsf{env}}\lambda_{\mathsf{env}}\varrho^t_{12}\mathrm{d}t. \tag{8.15}$$

In order to decide whether condition 3 does hold, we solve the dynamics in the same way as for the perfect driver. For the quite general case, the dynamics are quite involved and not very insightful. For the special class of initial states and by additionally requiring $\omega_{\mathsf{sys}} = \omega_{\mathsf{env}} \equiv \omega$, we still have quite complex solutions. Therefore, we additionally choose $\omega = 1$. With this we then find

$$\varrho^t_{12} = \frac{c_{\mathsf{env}} - c_{\mathsf{sys}}}{2}\sin\left(\lambda_{\mathsf{env}}t\right) + \frac{c_{\mathsf{env}} + c_{\mathsf{sys}} - 1}{2\sqrt{4+\lambda^2_{\mathsf{env}}}}\lambda_{\mathsf{env}}\sin\left(\sqrt{4+\lambda^2_{\mathsf{env}}}t\right) \tag{8.16}$$

$$\varrho^t_{21} = -\frac{c_{\mathsf{env}} - c_{\mathsf{sys}}}{2}\sin\left(\lambda_{\mathsf{env}}t\right) + \frac{c_{\mathsf{env}} + c_{\mathsf{sys}} - 1}{2\sqrt{4+\lambda^2_{\mathsf{env}}}}\lambda_{\mathsf{env}}\sin\left(\sqrt{4+\lambda^2_{\mathsf{env}}}t\right) \tag{8.17}$$

from which immediately follows $đQ^{(1)}_{\mathsf{env}} \neq -đQ^{(1)}_{\mathsf{sys}}$, in general[1]. Thus, condition 3 is generally not fulfilled, even for the special class of initial states with $\omega_{\mathsf{sys}} = \omega_{\mathsf{env}}$. We can use the analytic solution for the density operator in order to directly calculate the heat flow. For the special case considered above we easily find

$$\Delta Q_{\mathsf{env}} = \frac{c_{\mathsf{env}} - c_{\mathsf{sys}}}{2}\cos\left(\lambda_{\mathsf{env}}t\right) + \frac{c_{\mathsf{env}} + c_{\mathsf{sys}} - 1}{2\left(4+\lambda^2_{\mathsf{env}}\right)}\lambda^2_{\mathsf{env}}\cos\left(\sqrt{4+\lambda^2_{\mathsf{env}}}t\right), \tag{8.18}$$

$$\Delta Q_{\mathsf{sys}} = -\frac{c_{\mathsf{env}} - c_{\mathsf{sys}}}{2}\cos\left(\lambda_{\mathsf{env}}t\right) + \frac{c_{\mathsf{env}} + c_{\mathsf{sys}} - 1}{2\left(4+\lambda^2_{\mathsf{env}}\right)}\lambda^2_{\mathsf{env}}\cos\left(\sqrt{4+\lambda^2_{\mathsf{env}}}t\right). \tag{8.19}$$

Note, that the integration was performed without substituting any borders, thus we have given the antiderivative, here. In order to get the actual heat flows we have to renormalize so that $\Delta Q_{\mathsf{env}}(t=0) = \Delta Q_{\mathsf{sys}}(t=0) = 0$. As $\cos(0) = 1$, this can be done easily, here, giving the sine instead of the cosine.

If both spins start with the same inverse initial temperature, $\beta_{\mathsf{sys}} = \beta_{\mathsf{env}} \implies c_{\mathsf{sys}} = c_{\mathsf{env}}$, only the first addend vanishes (for $c_{\mathsf{env}} \neq \frac{1}{2}$) and we generally have a heat exchange, nevertheless. However, the second addend gives rise to a

[1] Note, that for $c_{\mathsf{sys}} = c_{\mathsf{env}} = \frac{1}{2}$ we have that $\varrho^t_{12} = 0 = \varrho^t_{21}\ \forall\ t$. This initial state would not give rise to any heat flow, as was to be expected since the Hamiltonian commutes with $\hat{\rho}^0$, then.

heat flow in second order coupling strength, λ_{env}^2. If this coupling strength is small, we approximately have $đQ_{\mathsf{sys}} \approx -đQ_{\mathsf{env}}$ due to

$$\Delta Q_{\mathsf{sys}} + \Delta Q_{\mathsf{env}} = \frac{c_{\mathsf{env}} + c_{\mathsf{sys}} - 1}{(4 + \lambda_{\mathsf{env}}^2)} \lambda_{\mathsf{env}}^2 \sin\left(\sqrt{4 + \lambda_{\mathsf{env}}^2}\, t\right), \tag{8.20}$$

which comes close to the perfect heat source for small λ_{env} as then $\Delta Q_{\mathsf{sys}} + \Delta Q_{\mathsf{env}} \approx 0$. In this sense, we have found the *almost* perfect heat source according to conditions 1 to 3. Note, that we have already substituted the cosine by the sine which we would have by a definite integral with borders as $\Delta Q_{\mathsf{sys}}(0) + \Delta Q_{\mathsf{env}}(0) = 0 + 0 = 0$.

8.2. Numerics

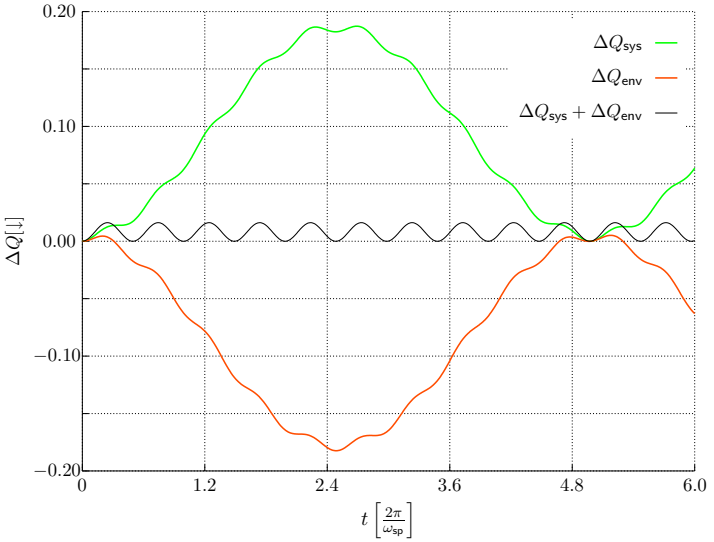

Figure 8.1.: Total heat flows ΔQ_{sys} (green) and ΔQ_{env} (orange) as well as the sum δQ (black) for $\hat{\rho}_{\mathsf{sys}}^0 = |{\downarrow}\rangle\langle{\downarrow}|$ over time t.

For the following discussion, we call one spin the environment, and the other one the system. The compound system starts in a factorizing state. The system is being measured initially, thus starts either in the ground state, $\hat{\rho}_{\mathsf{sys}}^0 = |{\downarrow}\rangle\langle{\downarrow}|$, or in the excited state, $\hat{\rho}_{\mathsf{sys}}^0 = |{\uparrow}\rangle\langle{\uparrow}|$. For the numerics we choose $\omega_{\mathsf{sys}} = \omega_{\mathsf{env}} = 1$, $\lambda_{\mathsf{env}} = 0.2$ and $\beta_{\mathsf{env}} = 1.5$. We solve the Schrödinger equation by exact diagonalization.

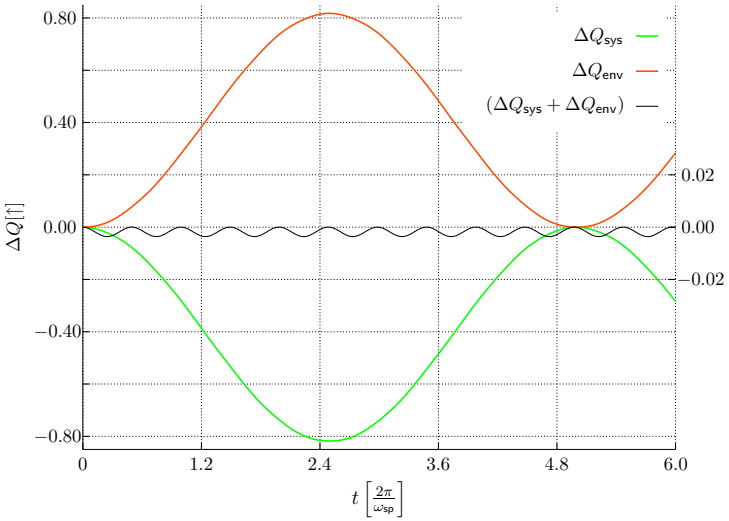

Figure 8.2.: Total heat flows ΔQ_{sys} (green) and ΔQ_{env} (orange) as well as the sum δQ (black) for $\hat{\rho}^0_{\mathsf{sys}} = |\uparrow\rangle\langle\uparrow|$ over time t. Note that the sum (black line) was multiplied by a factor of 10 in order to be visible here, thus the scale on the right-hand side applies for the black line without multiplication.

For the work according to LEMBAS we find indeed that $\Delta W_{\mathsf{sys}} = \Delta W_{\mathsf{dr}} = 0$. Thus, the two spins only exchange heat. The actual heat flows can be found in Fig. 8.1 for $\hat{\rho}^0_{\mathsf{sys}} = |\downarrow\rangle\langle\downarrow|$ and in Fig. 8.2 for $\hat{\rho}^0_{\mathsf{sys}} = |\uparrow\rangle\langle\uparrow|$. Note, that the heat flows do not compensate each other, as predicted by Eq. (8.20), which predicts a sinusoidal remainder for the sum. Indeed, the black curve representing $\delta Q \equiv \Delta Q_{\mathsf{sys}} + \Delta Q_{\mathsf{env}}$ exhibits a sinusoidal behavior. For $\hat{\rho}^0_{\mathsf{sys}} = |\uparrow\rangle\langle\uparrow|$, the total heat flow is much bigger than for $\hat{\rho}^0_{\mathsf{sys}} = |\downarrow\rangle\langle\downarrow|$. This is due to the fact that the environmental spin starts in a thermal state with an occupation probability for the ground state of about 80%, $c_{\mathsf{env}} \approx 0.8$, thus it can rather absorb than emit heat. Moreover, from Eq. (8.20) we have that

$$c_{\mathsf{env}} + c_{\mathsf{sys}} - 1 \approx \begin{cases} 0.8 & \text{for } c_{\mathsf{sys}} = 1 \iff \hat{\rho}^0_{\mathsf{sys}} = |\downarrow\rangle\langle\downarrow| \\ -0.2 & \text{for } c_{\mathsf{sys}} = 0 \iff \hat{\rho}^0_{\mathsf{sys}} = |\uparrow\rangle\langle\uparrow|\,, \end{cases} \tag{8.21}$$

which explains the sign as well as the absolute of δQ, which is only about $\frac{1}{4}$ for $\hat{\rho}^0_{\mathsf{sys}} = |\uparrow\rangle\langle\uparrow|$ of the absolute compared to $\hat{\rho}^0_{\mathsf{sys}} = |\downarrow\rangle\langle\downarrow|$. Due to that and the fact that the total heat flow is bigger for an initially excited system state, the scale for δQ had to be adapted in Fig. 8.2.

For comparison with the analytical result cf. Fig. 8.3. For further studies it is important to investigate how the error arising from numerical integration of the heat and work flows is influenced by the number of integration steps, N_{step}. The deviation of the numerically integrated heat flow into the system with respect to the analytical result, $\delta_{\mathsf{num}} Q_{\mathsf{sys}}$ is plotted in Fig. 8.4 for $\hat{\rho}^0_{\mathsf{sys}} = |\uparrow\rangle\langle\uparrow|$. The more integration steps N_{steps} are used, the less the deviation. However, the numerical effort increases approximately linear with increasing N_{step}. Thus, it seems reasonable to choose $N_{\mathsf{step}} \approx 3000$ for this time-interval.

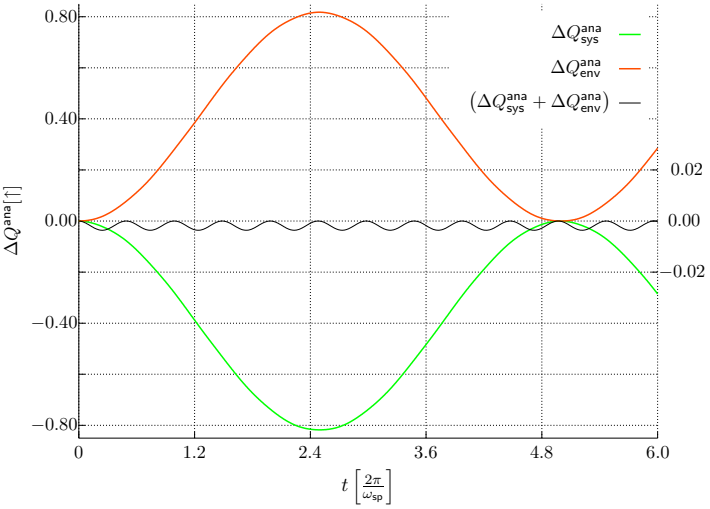

Figure 8.3.: Analytically calculated total heat flows ΔQ_{sys} (green) and ΔQ_{env} (orange) as well as the sum δQ (black) for $\hat{\rho}^0_{\mathsf{sys}} = |\uparrow\rangle\langle\uparrow|$ over time t. Note that δQ was multiplied by 10 in order to be visible here, thus the scale on the right-hand side applies for the black line without multiplication.

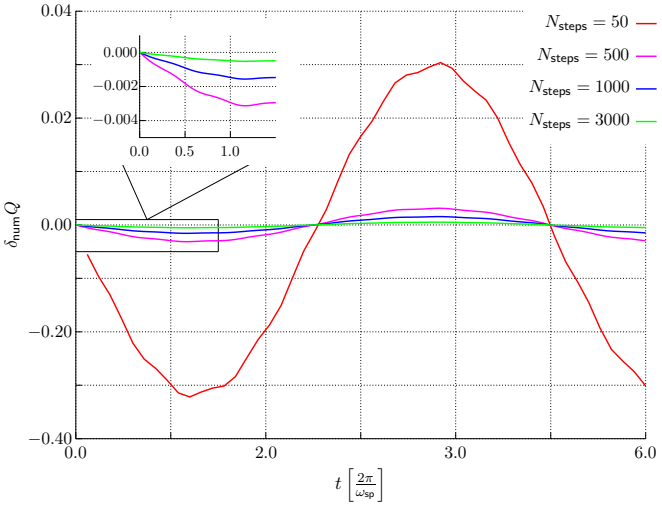

Figure 8.4.: Deviation $\delta_{\mathsf{num}}Q$ of numerical integration with respect to analytical result for different numbers of integration steps, N_{steps}. The inset shows the region from $t = 0$ to $t = 1.5$.

Part III.

Generalizations of the quantum Jarzysnki relation

9. Estimation methods for local effective free energy

9.1. Overview of estimation methods

In the following, we will consider different methods concerning local effective dynamics, which aim at predicting the local effective free energy change,

$$\Delta F^{\mathsf{eff}}_{\mathsf{sys}} = -\beta^{-1}_{\mathsf{sys}} \ln\left(\frac{Z^{\mathsf{eff}}_{\mathsf{sys}}(t)}{Z^{\mathsf{eff}}_{\mathsf{sys}}(0)}\right) = -\beta^{-1}_{\mathsf{sys}} \ln\left(\frac{\mathrm{Tr}\left\{\mathrm{e}^{-\beta_{\mathsf{sys}}\hat{H}'_{\mathsf{sys}}(t)}\right\}}{\mathrm{Tr}\left\{\mathrm{e}^{-\beta_{\mathsf{sys}}\hat{H}'_{\mathsf{sys}}(0)}\right\}}\right). \tag{9.1}$$

If not stated otherwise, we will choose the respective measurement basis to coincide with the energy-eigenbasis of the bare subsystem. Moreover, we will keep this measurement basis fixed over the whole procedure. The initial state of the system of interest is required to be canonical. According to their functionality we split the total system into a driving part (dr), the system of interest (sys) and an environment (env). The driver should be almost perfect (Sec. 5.2, $\Delta Q_{\mathsf{dr}} \approx 0$, in particular). Moreover, we require a physical separation of driver and environment, thus there is no direct coupling between these two functional parts. Then, for all estimation methods the system (sys) is projectively measured initially as well as at the end of the process. This procedure is then repeated many times giving a fluctuating quantity $\chi(f,i)$, say. Here, i and f denote the eigenstates the system has been projected into by the measurements. Then, the average $\overline{\mathrm{e}^{-\beta_{\mathsf{sys}}\chi(f,i)}}$ is taken, trying to estimate $\Delta F^{\mathsf{eff}}_{\mathsf{sys}}$, as is done by the JR (there, $\chi(f,i) = \Delta W(f,i)$). Only for bilocal EFT, the environment is also projectively measured immediately after the measurements on the system. There, we consider the average $\overline{\mathrm{e}^{-\beta_{\mathsf{sys}}\chi(f,i)}\mathrm{e}^{-\beta_{\mathsf{env}}\chi'(f',i')}}$.

For a better overview, we first give a short summary of the different estimation methods we want to consider in the following: (The bracket refers to respective measurements of subsystem (dr, sys, env), respectively.)

[$\cdot\boldsymbol{E}\cdot$] : **E**nergy **F**luctuation **T**heorem, EFT. Here, we consider two-time energy measurements E on the system of interest (sys), where we measure the system locally in the beginning and at the end of a process (cf. Sec. 9.2).

[$\cdot EE$] : bilocal EFT. The bilocal EFT will be of interest if we have two coupled systems where typically only one of them is driven. Here, we measure the effective energy of both systems (sys and env) in the beginning and at the end of the process, respectively (cf. also Chap. 4, Sec. 4.3). The instantaneous measurements are performed in a definite order (cf. Sec. 9.3).

[$W\cdot\cdot$], [$\cdot W\cdot$] : Jarzynski method. Since this method is directly linked to the JR we will call this the Jarzynski method. Here, only local measurements on the system (sys) are being performed. Then, we use the work given by LEMBAS as the fluctuating variable. We distinguish between [$\cdot W\cdot$], which uses the work performed on the system (sys) and [$W\cdot\cdot$], the work done by the driver (dr), respectively (cf. Sec. 9.4). The additional final measurement and the definition of work flow during that very measurement allows to define work along *trajectories*[1].

[$\cdot EQ$] : Crooks method. This estimation method is closely related to a proposal of Crooks. Here, the procedure is as in EFT. Additionally, however, we correct the total energy change of the system (sys) by the heat exchanged with its surroundings (env). We use the heat defined by LEMBAS (cf. Sec. 9.5).

Table 9.1 gives a summary of these methods as well as the necessary conditions under which they can be expected to give a good estimate for the free energy change.

9.2. EFT [$\cdot E\cdot$]

Here, the fluctuating quantity is the local effective energy corresponding to $\hat{H}_{\mathsf{sys}} + \hat{H}^{\mathsf{eff},1}_{\mathsf{sys}}$, E'_{sys}. The EFT coincides with the JR whenever we have no heat flow into the system since then $\Delta E'_{fi} = \Delta W_{fi}$ holds. The advantage of EFT is its clear concept with respect to heat and work. However, EFT is expected to fail when we have an additional heat flow into the system (sys). To be more precise, we consider a bipartite quantum system, considering one as the system of interest and the other as an environment (env), which enforces some effective time-evolution on the system. Classically, the JR was shown to hold for Hamiltonian dynamics, inter alia. Thus, if LEMBAS predicts that the only effect of the environment is to exchange work with the system, EFT should

[1] These trajectories are defined between the measured initial and final state, only. During the process no measurements are being performed. For a classical interpretation of thermodynamic values along trajectories we refer to [77].

Shorthand notation	Subsystems dr	sys	env	Necessary conditions for estimation method to give $\Delta F^{\mathsf{eff}}_{\mathsf{sys}}$
$[\cdot E \cdot]$	$\cdot$	E	$\cdot$	$\Delta Q_{\mathsf{sys}} = 0$
$[\cdot EE]$	$\cdot$	E	E	$\Delta F^{\mathsf{eff}}_{\mathsf{env}} = 0$; $E^{\mathsf{env}'}_{f':f} = E^{\mathsf{env}'}_{f'}$; $\rho^0_{\mathsf{env}} = \frac{\mathrm{e}^{-\beta_{\mathsf{env}} \hat{H}'_{\mathsf{env}}(0)}}{Z^0_{\mathsf{env}}}$
$[W \cdot \cdot]$	W	$\cdot$	$\cdot$	$\Delta Q_{\mathsf{dr}} = 0$; $\Delta W_{\mathsf{env}} = 0$
$[\cdot W \cdot]$	$\cdot$	W	$\cdot$	measurement induced work defined correctly
$[\cdot EQ]$	$\cdot$	E	Q	measurement induced heat taken into account

Table 9.1.: Estimation methods for tripartite system: Fluctuating local variables (energy E, work W, heat Q) of the respective functional part (driver dr, system sys, environment env) taken for estimating the local free energy of the system, $\Delta F^{\mathsf{eff}}_{\mathsf{sys}}$. The dot denotes that no variable is used from this part. The left column defines a short-hand notation, the right column gives the necessary conditions under which the methods can be expected to estimate $\Delta F^{\mathsf{eff}}_{\mathsf{sys}}$ reasonably well. $E^{\mathsf{env}'}_{f':f}$ denotes the effective energy-eigenvalue of the energy-eigenstate $|f'\rangle_{\mathsf{env}}$, given the system has been measured in the eigenstate $|f\rangle_{\mathsf{sys}}$.

hold. However, it does not seem straightforward to prove this expectation as one can have incoherent dynamics even for vanishing heat flows[2].

On the other hand, a classical driver should be in a pure state itself [33] (any classical system should be in a pure state in a non-ensemble view, of course). Then, after the initial measurement on the system has been performed, both system and environment are in pure states, respectively, as is the compound system. As the compound system is closed, it evolves unitarily, its von Neumann entropy staying constant. If now we have that the environment stays in a pure state throughout the time-evolution, then so does the system according to [25],

$$|S(\hat{\rho}_A) - S(\hat{\rho}_B)| \leq S(\hat{\rho}_{AB}) \leq S(\hat{\rho}_A) + S(\hat{\rho}_B). \tag{9.2}$$

The right-hand inequality is known as the *sub-additivity* of the von Neumann entropy, which reduces to an equality if the states factorize, $\hat{\rho}_{AB} = \hat{\rho}_A \otimes \hat{\rho}_B$. As the system's von Neumann entropy is constant at any time during the time-evolution, it receives no heat. As the purity of both system and environment stays 1, we know that the local system evolves unitarily [41]. From this we can readily infer that the local sum rule for the conditional probability holds

[2] Microcanonical coupling can lead to incoherent dynamics without any energy exchange, thus $\Delta Q = 0$, e. g.

as

$$\sum_i K_{fi}^{\mathsf{loc}} = \sum_i \mathrm{Tr}_{\mathsf{sys}}\Big\{ |f\rangle\langle f|\, \hat{U}_{\mathsf{sys}}^{\mathsf{eff}}(t)\, |i\rangle\langle i|\, \hat{U}_{\mathsf{sys}}^{\mathsf{eff}\,\dagger}(t) \Big\} = 1, \tag{9.3}$$

where we have used the completeness relation $\sum_i |i\rangle\langle i| = \hat{1}_{\mathsf{sys}}$ and unitarity $\hat{U}_{\mathsf{sys}}^{\mathsf{eff}}(t)\hat{U}_{\mathsf{sys}}^{\mathsf{eff}\,\dagger}(t) = \hat{1}_{\mathsf{sys}}$. Then it follows quite analogously to Sec. 2.2.1 that EFT works. As we have that $\Delta Q_{\mathsf{sys}} = 0$, EFT and JR coincide.

We conclude that if the environment starts in a pure state and remains pure during the whole process (classical driver) then we have no heat flow into the system according to Lembas and EFT does coincide with JR, giving the correct estimate for the free energy change.

9.3. Bilocal EFT $[\cdot EE]$

Here, we have two fluctuating quantities, namely the local effective energy of both systems, sys and env. We choose the measurements to be performed instantaneously one after the other (cf. Sec. 4.3). This is important, here, as a measurement on one of the systems does in general influence the state of the other one, too. Nevertheless, the measurement does not necessarily influence the effective Hamiltonian $\hat{H}^{\mathsf{eff},1}$ of the other system. If the effective Hamiltonian is not influenced by the first measurement, the proof in Sec. 4.3 remains valid and bilocal EFT should also hold for local effective energies as can be seen easily according to Eq. (4.14) and the remainder of the proof. If, however, the first measurement influences the local effective energy of the second system, we have $E'_{f'}(t) = E'_{f':f}(t)$ in Eq. (4.14) and thus bilocal EFT should fail, in general.

9.4. Jarzynski method $[W\cdot\cdot]$, $[\cdot W\cdot]$

Here, we want to use the work according to Lembas in order to formulate a quantum version of the Jarzynski relation. The advantage of this approach lies in the direct connection of this approach to the classical JR as, for both $[W\cdot\cdot]$ and $[\cdot W\cdot]$ we consider exponentially weighted averages of the work performed on the system (sys), just as in the classical JR. However, we face the problem of defining work for trajectories. Naturally, we could measure the system in the beginning of the process, giving an energy eigenstate. From this state, we could calculate the work for the subsequent process according to Lembas, giving $\Delta W_i^{\mathsf{Lem}}(t)$ as the fluctuating quantity. However, only the initial probability of measuring the system in a distinct energy-eigenstates gives rise to fluctuations, here.

A new approach would be to measure the system also at the end of the process. Then, if one could determine the work performed on the system during the final measurement, it would be possible to introduce the work according to LEMBAS for a distinct trajectory. The problem of defining heat and work for instantaneous projective measurements is discussed in App. C.

For the special case where the system ends in an energy-eigenstate without any measurement at the end of the process we expect $[W\cdot\cdot]$ and $[\cdot W\cdot]$ to give the correct estimate. This should be the case for an effective driving involving only $\hat{H}^{\mathsf{eff},1}_{\mathsf{sys}}$ with vanishing $\hat{H}^{\mathsf{eff},2}_{\mathsf{sys}}$.

For the more general case where $\hat{H}^{\mathsf{eff},2}_{\mathsf{sys}} \neq 0$, we know $[\cdot W\cdot]$ including the final measurement to estimate the free energy correctly for a situation described in Sec. 9.2, as then, according to App. C.4, we have that the change of internal energy due to the measurement, $\Delta U^M_{\mathsf{sys}}$, is solely work, $\Delta U^M_{\mathsf{sys}} = \Delta W^M_{\mathsf{sys}}$ even if the measurement basis does not coincide with the local effective energy-eigenbasis (keep in mind that the state of the system is pure). Then,

$$\Delta W^{\mathsf{Lem}}_{fi}(t) = \Delta W^M_{\mathsf{sys}}(f) + \Delta W^{\mathsf{Lem}}_i(t) = \Delta E'_{fi}, \tag{9.4}$$

coinciding with EFT and JR which are already known to give the correct free energy estimate (cf. Sec. 9.2).

Next, consider our total system composed of three quantum systems. If all three of them start in a pure state and one of them acts as an effective driver (dr) and the other as a perfect heat source (env) on the 3rd system (sys, without any direct coupling between the driver and heat source), one can essentially use the reasoning from above and arrive at the conclusion that the estimation via $[\cdot W\cdot]$ as well as $[\cdot EQ]$, described in the following section, should give $\Delta F^{\mathsf{eff}}_{\mathsf{sys}}$ correctly. However, one has to check carefully whether the connected parts conserve their original properties upon coupling, or if they influence each other in such a way that their effects upon the system (sys) are significantly changed. This is a well-known problem of modularization of quantum systems. Also, keep in mind that LEMBAS is introduced for bipartite systems, only, and it may show that locally considering the pairs driver-system (dr, sys) and system-heat source (sys, env) may lead to inconsistencies. This would be the case, e. g., for non-vanishing correlations between driver and heat source[3]. Thus, we additionally require that the pure state of the total system can be written as

$$\hat{\rho}^t_{\mathsf{tot}} = \hat{\rho}^t_{\mathsf{dr}} \otimes \left(\hat{\rho}^t_{\mathsf{sys}} \otimes \hat{\rho}^t_{\mathsf{env}} + \hat{C}^t_{\mathsf{se}}\right) \tag{9.5}$$

[3]Note, that even though we have required that driver and heat source do not interact directly, they may built up correlations via the system.

at any time t (this would hold for a classical perfect driver). The local von Neumann entropies of the system and the environment may change. At the end of the process, when the system (sys) is being measured, we have again that the total system as well as the driver and the system are in pure states, respectively. From [25] we then have that the heat source (env) is in a pure state after the measurement, too. If the heat source absorbs only heat during the measurement (cf. App. C for the definition of measurement induced energy flows), we have

$$\Delta U_{\mathsf{env}}(f,i) = \Delta Q^{\mathsf{Lem}}_{\mathsf{env}}(i) + \Delta Q^{M}_{\mathsf{env}}(f) = \Delta E'_{\mathsf{env}}(f,i) \tag{9.6}$$

and

$$\Delta W^{\mathsf{Lem}}_{fi}(t) = \Delta W^{M}_{\mathsf{sys}}(f) + \Delta W^{\mathsf{Lem}}_{i}(t) = \Delta E'_{fi}. \tag{9.7}$$

Thus, we find that $[\cdot W\cdot]$ then coincides with bilocal EFT and the Crooks estimation, $[\cdot EQ]$. As we have required that the measurement should not give rise to any work exchange between system and heat source, $\hat{H}^{\mathsf{eff},1}_{\mathsf{env}}$ should not change during measuring the system, thus it should not depend on the state of the system, generally (cf. App. C.3.2). This is just the requirement needed in Sec. 9.3 to proof that bilocal EFT gives the correct free energy change. Thus, if the requirements above are met, $[\cdot W\cdot]$ does not only coincide with bilocal EFT and $[\cdot EQ]$, but it should also give a good free energy estimate, as does $[\cdot EQ]$, then.

9.5. Crooks method $[\cdot EQ]$

This method is closely related to and was inspired by a proposal of Crooks [22]. The idea is to determine the work performed on the system indirectly by using the 1st law of thermodynamics. Here, the total energy change of the system is measured and then the heat flow into the environment is subtracted to recover the work on the system. Our approach is more general, as we do neither require the small coupling limit nor the environment to be a perfect heat bath as was done in [22]. Actually, the environment may be as small as a single spin, cf. Chap. 8

For the Crooks method, $[\cdot EQ]$, we use two-time measurements on the system as in EFT. Then, we determine the heat flow into the environment according to LEMBAS. Here, we have the fluctuation of the energy measurements, $\Delta E'_{fi}(t)$, as well as the heat flow into the environment, which might depend on the initial state of the measured system, $\Delta Q^{\mathsf{Lem}}_{i;\mathsf{env}}(t)$[4]. Here, the question arises whether

[4] Note that the index i refers to the state of the system (sys) and not to the environment (env).

one has to take into account that the final energy measurement does generally influence the environment, as we have already discussed in Sec. 9.4. Due to the correlations we expect co-jumps in the environment which should induce heat, there. For a slightly more detailed discussion we refer to the appendix, App. C. Taking into account co-jumps we can define heat along a *trajectory* in the two-time measurement sense, according to $\Delta Q^{\mathsf{Lem}}_{fi;\mathsf{env}}(t) = \Delta Q^{\mathsf{Lem}}_{i;\mathsf{env}}(t) + \Delta Q^{M}_{\mathsf{env}}(f)$, where, again, the index f refers to the system and the second addend denotes the heat flow into the environment due to a projective measurement on the system. By using the 1st law we can then recover the work performed onto the system, given by

$$\Delta W_{fi} = \Delta E'_{fi}(t) + \Delta Q^{\mathsf{Lem}}_{fi;\mathsf{env}}(t). \tag{9.8}$$

For the case where we have negligible correlations and thus almost no co-jumps, we expect that we can neglect the measurement effect and the Crooks estimator should give the correct result for the free energy without taking into account the final measurement for the heat flow.

10. Closed bipartite systems

Here, we restrict ourselves to a bipartite quantum system. The total system is supposed to be closed, being described by a time-independent Hamiltonian. In this chapter we focus on situations, where one subsystem acts as a driver (dr) for the other one (sys) (cf. Chaps. 6 and 7). We will discuss EFT and the Jarzynski method, here, as bilocal EFT as well as the Crooks method are not feasible for bipartite systems without environment, cf. Chap. 9.

10.1. Effectively driven system: SOM

We start by investigating the model system introduced in Chap. 6. As Lembas predicts that the oscillator is acting effectively as an external driver, $\Delta E'_{fi} = \Delta W_{fi}$, we expect that EFT ($[\cdot E \cdot]$) and the Jarzynski method ($[\cdot W \cdot]$, $[W \cdot \cdot]$) coincide and that both give the correct estimate for the free energy change. In Sec. 6.3, we have already numerically verified our findings from Secs. 6.1 and 6.2 that

$$\Delta Q^{\mathsf{Lem}}_{\mathsf{sys}} = 0 \text{ and } \Delta Q^{\mathsf{Lem}}_{\mathsf{env}} = 0. \tag{10.1}$$

We use the same parameter set as in the aforementioned section on numerics, $\omega_{\mathrm{sp}} = \omega_{\mathrm{osc}} = 1$, $\Omega_{\mathsf{int}} = -0.2$, $m = 45$, $\alpha = 3$ and $\beta^{\mathsf{eff}}_{\mathsf{sp}} = 0.85$. The oscillator is again being considered as the driver (dr) and the spin as the system of interest (sys).

Now, we investigate the deviation of EFT and the Jarzynski method from the exact free energy change. As

$$\frac{Z^{\mathsf{eff}}_{\mathsf{sys}}(t)}{Z^{\mathsf{eff}}_{\mathsf{sys}}(0)} = \mathrm{e}^{-\beta^{\mathsf{eff}}_{\mathsf{sys}} \Delta F^{\mathsf{eff}}_{\mathsf{sys}}}, \tag{10.2}$$

it is not crucial whether we consider the effective partition sums or the free energy change. Here and in the following chapters, we assume the initial partition sum, $Z^{\mathsf{eff}}_{\mathsf{sys}}(0)$ to be known, trying to determine the final partition sum $Z^{\mathsf{eff}}_{\mathsf{sys}}(t)$. To this end we define the relative deviation $\Delta^{Z}_{\mathsf{rel}}$ of EFT as well

as the Jarzynski method with respect to the correct $Z^{\mathsf{eff}}_{\mathsf{sys}}(t)$,

$$\Delta^{Z}_{\mathsf{rel}}(m) \equiv \frac{Z^{m}_{\mathsf{sys}}(t) - Z^{\mathsf{eff}}_{\mathsf{sys}}(t)}{Z^{\mathsf{eff}}_{\mathsf{sys}}(t)}, \tag{10.3}$$

where the index m will label the method used in order to obtain the final partition sum. Thus, $m \in \{[\cdot E \cdot], [\cdot W \cdot], [W \cdot \cdot]\}$, here. However, we face an additional problem, here. As we have seen in Sec. 6.3, the effective partition sum of the system (sys) may depend on the initially measured state of the system (sys), as the effective *driving protocol* may depend on this state. For the JR, however, it is assumed that the driving protocol can be reproduced perfectly for all repetitions. This implicit assumption may not only be problematic in our case but may also limit the practical applicability of the JR. For the spin (sys) we have two different possible measurement outcomes and therefore two different effective partition sums, $Z^{\mathsf{eff}}_{\mathsf{sys}}(t, \downarrow \,/\, \uparrow)$, for the exact time-evolution by solving the Schrödinger equation.

In the following we will use a combination of both, $Z^{\mathsf{eff}}_{\mathsf{sys}}(t, \downarrow)$ and $Z^{\mathsf{eff}}_{\mathsf{sys}}(t, \uparrow)$ as the *correct analytical* result, more precisely the weighted average of both, where the weight is determined by the initial occupation probability, given by the initial temperature, of the system (sys):

$$Z^{\mathsf{eff}}_{\mathsf{sys}}(t) \equiv \sum_{i=1}^{2} p(i) Z^{\mathsf{eff}}_{\mathsf{sys}}(t, i), \quad i = \begin{cases} 1: & \downarrow \\ 2: & \uparrow \end{cases}. \tag{10.4}$$

The initial occupation probability $p(i)$ is given by

$$p(i) = \frac{\mathrm{e}^{-\beta E'_i}}{Z^{\mathsf{eff}}_{\mathsf{sys}}(0)}, \tag{10.5}$$

as the system (sys) starts in a thermal state. If we do not want to use the weighted partition sum given by Eq. (10.4), this will be noted explicitly.

Here and in the following chapters, the figures on the estimation methods are all to be understood in the following way: The time t denotes the time elapsed after the initial measurement at $t = 0$, say. During this time, the total system evolves freely, without any further measurement or perturbation. Then, the final measurement takes place at time t. This process is repeated very often in order to estimate the free energy via the average given in Chap. 9. Every single time t denotes such a procedure.

Thus, the estimations of the free energy at a later time $\tau + \Delta t$ are to be understood not as a subsequent prediction after measurements at time $t = 0$ and $t = \tau$, but as a completely new set of processes (many repetitions) running undisturbed from initial time $t = 0$ to final time $\tau + \Delta t$.

10.1.1. EFT

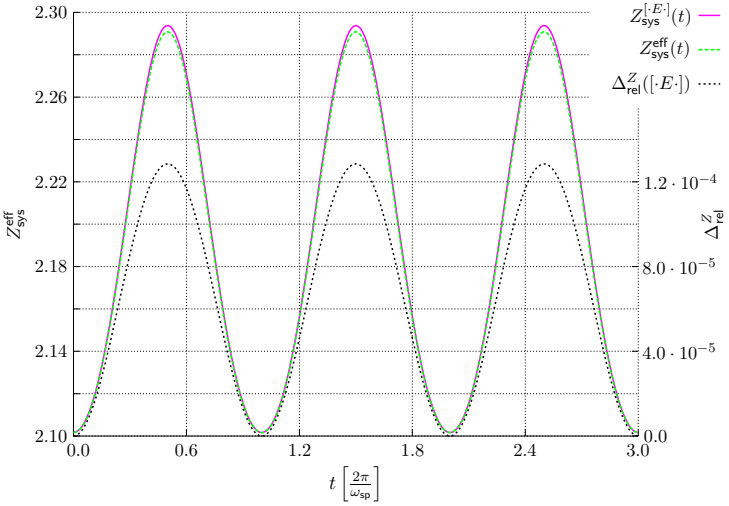

Figure 10.1.: Left scale: EFT estimation, $Z^{[\cdot E\cdot]}_{\mathsf{sys}}(t)$ (magenta line) and numerical exact $Z^{\mathsf{eff}}_{\mathsf{sys}}(t)$ (green dashed line) over t. Right scale: relative deviation, $\Delta^{Z}_{\mathsf{rel}}([\cdot E\cdot])$ (black dotted line).

We start by investigating EFT. As we can solve the Schrödinger equation by numerically exact diagonalization we do not need to integrate the fluctuating quantity (the effective energy). Thus, we do not expect any numerical errors to accumulate. The numerical result for EFT is shown in Fig. 10.1. As can be seen, the estimate $Z^{[\cdot E\cdot]}_{\mathsf{sys}}(t)$ for the effective partition sum at time t almost coincides with the numerical exact result, $Z^{\mathsf{eff}}_{\mathsf{sys}}(t)$, the relative deviation $\Delta^{Z}_{\mathsf{rel}}([\cdot E\cdot])$ being less than $1.3\cdot 10^{-4}\ \forall\ t$. The finite error is due to state-dependent driving. From Fig. 6.6 we know that the maximal relative deviation $\delta_{\mathsf{rel}} Z^{\mathsf{eff}}_{\mathsf{sys}}[\uparrow;\downarrow]$ lies at the order of 10^{-3} for the parameters chosen here. Due to the weighting we expect a smaller error here, which indeed happens to be the case. Nevertheless, the deviation found here can be explained solely by the state-dependent driving.

The numerics thus confirm our expectation: LEMBAS predicts only work exchange $\Longrightarrow$ EFT should give the correct free energy estimate. The reasoning could be reversed: As EFT holds, the energy exchange should be only work, as LEMBAS correctly predicts.

10.1.2. Jarzynski method

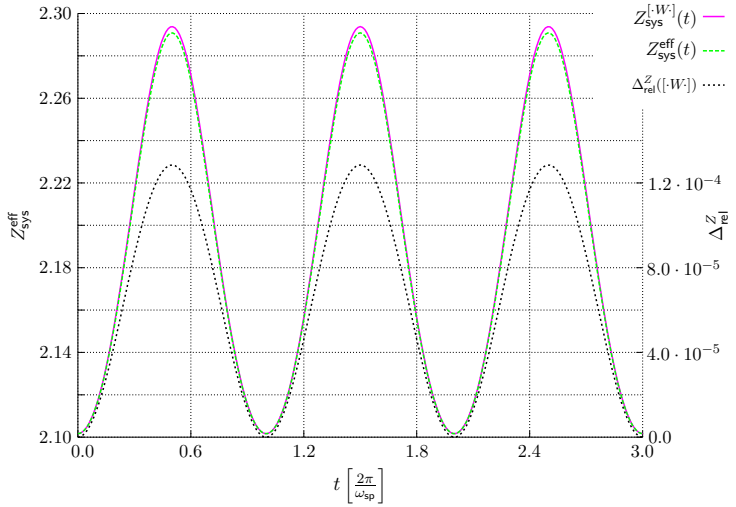

Figure 10.2.: Left scale: Jarzynski method estimation $Z_{\mathsf{sys}}^{[\cdot W\cdot]}(t)$ (magenta line) and numerical exact $Z_{\mathsf{sys}}^{\mathsf{eff}}(t)$ (green dashed line) over t. Right scale: relative deviation, $\Delta_{\mathsf{rel}}^{Z}([\cdot W\cdot])$ (black dotted line).

For SOM, we expect that the Jarzynski method coincides with EFT, as we have only work exchange and since the state of the system (sys) remains pure after the initial measurement throughout the dynamics, the final measurement only induces work if any energy is transferred to the system (sys) via the measurement. Moreover, from Sec. 6.2 we expect that $[\cdot W\cdot]$ coincides with $[W\cdot\cdot]$, as $\Delta W_{\mathsf{sys}}^{\mathsf{Lem}} = -\Delta W_{\mathsf{env}}^{\mathsf{Lem}}$. Indeed, our numerics confirms these expectations. Fig. 10.2 shows the numerical result for $[\cdot W\cdot]$ which coincides with $[W\cdot\cdot]$ as well as EFT from Fig. 10.1. Therefore, it is possible to use the work given by LEMBAS in order to estimate the effective partition sum in complete analogy to the classical Jarzynski relation.

10.2. Effectively driven system: Two-spin driver

Now, we investigate the model presented in Chap. 7 with respect to the JR. We choose the same parameters as in Sec. 7.7. From our previous studies in the aforementioned section, we expect that EFT coincides with the Jarzynski method and that both give the correct free energy estimate. Moreover, we

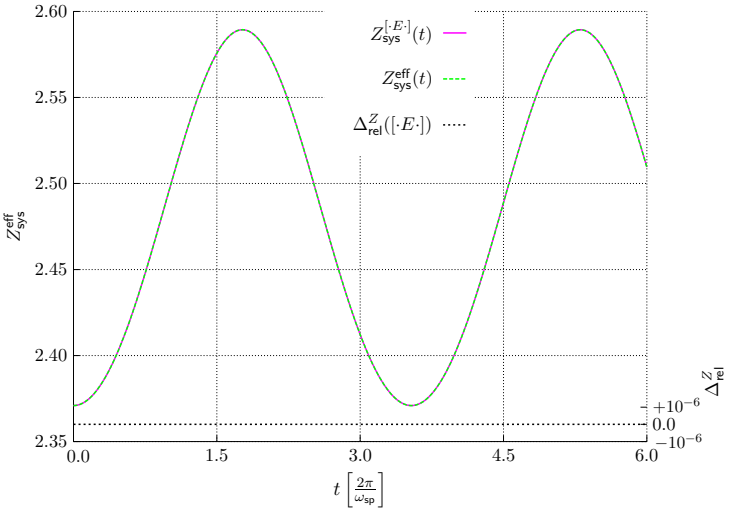

Figure 10.3.: EFT prediction $Z^{[\cdot E\cdot]}_{\mathrm{sys}}(t)$ as well as exact $Z^{\mathrm{eff}}_{\mathrm{sys}}(t)$ over t. Both lines coincide as confirmed by the relative deviation (black line), $\Delta^{Z}_{\mathrm{rel}}([\cdot E\cdot])$, for which the y-scale on the right-hand side applies.

expect that $Z^{\mathrm{eff}}_{\mathrm{sys}}(t,\downarrow) = Z^{\mathrm{eff}}_{\mathrm{sys}}(t,\uparrow) = Z^{\mathrm{eff}}_{\mathrm{sys}}(t)$, here, as we have found that the two-spin driver features state-independent driving.

10.2.1. EFT

For EFT, the system (sys) is measured initially and again at the end of the process. As above, $\Delta Q^{\mathrm{Lem}}_{\mathrm{sys}} = 0$, thus EFT coincides with the Jarzynski method and should be able to estimate the effective partition sum correctly. Fig. 10.3 confirms our expectations, as EFT gives the correct free energy estimate. Here, the result is exact within numerical accuracy. Again, the LEMBAS prediction that only work is being exchanged fits perfectly with the results on EFT and the JR.

10.2.2. Jarzynski method

We consider the work performed on the system (sys), $[\cdot W\cdot]$, as well as the work performed by the driver (dr), $[W\cdot\,\cdot]$. Fig. 10.4 confirms that $[\cdot W\cdot]$ gives the correct partition sum without deviations within numerical accuracy. The fact that $[W\cdot\,\cdot]$, which should also hold, in principle, shows deviations at the order of 10^{-4} is due to the numerical error of integration, cf. Sec. 7.7. Note, that

the deviation is not necessarily the same as in the aforementioned section, as for $[W\cdot\cdot]$, the integrated work is weighted exponentially. Thus, as for SOM in Sec. 10.1, we conclude that it is possible to formulate an effective quantum JR, here, which is in perfect agreement with the LEMBAS definition of heat and work. Both, the work performed on the system (sys) as well as the work performed by the driver (dr) given by LEMBAS can directly be used to obtain a quantum JR.

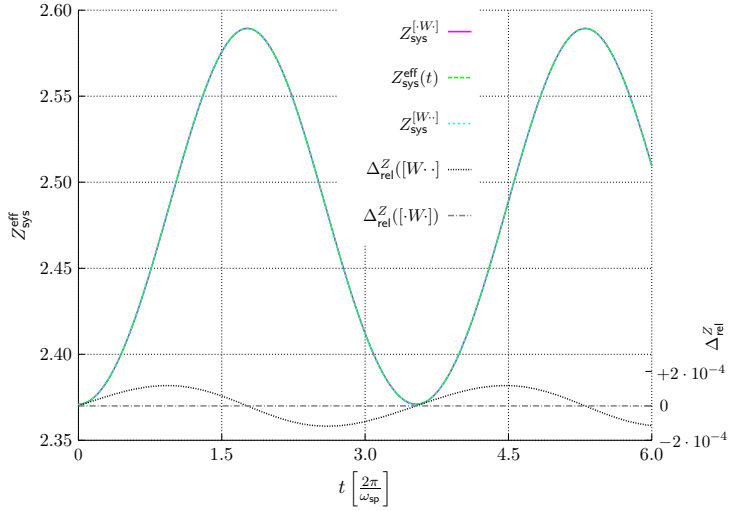

Figure 10.4.: Estimation of effective partition sum via Jarzynski method: $[\cdot W\cdot]$ and $[W\cdot\cdot]$ prediction as well as exact $Z^{\mathrm{eff}}_{\mathrm{sys}}(t)$. For the relative deviations of $[\cdot W\cdot]$ (grey line) and $[W\cdot\cdot]$ (black line) the scale on the right-hand side applies.

11. Additional one-spin environment: bilocal measurements

In Chap. 10 we have seen that it is possible to formulate effective quantum generalizations of the JR for bipartite closed quantum systems, in accord with LEMBAS. Here, we consider a quantum system which can be split into three subsystems. One part will be the system of interest (sys), while the other two will serve as driver (dr) and environment (env), cf. Chap. 9. We consider situations where the environment leads to a heat flow into the system, only. To this end, we combine the systems discussed in Chaps. 6 and 7 as drivers, and the system from Chap. 8 as the environment. Note, that we *cannot* trivially assume, that the systems coupled together still fulfill their roles as they did for the bipartite cases. Modularization may lead to loss of their original properties. Therefore, we have to check numerically whether, after plugging the parts together, they still have the same properties as for the unconnected parts - maybe at least approximately.

We start by considering bilocal measurements. Thus, we measure both, the system (sys) and the environment (env), initially as well as at the end of the process. Thus, we can consider bilocal EFT as well as the estimate via the Crooks method, here. As it is not necessary to measure the environment projectively for applying Crooks' method, this can be considered a special case, here. Moreover, not considering the final measurement of the environment, we can also investigate EFT as well as the Jarzynski method, here, implying the special case where the environment starts in a pure state. From our studies in Secs. 9.2- 9.5, we expect that all methods are able to give the correct partition sum estimate except EFT, as we expect a heat flow from the environment into the system. Here, the effective partition sum depends generally on both initially measured states if the effect of the driver is influenced by the initial state of system and environment. For the sake of clarity and brevity, we will consider $Z_{\mathsf{sys}}^{\mathsf{eff}}(t)$ as before, with the additional thermal weighting of the environment with its respective temperature. Conceptually, nothing new enters the discussion when taking into account the additional possibilities. Keep in

mind that the effective partition sum of the system is not directly influenced by the state of the environment but only indirectly by state-dependent driving.

11.1. Effective driving: SOM

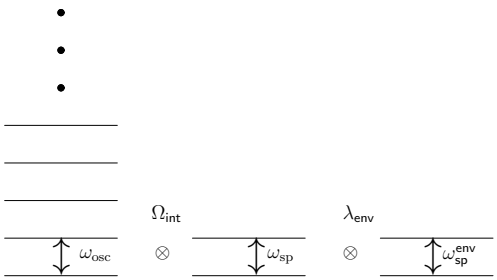

Figure 11.1.: SOM with additional spin with direct coupling to the system, only. The environmental spin will usually be coupled resonantly ($\omega_{\mathrm{sp}} = \omega_{\mathsf{sp}}^{\mathsf{env}}$) with coupling strength λ_{env}.

Here, we consider the model presented in Chap. 6 with an additional spin as the environment, coupled to the system (cf. Fig. 11.1). For the coupling we choose $\hat{H}_{\mathsf{se}} \equiv \lambda_{\mathsf{env}} \hat{\sigma}_x \otimes \hat{\sigma}_x$. Thus, the oscillator and the system alone represent the same model as in Chap. 6 (SOM), the two spins (system and environment) without the oscillator are identical with the model from Chap. 8. If we plug those two separate models together, we would expect that the effectively driven system (driven by the oscillator) exchanges heat with its environment, a perfect heat source. As LEMBAS was designed to explain heat and work flows in a bipartite scenario, we have to be careful with such a tripartite view as above. As already mentioned, the new system may behave quite differently than its separated parts would do. However, if the oscillator and the environment do not built up correlations in the time of interest, we could use LEMBAS for a split bipartite view of driver and system on one side, and system and environment on the other. As a criterion if this split bipartite view should be valid, we will use the Bures distance [12] between the true state $\hat{\rho}_{\mathsf{drenv}}$ and the factorizing one, $\hat{\rho}_{\mathsf{dr}} \otimes \hat{\rho}_{\mathsf{env}}$,

$$\mathcal{D}_B\left(\hat{\rho}_A, \hat{\rho}_B\right) = \sqrt{2\left(1 - \sqrt{\mathcal{F}(\hat{\rho}_A, \hat{\rho}_B)}\right)}, \tag{11.1}$$

with the fidelity $\mathcal{F}(\hat{\rho}_A, \hat{\rho}_B)$ defined through

$$\mathcal{F}(\hat{\rho}_A, \hat{\rho}_B) = \left[\mathrm{Tr} \left\{ \sqrt{\sqrt{\hat{\rho}_A} \hat{\rho}_B \sqrt{\hat{\rho}_A}} \right\} \right]^2 . \tag{11.2}$$

For our purpose, $\hat{\rho}_A$ and $\hat{\rho}_B$ are given by $\hat{\rho}_A = \hat{\rho}_{\mathsf{drenv}}$ and $\hat{\rho}_B = \hat{\rho}_{\mathsf{dr}} \otimes \hat{\rho}_{\mathsf{env}}$, respectively. If the combined state of the driver and the environment factorizes, we have that $\mathcal{D}_B(\hat{\rho}_A, \hat{\rho}_B) = 0$. Then, the split bipartite view of LEMBAS should work.

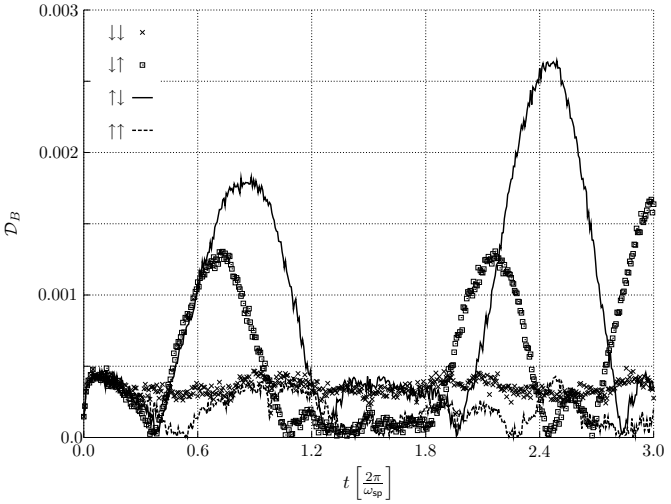

Figure 11.2.: Bures distance $\mathcal{D}_B$ over time elapsed, t, for the four different initial measurement outcomes, $\{\downarrow\downarrow, \downarrow\uparrow, \uparrow\downarrow, \uparrow\uparrow\}$. The left arrow refers to the system, the right one to the environment.

For our numerics we choose the same parameters as in Sec. 10.1 with the additional coupling strength $\lambda_{\mathsf{env}} = 0.15$. The environmental spin with $\omega_{\mathsf{env}} = \omega_{\mathsf{sys}} = 1$ is prepared in a canonical state with $\beta_{\mathsf{env}} = 0.85$. The Bures distance for the states, $\mathcal{D}_B$ is plotted in Fig. 11.2. As can be seen, the Bures distance remains relatively small during the whole process for all possible initial measurement outcomes. The largest values are reached for $\downarrow\uparrow$ and $\uparrow\downarrow$, respectively. The left arrow refers to the system (sys) and the right one to the environment (env). It can be understood intuitively that for opposite magnetization we have the largest values for the distance, because then, we have maximal heat exchange between system and environment which can lead to indirect correlations with the driver. Indeed, it was to be expected that the

driver and the environment can build up correlations, here, as we find easily that the coupling between driver and system, $\hat{H}_{\mathsf{int}}$, and the coupling between system and environment, $\hat{H}_{\mathsf{se}}$, do not commute, $[\hat{H}_{\mathsf{int}}, \hat{H}_{\mathsf{se}}] \neq 0$. However, as the Bures distance remains small the split bipartite view should work quite well.

Indeed, we numerically find that the purity of the driver, $P_{\mathsf{dr}}(t) \approx 1 \ \forall \ t$ and that $\Delta Q^{\mathsf{Lem}}_{\mathsf{dr}}(t) \approx 0 \ \forall \ t$. For the environment we find $\Delta Q^{\mathsf{Lem}}_{\mathsf{env}} \neq 0$, but $\Delta W^{\mathsf{Lem}}_{\mathsf{env}}(t) = 0 \ \forall \ t$. The environment thus maintains its functionality as a perfect heat source. For the system, we find that both, $\Delta W^{\mathsf{Lem}}_{\mathsf{sys}} \neq 0$ and $\Delta Q^{\mathsf{Lem}}_{\mathsf{sys}} \neq 0$. Due to these findings, we will adopt the way of speaking that the oscillator (driver) works on the system while the spin (environment) exchanges heat with the system. In the following we discuss the different methods introduced in Chap. 9 for estimating the local effective free energy of the system.

11.1.1. EFT

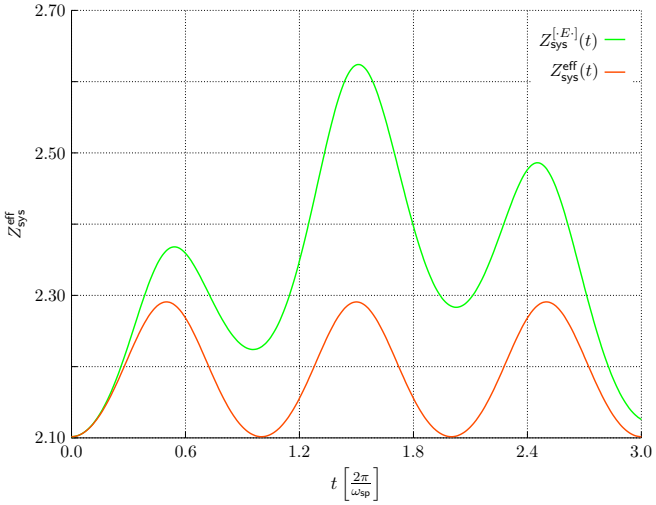

Figure 11.3.: EFT prediction for the effective partition sum, $Z^{[\cdot E\cdot]}_{\mathsf{sys}}(t)$ (green line), as well as numerically exact $Z^{\mathsf{eff}}_{\mathsf{sys}}(t)$ (orange line).

As LEMBAS predicts a heat flow into the system, we now expect EFT to fail. Note, that it does not coincide with the JR, then, as $\Delta E'_{fi} \neq \Delta W_{fi}$. Indeed, from Fig. 11.3 we can easily see that EFT is not able to give the correct $Z^{\mathsf{eff}}_{\mathsf{sys}}(t)$. The relative deviation $\Delta^{Z}_{\mathsf{rel}}([\cdot E\cdot])$, Eq. (10.3), rises fast, ranging up

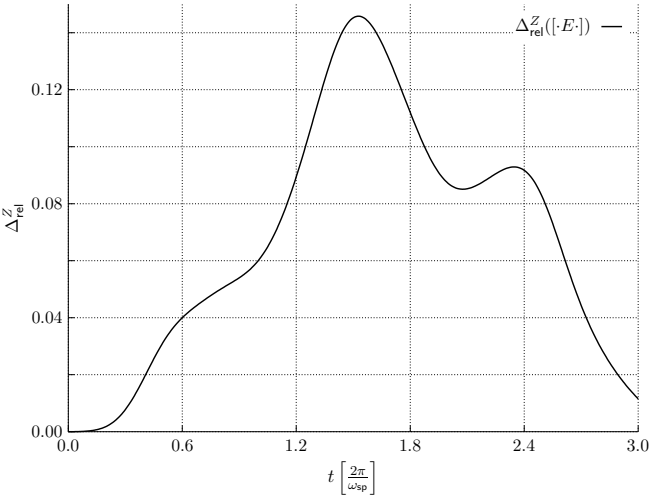

Figure 11.4.: Relative deviation $\Delta^Z_{\mathsf{rel}}([\cdot E\cdot])$ over t.

to over 14%, cf. Fig. 11.4. This large error cannot be explained by state-dependent driving as will be seen in the following sections. This would have come as a surprise as the deviation due to the state-dependency was rather small in Sec. 10.1.

Note that we did not take into account the measurements on the environment, here. Thus, we have studied a special situation where the environment starts in a pure state. The probability of finding a distinct pure state is given by the initial canonical distribution of the environmental spin.

This result shows, that the definition of heat and work according to LEMBAS is indeed feasible for this model. Although we deal with a single spin as a heat source, here, the prediction of LEMBAS that the energy flow from this spin into the system has to be considered as heat lead to our expectation that the estimation of the effective partition sum via EFT would fail, which has been confirmed numerically.

11.1.2. Bilocal EFT

According to our overview in Sec. 9.3, bilocal EFT should give a good estimate, here, as $\hat{H}'_{\mathsf{env}}$ does not depend on the state of the system[1]. Indeed, we find that bilocal EFT predicts almost correctly the effective partition sum, as

[1]This is due to the fact that $\hat{H}^{\mathsf{eff}}_{\mathsf{env}} = \hat{H}^{\mathsf{eff},2}_{\mathsf{env}}$, $\hat{H}^{\mathsf{eff},1}_{\mathsf{env}} = 0$.

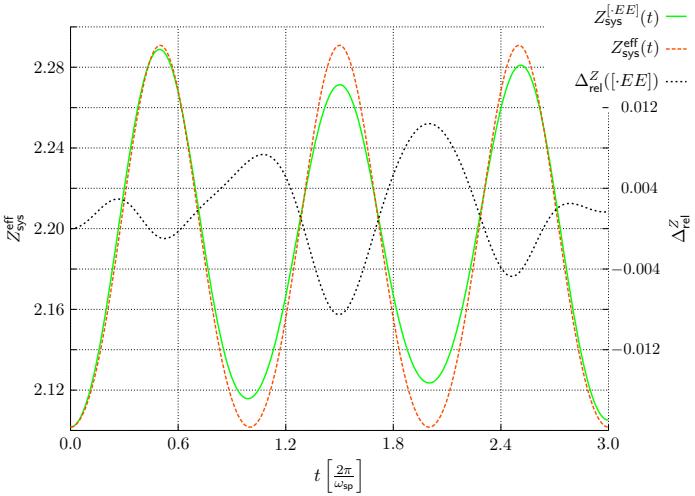

Figure 11.5.: Prediction of bilocal EFT, $Z_{\mathsf{sys}}^{[\cdot EE]}(t)$ (green line) as well as exact result for effective partition sum, $Z_{\mathsf{sys}}^{\mathsf{eff}}(t)$ (orange dashed line). For the relative deviation, $\Delta_{\mathsf{rel}}^{Z}([\cdot EE])$ (black dotted line), the scale on the right-hand side applies.

Fig. 11.5 shows. Here, we assume that the finite error, whose absolute value is less than 1.1% for the considered time t, arises due to the state-dependent driving and the fact, that we have a small heat flow into the driver. This assumption is backed by the fact that the sum rule for initial states of the conditional probability, $\sum_{i,i'} K_{ff',ii'} = 1$ (cf. Eq. (4.18)) is found to be fulfilled, numerically. Therefore, in the following the criterion for both Jarzynski and Crooks method to hold will be that they feature a relative deviation not significantly larger than the one we have found for bilocal EFT. In Sec. 11.4 we will further justify this assumption by substituting the oscillator (or the two-spin driver, respectively) by a classical external driver, modeled by an explicitly time-dependent Hamiltonian.

11.1.3. Crooks method

Here, we do not take the projective measurements on the environment into account. Thus, we consider the special case where the environment starts in a pure state, the probability of starting in a distinct energy-eigenstate being given by the initial canonical distribution. The heat flow into the environment will be determined according to LEMBAS. If we insisted on measuring the heat

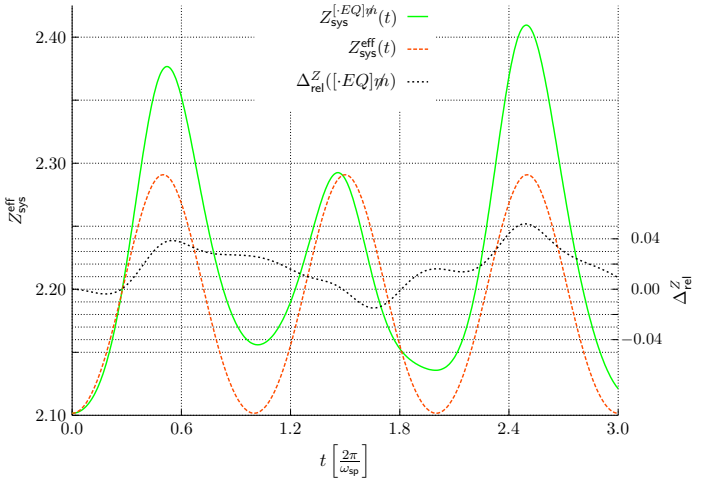

Figure 11.6.: Prediction of the Crooks method, $Z_{\mathsf{sys}}^{[\cdot EQ]\not m}(t)$ (green line) as well as exact result for effective partition sum, $Z_{\mathsf{sys}}^{\mathsf{eff}}(t)$ (orange dashed line). The crossed out $m, \not m$ accounts for the fact that the final measurement of the system has been ignored for the determination of the heat flow. For the relative deviation, $\Delta_{\mathsf{rel}}^{Z}([\cdot EQ]\not m)$ (black dotted line), the scale on the right-hand side applies.

flow via projective measurements, then Crooks method would coincide with bilocal EFT, here, as $\Delta E_{\mathsf{env}} = \Delta Q_{\mathsf{env}}$, $\Delta W_{\mathsf{env}} = 0$.

From an ensemble point of view, the system and the environment start in thermal states each. For a distinct process realization, however, they are projected into pure states due to the initial measurements. As the driver (oscillator) starts in a pure state, also, the total system has zero entropy, which is conserved by the unitary evolution. We already know that the oscillator's purity remains close to 1 during the time-evolution. The local purity of both system and the environment, however, gets as low as 0.5, the absolute minimum for a spin. The final measurement of the system will now cause the environmental state to be pure, too, as can be seen from Araki&Lieb [25]: The total system as well as the oscillator remain in pure states throughout the time-evolution. After the final projective measurement the state of the system is also pure, thus, the environmental state is necessary pure, too.

From this consideration we expect that ignoring the final measurement of the system by considering the heat flow up to this measurement, only, will lead to deviations from the correct effective partition sum of the system when

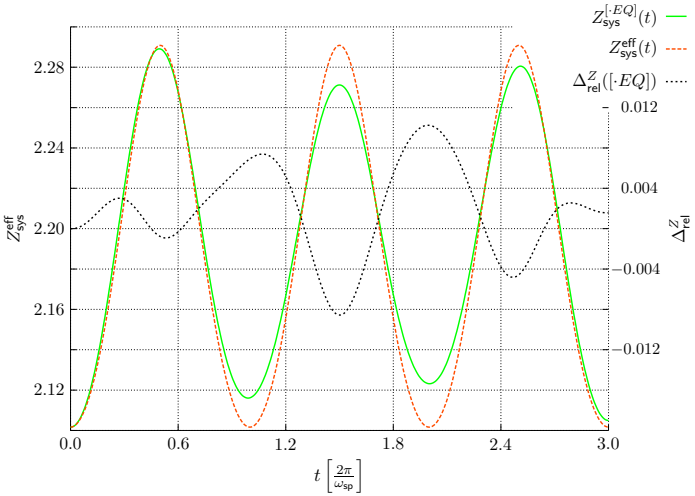

Figure 11.7.: Prediction of the Crooks method, $Z_{\mathsf{sys}}^{[\cdot EQ]}(t)$ (green line) as well as exact result for effective partition sum, $Z_{\mathsf{sys}}^{\mathsf{eff}}(t)$ (orange dashed line). For the relative deviation, $\Delta_{\mathsf{rel}}^{Z}([\cdot EQ])$ (black dotted line), the scale on the right-hand side applies. Hence, it is enlarged by a factor of 5.

applying Crooks' method as the environment will be in a mixed state, generally, implying a lack of knowledge with respect to the environmental state. Indeed, Fig. 11.6 clearly shows that the deviation of $\Delta_{\mathsf{rel}}^{Z}([\cdot EQ])$ can get as large as 5% during the time considered. This is much larger than the accepted deviation given by bilocal EFT of about 1%.

Next, we take into account the effect of the final measurement of the system on the environment. Here, we use our definition for the heat flow into the environment arising from the projective measurement on the system, Eqs. (C.26) and (C.27). Note that we have used $\mathrm{d}H'_{\mathsf{env}} = 0$ for the measurement as required for this definition[2]. Fig. 11.7 confirms that with this definition of measurement induced heat flow, $Z_{\mathsf{sys}}^{[\cdot EQ]}(t)$ coincides with the numerical exact result, $Z_{\mathsf{sys}}^{\mathsf{eff}}(t)$ within the tolerance specified by bilocal EFT. Indeed, the relative deviation of bilocal EFT and estimation via the Crooks method coincide within numerical accuracy. This should not come as a surprise as we know that the environment is in a pure state after the system has been measured. If this pure state is an energy-eigenstate, actually, then bilocal EFT and the

[2] $\mathrm{d}H'_{\mathsf{env}} = 0$ implies $E'^{\mathsf{env}}_{f':f} = E'^{\mathsf{env}}_{f'}$, thus the effective energy eigenvalues of the environment are independent of the state of the system, cf. condition on bilocal EFT, Sec. 4.3.

Crooks method should coincide, according to

$$\Delta Q^{\mathsf{Lem}}_{fi,\mathsf{env}} = \Delta Q^{\mathsf{Lem}}_{i,\mathsf{env}} + \Delta Q^{M}_{\mathsf{env}}(f) = \Delta U_{i,\mathsf{env}} + \Delta U^{M}_{\mathsf{env}}(f) = \Delta E^{\mathsf{env}}_{f'i'}, \quad (11.3)$$

where we have used $\Delta W_{\mathsf{env}} = 0$ and $\Delta W^{M}_{\mathsf{env}} = 0$ (cf. Eq. (C.27)) in the first step and $\Delta U_{i,\mathsf{env}} = \Delta U_{\mathsf{env}}$ by assuming state-independent driving. Thus, even for a heat source (according to LEMBAS) as small as a single spin, the estimation of the effective partition sum via the Crooks method gives quite good results. Again, the LEMBAS prediction that the system and the environment exchange only heat is in perfect accordance with the results obtained here.

11.1.4. Jarzynski method

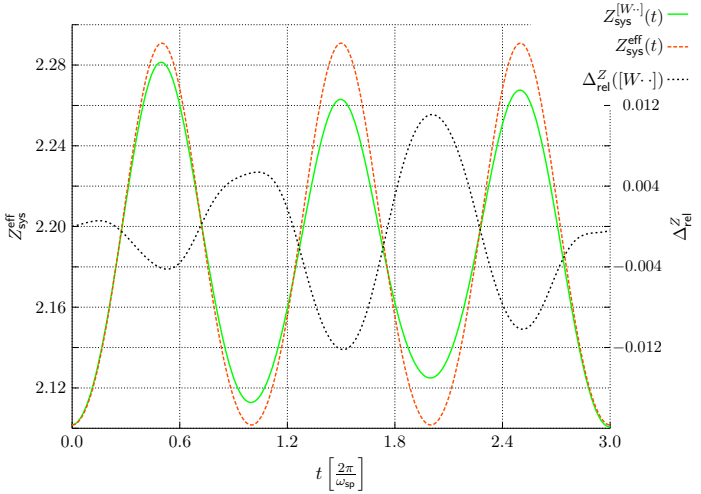

Figure 11.8.: Prediction of the Jarzynski method ($[W\cdot\cdot]$), $Z^{[W\cdot\cdot]}_{\mathsf{sys}}(t)$ (green line) for the effective partition sum, $Z^{\mathsf{eff}}_{\mathsf{sys}}(t)$ (exact result: orange dashed line). For the relative deviation, $\Delta^{Z}_{\mathsf{rel}}([W\cdot\cdot])$ (black dotted line), the scale on the right-hand side applies.

Here, we consider the estimation of the effective partition sum via the Jarzynski method. For $[W\cdot\cdot]$ the indirect measurement effect, if any, should give rise to a heat flow into the driver, only, according to Eqs. (C.26) and (C.27) (Note that $\mathrm{d}\hat{H}'_{\mathsf{env}} = 0$ as $\hat{H}^{\mathsf{eff},1}_{\mathsf{osc}} = 0$, cf. Eq. (6.9)). As the driver is almost in a pure state before the measurement, already, we expect that the effect of the measurement is negligible, anyway. Fig. 11.8 shows the prediction of $[W\cdot\cdot]$

compared to the numerical exact result for $Z^{\mathsf{eff}}_{\mathsf{sys}}(t)$ as well as the deviation. The deviation is slightly larger than the tolerance specified by bilocal EFT. This might arise from the fact that here, $\Delta W_{\mathsf{dr}} \neq \Delta W_{\mathsf{sys}}$, in general, as the spin is not in a pure state throughout the dynamics (cf. [31]). Moreover, an additional error may stem from the numerical integration of ΔW_{dr}[3]. Finally, the definition of measurement induced work exchange might not be good, here.

Next, we turn to $[\cdot W\cdot]$. Again, we expect the same error sources as for $[W\cdot\cdot]$. Here, we compare the results for the two different definitions of measurement induced work onto the system, method A as well as method B, cf. App. C.4. The latter definition was used for Fig. 11.9, which reveals that here, method B leads to deviations slightly larger than bilocal EFT. Therefore, it seems that this definition should not be used, here. Indeed, method A gives better results, as can be seen in Fig. 11.10. The deviation is about as small as for $[W\cdot\cdot]$, thus $[\cdot W\cdot]$ seems to give the correct partition sum estimate if method A is used for determination of work flow arising by the measurement. Note, that the differences between these two methods are small enough so that one cannot easily decide which method should be used in general in order to determine measurement induced work and heat flow.

This investigation shows that it is possible to formulate a local effective Jarzynski relation for quantum systems by using the LEMBAS definition of work. The Jarzynski method estimates the effective partition sum correctly even in the presence of a heat source, directly coupled to the driven system giving rise to non-negligible heat flow even during the process. The interpretation of the single spin as a heat source according to LEMBAS is backed up by the investigations of Secs. 11.1.1 and 11.1.3. Note, that the environment starts in a classical ensemble, here, in the sense that the environment, initially in a canonical state, is projected into an energy-eigenstate due to the measurement.

[3] As we solve the Schrödinger equation by numerical exact diagonalization, bilocal EFT does not suffer from numerical integration errors.

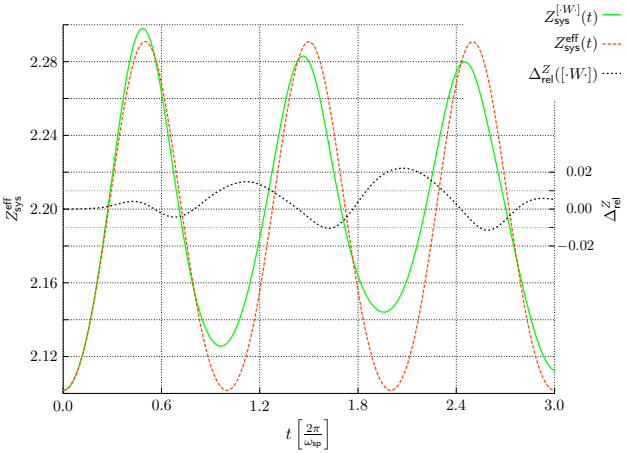

Figure 11.9.: Prediction of the Jarzynski method ($[\cdot W\cdot]$), $Z_{\mathsf{sys}}^{[\cdot W\cdot]}(t)$ (green line) as well as exact result for effective partition sum, $Z_{\mathsf{sys}}^{\mathsf{eff}}(t)$ (orange dashed line). Here, method B was used in order to determine the work exerted onto the system by the measurement. For the relative deviation, $\Delta_{\mathsf{rel}}^{Z}([\cdot W\cdot])$ (black dotted line), the scale on the right-hand side applies.

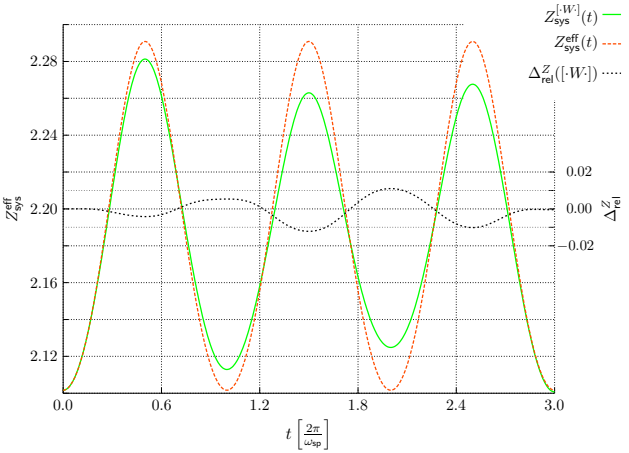

Figure 11.10.: Prediction of the Jarzynski method ($[\cdot W\cdot]$), $Z_{\mathsf{sys}}^{[\cdot W\cdot]}(t)$ (green line) as well as exact result for effective partition sum, $Z_{\mathsf{sys}}^{\mathsf{eff}}(t)$ (orange dashed line). Here, method A was used in order to determine the work exerted onto the system by the measurement. For the relative deviation, $\Delta_{\mathsf{rel}}^{Z}([\cdot W\cdot])$ (black dotted line), the scale on the right-hand side applies.

11.2. Two-spin driver

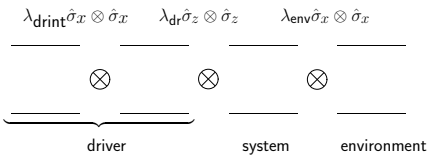

Figure 11.11.: Two-spin driver with system and environment. The environment is coupled to the system only.

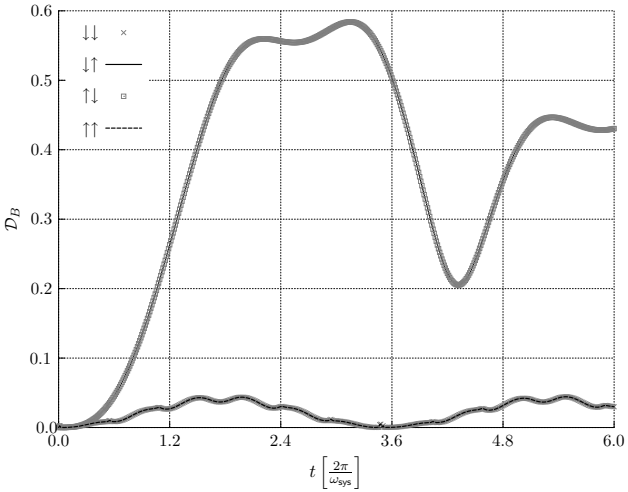

Figure 11.12.: Bures distance $\mathcal{D}_B$ between factorizing and true state of the combined system composed of driver and environment for the four different possible initial states. The left arrow refers to the system, the right one to the environment. The distance is the same for vanishing total magnetization and maximal magnetization.

In this section we are concerned with the two-spin driver. As we have seen in the previous sections, the oscillator, acting as an effective driver for the system, is relatively stable against adding an additional spin acting as environment. This stability is influenced by α and m, as has already been discussed.

We start with parameters as in Sec. 10.2, with the additional coupling

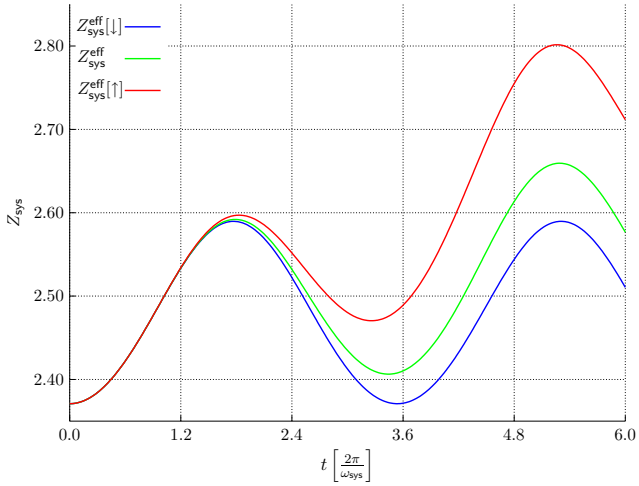

Figure 11.13.: Evolution of numerical exact effective partition sum of the system for starting in the ground state (blue line), in the excited state (red line) and for the thermal average thereof (green line).

strength, $\lambda_{\mathsf{env}} = 0.1$, resonant splitting of the environmental spin, $\omega_{\mathsf{env}} = \omega_{\mathsf{sys}} = 1$ and a canonical state with an inverse temperature of $\beta_{\mathsf{env}} = 1.5$. The coupling is comparatively strong. As $[\hat{H}_{\mathsf{drsys}}, \hat{H}_{\mathsf{se}}] \neq 0$, we expect that the environment will influence the driver. Indeed, we find that $\mathcal{D}_B$ gets as large as 0.6, cf. Fig. 11.12. Therefore, the split bipartite view may be problematic. Moreover, due to the strong correlations between driver and environment, the driver may loose its original properties, especially the state-independent driving. Indeed, Fig. 11.13 clearly shows that the effective partition sum evolves differently for different initial states[4]. Accordingly, we do expect that bilocal EFT will not give the correct estimate for the effective partition sum, here. However, its deviation from the thermal average $Z^{\mathsf{eff}}_{\mathsf{sys}}(t)$, cf. Eq. (10.4), should be smaller than for EFT, as is indeed confirmed by our numerics. The deviation of EFT gets as large as about 40% while for bl-EFT, it is less than 8% (again, the sum rule for the conditional probability $K_{ff',ii'}$, cf. Eq. (4.18) is found to be fulfilled numerically).

Now, we could proceed as for SOM, defining a tolerance for the deviation given by the bilocal EFT. However, as the deviation of the bilocal EFT is that large, the conclusions might be wrong due to an unidentified error source.

[4]For $Z^{\mathsf{eff}}_{\mathsf{sys}}[\downarrow]$ and $Z^{\mathsf{eff}}_{\mathsf{sys}}[\uparrow]$ we have assumed that the environment starts in the ground state, while for $Z^{\mathsf{sys}}_{\mathsf{eff}}(t)$, the weighting as described above has been performed.

Therefore, we consider a weaker coupling. Moreover, in order to minimize $[\hat{H}_{\mathsf{drsys}}, \hat{H}_{\mathsf{se}}] \propto \lambda_{\mathsf{dr}}\lambda_{\mathsf{env}}$, the coupling between driver and system will be reduced, while the other parameters are kept fixed.

11.3. Two-spin driver: Weak coupling

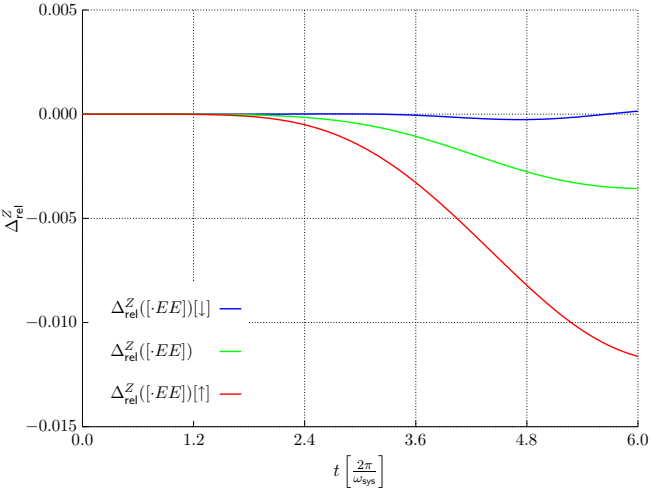

Figure 11.14.: Relative deviation Δ^Z_{rel} of bilocal EFT with respect to the numerical exact effective partition sums for $\hat{\rho}^0_{\mathsf{sys}} = |\downarrow\rangle\langle\downarrow|$ (blue line), $\hat{\rho}^0_{\mathsf{sys}} = |\uparrow\rangle\langle\uparrow|$ (red line) and the thermal average weighted by the initial temperature (green line), respectively.

For weaker couplings between driver and system, $\lambda_{\mathsf{dr}} = 0.1$ and $\lambda_{\mathsf{env}} = 0.05$, we find that the state-dependency of the driving protocol is dramatically reduced. Notably, the Bures distance between factorizing and exact driver-environment state is still relatively large and reaches values of about 0.3. Nevertheless, bilocal EFT gives a quite good estimate for the effective partition sum, as can be seen in Fig. 11.14. The relative deviation of EFT still reaches up to about 25%, which was to be expected if we have a heat flow into the system during the process. For estimation via the Crooks and Jarzynski method, the same holds true as already discussed in Sec. 11.1 and the respective subsections. We conclude that our results from Sec. 9.1 are perfectly confirmed by our numerics. Also, we can see that for relatively strong couplings, the original properties of the subpart of the quantum system are lost,

invalidating the estimation methods introduced, here. In order to show that the deviations of bilocal EFT and the Crooks method really are caused by state-dependent driving, we investigate a model with a perfect driver.

11.4. Classical external driver

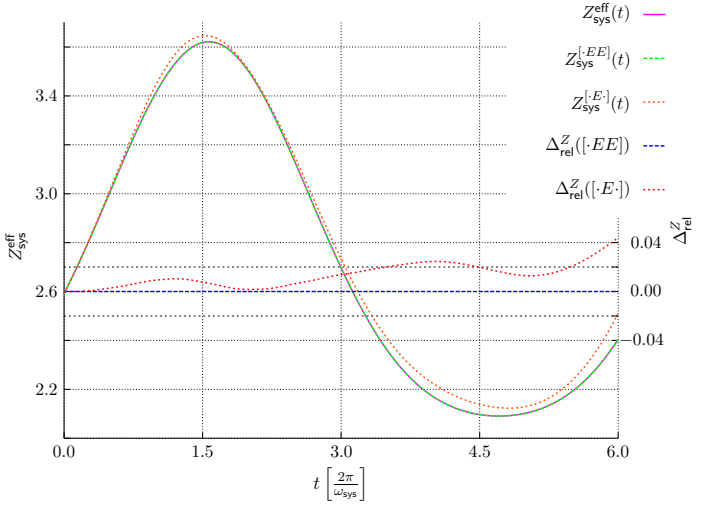

Figure 11.15.: Numerical exact effective partition sum $Z^{\mathsf{eff}}_{\mathsf{sys}}(t)$ (magenta), bilocal EFT prediction (green) and EFT prediction (orange). As the bilocal EFT prediction coincides with $Z^{\mathsf{eff}}_{\mathsf{sys}}(t)$, the latter line is covered by the former one. For the relative deviation of bilocal EFT (blue) and EFT (red), the scale on the right-hand side applies.

Here, we investigate two spins, one of which is driven externally by a perfect driver. The driving is realized by an explicitly time-dependent Hamiltonian of the system spin,

$$\hat{H}(t) = \frac{\omega_{\mathrm{sp}}(t)}{2}\hat{\sigma}_z \otimes \hat{1}_{\mathsf{env}} + \frac{\omega_{\mathsf{env}}}{2}\hat{1}_{\mathsf{sys}} \otimes \hat{\sigma}_z + \frac{\lambda_{\mathsf{env}}}{2}\hat{\sigma}_x \otimes \hat{\sigma}_x. \tag{11.4}$$

The model is thus equivalent to the ones presented in Secs. 11.1 and 11.2 despite of the time-dependent energy splitting of the system spin. For our numerics we choose $\omega_{\mathsf{env}} = 1$ and $\lambda_{\mathsf{env}} = 0.05$. Moreover, the driving is

supposed to be realized sinusoidal,

$$\omega_{\mathrm{sp}}(t) = \frac{1}{2}\left[1 + 0.6\sin\left(\frac{t}{2\pi}\right)\right]. \tag{11.5}$$

First, our numerics confirm that $Z_{\mathsf{sys}}^{\mathsf{eff}}(t)$ is independent of the initial state. Second, Fig. 11.15 shows that bilocal EFT does indeed give the correct estimate for $Z_{\mathsf{sys}}^{\mathsf{eff}}(t)$, as both curves coincide and the relative deviation vanishes. Also, EFT does fail, its relative deviation reaches 4% during the time span investigated. Moreover, Fig. 11.16 confirms that the estimation using the Crooks method gives the correct estimate (within a deviation smaller than $3 \cdot 10^{-5}$ which stems from numerical integration).

However, Fig. 11.16 also reveals that the Jarzynski method does not estimate the effective partition sum correctly. Both definitions of measurement induced work, method A and method B, do lead to deviatons from the correct effective partition sum. This could not be seen from the studies above, where the state-dependent driving covered this finding. This is clearly a hint that both *ad hoc* definitions of measurement induced heat and work would have to be improved for gaining better estimates using the Jarzynski method. Also, one may argue that the coupling to the environment is too strong for feasible definitions of thermodynamic properties, here. Indeed, for weaker couplings we find that the relative deviations gets smaller. Of course, it is possible to generalize the definition of effective partition sums for interacting systems in another way as is done in this thesis using LEMBAS (cf., e. g. [7, 11]). However, the use and meaning of different generalizations of thermodynamic variables remains debatable especially when strong couplings are involved.

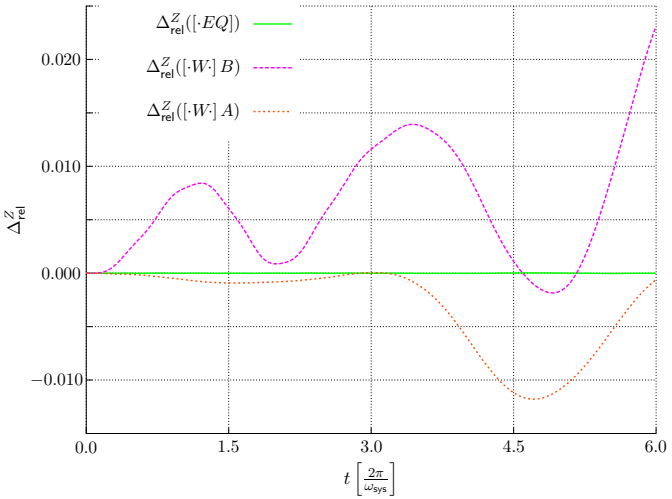

Figure 11.16.: Relative deviation of both the Crooks method (green) and the Jarzynski method, for which both definitions of measurement induced work, method B (magenta) and method A (orange) were used.

12. Additional one-spin environment: local measurements

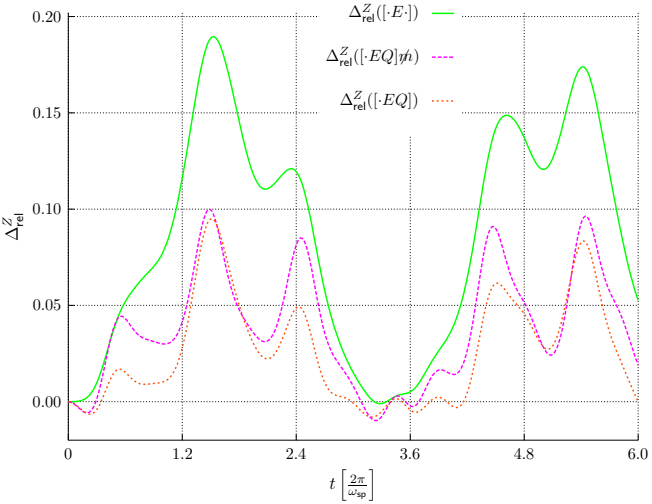

Figure 12.1.: Relative deviations Δ^Z_{rel} of EFT (green) as well as of estimation via the Crooks method ($[\cdot EQ]$, orange line). The magenta line gives the estimation of Crooks' method if the heat flow into the environment arising from the final measurement of the system was ignored, $[\cdot EQ]\not\hbar$.

In the previous chapter we have studied a tripartite quantum system. One part acted as a driver (dr) onto the second part, the system (sys), which was coupled to an environment (env). We study the same model as in Chap. 11, Sec. 11.1, depicted in Fig. 11.1. Here, however, only the system (sys) is being measured locally (in contrast to the previous chapter where system (sys) and environment (env) have each been measured locally). Then, we investigate the EFT and the estimation via both Crooks and Jarzynski method. For

the Crooks method, we assume that we could measure the heat flow into the environment (env) without using projective measurements, there. As the environment (env) starts in a thermal state, now, it will generally be in a mixed state after the final measurement on the system (sys) has been performed. Therefore, it is questionable whether the Crooks method will give the correct estimate for the effective partition sum of the system (sys).

We use the same parameter set as in Sec. 11.1. From our numerics we find that the Bures distance between the true combined state of driver and environment and the factorizing state is very small. Thus, the tripartite view should work well (cf. the discussion in Sec. 11.1). Moreover, we have that the driving is state-independent within very good approximation.

Fig. 12.1 shows the relative deviation of EFT and the Crooks method. As can be seen, EFT fails to give the correct estimate as expected, but so does Crooks' method. The latter has smaller deviations, and as in Sec. 11.1.3, ignoring the measurement induced heat flow leads to even larger deviations (at least most of the time). As mentioned above, as the environment starts in a mixed state and also ends in one, we have a lack of information. The state of system and environment combined is not pure. Keep in mind that if it would be a statistical mixture (as in Chap. 11), where the environment was pure after the measurement, then, Crooks method would estimate the partition sum correctly. So, the fact that it fails here can be considered a quantum effect in this sense[1]. This effect is discussed in more detail in Sec. 12.1.

Of course, one may argue that the definition of measurement induced heat and work is flawed: In Eq. (C.26) and (C.27) we have assumed that the total change of internal energy is to be considered as heat, there. However, according to Sec. C.4, the share of energy change attributed to changing the state unitarily (without changing von Neumann entropy) should be counted as work. So, with a more elaborate definition of measurement induced heat, one may find that the Crooks method is able to give the correct estimate.

However, it should not come as a surprise that the lack of knowledge due to the mixed state of the environment may lead to deviations of the estimator for the effective partition sum.

For the Jarzynski method, we find deviations comparable to the ones obtained in the previous chapter. It seems that this method is only slightly influenced by the fact that the environment is in a mixed state for single process realizations, here.

[1] If it would be possible to measure the heat flow into the environment without performing projective measurements on the environment, it could be possible to confirm this quantum deviation, allowing for differentiating between *subjective* lack of knowledge (statistical mixture) and *objective* lack of knowledge (quantum mixed state).

12.1. Quantum deviation of the Crooks method

We discuss the quantum deviation of the Crooks method described above for an externally driven spin (sys) coupled to an environmental spin (env). This model has already been discussed in Sec. 11.4 for bilocal measurements. Here, we use the Hamiltonian given in Eq. (11.4) with the explicit driving according to Eq. (11.5). Moreover, we choose $\omega_{\mathsf{env}} = 1$ and $\lambda_{\mathsf{env}} = 0.07$. The initial state of the compound system is given by

$$\left(\hat{\rho}^0\right)_{ij,i'j'} = \frac{\mathrm{e}^{-\beta_{\mathsf{sys}} E_i^{\mathsf{sys}}}}{Z_{\mathsf{sys}}^0} \cdot \frac{\mathrm{e}^{-\beta_{\mathsf{env}} E_{i'}^{\mathsf{env}}}}{Z_{\mathsf{env}}^0} \delta_{ij}\delta_{i'j'}, \tag{12.1}$$

which corresponds to a factorizing state with canonical distributions of system (sys) and environment (env) with the respective inverse temperatures β_{sys} and β_{env}. Now, we compare two different settings:

subjective lack of knowledge: We have to describe the state as an ensemble. Both, system (sys) and environment (env) are in a pure state initially for a single process realization, but we do not know which one (classical interpretation). For many repetitions the probability that system and environment have been in a distinct state initially is given by the canonical distribution each, c. f. Eq. (12.1). (This scenario coincides with bilocal measurements).

objective lack of knowledge: Both, system (sys) and environment (env) are in mixed states initially. Measuring the system (sys) locally does project it into a pure state, but the environment, which is not affected by the measurement, remains in a mixed state even for a single process realization.

The second setting is clearly quantum as it involves mixed states of single systems.

In the following, we study EFT as well as both, Jarzynski and Crooks method. We compare their predictions for $Z_{\mathsf{sys}}^{\mathsf{eff}}(t)$ for the case where a) the environment starts in a pure state with probabilities given by Eq. (12.1) for single process realizations and b) the environment starts in a mixed state. For the Crooks method we assume that, in the latter case, it would be possible to determine the heat flow into the environment without measuring the environmental state projectively.

As Fig. 12.2 shows, both initial states lead to exactly the same deviation when using the EFT estimator (green and red line). Obviously, by averaging over the ensemble of measurements, we have no additional information on the

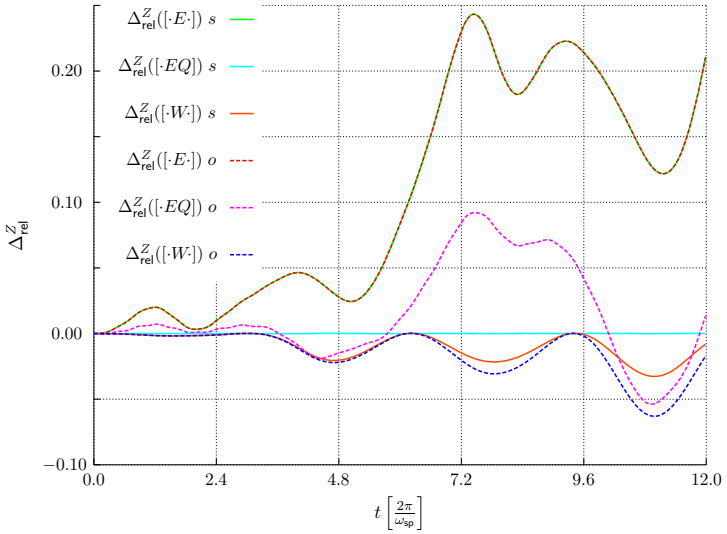

Figure 12.2.: Relative deviations Δ^Z_{rel} of EFT and both Crooks and Jarzynski method (measurement induced work determination method A). The index s (subjective lack of knowledge) refers to pure initial states of the environment while o (objective lack of knowledge) refers to a mixed environmental state. Note that for EFT, both initial states lead to the same large relative deviation.

state of the system (sys) and we have no way to differ between subjective and objective lack of knowledge. Note that the deviations found for SOM for local and bilocal measurements do not coincide due to state-dependent driving.

As we have already seen, estimation using the Crooks method gives the exact result for $Z^{\mathsf{eff}}_{\mathsf{sys}}(t)$ (cyan line) if the environment was in a pure state initially, but it produces relatively large deviations for a mixed state (magenta line). The Jarzynski method estimator shows deviations for both initial states, however, after about half of the considered process time, the deviation is less for a pure initial state of the environment than for the mixed state (orange and blue line). This might come as a surprise at first glance, since for the Jarzynski method, only local measurements on the system (sys) are performed. Thus, the additional lack of information concerning the environment does not enter the discussion directly, here. However, the state of the system (sys) is influenced by the environment and this influence depends, in general, on the state of the environment. Unfortunately, it remains unclear how $\Delta W^{\mathsf{Lem}}_{\mathsf{sys}}$ can be measured for general systems.

Again, we have seen that by using the LEMBAS separation of energy exchange into heat and work we are able to discuss local fluctuation theorems. The fact that both Crooks and Jarzynski method estimators lead to relatively large deviations for objective lack of knowledge is not too problematic, here. First, for short process times both methods estimate the effective partition sum of the system (sys) quite well (deviation of maximally about 1% up to $t \approx 4{\times}2\pi$) which indicates that for weaker coupling the estimates will improve. Indeed, our numerics show that reduction of the coupling strength leads to better estimates. Second, it is not clear whether the direct generalization of the JR, the estimation via the Jarzynski method, should be able to predict the effective partition sum for large heat flows into the system correctly.

13. Spin-oscillator model with additional two-spin environment

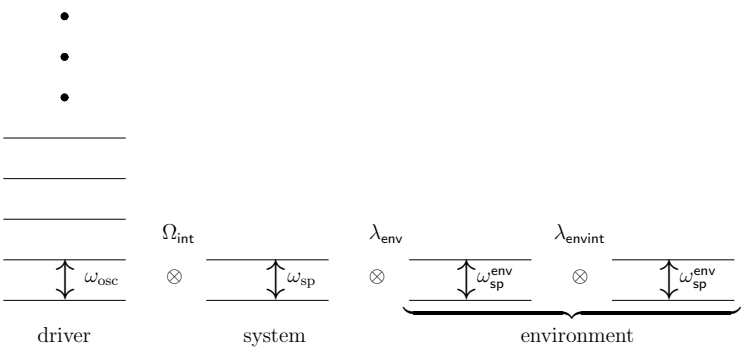

Figure 13.1.: The oscillator (driver) is coupled to the system, which is itself coupled directly to one environmental spin. The environment consists of two spins. These are coupled resonantly with interaction strength $\lambda_{\mathsf{envint}}$.

Up to now, we have investigated an effectively driven system (sys) coupled to a small environment (1 spin only). Here, we investigate a model quite analogue to Chap. 11.2, cf. Fig. 13.1, but the environment (env) is extended by an additional spin. The environment internal coupling is chosen to be $\hat{H}_{\mathsf{int}}^{\mathsf{env}} = \lambda_{\mathsf{envint}} \hat{\sigma}_x \otimes \hat{\sigma}_x$, thus we expect that only heat flows inside the environment, cf. Chap. 8. Dependent on the initial states of the environmental spins, they will mainly swap energy between each other. In a semi-classical picture the dynamics could be described as spin-flips with a certain frequency. For the coupling of the system (sys) to the environment (env), we choose either $\hat{H}^{\mathsf{se}} = \lambda_{\mathsf{env}} \hat{\sigma}_x \otimes \hat{\sigma}_x$, cf. Sec. 13.1 or the coupling described in the paragraph below. If the flipping frequency is very high, we expect that the environment will loose its possibility to exchange heat with the system, validating EFT (high flipping frequency means effectively a totally mixed state even when taking time averages over short time spans).

If the coupling between system and environment is chosen as $\hat{H}_z^{\mathsf{se}} = \lambda_{\mathsf{env}} \hat{\sigma}_z \otimes \hat{\sigma}_z$, cf. Sec. 13.2, we have that the state of the first environmental spin influences the effective splitting of the system[1]. Thus, the effective partition sum of the system (sys) depends on the state of the environment. If, however, the environmental spin coupled to the system undergoes very fast oscillations (flippings in the semi-classical picture), then we expect that this dependency can no longer be resolved. This scenario is reminiscent of NMR, where exchange or motion narrowing of spectral lines can occur [28]. Thus, for very small $\lambda_{\mathsf{envint}}$ we expect that the extremal cases $|\downarrow\rangle\langle\downarrow|$ and $|\uparrow\rangle\langle\uparrow|$ of the connecting environmental spin can be resolved for fast enough process protocols while for strong $\lambda_{\mathsf{envint}}$, they will become indistinguishable as the time-average of the environmental spin looks like a totally mixed one, even for short time spans averaged over. Of course, if we choose to average over a very long time span, then the average will also look like this state for weak $\lambda_{\mathsf{envint}}$.

We start by investigating the heat exchanging interaction.

13.1. Environment as heat source

As described above, we expect that fast flipping dynamics of the border spin of the environment (env) (cf. Fig. 13.1, 2nd spin from the left coupled to the system directly) reduces the heat flow into the system, as then the spin assumes an effective totally mixed state (in the time-averaging sense described above). For our numerics, we choose the same parameters as in Chap. 11, Sec. 11.1. The border spin starts in a thermal state with inverse temperature $\beta_{\mathsf{sp2}} = \beta_{\mathsf{sys}}$, the other environmental spin in the inverse state, thus $(\hat{\rho}_{\mathsf{sp3}})_{ij} = \mathsf{diag}\left[(\hat{\rho}_{\mathsf{sp2}})_{11}, (\hat{\rho}_{\mathsf{sp2}})_{00}\right]$ so that they can perform optimal swaps with respect to the initial occupancy.

Fig. 13.2 confirms that the stronger the environment internal coupling $\lambda_{\mathsf{envint}}$, the smaller the relative deviation of the EFT prediction. For $\lambda_{\mathsf{envint}} = 1.50$, the relative deviation is less than 1% for the time investigated, here. For relatively weak coupling, it gets as large as about 20%. Also, our numerics confirm that the heat flow according to LEMBAS is reduced the stronger $\lambda_{\mathsf{envint}}$. Therefore, if an experimenter has only limited control over the environment (decoupling impossible), it may be possible to reduce environment induced perturbances through strong driving (by a laser, e. g.) of the environment.

Note that the environment is not in a pure state, here. More precisely, the initial state is even non-diagonal in the energy-eigenbasis of the environment as we have prepared the states into eigenstates of the bare environmental

[1] With this coupling, the environment can be identified as the two-spin driver from Chap. 7, in principle. However, the initial state of both spins is generally not pure, here!

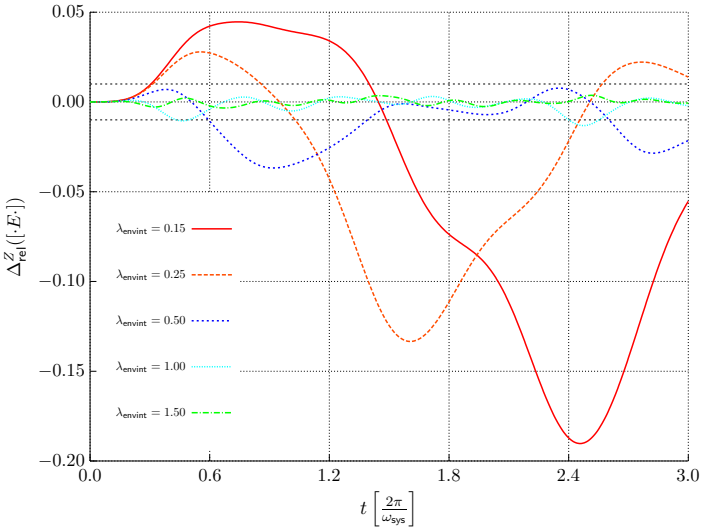

Figure 13.2.: Relative deviation of EFT $\Delta^Z_{\mathsf{rel}}([\cdot E\cdot])$ over process time t for five different environmental internal coupling strengths, $\lambda_{\mathsf{envint}} = 0.15$ (red), $\lambda_{\mathsf{envint}} = 0.25$ (orange), $\lambda_{\mathsf{envint}} = 0.50$ (blue), $\lambda_{\mathsf{envint}} = 1.00$ (cyan) and $\lambda_{\mathsf{envint}} = 1.50$ (green). The dotted lines around 0.00 mark -0.01 and 0.01, respectively.

spins disregarding their interaction. Therefore we expect that the Jarzynski method estimator shows deviations from the exact effective partition sum. As the environment is even larger than before, the deviations might be more severe. Indeed, Fig. 13.3 shows that we have quite large deviations for the Jarzynski method. Similarly to EFT, the deviation gets smaller the stronger $\lambda_{\mathsf{envint}}$, as then the dynamics of the system (sys) is almost not influenced by the environment, reducing this model effectively to SOM discussed in Sec. 10.1.

Moreover, we have chosen relatively strong couplings here. In thermodnyamical settings it is usually important that different systems are only coupled weakly. This is quite intuitive, because the separation of a system into different subparts seems only natural if the interaction energy between the subparts is weak, otherwise one would consider them to be a natural entity[2]. Indeed, if we reduce the coupling between system and environment to

[2]It would be interesting to study situations where $\lambda_{\mathsf{env}} \gg \lambda_{\mathsf{envint}}$. There, we would expect that choosing the two left-most spins as the system under consideration (sys) and only the third spin as the environment (env) would give much better results concerning the estimation methods of the effective partition sum than the separation used in this

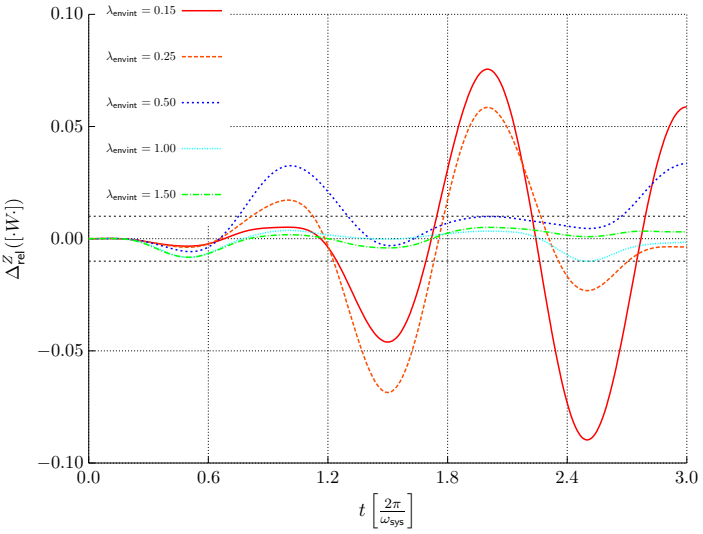

Figure 13.3.: Relative deviation of Jarzynski method estimator, $\Delta^Z_{\text{rel}}([\cdot W\cdot])$, over process time t for five different environmental internal coupling strengths, $\lambda_{\text{envint}} = 0.15$ (red), $\lambda_{\text{envint}} = 0.25$ (orange), $\lambda_{\text{envint}} = 0.50$ (blue), $\lambda_{\text{envint}} = 1.00$ (cyan) and $\lambda_{\text{envint}} = 1.50$ (green). The dotted lines around 0.00 mark -0.01 and $+0.01$, respectively.

$\lambda_{\text{env}} = 0.01$, we find for $\lambda_{\text{envint}} = 0.03$ that the relative deviations of both, EFT (less heat flow) as well as that of the Jarzysnki method are reduced. There, $\Delta^Z_{\text{rel}}([\cdot E\cdot])$ reaches as high as 1.2%, while $\Delta^Z_{\text{rel}}([\cdot W\cdot])$ is less than 0.4% for the time span investigated.

13.2. Environment as perturbation

We investigate the model as depicted in Fig. 13.1 with $\hat{H}^{\text{se}}_z = \lambda_{\text{env}}\hat{\sigma}_z \otimes \hat{\sigma}_z$, as described at the beginning of this chapter. We start with two different initial states of the environment (env), $\hat{\rho}^0_{\text{env}}(\downarrow\uparrow) = |\downarrow\uparrow\rangle\langle\downarrow\uparrow|$ and $\hat{\rho}^0_{\text{env}}(\uparrow\downarrow) = |\uparrow\downarrow\rangle\langle\uparrow\downarrow|$. Both states are pure and lead to perfect energy swapping between the isolated environmental spins. Due to the coupling to the system (sys), this dynamics may be disturbed, however. Note that both intitial states allow for identification of the environment with the perfect driver from Chap. 7. As we have no heat flow into the system (sys) according to LEMBAS, here, we expect EFT to

chapter.

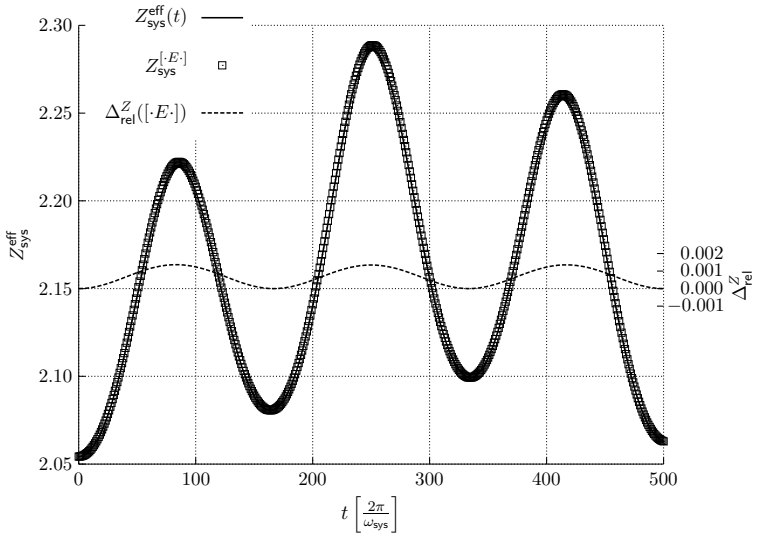

Figure 13.4.: Effective partition sum $Z^{\mathsf{eff}}_{\mathsf{sys}}$ as well as EFT estimator $Z^{[\cdot E\cdot]}_{\mathsf{sys}}$ for $\lambda_{\mathsf{env}} = \lambda_{\mathsf{envint}} = 0.1$. Both coincide with small deviations $\Delta^{Z}_{\mathsf{rel}}([\cdot E\cdot])$, for which the scale on the right-hand side applies (ten times enlarged).

hold. Indeed, as can be seen from Fig. 13.4, EFT estimates the effective partition sum numerically exact within the deviation arising from state-dependent driving. Moreover, we find that the estimation via the Jarzynski method shows exactly the same deviation as EFT, here. Again, the defintion of work according to Lembas explains perfectly why EFT does give the correct estimate and using this work directly in the Jarzynski method gives the correct effective partition sum.

Although the environment (env) could be seen as a driver, we want to consider it as a perturbation, in the following. The oscillator is interpreted as the external driver (dr) and the effective partition sum we aim to determine is given by the effect of the oscillator (dr) on the system (sys), only.

For our numerics we choose a fixed final measurement time interval $t_f + \delta\tau$, where $\delta\tau$ is randomly chosen from $\pm 0.1 \cdot t_f$. Then, the result obtained for EFT is averaged over. This is done to represent the fact that the final measurement time might not be perfectly reproducable. Moreover, as we have chosen definite initial states, we have not accounted for the fact that the state of the environment (env) might already be random initially. With these choices, we expect that EFT gives the unperturbed effective partition sum for strong

$\lambda_{\mathsf{envint}}$ and thus fast flipping dynamics (fast compared to the driving velocity), while for very weak $\lambda_{\mathsf{envint}}$ and slow dynamics it should give $Z^{\mathsf{eff}}_{\mathsf{sys}}(\downarrow)$ and $Z^{\mathsf{eff}}_{\mathsf{sys}}(\uparrow)$ for the corresponding initial states of the environment, respectively. The argument of the effective partition sum refers to the state of the environmental spin coupled to the system directly, here. For the parameters chosen we readily obtain $Z^{\mathsf{eff}}_{\mathsf{sys}}(\downarrow) \approx 2.2034$, $Z^{\mathsf{eff}}_{\mathsf{sys}}(\uparrow) \approx 2.3933$, while for the unperturbed partition sum we find $Z^{\mathsf{eff}}_{\mathsf{sys}} \approx 2.2901$. Fig. 13.5 confirms that for weak $\lambda_{\mathsf{envint}}$, EFT is able to differ between the effective partition sum for the limiting cases of the first environmental spin being either in the ground or the excited state, while for strong $\lambda_{\mathsf{envint}}$, EFT gives the correct unperturbed parititon sum. Note, that EFT does not approach $Z^{\mathsf{eff}}_{\mathsf{sys}}$ with increasing $\lambda_{\mathsf{envint}}$ monotoneously. This is due to the fact that we exactly reproduce the inital conditions, while only the final measurement time has an artificially introduced uncertainty. As the environmental spins perform oscillations, it might happen that we come already close to $Z^{\mathsf{eff}}_{\mathsf{sys}}$ in the final measurement time interval for relatively weak $\lambda_{\mathsf{envint}}$.

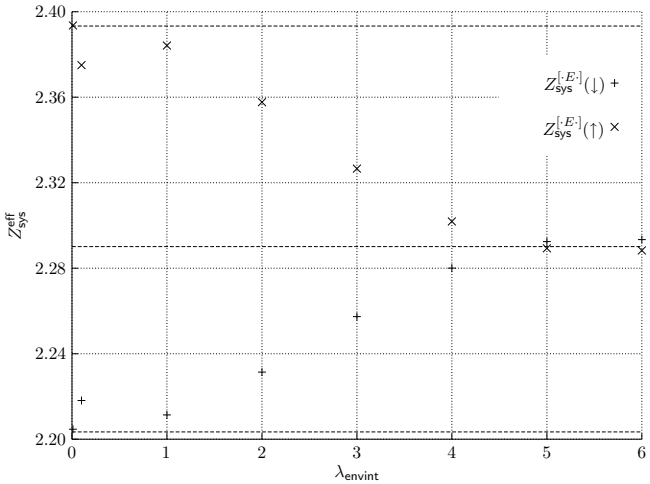

Figure 13.5.: Effective partition sums according to EFT for different initial states of the environment, $Z^{[\cdot E\cdot]}_{\mathsf{sys}}(\downarrow)$ and $Z^{[\cdot E\cdot]}_{\mathsf{sys}}(\uparrow)$, over the internal coupling of the environment, $\lambda_{\mathsf{envint}}$. The dashed horizontal lines denote the numerical exact partition sums $Z^{\mathsf{eff}}_{\mathsf{sys}}(\downarrow) = 2.2034$, $Z^{\mathsf{eff}}_{\mathsf{sys}}(\uparrow) = 2.3933$ as well as the unperturbed partition sum $Z^{\mathsf{eff}}_{\mathsf{sys}} = 2.2901$, respectively.

14. Bipartite three-spin model with thermalizing environment

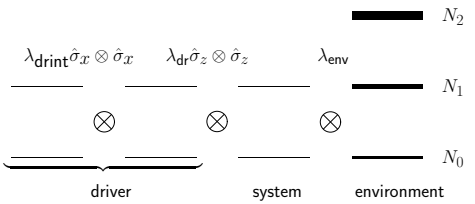

Figure 14.1.: Spin acting as system (sys) coupled to an effective driver (the two leftmost spins) and an environment (env), whose spectrum is modeled as three energy bands with rising degeneracy N_0, N_1 and N_2.

Up to now, the models considered have been fully quantum with respect to the dynamics following the initial measurements (process), however, the initial conditions were chosen without explaining how they might arise by also considering only quantum systems. Here, we investigate a quantum model which features thermalization of the system (the initial state chosen in the preceeding sections) as well as effective driving. We combine the two-spin driver (dr) from Chap. 7, Eq. (7.1), acting on the system of interest (sys) and a thermalizing environment (env) as described by Eq. (5.15) in Sec. 5.3.1 (cf. Fig. 14.1). Of course, the two-spin driver may be influenced by the environment (env) indirectly and vice versa, but for small enough coupling strengths both subsystems should keep their original properties when considering short time scales.

Here, we have chosen the two-spin driver to keep the numerical effort on a tolerable level, although we have seen that it reacts much more sensitive to modularization than the oscillator, cf. Secs. 11.1 and 11.2. First, we choose a system−environment coupling as discussed in the first part of Sec. 5.3.2, as then, the system (sys) should only receive heat from the environment (env) according to LEMBAS. Then, we show that a system−environment coupling discussed in the second part of Sec. 5.3.2 does indeed lead to a partially working environment despite of its apparent thermalization behavior.

14.1. EFT and Jarzynski method

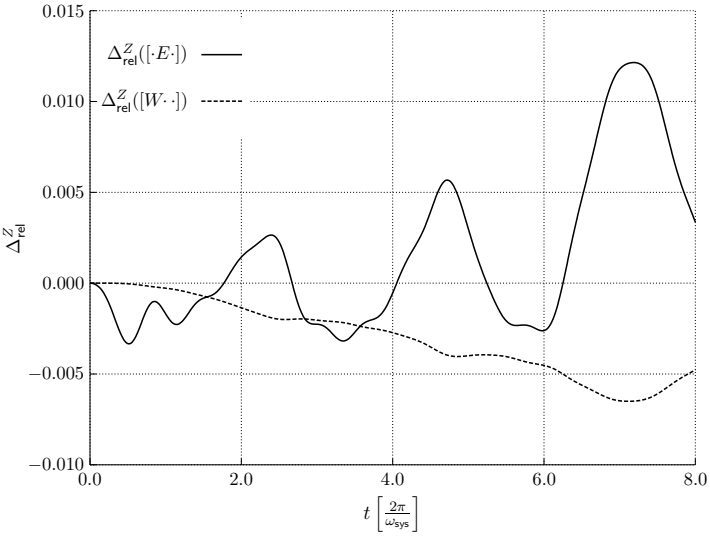

Figure 14.2.: Relative deviation of estimation via both EFT, $\Delta^Z_{\mathsf{rel}}([\cdot E\cdot])$, and the Jarzynski method, $\Delta^Z_{\mathsf{rel}}([W\cdot\cdot])$.

Here, we investigate both, EFT and estimation via the Jarzynski method, $[W\cdot\cdot]$. For the latter, we only consider the two spins (dr) as the work source, treating the environment (env) as a heat source. This heat source (env) has partially bath properties, namely that it is able to thermalize the system, however, it is far from being a perfect bath as its own state is not canonical and does change markedly during the observation time. As LEMBAS predicts only heat exchange between system (sys) and environment (env), we expect EFT to fail but the Jarzynski relation to give a godd estimate of the effective partition sum.

Indeed, as Fig. 14.2 shows, the Jarzynski method gives a quite good estimate of the effective parition sum while the estimation of EFT is worse most of the time. There are two reasons for the deviation of the Jarzynski method: First, the investigation of the Bures distance reveals that it rapidly rises up to around 0.6 on average and the absolute of the interaction energy between system (sys) and environment (env) fluctuates around 0.03, which is still relatively large compared to the absolute value of internal energy of the system (sys) which lies at about 0.1. Note, that if we choose a very weak coupling between the system and the thermalizing environment, the latter can be considered

decoupled during the process as the dynamics are usually much slower due to the weak coupling. The investigations of the previous chapters without a thermalizing environment can thought of as belonging to such a weak coupling scenario.

In the following section, we want to investigate the completely random coupling discussed in the second part of Sec. 5.3.2.

14.2. EFT and Jarzynski method for partially working environment

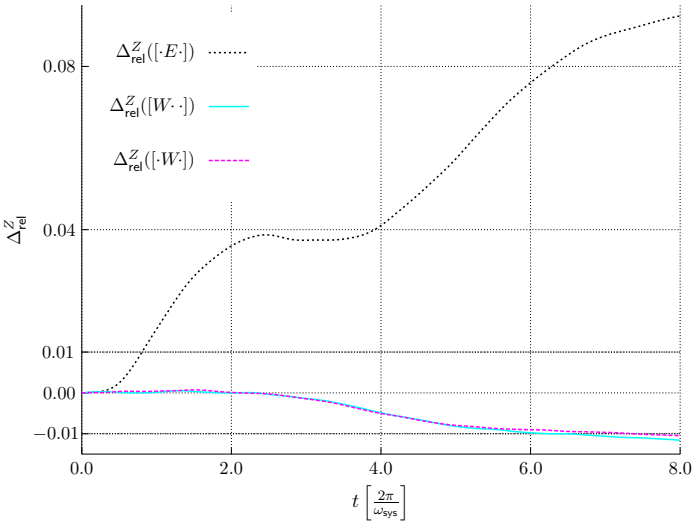

Figure 14.3.: Relative deviation of both, EFT, $\Delta^Z_{\mathsf{rel}}([\cdot E\cdot])$, and estimation via the Jarzynski method, $\Delta^Z_{\mathsf{rel}}([W\cdot\cdot])$ and $\Delta^Z_{\mathsf{rel}}([\cdot W\cdot])$.

We investigate the same model as in the previous section but with the system−environement coupling introduced in Sec. 5.3.1. As we have seen this coupling leads to faster thermalization. However, LEMBAS does predict a non-vanishing work exchange between the spin (sys) and the environment (env) for this kind of coupling. When only considering the effect of this environement (env) onto the system (sys) without performing a LEMBAS analysis, one might be tempted to think of this environment as a heat bath, as it thermalizes the system (sys). As a consequence the total energy exchange between system and environment could then be interpreted as heat which could lead to violations of

the Clausius inequality and subsequently to cyclic processes violating Carnot efficiency (cf. also Chap. 16).

For our numerics we choose the same parameters as in Sec. 13.1, however the coupling strength between system and environment, λ_{env}, cannot be compared directly to that of the aforementioned section as the coupling is different. As a more independent means of measuring coupling strength we take the interaction energy, which is found to fluctuate around -0.03 and $+0.01$ (depending on the initially measured state), approximately. Thus, the interaction is a little bit weaker, here. The Bures distance gives results comparable to the previous section. As can be seen from Fig. 14.3, EFT shows large deviations from the numerical exact effective partition sum as we have a larger heat flow, here. The deviation of the Jarzynski method taking only the two-spin driver as a work source (dr), $[W\cdot\,\cdot]$, shows moderate deviations of about 1%. If this error is solely due to the fact that the work flow from the environment (env) has been ignored, then using the total work exerted onto the system (sys) by both driver and environment ($[\cdot W\cdot]$) should give a significantly better estimate. However, Fig. 14.3 reveals that the estimation given by $[\cdot W\cdot]$ does almost coincide with the one given by $[W\cdot\,\cdot]$.

To get a clearer picture, we consider the model as in Sec. 5.3.2 without any driver. Considering any energy flow from the environment as heat, we would trivially find $\Delta W_{\mathsf{dr}} = 0 = \Delta W_{\mathsf{sys}}$ from which immediately follows $Z^{\mathsf{eff}}_{\mathsf{sys}}(t) = Z^{\mathsf{eff}}_{\mathsf{sys}}(0)$ according to the Jarzynski method. However, using LEMBAS, we find that $\Delta W^{\mathsf{Lem}}_{\mathsf{sys}} \neq 0$. In this setting, the estimation using $\Delta W_{\mathsf{sys}} = 0$ deviates about 1.3% from the exact effective partition sum, while using $\Delta W^{\mathsf{Lem}}_{\mathsf{sys}}$ leads to deviations of about 0.7%. This can be seen as an additional hint that the environment acts indeed partially as a work source on the system.

The investigations of this chapter confirm that a thermalizing environment could in principle be used to obtain a canonical state. It is not necessary to remove the coupling to this environment for weak coupling strengths for investigations of the Jarzynski relation using the work according to LEMBAS as the Jarzynski method gives quite good estimates for the effective partition sum. However, when applying the EFT the thermalizing environment should be decoupled because otherwise the estimation of EFT might differ significantly from the correct effective partition sum. Only if the process would be performed very fast so that $\Delta Q_{\mathsf{env}} \approx 0$ during process time EFT can be expected to give a good estimate.

15. Non-adiabatic driving

Up to now, we have considered situations, where the driving was adiabatic in the following sense: The effect of the driver (oscillator and two-spin driver, respectively) on the system (sys) without any environment (env) was adiabatic as it did only change the effective splitting of the system without inducing any transitions in the basis of the bare system Hamiltonian. This is essentially a feature of the fact that for both drivers discussed in Chaps. 6 and 7 we have that the coupling between driver and system fulfills $[\hat{H}^{\mathsf{int}}_{\mathsf{driver-sys}}, \hat{H}_{\mathsf{sys}}] = 0$. In this chapter we will deal with situations where the commutator does not vanish. Despite the fact that the instantaneous energy-eigenbasis will change due to the driving, we study what happens when keeping the measurement basis fixed, coinciding with the energy eigenbasis of the bare system Hamiltonian.

15.1. External driving

We start by investigating external driving, where the time-dependency of the system (sys) is explicitly contained in the Hamiltonian. We consider a single TLS, its Hamiltonian given by

$$\hat{H}(t) \equiv \frac{\omega_{\mathsf{sp}}}{2}\hat{\sigma}_z + \lambda_{\mathsf{dr}} \sin\left(\omega_{\mathsf{dr}} t\right) \hat{\sigma}_x, \tag{15.1}$$

where the second addend arises from external driving. The measurement basis is chosen to coincide with the energy-eigenbasis of the bare system spin. As we have unitary evolution, here ($\Longrightarrow \Delta S = 0 \Longrightarrow \Delta Q^{\mathsf{Lem}} = 0$), we expect that EFT gives the correct result for the effective partition sum. Also, the Jarzynski method should estimate the effective partition sum correctly. For the choices above we have that the effective parition sum of the system is constant, $Z^{\mathsf{eff}}_{\mathsf{sys}}(t) = Z^{\mathsf{eff}}_{\mathsf{sys}}(0)\ \forall\ t$, as $\hat{H}^{\mathsf{eff}}_{\mathsf{sys}}(t) = \hat{H}^{\mathsf{eff},2}_{\mathsf{sys}}(t)$, $\hat{H}^{\mathsf{eff},1}_{\mathsf{sys}}(t) = 0\ \forall\ t$.

Fig. 15.1 shows the result for $\lambda_{\mathsf{dr}} = 0.4$ and $\omega_{\mathsf{dr}} = (2\pi)^{-1}$. As can be seen, EFT works perfectly, as does the Jarzynski method, $[\cdot W \cdot]$, when method B is used in order to determine measurement induced work into the system (sys). However, when choosing method A for determination of measurement induced work, we have large deviations from the numerical exact partition sum. We want to stress the fact that completely ignoring the energy flow during the

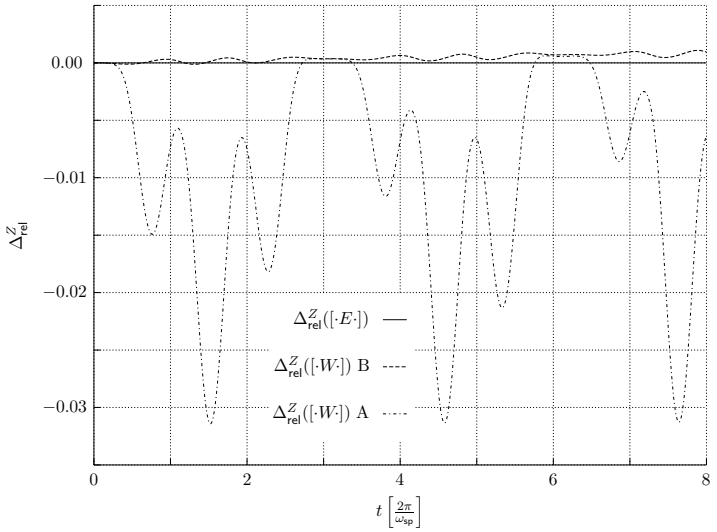

Figure 15.1.: Relative deviations of EFT, $\Delta^Z_{\mathsf{rel}}([\cdot E\cdot])$ and the Jarzynski method using both definitions of measurement induced work flow, method A ($\Delta^Z_{\mathsf{rel}}([\cdot W\cdot])$ A) as well as method B ($\Delta^Z_{\mathsf{rel}}([\cdot W\cdot])$ B).

final measurement, thus taking only $\Delta W_i^{\mathsf{Lem}}$ (the work performed onto the system during the process up to the measurement) for the estimate via the Jarzynski method, leads to deviations from the correct effective partition sum of up to 12% and over about 6% on average. Thus, it is important to take the measurement effect into account.

In order to generalize the situation, we now choose a slightly altered external driving,

$$\hat{H}(t) \equiv \frac{\omega_{\mathrm{sp}}}{2}\hat{\sigma}_z + \lambda_{\mathsf{dr}} \sin\left(\omega_{\mathsf{dr}} t\right)\left(\hat{\sigma}_x + \hat{\sigma}_z\right), \tag{15.2}$$

combining adiabatic and non-adiabatic driving. For this coupling with the same parameters as before, we find that still EFT gives exactly the correct estimate. As above, the Jarzynski method estimates the effective partition sum of the system quite well only if method B for determining measurement induced work flow is chosen. However, we expect that the quality of the estimator might be influenced by an environment.

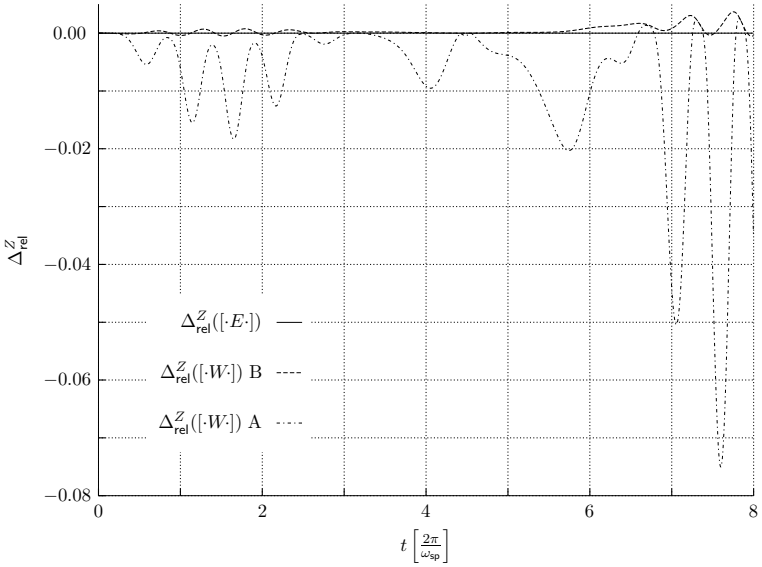

Figure 15.2.: Relative deviations of EFT, $\Delta^Z_{\mathsf{rel}}([\cdot E\cdot])$ and the Jarzynski method using both definitions of measurement induced work flow, method A ($\Delta^Z_{\mathsf{rel}}([\cdot W\cdot])$ A) as well as method B ($\Delta^Z_{\mathsf{rel}}([\cdot W\cdot])$ B).

15.1.1. External driving: Additional one-spin environment

We use the driving given by the Hamiltonian in Eq. (15.1). But, we couple an additional spin to the system as done in Chap. 11 and consider bi-local measurements. Due to the different driving, leading to off-diagonal elements in the density operator, in general, we find that the environment is not a pure heat source, here, but also acts partially as a driver,

$$\Delta W^{\mathsf{Lem}}_{\mathsf{env}} \neq 0 \;\text{ and }\; \Delta Q^{\mathsf{Lem}}_{\mathsf{env}} \neq 0. \tag{15.3}$$

However, it still holds that $\hat{H}^{\mathsf{eff}}_{\mathsf{env}} = \hat{H}^{\mathsf{eff},2}_{\mathsf{env}}$, which gives that the effective Hamiltonian (and thus the effective partition sum) of the environment is not influenced by a measurement of the system. Thus, in comparison with Sec. 4.3 and Chap. 11, we expect that bilocal EFT gives the correct estimate, while EFT fails. Moreover, as we have that the environment acts as both, heat and work source, the Jarzynski method will most likely fail to give a good estimate of the effective partition sum of the system. Indeed, Fig. 15.3 confirms our expectations: While bilocal EFT gives the exact effective partiton sum, EFT shows large deviations. Moreover, the Jarzynski method estima-

tor also shows deviations from the numerical exact result. Again, method B gives better estimates than method A. As both methods suffer from relatively large deviations, this might show that we have chosen too strong couplings or, that the mixed effects of the environment as both, heat and work source, are problematic for the interpretations used here.

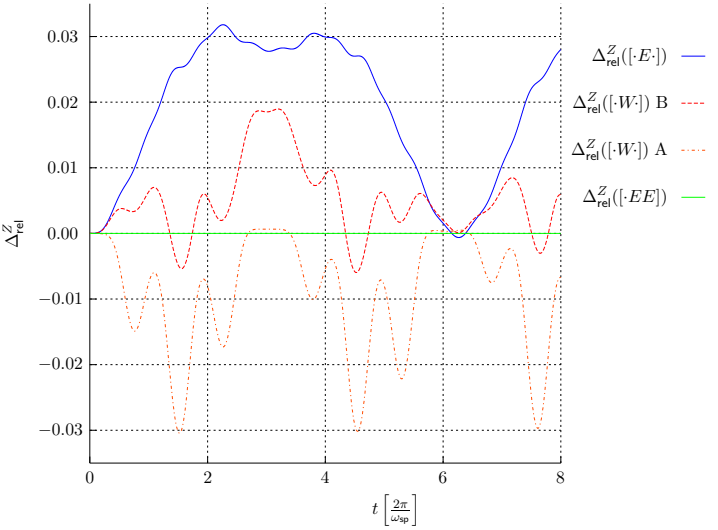

Figure 15.3.: Relative deviations of EFT (blue line), bilocal EFT (green line), as well as for the Jarzynski method using both, method B (red line) and method A (orange line).

15.2. SOM

Now, we return to closed quantum systems and local effective dynamics. In the following, we use the model system from Chap. 6, depicted in Fig. 6.1. However, we choose a different coupling between the oscillator (dr) and the spin (sys), the Jaynes-Cummings interaction, $\hat{H}_{\mathsf{int}} \equiv \frac{\Omega_{\mathsf{int}}}{2}\left(\hat{\sigma}_+ \otimes \hat{a} + \hat{\sigma}_- \otimes \hat{a}^\dagger\right)$. This should give rise to a similar driving as in the previous section. However, according to LEMBAS, the new coupling leads to heat and work exchange between the oscillator (dr) and the system (sys). Nevertheless, we will call the oscillator a driver in the remainder of this section. From [41] we know that the larger α, the more accurate the factorization approximation for finte times t, thus, the less heat flows between system and driver. As already discussed,

the numerical effort grows with α, thus we cannot choose α too large. As long as the purity of the oscialltor remains close to 1, the Jarzynski method should give acceptable estimates for the effective partition sum. Moreover, as we have a heat flow into the system according to LEMBAS we expect EFT to fail. Numerical results for $\alpha = 6$, $m = 190$ and $\Omega_{\mathsf{int}} = -0.03$ can be found in Fig. 15.4. As expected, EFT fails to estimate the effective partition sum correctly, as according to LEMBAS we have heat and work transfer from the oscillator. Only in the beginning of the process, where the purity of the oscillator has not dropped too much, yet, the Jarzynski method gives an excellent estimate of $Z^{\mathsf{eff}}_{\mathsf{sys}}(t)$. However, the devitation grows fast for dropping purity.

Again, the expectations from LEMBAS interpretation of heat and work is in accordance with our numerical results. As already mentioned above, it shows that mixed behavior as heat and work source of a single quantum system is problematic for the estimation methods considered here.

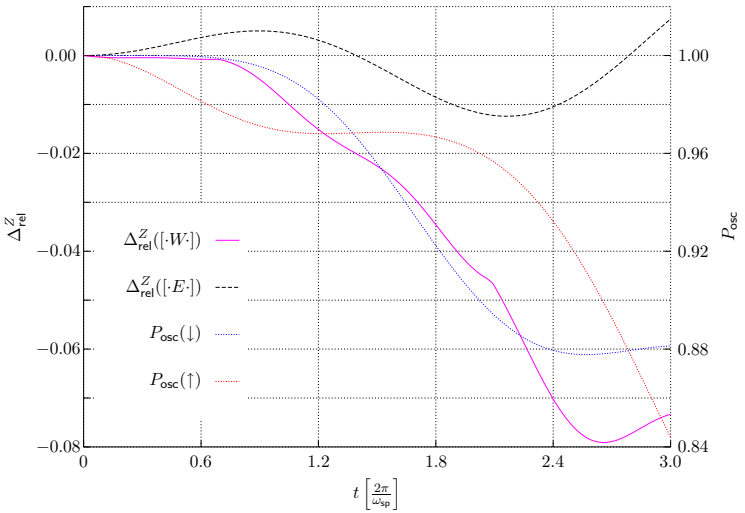

Figure 15.4.: Left-hand scale: Deviations of both EFT and estimation via Jarzynski method. Right-hand scale: Purity of the oscillator for $\hat{\rho}^0_{\mathsf{sys}} = |\downarrow\rangle\langle\downarrow|$ (blue) as well as $\hat{\rho}^0_{\mathsf{sys}} = |\uparrow\rangle\langle\uparrow|$ (orange).

Part IV.

Quantum Jarzynski relation and cyclic processes

16. Cyclic processes

Besides describing relaxation into thermal equilibrium, one of the most important applications of thermodynamics is its description of cyclic processes. When discussing cyclic processes with quantum systems as the working agent, the generally discrete spectrum allows for new features, usually not present in classical systems. In particular, the (classical) heat baths may be taken to be coupled to specific transitions of the spectrum of the system only, cf. [16, 27, 40]. Other investigations are concerned with scenarios where an external control enables both coupling and decoupling from the heat baths or, via adapted filters, lead to effective coupling to only one heat bath at a time [15, 38, 63, 70]. Some of these works are also concerned with non-quasistationary processes, considering the efficiency for maximum power output as first discussed in [18].

Here, we try to make use of the Jarzynski relation and LEMBAS in order to investigate cyclic processes with quantum systems, which are driven in finite time (and thus may reach states far from thermal equilibrium). We restrict ourselves to perfect heat baths, though. For our purpose, a perfect heat bath...

1. exchanges only heat with its surroundings, $\mathrm{d}U_{\mathsf{bath}} = \mathrm{d}Q_{\mathsf{bath}}$,
2. imposes a canonical state within finite relaxation time τ_R onto the system coupled to. This canonical state has the same temperature as the bath, $T_{\mathsf{sys}} = T_{\mathsf{bath}}$,
3. gives rise to pure heat flow into the system coupled to.

We consider cyclic processes between two heat baths of different temperature, restricting ourselves to the case where the system works as a heat engine. Focus will be laid on the efficiency η of these engines.

As we work in a field connecting quantum mechanics and thermodynamics, here, we face the following problem: *Adiabatic* in the thermodynamic sense describes a process without heat flow into the system while in quantum mechanics, it denotes a process without any transitions in the instantaneous eigenbasis of the density operator. In order to avoid confusion, we will use the term "quadiabatic" in order to denote adiabatic in the quantum mechanical sense.

As focus will be laid on the efficiency of the cyclic processes investigated, we give the standard textbook definition of efficiency of a cyclic process [54, 79, 82, 83]:

$$\eta_{\mathsf{id}} \equiv \frac{\text{work output of machine}}{\text{heat absorbed at hot bath}} \,. \tag{16.1}$$

Most textbooks deal with ideal cyclic processes in standard thermodynamics. Therefore, this definition is of course justified, but may lead to confusion when considering more general situations. Especially, it has been implicitly assumed that the heat emitted from the hot bath equals the heat absorbed by the working agent (the index id accounts for that idealization). This holds for standard idealizations in thermodynamics (extensitivity), but when considering situations where energy is not extensive or where we have a heat leakage between hot and cold bath via the system, e. g., then this definition should be replaced by the more strict and more general definition given, e. g., in [26, 64],

$$\eta \equiv \frac{\text{work output of machine}}{\text{heat withdrawn from hot bath}} \,. \tag{16.2}$$

This distinction between η_{id} and η will become important in Sec. 17. We think that the latter definition is the better one, because when considering an engine designed to convert heat into work, one usually has to heat up the hot bath (by sun power, chemical or nuclear reactions, e. g.). Then, one also has to pay for leakage or intrinsic losses of heat conduction from the hot bath into the system. Thus, it is much more interesting to know how much energy is withdrawn from the hot bath than how much heat actually arrived at the system subjected to the cyclic process. Only when considering idealized situations as described above, the definitions coincide.

For the remainder of this thesis, we will use the following sign convention: If the internal energy of the considered system grows due to an energy flow, it will be associated with a positive sign for the energy flow. If the internal energy decreases, the corresponding energy flow will have a negative sign.

16.1. Quantum Otto cycle

The classical Otto cycle (cOC) combines *adiabates* and *isochors*. The quantum variant thereof (qOC), which we are going to investigate, also combines these two process types. As the von Neumann entropy is constant for unitary processes and thus according to Lembas no heat flows into or out of the unitarily evolving system, we will realize the adiabates of the qOC by unitary processes. The isochors (constant volume) correspond to process steps where

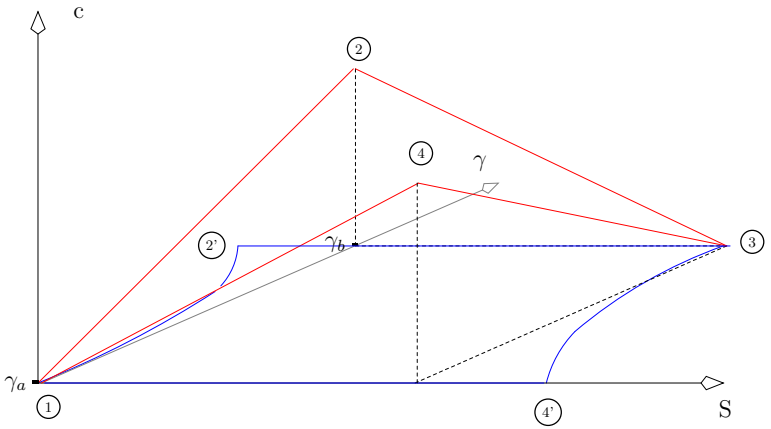

Figure 16.1.: Schematics of qOC (red curves) in an entropy S (x-axis), control parameter γ (y-axis, "volume") and canonicity c (z-axis) plot. $1 \longrightarrow 2$ and $4 \longrightarrow 1$ represent the adiabatic steps ($\Delta S = 0 \implies \Delta Q^{\mathsf{Lem}} = 0$) and $2 \longrightarrow 3$ as well as $4 \longrightarrow 1$ the isochoric steps ($\gamma = \text{const.}$). The blue curve describes a quasi-classical Stirling process combining isotherms ($1 \longrightarrow 2'$, $3 \longrightarrow 4'$) and isochors ($2' \longrightarrow 3$, $4' \longrightarrow 1$). At point 1 and 3 the system is in a canonical state with inverse temperature β_1 and β_3, respectively. The adiabates are driven between γ_a and γ_b.

the control parameter $\gamma(t)$ of the Hamiltonian is kept fixed. A schematic of the qOC is shown in Fig. 16.1. There, we have introduced the *canonicity*: It describes if the state of the system is canonical ($c = 0$) or not ($c \neq 0$). For our purpose, we do not have to know how *far away* from the canonical state the system actually is. Therefore, c does not necessarily have to fulfill any conditions on usual measures. It is just used to stress the fact that quite generally, after a unitary transformation, a formerly canonical state will most likely end up in a non-canonical one[1]. The blue curve in Fig. 16.1, which lies in the S/γ-plane ($c = 0$), can therefore be identified with a process from standard thermodynamics, as the system is always in a canonical state (quasistatic processes). Here, the blue curves describe a Stirling process (combinations of isothermal and isochoric process steps).

The quantum Otto cycle depicted as the red curve in Fig. 16.1 thus leads to non-canonical states, naturally. As we allow for arbitrary speed of the unitary

[1] Consider, e. g., a process which only deforms the energy spectrum of a system without inducing any transitions. If the system has more than two non-degenerate energy levels, the state after deformation will no longer be canonical, in general.

processes here, the only limits on how fast the cycle can be completed are given by the thermal relaxation duration of the system coupled to the hot and cold bath, respectively.

16.2. Jarzynski relation and unitary process steps

We investigate exemplarily the process step $1 \longrightarrow 2$ (cf. Fig. 16.1). As the system starts in thermal equilibrium at (1) with inverse temperature β_1 and as the process step is unitary, we know the JR to give the correct estimate,

$$\overline{\mathrm{e}^{-\beta_1 \Delta W_{12}^{fi}}} = \mathrm{e}^{-\beta_1 \Delta F^{\mathsf{iso}}(\gamma_a, \gamma_b)}. \tag{16.3}$$

The index fi stresses the fact that we consider work along trajectories, here, rather than an averaged work. Note, that $\Delta F^{\mathsf{iso}}(\gamma_a, \gamma_b)$ refers to the isothermal free energy difference. As the blue curve $1 \longrightarrow 2'$ corresponds to an isothermal process from γ_a to γ_b, we have $\Delta F^{\mathsf{iso}}(\gamma_a, \gamma_b) = \Delta F_{12'}$. Moreover, we have for the isothermal process $\Delta W_{12'} = \Delta F_{12'}$, and by using Jensen's inequality [47] we arrive at

$$\Delta W_{12} \geq \Delta W_{12'}. \tag{16.4}$$

For a hypothetical[2] process from (2) to (2'), $2 \longrightarrow 2'$, realized by coupling the system in state (2) to the heat bath with β_1, we would have $\Delta U(2, 2') = \Delta Q_{22'}$, and as $\Delta U(1, 2') = \Delta U(1, 2) + \Delta U(2, 2')$, we arrive at

$$\Delta W_{12'} + \Delta Q_{12'} = \Delta W_{12} + \Delta Q_{22'}, \tag{16.5}$$

from which follows with Eq. (16.4) that

$$\Delta Q_{12'} \geq \Delta Q_{22'}. \tag{16.6}$$

For the process step $3 \longrightarrow 4$ analogous inequalities can be derived.

Next, we turn to consequences for the entropy. For the isothermal process $1 \longrightarrow 2'$, we have

$$\Delta S_{12'} \geq \beta_1 \Delta Q_{12'}, \tag{16.7}$$

where the equality holds for reversible processes. As $\Delta S_{12} = 0$, we have that $\Delta S_{12} + \Delta S_{22'} = \Delta S_{22'} = \Delta S_{12'}$, and therefore

$$\Delta S_{22'} \geq \beta_1 \Delta Q_{12'} \geq \beta_1 \Delta Q_{22'}. \tag{16.8}$$

Thus, for the hypothetical process $2 \longrightarrow 2'$ the Clausius inequality is naturally fulfilled. Of course, the same reasoning holds for the process $4 \longrightarrow 4'$.

[2] By hypothetical we mean that we do not want to perform this process, here. It does not mean that such a process would be impossible to perform, in principle.

16.3. Quantum Otto compared to Stirling

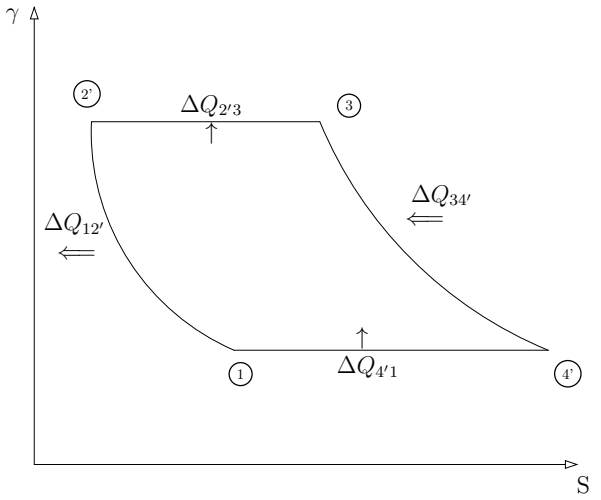

Figure 16.2.: Schematic of the classical Stirling process: control parameter γ ("volume") vs. entropy S. The unusual choice of S is for better comparison with Fig. 16.1, where the blue lines correspond to the process depicted here. Ideally, the heat flows $\Delta Q_{2'3}$ and $\Delta Q_{4'1}$ compensate each other; the heat $\Delta Q_{4'1}$ is stored and re-used for step $2' \longrightarrow 3$. Thus, only the heat $\Delta Q_{34'}$ is withdrawn from the hot bath.

As we have seen in the previous section, the quantum Otto cycle can be compared to the Stirling cycle lying in the canonical S/γ-plane ($c = 0$) (cf. Fig. 16.2). Therefore, it seems natural to compare the efficiency of the qOC, η_{qOC}, with that of a classical Stirling machine, η_{Stir}. In the following we will use the findings from Sec. 16.2 in order to find an upper bound for η_{qOC}. If not stated otherwise, we choose $T_3 > T_1 \Longrightarrow \beta_3 < \beta_1$. For comparison with the classical Stirling cycle one could think of γ_a corresponding to some "volume" V_a^{-1} and γ_b to V_b^{-1}. The larger γ, the smaller the volume. We choose this kind of identifying γ with V because of the analogy with the potential well: Enlarging γ can be intuitively compared to dilate the energy spectrum, thus larger energy level spacing, which means a compression of the potential well (smaller width).

In the classical Stirling process (cf. Fig. 16.2) we have heat flows during all process steps: Heat is dispensed into the cold bath during isothermal compression ($\Delta Q_{12'}$), then, heat is absorbed during the isochoric heating ($\Delta Q_{2'3}$)

and the subsequent isothermal expansion ($\Delta Q_{34'}$). In the last step heat is dispensed during the isochoric cooling ($\Delta Q_{4'1}$). The isothermal heat flows compensate each other, so, the most efficient way to realize a Stirling process is to store the heat dispensed during the isochoric cooling and re-use it for the isochoric heating[3]. Then, no additional heat has to be taken from the hot bath rendering the process most efficient. The efficiency of the ideal Stirling process is thus given by

$$\eta_{\mathsf{id}}^{\mathsf{Stir}} = -\frac{\Delta W_{12'} + \Delta W_{34'}}{\Delta Q_{34'}}. \tag{16.9}$$

The minus sign accounts for the sign convention that work performed *by* the system is negative.

For the qOC, we have by definition

$$\eta_{\mathsf{id}}^{\mathsf{qOC}} = -\frac{\Delta W_{12} + \Delta W_{34}}{\Delta Q_{23}}. \tag{16.10}$$

From Eq. (16.4) we have

$$\begin{aligned} &\Delta W_{12} \geq \Delta W_{12'} \ \text{ and } \ \Delta W_{34} \geq \Delta W_{34'} \\ &\qquad \Longrightarrow -\left(\Delta W_{12} + \Delta W_{34}\right) \leq -\left(\Delta W_{12'} + \Delta W_{34'}\right). \end{aligned} \tag{16.11}$$

Using this inequality and combining Eq. (16.9) with Eq. (16.10), gives

$$\eta_{\mathsf{id}}^{\mathsf{qOC}} \leq \frac{\Delta Q_{34'}}{\Delta Q_{23}} \eta_{\mathsf{id}}^{\mathsf{Stir}}. \tag{16.12}$$

As the work output for the qOC is smaller than that of the classical Stirling cycle (cf. Eq. (16.11)), we have that the efficiency of qOC can only be larger than that of Stirling if the heat input from the hot bath is smaller for qOC than for Stirling. Actually, as the ideal Stirling process reaches Carnot efficiency, we expect that qOC cannot be more efficient than Stirling.

However, with $\Delta Q_{2'3} + \Delta Q_{4'1} = 0$ and $\oint U_{\mathsf{sys}} = 0$, we find that

$$\Delta Q_{23} + \Delta Q_{41} \geq \Delta Q_{12'} + \Delta Q_{34'}, \tag{16.13}$$

giving an upper bound $\Delta Q_{41} \geq \Delta Q_{12'}$ for $\Delta Q_{34'} > \Delta Q_{23}$, which does not help to limit the efficiency, here. Therefore, we turn to a closer study involving entropy.

[3] Technical implementations actually do exactly this: They try to store the heat dispensed during isochoric cooling in a regenerator in order to feed it back to the system during isochoric heating.

17. Efficiency of quantum Otto cycle

We start by investigating the change of von Neumann entropy for a relaxation process, where only one bath is coupled to the system:

$$\Delta S_{\mathsf{sys}} + \Delta S_{\mathsf{bath}} \geq \Delta S_{\mathsf{sys\,bath}} = 0, \tag{17.1}$$

as the compound system is supposed to evolve unitarily. The heat bath, being perfect, obeys the Clausius equality, giving

$$\Delta S_{\mathsf{sys}} \geq -\Delta S_{\mathsf{bath}} = -\frac{\Delta Q_{\mathsf{bath}}}{T_{\mathsf{bath}}}. \tag{17.2}$$

As we allow for non-extensive energy, here (the interaction energy might be non-negligible compared to the energy of the quantum system), we *cannot* assume the heat flows from the bath and into the system to be equal, here.

Now, we investigate the process step $2 \longrightarrow 3$ from Fig. 16.1 more closely, dividing it into three steps: First, the system is coupled to the bath; second, the system relaxes into thermal equilibrium with $T_{\mathsf{sys}} = T_3$; third, the system is decoupled from the bath. Then, we have for the system

$$\underset{t=0}{\text{uncoupled}} \xrightarrow[đQ_{\mathsf{sys}}+đW_{\mathsf{sys}}]{\text{coupling}} \underset{t=0^+}{\text{coupled}} \xrightarrow[đQ_{\mathsf{sys}}]{\text{relax}} \underset{t=T}{\text{canonical}} \xrightarrow[đQ_{\mathsf{sys}}+đW_{\mathsf{sys}}]{\text{decoupling}} \underset{t=T^+}{\text{decoupled canonical}}. \tag{17.3}$$

For the bath, this reads analogously besides the fact that for the bath we have $đW_{\mathsf{bath}} = 0$. The coupling is supposed to be realized very fast, so that the dynamics of the system and the bath can be neglected in that time, therefore we consider the coupling to be instantaneous.

We start by investigating the decoupling, because there, the state of the system is known to be canonical, $\hat{\rho}_{\mathsf{sys}}^{T^+} = \hat{\rho}_{\mathsf{sys}}^{\mathsf{can}}$,

$$\Delta U_{\mathsf{sys}}^{\mathsf{decoup}} = \mathrm{Tr}\left\{\hat{H}_{\mathsf{sys}}\hat{\rho}_{\mathsf{sys}}^{\mathsf{can}}\right\} - \mathrm{Tr}\left\{\hat{H}'\hat{\rho}_{\mathsf{sys}}^{\mathsf{can}}\right\} = -\mathrm{Tr}\left\{\hat{H}_{\mathsf{sys}}^{\mathsf{eff}}\hat{\rho}_{\mathsf{sys}}^{\mathsf{can}}\right\}, \tag{17.4}$$

where we have already used that $\hat{\rho}_{\mathsf{sys}}^{\mathsf{can}}$ is diagonal in the energy-eigenbasis. Denoting the interaction between system and bath by $\sigma(t)\hat{H}_{\mathsf{se}}$, we can rewrite

the last expression, giving

$$\begin{aligned}\Delta U_{\mathsf{sys}}^{\mathsf{decoup}} &= -\mathrm{Tr}_{\mathsf{sys}}\left\{\hat{\rho}_{\mathsf{sys}}^{\mathsf{can}}\mathrm{Tr}_{\mathsf{bath}}\left[\hat{H}_{\mathsf{se}}(\hat{1}_{\mathsf{sys}}\otimes\hat{\rho}_{\mathsf{bath}})\right]\right\}\\ &= -\mathrm{Tr}_{\mathsf{bath}}\left\{\hat{\rho}_{\mathsf{bath}}\mathrm{Tr}_{\mathsf{sys}}\left[\hat{H}_{\mathsf{se}}(\hat{\rho}_{\mathsf{sys}}^{\mathsf{can}}\otimes\hat{1}_{\mathsf{bath}})\right]\right\}\\ &= -\mathrm{Tr}\left\{\hat{\rho}_{\mathsf{bath}}\hat{H}'_{\mathsf{bath}}\right\}. \end{aligned} \tag{17.5}$$

For the coupling strength $\sigma(t)$ we have used $\sigma(t) = \theta(0)-\theta(T)$, with $\theta(\tau)$ being the step function, thus the coupling is turned on instantaneously at $t = 0$ and turned off at $t = T$. Moreover, we have used that the state of the bath does not change and is diagonal in its energy-eigenbasis. We recognize this expression as $\Delta Q_{\mathsf{bath}}^{\mathsf{decoup}}$. As we have according to Lembas that $\Delta U_{\mathsf{sys}}^{\mathsf{decoup}} = \Delta W_{\mathsf{sys}}^{\mathsf{decoup}}$, and since $\Delta W_{\mathsf{sys}}^{\mathsf{decoup}} = \Delta W_{\mathsf{bath}}^{\mathsf{decoup}}$, we find that the interdiction of extracting work from the bath leads to[1]

$$\Delta U_{\mathsf{sys}}^{\mathsf{decoup}} = \Delta U_{\mathsf{bath}}^{\mathsf{decoup}} = 0. \tag{17.6}$$

17.1. "Quadiabatic" processes

Now, let us suppose that the initial state of the system is also diagonal. This would be the case for quadiabatic processes, where $K_{fi} = \delta_{fi}$, thus the canonical states remain diagonal during the unitary process. Then, the same reasoning as above holds for the coupling process, giving $\Delta U_{\mathsf{sys/bath}}^{\mathsf{couple}} = 0$. This then gives for the complete process $2 \longrightarrow 3$ including both the coupling and decoupling

$$\Delta U_{\mathsf{sys}}(0 \longrightarrow T^+) = \Delta Q_{\mathsf{sys}} \;\text{ and }\; \Delta U_{\mathsf{bath}}(0 \longrightarrow T^+) = \Delta Q_{\mathsf{bath}}(0 \longrightarrow T^+), \tag{17.7}$$

where we have already used that the energy flow into the system due to the bath is only heat. Note, that $\Delta Q_{\mathsf{sys}} \neq \Delta Q_{\mathsf{bath}}$, in general. Now, we compare

[1] Note, that for both, the perfect heat source (cf. Chap. 8) as well as for the thermalizing environment (cf. Sec. 5.3.2, second type of coupling), we have indeed that the internal energy does not change when coupling system and environment in diagonal states. Only for the first type of coupling discussed in Sec. 5.3.2, we would have a change of internal energy. However, as we have seen, this coupling gives rise to a work exchange, anyway, prohibiting this model to be seen as a pure heat source.

this with the internal energy of system and bath combined,

$$U(0) = \mathrm{Tr}\left\{(\hat{H}_{\mathsf{sys}} + \hat{H}_{\mathsf{bath}})\hat{\rho}^{0}_{\mathsf{sys\ bath}}\right\} = U_{\mathsf{sys}}(0) + U_{\mathsf{bath}}(0) \tag{17.8}$$

$$U(T^{+}) = \mathrm{Tr}\left\{(\hat{H}_{\mathsf{sys}} + \hat{H}_{\mathsf{bath}})\hat{\rho}^{T^{+}}_{\mathsf{sys\ bath}}\right\} = U_{\mathsf{sys}}(T^{+}) + U_{\mathsf{bath}}(T^{+}) \tag{17.9}$$

$$\Longrightarrow \Delta U(0 \longrightarrow T^{+}) = \Delta U^{\mathsf{coupling}} = \Delta Q_{\mathsf{sys}}(0 \longrightarrow T^{+}) + \Delta Q_{\mathsf{bath}}(0 \longrightarrow T^{+}). \tag{17.10}$$

Here, we have denoted $\Delta U(0 \longrightarrow T^{+})$ as $\Delta U^{\mathsf{coupling}}$, as during the relaxation the energy of the compound system is constant. Thus, any change of the compound energy can be considered to be coupling effects. Of course, analogous relations hold for the process step $4 \longrightarrow 1$.

With $\Delta Q_{\mathsf{sys}}(0 \longrightarrow T^{+}) = \Delta Q^{\mathsf{sys}}_{23}$ and $\Delta Q_{\mathsf{bath}}(0 \longrightarrow T^{+}) = \Delta Q^{\mathsf{bath}}_{23}$ and $\Delta U(0 \longrightarrow T^{+}) = \Delta W^{\mathsf{coupling}}_{23}$, we have

$$-\Delta Q^{\mathsf{bath}}_{23} = \Delta Q^{\mathsf{sys}}_{23} - \Delta W^{\mathsf{coupling}}_{23}. \tag{17.11}$$

An analogous relation holds for $4 \longrightarrow 1$. Using Eq. (17.11) in Eq. (17.2), we find

$$\Delta S^{\mathsf{sys}}_{23} \geq \frac{\Delta Q^{\mathsf{sys}}_{23} - \Delta W^{\mathsf{coupling}}_{23}}{T_3}, \tag{17.12}$$

where we have inserted the temperature of the bath $T_{\mathsf{bath}} = T_3$. Analogously, we have

$$\Delta S^{\mathsf{sys}}_{41} \geq \frac{\Delta Q^{\mathsf{sys}}_{41} - \Delta W^{\mathsf{coupling}}_{41}}{T_1}. \tag{17.13}$$

Then, taking into account the coupling and decoupling processes, we have for the work output $\delta W^{\mathsf{out}}_{\mathsf{cycle}}$ over a complete cycle

$$\delta W^{\mathsf{out}}_{\mathsf{cycle}} = -\left(\Delta W_{12} + \Delta W^{\mathsf{coupling}}_{23} + \Delta W_{34} + \Delta W^{\mathsf{coupling}}_{41}\right). \tag{17.14}$$

With the definition Eq. (16.2) for the efficiency η we get

$$\eta_{\mathsf{qOC}} = \frac{\delta W^{\mathsf{out}}_{\mathsf{cycle}}}{-\Delta Q^{\mathsf{bath}}_{23}} = -\frac{\Delta W_{12} + \Delta W^{\mathsf{coupling}}_{23} + \Delta W_{34} + \Delta W^{\mathsf{coupling}}_{41}}{\Delta Q^{\mathsf{sys}}_{23} - \Delta W^{\mathsf{coupling}}_{23}}, \tag{17.15}$$

where we have used definition (17.14) and Eq. (17.11), respectively. For a cyclic process we have

$$\oint U_{\mathsf{sys}} = 0 \implies \Delta W^{\mathsf{sys}}_{12} + \Delta W^{\mathsf{sys}}_{34} = -\Delta Q^{\mathsf{sys}}_{23} - \Delta Q^{\mathsf{sys}}_{41}, \tag{17.16}$$

as well as

$$\oint S_{\mathsf{sys}} = 0 \implies \Delta S_{23}^{\mathsf{sys}} + \Delta S_{41}^{\mathsf{sys}} = 0, \tag{17.17}$$

which gives after insertion of Eqs. (17.12) and (17.13)

$$\frac{\Delta Q_{23}^{\mathsf{sys}} - \Delta W_{23}^{\mathsf{coupling}}}{T_3} + \frac{\Delta Q_{41}^{\mathsf{sys}} - \Delta W_{41}^{\mathsf{coupling}}}{T_1} \leq 0. \tag{17.18}$$

We solve this equation for $\Delta Q_{41}^{\mathsf{sys}}$, giving

$$\Delta Q_{41}^{\mathsf{sys}} \leq -\frac{T_1}{T_3}\left(\Delta Q_{23}^{\mathsf{sys}} - \Delta W_{23}^{\mathsf{coupling}}\right) + \Delta W_{41}^{\mathsf{coupling}}. \tag{17.19}$$

Now, we substitute Eqs. (17.16) and (17.19) into the expression for the efficiency, Eq. (17.15), which then reads

$$\eta_{\mathsf{qOC}} \leq \frac{\left(\Delta Q_{23}^{\mathsf{sys}} - \Delta W_{23}^{\mathsf{coupling}}\right)\left(1 - \frac{T_1}{T_3}\right)}{\Delta Q_{23}^{\mathsf{sys}} - \Delta W_{23}^{\mathsf{coupling}}} = 1 - \frac{T_1}{T_3} = \eta_{\mathsf{Carnot}}. \tag{17.20}$$

Thus, we have found that the efficiency of the quantum Otto cycle is less than or equal to Carnot efficiency. Note, that if we would have used definition (16.1) for the efficiency, it would have been possible to exceed Carnot efficiency for $\Delta W_{23}^{\mathsf{coupling}} < 0$.

17.2. "Non-quadiabatic" unitary processes

For the calculations above we have assumed that the state of the system is diagonal in the energy-eigenbasis of the system Hamiltonian after the unitary process step (this assumption was necessary for identifying $\Delta U_{\mathsf{sys/bath}}^{\mathsf{couple}} = 0$). Here, we consider more general situations where we assume the density operator to feature off-diagonal elements in the energy-eigenbasis of the system Hamiltonian. First, we note that we could use a micro canonical coupling ($[\hat{H}_{\mathsf{sys}}, \hat{H}_{\mathsf{se}}] = 0$) in order to get rid of the off-diagonal elements (cf. [44], e. g.). As such a coupling does not alter the effective internal energy of the system during the evolution ($[\hat{H}'_{\mathsf{sys}}, \hat{H}_{\mathsf{se}}] = 0$ in Eq. (5.8)) and we thus have $\Delta Q_{\mathsf{sys}}^{\mathsf{Lem}} = 0$, it is always possible to prepare the density operator in a diagonal state without any energy investment. Thus, for this process we have that $\Delta S_{\mathsf{sys}}^{\mathsf{micro}} \geq 0$, where the equality only holds if the system has already been in a diagonal state. From this we readily infer

$$\Delta S_{\mathsf{sys}}^{\mathsf{micro}} \geq \Delta Q_{\mathsf{sys}}^{\mathsf{Lem,\ micro}} = 0, \tag{17.21}$$

which shows that this process is irreversible. For partially irreversible processes one expects the efficiency of cyclic processes to be smaller than for reversible ones. That this does also hold here will be shown in the following.

As Eqs. (17.8) and (17.9) are still valid, we find

$$\Delta W_{23}^{\mathsf{coupling}} = \Delta Q_{23}^{\mathsf{sys}} + \Delta Q_{23}^{\mathsf{bath}} + \Delta W_{2}^{\mathsf{sys,\ couple}}, \tag{17.22}$$

where the last addend accounts for the fact that the coupling can perform work on the system. Also, it is easy to find an equivalent expression for $\Delta W_{41}^{\mathsf{coupling}}$. Then, Eq. (17.16) reads

$$\Delta W_{12}^{\mathsf{sys}} + \Delta W_{34}^{\mathsf{sys}} = -\Delta Q_{23}^{\mathsf{sys}} - \Delta Q_{41}^{\mathsf{sys}} - \Delta W_{2,4}^{\mathsf{sys,\ couple}}. \tag{17.23}$$

Using this expression and Eq. (17.22) we find

$$\eta_{\mathsf{qOC}} = \frac{\Delta Q_{23}^{\mathsf{sys}} + \Delta Q_{41}^{\mathsf{sys}} - \Delta W_{23}^{\mathsf{coupling}} - \Delta W_{41}^{\mathsf{coupling}} + \Delta W_{2,\,4}^{\mathsf{sys\ couple}}}{\Delta Q_{23}^{\mathsf{sys}} - \Delta W_{23}^{\mathsf{coupling}} + \Delta W_{2}^{\mathsf{sys,\ couple}}}, \tag{17.24}$$

which can be simplified to

$$\eta_{\mathsf{qOC}} = 1 + \frac{\Delta Q_{41}^{\mathsf{sys}} - \Delta W_{41}^{\mathsf{coupling}} + \Delta W_{4}^{\mathsf{sys\ couple}}}{\Delta Q_{23}^{\mathsf{sys}} - \Delta W_{23}^{\mathsf{coupling}} + \Delta W_{2}^{\mathsf{sys,\ couple}}} = 1 + \frac{\Delta Q_{41}^{\mathsf{bath}}}{\Delta Q_{23}^{\mathsf{bath}}}. \tag{17.25}$$

For the functionality as a heat engine it is necessary that heat is withdrawn from the hot bath, $\Delta Q_{23}^{\mathsf{bath}} < 0$, and heat is dispensed into the cold bath, $\Delta Q_{41}^{\mathsf{bath}} > 0$. Thus, the last addend of Eq. (17.25) is necessarily negative. For maximal efficiency this addend should be minimized. As the signs are reversed for the system, we have that in

$$\eta_{\mathsf{qOC}} = 1 + \frac{\Delta Q_{41}^{\mathsf{sys}} - \Delta W_{41}^{\mathsf{coupling}} + \Delta W_{4}^{\mathsf{sys\ couple}}}{\Delta Q_{23}^{\mathsf{sys}} - \Delta W_{23}^{\mathsf{coupling}} + \Delta W_{2}^{\mathsf{sys,\ couple}}}, \tag{17.26}$$

the numerator is negative while the denominator is positive. Thus, in order to minimize the last addend we should maximize both, numerator and denominator.

To this end, we note that we have

$$\Delta U_{\mathsf{sys}}^{\mathsf{quad}}(1 \longrightarrow 3) = \Delta U_{\mathsf{sys}}(1 \longrightarrow 3), \tag{17.27}$$

with $\Delta U_{\mathsf{sys}}^{\mathsf{quad}}(1 \longrightarrow 3)$ being the change of internal energy during a process from state (1) to state (3), with $1 \longrightarrow 2$ being performed quadiabatically,

compared to the change of internal energy $\Delta U_{\mathsf{sys}}(1 \longrightarrow 3)$ with an arbitrary process $1 \longrightarrow 2$. The equality is a direct consequence of U_{sys} being a state function. From this we have

$$\Delta W_{12}^{\mathsf{sys,\ quad}} + \Delta Q_{23}^{\mathsf{sys\ quad}} = \Delta W_{12}^{\mathsf{sys}} + \Delta Q_{23}^{\mathsf{sys}} + \Delta W_{2}^{\mathsf{sys,\ couple}}. \tag{17.28}$$

Inserting this expression and an analogous one for the process step $4 \longrightarrow 1$ into Eq. (17.26), we find for the efficiency

$$\eta_{\mathsf{qOC}} = 1 + \frac{\Delta W_{34}^{\mathsf{sys,\ quad}} - \Delta W_{34}^{\mathsf{sys}} + \Delta Q_{41}^{\mathsf{sys,\ quad}} - \Delta W_{41}^{\mathsf{coupling}}}{\Delta W_{12}^{\mathsf{sys,\ quad}} - \Delta W_{12}^{\mathsf{sys}} + \Delta Q_{23}^{\mathsf{sys,\ quad}} - \Delta W_{23}^{\mathsf{coupling}}}. \tag{17.29}$$

Note, that the efficiency for quadiabatic steps $1 \longrightarrow 2$ and $3 \longrightarrow 4$ given in Eq. (17.15) can be written as

$$\eta_{\mathsf{qOC}}^{\mathsf{quad}} = 1 + \frac{\Delta Q_{41}^{\mathsf{sys,\ quad}} - \Delta W_{41}^{\mathsf{coupling}}}{\Delta Q_{23}^{\mathsf{sys,\ quad}} - \Delta W_{23}^{\mathsf{coupling}}}. \tag{17.30}$$

A comparison with Eq. (17.29) shows that we have an additional addend in both, numerator and denominator, reading

$$\Delta W_{34}^{\mathsf{sys,\ quad}} - \Delta W_{34}^{\mathsf{sys}} \ \text{ and } \ \Delta W_{12}^{\mathsf{sys,\ quad}} - \Delta W_{12}^{\mathsf{sys}}, \tag{17.31}$$

respectively. As explained above, for maximal efficiency both these expressions should be maximal. Thus, the work during the unitary processes should be minimized[2].

For passive states, given by

$$p(E_i) > p(E_j) \Leftrightarrow i < j, \tag{17.32}$$

with $p(E_{i/j})$ denoting the occupation probability of energy eigenstate E_i and E_j, respectively, it is known [81] that for a finite system under the influence of $\hat{H}(t) = \hat{H} + \hat{h}(t)$ with $\hat{h}(0) = \hat{h}(\tau) = 0$ we have that

$$\Delta U(0,\tau) = \mathrm{Tr}\left\{\hat{H}\hat{\rho}(\tau)\right\} - \mathrm{Tr}\left\{\hat{H}\hat{\rho}(0)\right\} \geq 0. \tag{17.33}$$

A generalization for $\hat{h}(\tau) \neq 0$ can be found in [3]. There, it is shown that if no unavoided level crossings occur, minimal work input during a unitary process is reached for quadiabatic process implementation.

[2] This meets the expectations, since minimal ΔW^{sys} means maximal work output or minimal work input, respectively, due to the sign convention.

Here, we present a proof which allows for a slight generalization to processes with unavoided level crossings, cf. also [1]. As we consider unitary processes we trivially have $\Delta U = \Delta W = \overline{E(T)} - \overline{E(0)}$ and minimizing ΔW is thus equivalent to minimizing $\overline{E(T)} = \mathrm{Tr}\left\{\hat{H}(T)\hat{\rho}(T)\right\}$. For the sake of simplicity we assume that we have no degeneracies in the spectra of both initial and final Hamiltonian. Minimizing the average energy of the final state of the system means to maximize the occupation probabilities for low lying energy levels. So, minimal work would mean that only the ground state with the corresponding energy E_0 is occupied after the process, $p^T(E_0) = 1$. However, for unitary processes the sum rule for the conditional probability,

$$\sum_i K_{fi}(T) = 1 \tag{17.34}$$

(cf. Sec. 2.2.1), sets a restriction on the possibility to occupy certain states[3]. Here, the initial state is required to be passive. Now, we start by trying to maximize the final occupation probability of the ground state,

$$p^T(E_0) = \sum_{i=0}^{N} K_{0i} p^0(E_i) \leq p^0(E_0) \sum_{i=0}^{N} K_{0i} = p^0(E_0), \tag{17.35}$$

where we have successively used that we have a passive state and then the sum rule for unitary processes. Thus, we have maximal ground state occupancy for $K_{0i} = \delta_{i0} \Longrightarrow K_{f0} = \delta_{f0},\ K_{00} = 1$. Next, we try to maximize $p^T(E_1)$, the first excited state,

$$p^T(E_1) = \sum_{i=1}^{N} K_{1i} p^0(E_i) \leq p^0(E_1) \sum_{i=1}^{N} K_{2i} = p^0(E_1), \tag{17.36}$$

where the same reasoning as above can be used. Note that the sum runs from $i = 1$, as $K_{10} = 0$ due probability normalization, $\sum_f K_{fi} = 1$, and the fact that we already have $K_{00} = 1$. Thus, if we want to maximize $p^T(E_1)$ any further this is only possible at the cost of diminishing $p^T(E_0)$, which would enlarge the average energy. We can go on with this reasoning subsequently for every $p^T(E_i)$, giving that the average energy is minimized for $K_{fi} = \delta_{fi}$, if the process does not feature any level crossings. Introducing any off-diagonal

[3] As long as the final (complete) basis set can be mapped upon the initial one, the measurement basis does not necessarily have to coincide with the current energy-eigenbasis. Although the choice of the measurement basis influences the actual value of the minimal work average, it does not influence how this minimal value is reached.

elements without changing the diagonal ones does change the von Neumann entropy, rendering the process non-unitary.

Moreover, from this proof it is obvious how this statement can be generalized further: If we have level crossings, we have to ensure that during the unitary process we have transitions such that the initially k-th lowest energy level is mapped upon the k-th lowest after the process. Then, the work during the process is minimal for unitary processes.

It is even possible to use this proof for a generalization to non-passive, diagonal states: The process should be performed in such a way, that the energy level with the k-th largest occupation probability $p^0(E_i)$ is mapped upon the k-th energy level at the end of the process (cf. Fig. for a clarifying example with a five-level system). The transitions can in principle be performed unitarily as the von Neumann entropy at the end of the process equals the initial one. Thus, we have found a quite general way to minimize the work during a unitary process for initially diagonal states. The initial state being passive or not, the work is minimal for diagonal final states.

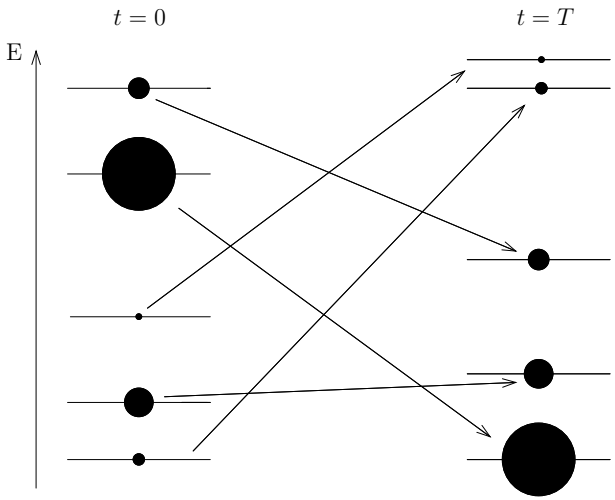

Figure 17.1.: Here, the energy spectrum of a five-level system is depicted. On the left-hand side the spectrum for $t = 0$ is depicted, on the right-hand side the spectrum after the process has been completed at $t = T$. The larger the circle the more probable the energy level is occupied. The arrows indicate the transitions leading to minimal work. Note, that the von Neumann entropy is equal at $t = 0$ and $t = T$. This process, can thus, in principle, be realized unitarily.

As the unitary process steps in the qOC start in a canonical state, which is passive, we have that if no unavoided level crossings occur, the work during the quadiabatic process ($K_{fi} = \delta_{fi}$) is minimal. Even for processes with unavoided level crossings, the work is minimized for diagonal final states, which fulfill the condition set in Sec. 17.1, irrespective of the fact that they do not have to be quadiabatic in the strict sense.

As a consequence, we have that both,

$$\Delta W_{12}^{\mathsf{sys}} \geq \Delta W_{12}^{\mathsf{sys\ quad}} \text{ and } \Delta W_{34}^{\mathsf{sys}} \geq \Delta W_{34}^{\mathsf{sys\ quad}}. \tag{17.37}$$

Thus, we have that $\eta_{\mathsf{qOC}} \leq \eta_{\mathsf{qOC}}^{\mathsf{diag}} \leq \eta_{\mathsf{Carnot}}$, with $\eta_{\mathsf{qOC}}^{\mathsf{diag}}$ being the efficiency calculated in Sec. 17.1 for diagonal system states (2) and (4), where we have already used that this is more general than quadiabatic processes. This finding meets our expectations: The qOC is maximally as efficient as the Carnot cycle between baths with respective temperatures T_1 and T_3 and if we have process steps which are performed irreversible, the efficiency decreases.

17.3. Quantum and classical Otto efficiency

Up to now, the efficiency of qOC has only been compared to the classical Carnot efficiency. Here, we aim at a comparison with the classical Otto efficiency. To this end, we discuss a special class of processes, which does not lead to unavoided level crossings. In Secs. 17.1 and 17.2 we have shown that quadiabatic processes lead to highest efficiency for cyclic processes and that this efficiency is less than Carnot. However, as we consider the quantum analogue of the Otto cycle, it would be interesting to compare the efficiency of qOC with the classical Otto efficiency. For the classical Otto cycle an ideal gas is taken as the working medium, usually. Then, one finds [26, 30]

$$\eta_{\mathsf{Otto}}^{\mathsf{class}} = 1 - \frac{T_4 - T_1}{T_3 - T_2} = 1 - \left(\frac{V_2}{V_1}\right)^{\kappa - 1}, \tag{17.38}$$

with V_1 being the larger and V_2 being the smaller volume and $\kappa \equiv \frac{c_p}{c_V}$, the ratio of specific heat capacity at constant pressure (c_p) and constant volume (c_V), respectively. For an ideal gas one can identify $\kappa = \frac{f+2}{f}$, f being the degrees of freedom (usually one has $f = 3$ as only translatory degrees of freedom are present for ideal gases).

For the comparison with η_{qOC} we face the following problems (cf. Eq. (17.38)): First, neither T_2 nor T_4 is properly defined as the corresponding states of the system are not canonical, in general. Second, the definition of volume and

heat capacities for arbitrary systems seems far from being straightforward. Due to these problems, we discuss the efficiency of qOC for a special class of energy spectra, being of the form (cf. [38])

$$E_n(\gamma) = f(\gamma)E_n, \tag{17.39}$$

where γ denotes the control parameter and $f(\gamma)$ an arbitrary continuously differentiable real-valued function. Thus, we only allow spectral deformations, like, e. g., a single particle in a one-dimensional potential well of variable width $L(t)$, $E_n = \frac{\pi^2 n^2}{2mL^2(t)}$ with $f(\gamma) = L^{-2}(t)$, here.

With Eq. (17.39) we find (cf. also Fig. 16.1)

$$\Delta W_{12}^{\mathsf{sys}} = \sum_n \left[f(\gamma_b) - f(\gamma_a)\right] E_n \rho_{nn}, \tag{17.40}$$

$$\Delta W_{34}^{\mathsf{sys}} = \sum_m \left[f(\gamma_a) - f(\gamma_b)\right] E_m \tilde{\rho}_{mm}, \tag{17.41}$$

where we have used that we perform the process quadiabatically. For the heat flow into the system we have

$$\Delta Q_{23}^{\mathsf{sys}} = f(\gamma_b) \sum_{m,n} \left[E_m \tilde{\rho}_{mm} - E_n \rho_{nn}\right]. \tag{17.42}$$

Substituting these expressions into Eq. (17.15) gives

$$\eta_{\mathsf{qOC}} = \frac{\sum_{m,n} \left[E_m \tilde{\rho}_{mm} - E_n \rho_{nn}\right] \left[f(\gamma_b) - f(\gamma_a)\right] - \Delta W_{23}^{\mathsf{coupling}} - \Delta W_{41}^{\mathsf{coupling}}}{\sum_{m,n} \left[E_m \tilde{\rho}_{mm} - E_n \rho_{nn}\right] f(\gamma_b) - \Delta W_{23}^{\mathsf{coupling}}}. \tag{17.43}$$

For negligible coupling strength, we find

$$\eta_{\mathsf{qOC}} = 1 - \frac{f(\gamma_a)}{f(\gamma_b)}, \tag{17.44}$$

which translates into the classical Otto efficiency, as $f(\gamma_a)$ corresponds to smaller "volume" as discussed in Sec. 16.3.

Another approach would be to define effective temperatures for both system states (2) and (4). To this end, we consider the internal energy of the system in state (1) first, giving

$$U(1) = \frac{1}{Z_1} \sum_n \mathrm{e}^{-\beta_1 E_n(1)} E_n(1) = \frac{1}{Z_1} \sum_n \mathrm{e}^{-\beta_1 f(\gamma_a) E_n} f(\gamma_a) E_n. \tag{17.45}$$

As we consider most efficient processes (quadiabatic), we have for the internal energy of the system in state (2),

$$U(2) = \frac{1}{Z_1}\sum_n \mathrm{e}^{-\beta_1 E_n(1)} E_n(2) = \frac{1}{Z_1}\sum_n \mathrm{e}^{-\beta_1 \frac{f(\gamma_a)}{f(\gamma_b)} E_n(2)} f(\gamma_b) E_n. \quad (17.46)$$

From the exponential of the last addend of Eq. (17.46), we get a possible definition of effective temperature for state (2)[4],

$$\frac{1}{T_2} \equiv \beta_2^{\mathsf{eff}} \equiv \beta_1 \frac{f(\gamma_a)}{f(\gamma_b)} \implies T_2 = T_1 \frac{f(\gamma_b)}{f(\gamma_a)}. \quad (17.47)$$

Analogously we find for state (4)[5],

$$\frac{1}{T_4} \equiv \beta_4^{\mathsf{eff}} \equiv \beta_3 \frac{f(\gamma_b)}{f(\gamma_a)} \implies T_4 = T_3 \frac{f(\gamma_a)}{f(\gamma_b)}. \quad (17.48)$$

Combining Eqs. (17.47) and (17.48), we find

$$T_4 - T_1 = \frac{f(\gamma_a)}{f(\gamma_b)} (T_3 - T_2), \quad (17.49)$$

which, solved for $\frac{f(\gamma_a)}{f(\gamma_b)}$, immediately yields in Eq. (17.44)

$$\eta_{\mathsf{qOC}} = 1 - \frac{T_4 - T_1}{T_3 - T_2}. \quad (17.50)$$

This equals the efficiency of the classical Otto cycle.

17.4. Comparison to Curzon-Ahlborn efficiency

Technical applications usually aim at maximizing the power output of engines rather than maximizing efficiency. For a fairly simple model, Curzon and Ahlborn showed that the efficiency of a Carnot Engine at Maximum Power output is given by [18]

$$\eta_{CA} = 1 - \sqrt{\frac{T_1}{T_3}}, \quad (17.51)$$

[4] Note, that the exponential in the partition sum can be treated analogously.

[5] Note, that our generalized temperatures are consistent with the finding for the reversible classical Otto cycle with ideal gases (constant heat capacity), $T_2 T_4 = T_1 T_3$, cf. [30].

with T_1 being the temperature of the cold bath and T_3 being the temperature of the hot one. Here, we assume the system to feature a constant heat capacity c_V and heat exchange proportional to the temperature difference,

$$\dot{Q} = -k\Delta T. \tag{17.52}$$

Using $c_V = \frac{1}{m}\frac{\partial Q}{\partial T}$ and requiring $\dot{c}_V = \dot{m} = 0$, we have

$$\dot{Q} = -k\left(T(t) - T_B\right) = mc_v\dot{T}(t), \tag{17.53}$$

where $T(t)$ is the temperature of the system after time t elapsed since coupling the system to the bath of temperature T_B. For $2 \longrightarrow 3$ we get after integration

$$T^*(t) = (T_2^* - T_3)\exp\left\{-\frac{k}{mc_V}t\right\} + T_3, \tag{17.54}$$

with the boundary conditions $T^*(0) \stackrel{!}{=} T_2^*$ and $T^*(\infty) \longrightarrow T_3$. The asterisk accounts for the fact that a generalized definition was used for the respective temperature as the system might not be in a canonical state. Note that the heat transport equations are supposed to hold for the effective temperatures and states out of equilibrium. Of course, analogous relations hold for the process $4 \longrightarrow 1$. T_2^* as well as T_4^* depend on the actual system temperatures $T^*(t_d)$ in the states (1') and (3') which have been reached after coupling the system to the respective heat baths for time t_d. With this, we find for ΔQ_{23} (with $k = 1$, $c_V = 1$, $m = 1$ and $r \equiv \frac{f(\gamma_b)}{f(\gamma_a)}$ for the sake of simplicity),

$$\Delta Q_{23}(t_d^a, t_d^b) = -\left(1 - \mathrm{e}^{-t_d^a}\right)\left(T_3 - \frac{T_3\mathrm{e}^{-t_d^b}\left(1 - \mathrm{e}^{-t_d^a}\right) + rT_1\left(1 - \mathrm{e}^{-t_d^b}\right)}{1 - \mathrm{e}^{-(t_d^a + t_d^b)}}\right), \tag{17.55}$$

where t_d^a and t_d^b denote the relaxation time at the hot bath T_3 (t_d^a) and cold bath T_1 (t_d^b), respectively. A quite analogous relation holds for $\Delta Q_{41}(t_d^a, t_d^b)$.

Using these relations and assumptions it is then easy to show, that

$$\eta_{\mathsf{qOC}} = \frac{\Delta Q_{23}(t_d^a, t_d^b) + \Delta Q_{41}(t_d^a, t_d^b)}{\Delta Q_{23}(t_d^a, t_d^b)} = 1 - \frac{f(\gamma_a)}{f(\gamma_b)}, \tag{17.56}$$

independent of the relaxation times t_d^a and t_d^b! This result is in accordance with the findings in [38] for a control-theoretic model. The power output,

$$\dot{W} = \frac{\Delta Q_{23} + \Delta Q_{41}}{\Delta t_{\mathsf{cycle}}}, \tag{17.57}$$

however, does in general depend on the process time, especially when taking into account that the unitary steps may be performed arbitrarily fast, but for realistic situations, still in finite time.

17.5. Surviving correlations

At the beginning of Chap. 17, we have implicitly assumed that we have no initial correlations between the system and the bath. Generally, however, there might be correlations between system and bath surviving the contact and thermalization with the other bath. Therefore, we generalize the proof of Sec. 17.1 by using the strong subadditivity of the von Neumann entropy [17],

$$S(\hat{\rho}_{ABC}) + S(\hat{\rho}_B) \leq S(\hat{\rho}_{AB}) + S(\hat{\rho}_{BC}), \tag{17.58}$$

for the total state consisting of the system B and both heat baths, A and C. The initial state is supposed to factorize,

$$\hat{\rho}^0_{ABC} = \hat{\rho}^0_A \otimes \hat{\rho}^0_B \otimes \hat{\rho}^0_C. \tag{17.59}$$

As the correlations will generally depend on the history of the system, thus on the number of cycles the engine has already run through, we have to keep count of the actual cycle n. In order not to confuse n with the states $\textcircled{1}\ldots\textcircled{4}$, we will rename the states to $\textcircled{1}\!\!\rightarrow a$, $\textcircled{2}\!\!\rightarrow b$, and so on. Thus, the relaxation from $4 \longrightarrow 1$ will now read for the n-th cycle as $d_n \longrightarrow a_{n+1}$. In the following, we will use the short-hand notation $n^+ \equiv n + 1$.

As the baths are decoupled for most process steps we find

$$S_A(a_n) = S_A(b_n) \ \text{ and } \ S_A(c_n) = S_A(d_n) = S_A(a_{n^+}) = S_A(b_{n^+}), \tag{17.60}$$

$$S_C(a_n) = S_C(b_n) = S_C(c_n) = S_C(d_n). \tag{17.61}$$

For the system we have due to the unitary process steps

$$S_B(a_n) = S_B(b_n) \ \text{ and } \ S_B(c_n) = S_B(d_n). \tag{17.62}$$

Moreover, for a cyclic process we necessarily have

$$S_B(a_n) = S_B(a_{n^+}). \tag{17.63}$$

Also, as the compound system is closed, we have that

$$S_{ABC} = S^0_{ABC} = S^0_A + S^0_B + S^0_C, \tag{17.64}$$

as we have required the state to factorize initially.

We start by investigating the entropy for the n-th cycle at point c, using Eq. (17.58),

$$S_{ABC}(c_n) + S_B(c_n) \leq S_{AB}(c_n) + S_{BC}(c_n). \tag{17.65}$$

Also, we know that $S_{AB}(c_n) \leq S_A(c_n) + S_B(c_n)$ and $S_{BC}(c_n) \leq S_B(c_n) + S_C(c_n)$. With this and Eq. (17.64) we find

$$\begin{aligned} &S^0_{ABC} + S_B(c_n) \leq S_A(c_n) + S_B(c_n) + S_B(c_n) + S_C(c_n) \\ &\quad \Longrightarrow \Delta S_B(b_n, c_n) \geq -\Delta S_A(0, c_n) - \Delta S_C(0, a_n), \end{aligned} \tag{17.66}$$

where we have also used Eqs. (17.61) and (17.63). Here, $\Delta S_X(i, f) \equiv S_X(f) - S_X(i)$. We require the Clausius equality to be fulfilled for the baths and thus, quite analogous to Sec. 17, we find

$$-\Delta Q_A(0, c_n) = \Delta Q^a_B(0, c_n) - \Delta W^{\text{coupling}}_A(0, c_n) \text{ and} \tag{17.67}$$

$$-\Delta Q_C(0, c_n) = \Delta Q^c_B(0, c_n) - \Delta W^{\text{coupling}}_C(0, c_n), \tag{17.68}$$

where the upper index at the heat flow into the system, $\Delta Q^{a/c}_B$, denotes the heat flow arising from coupling to the respective bath A/C and $\Delta W^{\text{coupling}}_{A/C}$ the work for coupling and decoupling to the respective baths. Note, that both, $\Delta Q(0, c_n)$ as well as $\Delta W^{\text{coupling}}(0, c_n)$ denote the *total* heat flow and work due to coupling, respectively. They are thus already summed up for the n cycles up to point c, e. g., we have $\Delta Q^a_B(0, c_n) = \sum_{i=1}^n \Delta Q^a_B(b_i, c_i)$. Inserting Eqs. (17.67) and (17.68) into Eq. (17.66) we find using the Clausius equality for the baths

$$\Delta S_B(0, c_n) \geq \frac{\Delta Q^a_B(0, c_n) - \Delta W^{\text{coupling}}_A(0, c_n)}{T_A} + \frac{\Delta Q^c_B(0, c_n) - \Delta W^{\text{coupling}}_C(0, c_n)}{T_C}. \tag{17.69}$$

Now, we consider the step $4 \longrightarrow 1$ in order to close the cycle. We start by investigating the first cycle only, where we have

$$\hat{\rho}_{ABC}(d_1) = \hat{\rho}_{AB}(d_1) \otimes \hat{\rho}_C(d_1) \quad \Longrightarrow S_{ABC}(d_1) = S_{AB}(d_1) + S_C(d_1), \tag{17.70}$$

as bath C has not yet interacted with the rest of the system which was initially factorized. Thus, we have

$$\Delta S_{BC}(d_1) = S_B(d_1) + S_C(d_1) \text{ and } S_{BC}(a_2) \leq S_B(a_2) + S_C(a_2), \tag{17.71}$$

from which readily follows

$$\Delta S_{BC}(d_1, a_2) \leq \Delta S_B(d_1, a_2) + \Delta S_C(d_1, a_2). \tag{17.72}$$

During the process step $d \longrightarrow a$ bath A is decoupled, thus system B and bath C combined evolve unitarily. Therefore, $\Delta S_{BC}(d_1, a_2) = 0$ giving

$$\Delta S_B(d_1, a_2) \geq -\Delta S_C(d_1, a_2). \tag{17.73}$$

Again, quite analogous to Sec. 17.1 we thus have

$$\Delta S_B(d_1, a_2) \geq \frac{\Delta Q_B^c(d_1, a_2) - \Delta W_C^{\text{coupling}}(d_1, a_2)}{T_C}. \tag{17.74}$$

Now, we use $\Delta S_B(d_n, a_{n^+}) = \Delta S_B(d_{n'}, a_{n'+1}) \; \forall \; \{n, n'\}$ as well as the cyclicity of the process in order to get

$$\Delta S_B(0, d_n) + \Delta S_B(d_n, a_{n^+}) = \Delta S_B(0, c_n) + \Delta S_B(d_1, a_2) \stackrel{!}{=} 0, \tag{17.75}$$

which is then used in combination with Eqs. (17.69) and (17.74) to give

$$\begin{aligned} 0 \geq & \frac{\Delta Q_B^a(0, c_n) - \Delta W_A^{\text{coupling}}(0, c_n)}{T_A} + \frac{\Delta Q_B^c(0, c_n) - \Delta W_C^{\text{coupling}}(0, c_n)}{T_C} \\ & + \frac{\Delta Q_B^c(d_1, a_2) - \Delta W_C^{\text{coupling}}(d_1, a_2)}{T_C}. \end{aligned} \tag{17.76}$$

As we have $\Delta Q_B^c(d_1, a_2) = \Delta Q_B^c(d_n, a_{n^+})$ and as bath A is decoupled from the system during steps $c_n \longrightarrow a_{n^+}$, we can rewrite this expression giving

$$\begin{aligned} 0 \geq & \frac{\Delta Q_B^a(0, a_{n^+}) - \Delta W_A^{\text{coupling}}(0, a_{n^+})}{T_A} + \frac{\Delta Q_B^c(0, a_{n^+}) - \Delta W_C^{\text{coupling}}(0, a_{n^+})}{T_C} \\ & + \frac{\Delta W_C^{\text{coupling}}(d_n, a_{n^+}) - \Delta W_C^{\text{coupling}}(d_1, a_2)}{T_C}. \end{aligned} \tag{17.77}$$

With the abbreviation

$$\delta \Delta W_C^{\text{coupling}} \equiv \Delta W_C^{\text{coupling}}(d_n, a_{n^+}) - \Delta W_C^{\text{coupling}}(d_1, a_2) \tag{17.78}$$

we get from Eq. (17.77)

$$\begin{aligned} \Delta Q_B^c(0, a_{n^+}) \leq & -\frac{T_C}{T_A}\left[\Delta Q_B^a(0, a_{n^+}) - \Delta W_A^{\text{coupling}}(0, a_{n^+})\right] \\ & + \Delta W_C^{\text{coupling}}(0, a_{n^+}) - \delta \Delta W_C^{\text{coupling}}. \end{aligned} \tag{17.79}$$

For the efficiency η_{n^+} of this cyclic process up to the $(n+1)$-th cycle we have

$$\eta_{n^+} = \frac{\Delta Q_B^a(0,a_{n^+}) + \Delta Q_B^c(0,a_{n^+}) - \Delta W_A^{\mathsf{coupling}}(0,a_{n^+}) - \Delta W_C^{\mathsf{coupling}}(0,a_{n^+})}{\Delta Q_B^a(0,a_{n^+}) - \Delta W_A^{\mathsf{coupling}}(0,a_{n^+})} \tag{17.80}$$

where we have already used $\oint U_B \stackrel{!}{=} 0$ and the definition of work output Eq. (17.14) analogous to Sec. 17.1. Inserting Eq. (17.79) into the efficiency we find

$$\eta_{n^+} \leq \underbrace{1 - \frac{T_C}{T_A}}_{\eta_{\mathsf{Carnot}}} - \frac{\delta \Delta W_C^{\mathsf{coupling}}}{\Delta Q_B^a(0,a_{n^+}) - \Delta W_A^{\mathsf{coupling}}(0,a_{n^+})}. \tag{17.81}$$

As for the determination of the efficiency of cyclic processes the limit $n \longrightarrow \infty$ should be taken, we investigate the last addend of Eq. (17.81) more closely. The denominator represents the *total* heat withdrawn from the hot bath during n cycles. As the heat engine should never loose its functionality, the *total* heat withdrawn from the hot bath will steadily grow,

$$\lim_{n\longrightarrow\infty} \left[\Delta Q_B^a(0,a_{n^+}) - \Delta W_A^{\mathsf{coupling}}(0,a_{n^+})\right] \longrightarrow \infty. \tag{17.82}$$

The numerator describes the difference of the work during coupling and decoupling between the first and the n-th cycle. As single coupling events should lead to finite energy changes, only, the numerator is a finite value not growing monotonously with n. Therefore, the last addend of Eq. (17.81) can be neglected savely for large n, giving

$$\lim_{n^+\longrightarrow\infty} \eta_{n^+} \leq 1 - \frac{T_C}{T_A} = \eta_{\mathsf{Carnot}}. \tag{17.83}$$

Thus, the efficiency qOC is maximally equal to the Carnot efficiency even for surviving correlations between the baths and system.

18. Conclusion

This thesis has been concerned with non-equilibrium phenomena for quantum systems. We were especially interested in quantum generalizations of the Jarzynski relation. Our approach focused on modular closed quantum systems with a time-independent Hamiltonian, trying to formulate the Jarzynski relation (JR) for a local part of the compound system.

Typically, the local effective observables of this part turn out to be time-dependent. For our purpose it is crucial to separate the energy exchange between the part of interest (sys) and its environment into heat and work for arbitrary processes. To this end we have used LEMBAS (Local Effective Measurement Basis) which suggests that this separation depends on the measurement basis. For our studies we have used the initial energy eigenbasis of the bare system (sys) as a fixed measurement basis. Moreover, we have used the LEMBAS idea to introduce measurement induced heat and work flows, also.

Before considering the JR, we have identified quantum environments with specific functionalities with respect to the system (sys) by using LEMBAS. These environments are actually quite small: as drivers (dr) we have investigated the spin-oscillator model (SOM, cf. [31]) and the bipartite three-spin model, as a heat source we have discussed a two-spin model where the environment is as small as a single spin. That the LEMBAS definition of heat and work is indeed feasible has been confirmed by the subsequent studies of the local quantum JR. Attention has to be paid when coupling several of these *modules* together as they might loose their original functionality.

We have then proposed different methods of investigating the JR for quantum systems which refer to different perspectives of an observer. All methods involve two-time projective measurements of the system of interest (sys) both initially and at the end of the process. This energy difference could be used directly for estimating the free energy change. We call this method the energy fluctuation theorem (EFT). The probably most direct way of generalizing the JR to local effective observables is to use the work (given by LEMBAS) exerted onto the system (sys) during the process between the two eigenstates the system has been projected into by the measurements (Jarzynski method). As it may be inconvenient to determine the work onto the system (sys) directly we have also introduced a generalized method based on a proposal by Crooks [22], which we name Crooks method. Here, the total energy change of the system

(sys) is corrected by the heat flow into the environment, giving the work onto the system according to the first law. Finally, bilocal EFT involves initial and final measurements on both, system and environment.

We find that if we have no heat flow (according to LEMBAS) into the system (sys) during the process, EFT coincides with both the Jarzynski as well as the Crooks method and they all estimate the free energy change correctly. Coupling the system (sys) to a driving environment (dr) as well as to a heat source (env), which may be as small as a single spin, EFT fails to give a good estimate while Crooks and the Jarzynski method give reasonable estimates for moderate coupling strengths. This confirms that the LEMBAS definition of heat and work is indeed feasible, here. The fact that the energy exchange between the system (sys) and environment (env) is interpreted as heat explains why EFT fails in this setup. Moreover, the direct use of work for the Jarzynski method as well as the use of heat in the Crooks method show that the LEMBAS definitions are suitable for investigations of local effective quantum Jarzynski relations.

All methods investigated have in common that the effect of the measurement of the system on both, system (direct effect) and environment (indirect effect) have to be taken into account for gaining reasonable estimates. This fact shows especially clear for effective drivers influencing the local energy-eigenstates. Ignoring the effects of the measurement leads to a lack of knowledge which reflects in deviations of the estimate from the correct free energy change. However, this is also true for environments in mixed states even if the measurement effects are taken into account. There, only bilocal EFT gives good estimates.

Thus, for reasonable coupling strengths it is possible to get good estimates for the effective free energy change using the methods introduced here, even for locally non-unitary dynamics (as in the case of the system being coupled to a driving environment and a heat source). However, non-unitarity can also lead to deviations of the estimation given by the JR from the free energy change.

In this context we have investigated an externally controlled model, a potential well with variable width. There we find that non-equilibrium processes driving the system far away from equilibrium reveal that idealizations, typical and reliable for classical thermodynamics and quasi-static processes, may become problematic. The infinitely high potential steps (causing non-unitarity) are responsible for the JR to fail, while it could be shown to hold for finite, arbitrarily high potentials. Moreover this model showed that bad statistics may render experimental application of the JR inefficient. Possible solutions to this problem might involve optimal work protocols or, as discussed in this thesis, new measurement strategies.

Finally, we have used the acquired results and insights from the JR as well as LEMBAS in order to discuss the efficiency of a quantum Otto cycle. Within our setting, we were able to show that the efficiency does not exceed Carnot efficiency and that coherences in the density operator of the system do not improve the efficiency. For a specific class of processes and adequate generalizations of temperature and volume we have been able to show that the efficiency of the classical Otto process is an upper bound for the quantum Otto cycle and that this efficiency is independent of the velocity this Otto cycle is run through.

It would be interesting to investigate the effect of larger systems and environments on the JR. Also, a more elaborate definition of measurement induced heat and work flows may help not only for a better understanding of fluctuation theorems but, more general, for the effect of the measurement on the measured system itself as well as on its surroundings via correlations. Studying other fluctuation theorems for closed quantum systems, like the Crooks fluctuation theorem, could lead to new insights into non-equilibrium thermodynamics. Furthermore, it would be interesting to study different cyclic processes with respect to efficiency and maximum power output using, e. g., results from the quantum JR.

In conclusion, we have shown that thermodynamical concepts of non-equilibrium phenomena may still apply to small closed quantum systems. Fluctuation theorems for quantum systems can be helpful for further investigations of cyclic processes involving non-equilibrium process steps. Hopefully, this work helps for a deeper understanding of non-equilibrium aspects of quantum systems.

Part V.

Appendices

A. Theorem of expansion

We recognize this problem as a special case of the Sturm-Liouville Eigenvalue Problem [29]. Generally it is formulated the following way: Given the homogeneous boundary condition problem in the interval $J = [a, b]$,

$$Lu + \lambda w(x)u = 0,\ R_1 u = R_2 u = 0 \tag{A.1}$$

with

$$Lu \equiv [p(x)u']' + q(x)u \tag{A.2}$$

and the linear boundary conditions

$$R_1 u \equiv \alpha_1 u(a) + \alpha_2 u'(a) \tag{A.3}$$

$$R_2 u \equiv \gamma_1 u(b) + \gamma_2 u'(b) \tag{A.4}$$

where $(\alpha_1, \alpha_2) \neq (0, 0)$ and $(\gamma_1, \gamma_2) \neq (0, 0)$, we want to find the eigenvalues and eigenfunctions of this problem. It is required that $\alpha_k, \gamma_k, \lambda \in \mathbb{R}$, $p(x)$ are continuous and differentiable, $q(x)$ continuous and $w(x)$ continuous and positive. Moreover, $p(x)$, $q(x)$ and $w(x)$ are supposed to be real-valued. Herein, λ is called an eigenvalue of this problem if Eq. (A.1) has a non-trivial solution $\tilde{u}(x)$; $\tilde{u}(x)$ is then called an eigenfunction to the eigenvalue λ. From Ref. [29] one then finds that the eigenvalues are non-degenerate and that they form a strictly increasing sequence with $\lambda_n \to \infty$. The eigenfunctions to different eigenvalues are orthogonal to each other.

The so-called *theorem of expansion* [29] states, that given Eq. (A.1) with eigenvalues $\lambda_1, \lambda_2, \ldots$ ordered according to their modulus, $\lambda_1 < \lambda_2 \ldots$ and any function $\nu(x) \in C[a, b]$ which is piecewise continuously differentiable and vanishes in all boundaries of [a,b] where the eigenfunction u_1 of the smallest eigenvalue λ_1 equals zero, then there exists always the following expansion of the function $\nu(x)$,

$$\nu(x) = \sum_{n=1}^{\infty} c_n u_n(x) \text{ with } c_n \equiv \int_a^b w(t)\nu(t)u_n(t)\mathrm{d}t, \tag{A.5}$$

where the expansion is an absolute and uniformly convergent series of the eigenfunctions $u_n(x)$. Here, $C[a, b]$ denotes the set of continuous functions $g : J \to \mathbb{R}$.

B. Perfect work source: two-spin driver

B.1. Exemplary study of operator transformation

We transform the local Hamiltonian of the 1st spin, $\hat{H}^{\mathsf{sp1}}$, given by

$$\hat{H}^{\mathsf{sp1}} = \frac{\omega}{2}\hat{\sigma}_z \otimes \hat{1}_{23}, \tag{B.1}$$

into the operator basis introduced in Sec. 7.1, $\hat{H}^{\mathsf{sp1}}_{\mathfrak{B}}$. We get

$$\begin{aligned}
\hat{H}^{\mathsf{sp1}}_{\mathfrak{B}} &= \frac{\omega}{2}\sum_{\mu\mu'\mu''} \mathrm{Tr}\left\{\left(\hat{\sigma}_z \otimes \hat{1}_{23}\right)\mathfrak{B}_\mu \otimes \mathfrak{B}_{\mu'} \otimes \mathfrak{B}_{\mu''}\right\}\mathfrak{B}_\mu \otimes \mathfrak{B}_{\mu'} \otimes \mathfrak{B}_{\mu''} \\
&= \frac{\omega}{2}\left(\mathrm{Tr}\left\{\hat{\sigma}_z\eta\hat{1}\right\}\mathfrak{B}_0 + \sum_{i=x,y,z}\mathrm{Tr}\left\{\hat{\sigma}_z\eta\hat{\sigma}_i\right\}\mathfrak{B}_i\right) \otimes \eta^{-1}\mathfrak{B}_0 \otimes \eta^{-1}\mathfrak{B}_0 \\
&= \eta^{-1}\omega\mathfrak{B}_3 \otimes \mathfrak{B}_0 \otimes \mathfrak{B}_0,
\end{aligned} \tag{B.2}$$

where we have used Eq. (7.7), $\mathrm{Tr}\{\hat{\sigma}_z\} = 0$, $\hat{\sigma}_z\hat{\sigma}_i = \delta_{iz}\hat{1}$ and $\mathrm{Tr}\left\{\hat{1}\right\} = 2$.

B.2. On the solution of a set of ODEs

Suppose we have found an orthonormal set of eigenvectors $\vec{x}_E$, given as the columns of a transformation matrix $\mathcal{T}$. Then, we have that

$$\mathcal{A}\left(\mathcal{T}\vec{e}_i\right) = a_i\left(\mathcal{T}\vec{e}_i\right), \tag{B.3}$$

with $\vec{e}_i$ being an element of the orthonormal basis vector set and a_i the eigenvalue of $\vec{x}^i_E$. If we want to diagonalize $\mathcal{A}$, we have to invert $\mathcal{T}$, which is the conjugate transpose of $\mathcal{T}$ in this case, using

$$\left(\vec{e}_i^{\,\dagger}\mathcal{T}^\dagger\right)\mathcal{A}\left(\mathcal{T}\vec{e}_j\right) = a_j\vec{e}_i^{\,\dagger}\mathcal{T}^\dagger\mathcal{T}\vec{e}_j = a_j\vec{e}_i^{\,\dagger}\vec{e}_j = a_j\delta_{ij}, \tag{B.4}$$

with δ_{ij} being the Kronecker-delta. Here, we have used $\mathcal{T}^\dagger\mathcal{T} = \mathsf{id}$ and that we have an orthonormal basis vector set, thus $\vec{e}_i^{\,\dagger}\vec{e}_j = \delta_{ij}$. We immediately see from this coefficient representation of $\mathcal{A}$ that this is now a diagonal matrix. From this we can immediately infer that $\tilde{\mathcal{A}}$ given by

$$\tilde{\mathcal{A}} = \mathcal{T}^\dagger\mathcal{A}\mathcal{T} \tag{B.5}$$

is diagonal. Introducing the vector $\vec{\tilde{\rho}}$ by

$$\vec{\tilde{\rho}} \equiv \mathcal{T}^\dagger\vec{\rho}, \;\; \dot{\vec{\tilde{\rho}}} = \mathcal{T}^\dagger\dot{\vec{\rho}}, \tag{B.6}$$

we can rewrite Eq. (7.95), giving

$$\dot{\vec{\rho}}(t) = \mathcal{T}\dot{\vec{\tilde{\rho}}}(t) = \mathcal{A}\vec{\rho}(t) = \mathcal{A}\mathcal{T}\vec{\tilde{\rho}}(t) \implies \dot{\vec{\tilde{\rho}}}(t) = \mathcal{T}^\dagger\mathcal{A}\mathcal{T}\vec{\tilde{\rho}}(t). \tag{B.7}$$

Substituting Eq. (B.5), we get

$$\dot{\vec{\tilde{\rho}}}(t) = \tilde{\mathcal{A}}\vec{\tilde{\rho}}(t) \tag{B.8}$$

with the formal solution

$$\vec{\tilde{\rho}}(t) = \mathrm{e}^{\tilde{\mathcal{A}}t}\vec{\tilde{\rho}}(0). \tag{B.9}$$

Transforming back into the original basis yields

$$\vec{\tilde{\rho}}(t) = \mathcal{T}\vec{\rho}(t) = \mathrm{e}^{\tilde{\mathcal{A}}t}\mathcal{T}\vec{\rho}(0), \tag{B.10}$$

which finally gives

$$\vec{\rho}(t) = \mathcal{T}^\dagger\mathrm{e}^{\tilde{\mathcal{A}}t}\mathcal{T}\vec{\rho}(0). \tag{B.11}$$

As the matrix exponent of the diagonalized matrix is nothing but its diagonal entries in the exponent, the solution can be found easily once the unitary transformation $\mathcal{T}$ is known.

B.3. On reciprocal basis sets

In principle, what we have is a transformation $\mathcal{R}$, which transforms a basis vector $|e_i\rangle$ into an eigenvector $|x_E^i\rangle$,

$$\mathcal{R}\,|e_i\rangle = |x_E^i\rangle \;\text{ with }\; \mathcal{A}\,|x_E^i\rangle = a_i\,|x_E^i\rangle\,. \tag{B.12}$$

These eigenvectors form a set of non-orthogonal basis vectors, thus

$$\langle x_e^i | x_E^j \rangle = C_{ij} \overset{!}{\neq} \delta_{ij}. \tag{B.13}$$

The inequality is due to the fact that the vectors are not orthogonal. As a consequence,

$$\sum_i R_{ji}^* R_{ij} \neq \delta_{ij}, \tag{B.14}$$

as would be expected for unitary matrices. Here, R_{ji}^* denote the complex conjugate coefficients of $\mathcal{R}$. Transposing interchanges the indices. Thus, as $\mathcal{R}$ does not contain orthogonalized eigenvectors, it is not unitary.

From the theory of non-orthogonal basis vectors (cf., e. g. [67]) we know that

$$\mathcal{R}^\dagger \neq \mathcal{R}^{*^T}, \tag{B.15}$$

or in coefficient notation,

$$R_{ij}^\dagger \neq R_{ji}^*. \tag{B.16}$$

Consider a non-orthogonal basis set $\{|\varphi_i\rangle\}$. A helpful tool for non-orthogonal basis sets is the reciprocal basis set $\{|\chi_i\rangle\}$, defined through

$$\langle \chi_i | \varphi_j \rangle = \delta_{ij}. \tag{B.17}$$

The transformation between the two basis sets is given by

$$|\chi_i\rangle = \sum_j \bar{C}_{ij} \, |\varphi_j\rangle \, . \tag{B.18}$$

With the definition of

$$\langle \varphi_i | \varphi_j \rangle \equiv C_{ij} \tag{B.19}$$

we then find

$$\delta_{ik} = \sum_j \bar{C}_{ij} \, \langle \varphi_j | \varphi_k \rangle \implies \mathsf{id} = \bar{C} C. \tag{B.20}$$

Then, the adjoint of an operator is defined through the complex conjugate transpose of its coefficient representation in the reciprocal basis rather than in the original basis,

$$\mathcal{G}^\dagger = \underset{\cdot}{\mathcal{G}}^{*^T}, \tag{B.21}$$

where $\dot{\mathcal{G}}$ denotes the operator $\mathcal{G}$ given in the reciprocal basis.

In our context, we have that

$$\mathcal{T}^\dagger \mathcal{T} = C, \tag{B.22}$$

thus, if we are able to find the inverse $\bar{C}$ of C, we have

$$\mathcal{T}^{-1} = \bar{C}\mathcal{T}^\dagger. \tag{B.23}$$

Indeed, MATHEMATICA is able to invert C, thus we get the analytical solution for arbitrary initial states, given by

$$\vec{\rho}(t) = \mathcal{T} \mathrm{e}^{\tilde{A}t} \bar{C} \mathcal{T}^\dagger \vec{\rho}(0). \tag{B.24}$$

With this we can now give the general solution of the set of ODE for the coefficients of the density operator.

C. LEMBAS and Measurement

In this chapter, we are concerned with the question whether we can unambiguously define measurement induced heat and work flows in the sense of LEMBAS. The effect of projective measurements on the distribution of work has already been considered from a different point of view in [78], e. g. Here, we consider a bipartite system, being described by

$$\hat{\rho} = \hat{\rho}_{\mathsf{sys}} \otimes \hat{\rho}_{\mathsf{env}} + \hat{C}_{\mathsf{se}}. \tag{C.1}$$

We want to consider the energy flows while measuring subsequently both systems locally. We consider only instantaneous, projective energy measurements via $\hat{P}_n = (|n\rangle\langle n| \otimes \hat{1}_{\mathsf{env}})$. The measurement basis is chosen to coincide with the bare local energy-eigenbasis, $\{|n\rangle\}$, for the following considerations.

C.1. Local states after measurement

We start with measuring the system. We find for the density operator after measuring the system in the energy-eigenstate $|n\rangle$:

$$\hat{\rho}^{+}(n) = \frac{\hat{P}_n \hat{\rho} \hat{P}_n}{q_n} \quad \text{with} \quad q_n = \mathrm{Tr}\left\{\hat{P}_n \hat{\rho} \hat{P}_n\right\} = \left(\hat{\rho}_{\mathsf{sys}}\right)_{nn}, \tag{C.2}$$

where we have used that $\mathrm{Tr}_{\mathsf{env}}\{\hat{C}_{\mathsf{se}}\} = 0$. The superscript + denotes the fact that the system has been measured, thus the time at which we consider the density operator is $\hat{\rho}^{t+\mathrm{d}t}$ with $\mathrm{d}t \longrightarrow 0$. The time at which the measurement is being performed will be set to 0 in the following.

The compound state after this local measurement is given by

$$\hat{\rho}^{+}(n) = |n\rangle\langle n| \otimes \hat{\rho}^{0}_{\mathsf{env}} + \hat{P}_n \hat{C}_{\mathsf{se}} \hat{P}_n \frac{1}{q_n}. \tag{C.3}$$

The state of the environment is thus influenced by measuring the system as

can be seen easily due to

$$\hat{\rho}^{+}_{\mathsf{env}}(n) = \mathrm{Tr}_{\mathsf{sys}}\{\hat{\rho}^{+}(n)\} = \hat{\rho}^{0}_{\mathsf{env}} + \mathrm{Tr}_{\mathsf{sys}}\left\{\hat{P}_n\hat{C}_{\mathsf{se}}\right\}\frac{1}{q_n}$$
$$= \sum_{n'p'}\left[(\hat{\rho}_{\mathsf{env}})_{n'p'} + \frac{1}{q_n}\langle nn'|\,\hat{C}_{\mathsf{se}}\,|np'\rangle\right]|n'\rangle\langle p'|\,. \tag{C.4}$$

In the first step we have used the cyclic property of the partial trace for local operators, $\mathrm{Tr}_{\mathsf{sys}}\{\hat{P}_n\hat{C}_{\mathsf{se}}\hat{P}_n\} = \mathrm{Tr}_{\mathsf{sys}}\{\hat{P}^2_n\hat{C}_{\mathsf{se}}\}$ and that $\hat{P}^2_n = \hat{P}_n$.

In contrast, for the ensemble measurement[1] we have:

$$\hat{\rho}^{+}_{\mathsf{env}} = \sum_n \hat{\rho}^{+}_{\mathsf{env}}(n)q_n = \hat{\rho}^{0}_{\mathsf{env}} + \sum_{n'p'}\langle nn'|\,\hat{C}_{\mathsf{se}}\,|np'\rangle\,|n'\rangle\langle p'| = \hat{\rho}^{0}_{\mathsf{env}}, \tag{C.5}$$

thus, no change can be seen. In the last step we have used that $\mathrm{Tr}_{\mathsf{sys}}\{\hat{C}_{\mathsf{se}}\} = 0$.

The state of the system changes, however, if there are coherences present initially, as

$$\hat{\rho}^{+}_{\mathsf{sys}} = \sum_n q_n\hat{\rho}^{+}_{\mathsf{sys}}(n) = \mathsf{diag}\left(\hat{\rho}^{0}_{\mathsf{sys}}\right) \equiv \hat{\rho}^{D}_{\mathsf{sys}}. \tag{C.6}$$

Since we measure in the energy-eigenbasis of the bare system Hamiltonian, only the diagonal elements in this basis are recovered.

C.2. Internal energy change

In order to define work and heat induced by a measurement, we first start with investigating the change of internal energy due to a measurement. As we expect the internal energy of both subsystems to change, we consider them separately.

C.2.1. System

The effective internal energy of the system before the measurement is defined as [33]

$$U_{\mathsf{sys}} = \mathrm{Tr}\left\{\hat{H}'_{\mathsf{sys}}\hat{\rho}_{\mathsf{sys}}\right\}. \tag{C.7}$$

[1] By the notion of ensemble measurement we understand many repeated measurements on equally prepared states

After the system has being measured in a distinct energy-eigenstate, we have

$$U^+_{\mathsf{sys}} = \mathrm{Tr}\left\{\hat{H}'^+_{\mathsf{sys}}\hat{\rho}^+_{\mathsf{sys}}\right\} = \sum_n q_n \mathrm{Tr}\left\{\hat{H}'^+_{\mathsf{sys}}(n)\hat{\rho}^+_{\mathsf{sys}}(n)\right\} \equiv \sum_n q_n U^+_{\mathsf{sys}}(n). \tag{C.8}$$

Here, we have defined the internal energy $U^+_{\mathsf{sys}}(n)$ of the system for a specific measurement outcome. Note, that generally $\hat{H}'_{\mathsf{sys}}$ does change due to the measurement as $\hat{H}'_{\mathsf{sys}} = \hat{H}_{\mathsf{sys}} + \hat{H}^{\mathsf{eff},1}_{\mathsf{sys}}$ and the latter addend depends on $\hat{\rho}_{\mathsf{env}}$. More precisely, we have

$$\begin{aligned}\hat{H}^{\mathsf{eff},1^+}_{\mathsf{sys}}(n) &= \mathsf{diag}\left(\mathrm{Tr}_{\mathsf{env}}\left\{\hat{H}_{\mathsf{se}}\hat{1}\otimes\hat{\rho}^+_{\mathsf{env}}(n)\right\}\right) \\ &\overset{(C.4)}{=} \hat{H}^{\mathsf{eff},1}_{\mathsf{sys}} + \mathsf{diag}\left(\mathrm{Tr}_{\mathsf{env}}\left\{\hat{H}_{\mathsf{se}}\mathrm{Tr}_{\mathsf{sys}}\left[\hat{P}_n\hat{C}_{\mathsf{se}}\right]\right\}\right) q_n^{-1}. \end{aligned} \tag{C.9}$$

Note, that for $\hat{H}^{\mathsf{eff},1}_{\mathsf{sys}}$ we only have to take the part of $\hat{H}^{\mathsf{eff}}_{\mathsf{sys}}$ which commutes with the measurement basis into account. As the measurement basis is chosen to coincide with the local Hamiltonian, we take the diagonal elements in the energy-basis representation. For an ensemble measurement, we have

$$\begin{aligned}U^+_{\mathsf{sys}} &= \sum_n q_n \mathrm{Tr}\left\{[\hat{H}_{\mathsf{sys}} + \hat{H}^{\mathsf{eff},1^+}_{\mathsf{sys}}(n)]\hat{\rho}^+_{\mathsf{sys}}(n)\right\} \\ &= \mathrm{Tr}\left\{(\hat{H}_{\mathsf{sys}} + \hat{H}^{\mathsf{eff},1}_{\mathsf{sys}})\hat{\rho}^D_{\mathsf{sys}}\right\} + \sum_n \mathrm{Tr}_{\mathsf{sys}}\left\{\mathrm{Tr}_{\mathsf{env}}\left[\hat{H}_{\mathsf{se}}\mathrm{Tr}_{\mathsf{sys}}\left(\hat{P}_n\hat{C}_{\mathsf{se}}\right)\right]|n\rangle\langle n|\right\}, \end{aligned} \tag{C.10}$$

where we have used Eqs. (C.4) and (C.9), respectively. In the second addend we can take the complete $\hat{H}^{\mathsf{eff}}_{\mathsf{sys}}$, here, as $\hat{\rho}^+_{\mathsf{sys}}(n) = |n\rangle\langle n|$ trivially has only diagonal elements in the energy-basis representation. The same reasoning allows to identify

$$\mathrm{Tr}\left\{\hat{H}'_{\mathsf{sys}}\hat{\rho}^D_{\mathsf{sys}}\right\} = \mathrm{Tr}\left\{\hat{H}'_{\mathsf{sys}}\hat{\rho}_{\mathsf{sys}}\right\} = U_{\mathsf{sys}}. \tag{C.11}$$

Rewriting the second addend of Eq. (C.10), U^c_{sys}, we get

$$U^c_{\mathsf{sys}} = \sum_n \mathrm{Tr}\left\{\hat{H}_{\mathsf{se}}\left[|n\rangle\langle n|\otimes\mathrm{Tr}_{\mathsf{sys}}\left(\hat{P}_n\hat{C}_{\mathsf{se}}\right)\right]\right\}, \tag{C.12}$$

which vanishes only for $\hat{C}_{\mathsf{se}} = 0$, generally. Thus, by measuring the system its internal energy according to LEMBAS may be changed even in an ensemble measurement if $\hat{H}'_{\mathsf{sys}}$ depends on the state of the environment!

For a single measurement outcome we find for the change of the internal energy due to the measurement

$$\begin{aligned}\Delta U^M_{\mathsf{sys}}(n) &= U^+_{\mathsf{sys}}(n) - U_{\mathsf{sys}} \\ &= \mathrm{Tr}\left\{\left[\hat{H}_{\mathsf{sys}} + \hat{H}^{\mathsf{eff},1^+}_{\mathsf{sys}}(n)\right]|n\rangle\langle n| - \left[\hat{H}_{\mathsf{sys}} + \hat{H}^{\mathsf{eff},1}_{\mathsf{sys}}\right]\hat{\rho}_{\mathsf{sys}}\right\}.\end{aligned} \tag{C.13}$$

A separation of energy flow into a part which changes the local von Neumann entropy and a contribution that does not, does not seem to be straightforward. As a direct consequence it is awkward to define measurement induced heat and work flow into the system this way.

Now, we investigate what happens to the internal energy of the environment.

C.2.2. Environment

Analogously to the system, the internal energy of the environment is defined as

$$U_{\mathsf{env}} = \mathrm{Tr}\left\{\hat{H}'_{\mathsf{env}}\hat{\rho}_{\mathsf{env}}\right\}. \tag{C.14}$$

After the projective measurement on the system the internal energy of the environment reads

$$U^+_{\mathsf{env}} = \mathrm{Tr}\left\{\hat{H}'^+_{\mathsf{env}}\hat{\rho}^+_{\mathsf{env}}\right\} = \sum_n q_n \mathrm{Tr}\left\{\hat{H}'^+_{\mathsf{env}}(n)\hat{\rho}^+_{\mathsf{env}}(n)\right\} \equiv \sum_n q_n U^+_{\mathsf{env}}(n). \tag{C.15}$$

For the effective Hamiltonian of the environment after the measurement we have

$$\hat{H}^{\mathsf{eff},1^+}_{\mathsf{env}}(n) = \mathsf{diag}\left(\mathrm{Tr}_{\mathsf{sys}}\left\{\hat{H}_{\mathsf{se}}(|n\rangle\langle n| \otimes \hat{1}_{\mathsf{env}})\right\}\right). \tag{C.16}$$

With this we find for an ensemble measurement

$$\begin{aligned}U^+_{\mathsf{env}} &= \sum_n q_n \mathrm{Tr}\left\{[\hat{H}_{\mathsf{env}} + \hat{H}^{\mathsf{eff},1^+}_{\mathsf{env}}(n)]\hat{\rho}^+_{\mathsf{env}}(n)\right\} \\ &= \mathrm{Tr}\left\{\hat{H}_{\mathsf{env}}\hat{\rho}_{\mathsf{env}}\right\} + \sum_n \mathrm{Tr}\left\{\hat{H}^{\mathsf{eff},1^+}_{\mathsf{env}}(n)\left[q_n\hat{\rho}^0_{\mathsf{env}} + \mathrm{Tr}_{\mathsf{sys}}\left\{\hat{P}_n\hat{C}_{\mathsf{se}}\right\}\right]\right\},\end{aligned} \tag{C.17}$$

where we have used Eqs. (C.5) and (C.4), respectively. Thus, as for the system, the internal energy of the environment may change during an ensemble

measurement. Even for vanishing correlations, $\hat{C}_{\mathsf{se}} = 0$, the internal energy of the environment can change in an ensemble measurement according to Eq. (C.17). Only if we would have $\hat{\rho}^0_{\mathsf{sys}} = \hat{\rho}^D_{\mathsf{sys}}$ we could identify

$$\sum_n \mathrm{Tr}\left\{\hat{H}^{\mathsf{eff},1^+}_{\mathsf{env}}(n) q_n \hat{\rho}^0_{\mathsf{env}}\right\} \overset{(C.16)}{=} \mathrm{Tr}\left\{\hat{H}^{\mathsf{eff},1}_{\mathsf{env}} \hat{\rho}^0_{\mathsf{env}}\right\}, \tag{C.18}$$

leading to $U^+_{\mathsf{env}} = U_{\mathsf{env}}$.

For a single measurement outcome we find for the change of internal energy of the environment

$$\begin{aligned}\Delta U^M_{\mathsf{env}}(n) &= U^+_{\mathsf{env}}(n) - U_{\mathsf{env}} \\ &= \mathrm{Tr}\left\{\left[\hat{H}_{\mathsf{env}} + \hat{H}^{\mathsf{eff},1^+}_{\mathsf{env}}(n)\right]\hat{\rho}^+_{\mathsf{env}}(n) - \left[\hat{H}_{\mathsf{env}} + \hat{H}^{\mathsf{eff},1}_{\mathsf{env}}\right]\hat{\rho}^0_{\mathsf{env}}\right\}.\end{aligned} \tag{C.19}$$

Again, as for the system, it looks like there is no straightforward way to define measurement induced heat and work flow, here.

As we face the aforementioned problems we try to find special cases, where we can unambiguously define measurement induced work and heat.

C.3. Special cases

Here, we want to consider situations where we are able to separate measurement induced energy flow into heat and work despite the problems discussed in Sec. C.2.

C.3.1. Local pure states

We require the system to be in a pure state locally. Then, if we perform a measurement on the system, its local von Neumann entropy does not change. Therefore, the change of internal energy can be attributed to work, only. Thus, we then have that

$$\Delta U^M_{\mathsf{sys}}(n) = \Delta W^M_{\mathsf{sys}}(n). \tag{C.20}$$

Therefore, if the system has been measured at some time in the past, $-\tau$, and has afterwards evolved unitarily, we have that

$$\begin{aligned}\Delta U_{\mathsf{sys}}(f,i) &= \Delta U^M_{\mathsf{sys}}(f) + \Delta U^{-\tau,0}_{\mathsf{sys}}(i) \\ &= \Delta W^M_{\mathsf{sys}}(f) + \Delta W^{\mathsf{Lem}}_{\mathsf{sys}}(i) = \Delta W^{\mathsf{Lem}}_{fi} = \Delta E'_{fi}.\end{aligned} \tag{C.21}$$

This is consistent with our definition of work between two energy-eigenstates for unitary evolution (cf. Sec. 2.2.1[2]) where we have argued that only work is being performed on the system and we thus have for two-time measurements

$$\Delta E'_{fi} = \Delta W_{fi}. \tag{C.22}$$

Note that if we would have

$$\Delta U^M_{\mathsf{sys}}(n) \neq \Delta W^M_{\mathsf{sys}}(n) \tag{C.23}$$

for measuring pure states, then

$$\Delta E'_{fi} \neq \Delta W_{fi}, \tag{C.24}$$

which would lead to

$$\overline{\mathrm{e}^{-\beta \Delta W_{fi}}} \neq \overline{\mathrm{e}^{-\beta \Delta E_{fi}}} = \mathrm{e}^{-\beta \Delta F}, \tag{C.25}$$

which would mean a violation of JR for closed quantum systems (As EFT would hold but not coincide with JR).

C.3.2. State-independent effective Hamiltonian of environment

Suppose that $\hat{H}^{\mathsf{eff},1}_{\mathsf{env}}$ does not depend on the state of the system ($\hat{H}^{\mathsf{eff},2}_{\mathsf{env}}$ might do so). Using $\hat{H}^{\mathsf{eff},1}_{\mathsf{env}} = \hat{H}^{\mathsf{eff},1^+}_{\mathsf{env}}(n)\ \forall\ n$ in Eq. (C.19) gives

$$\begin{aligned}\Delta U^M_{\mathsf{env}}(n) &= \mathrm{Tr}\left\{\hat{H}'_{\mathsf{env}}\left[\hat{\rho}^{+}_{\mathsf{env}}(n) - \hat{\rho}^{0}_{\mathsf{env}}\right]\right\} \\ &= \mathrm{Tr}\left\{\left(\hat{P}_n \otimes \hat{H}'_{\mathsf{env}}\right)\hat{C}_{\mathsf{se}}\right\} q_n^{-1},\end{aligned} \tag{C.26}$$

where we used Eq. (C.4) in the last step. As from $\hat{C}_{\mathsf{se}} = 0 \Longrightarrow \Delta U^M_{\mathsf{env}}(n) = 0$ and since here, $\hat{\rho}_{\mathsf{env}}$ changes due to the measurement (via correlations) but $\hat{H}^{\mathsf{eff},1}_{\mathsf{env}}$ does not, we will use the *ad hoc* definition

$$\hat{H}^{\mathsf{eff},1}_{\mathsf{env}} = \hat{H}^{\mathsf{eff},1^+}_{\mathsf{env}}(n)\ \forall\ n \implies \Delta U^M_{\mathsf{env}}(n) = \Delta Q^M_{\mathsf{env}}(n). \tag{C.27}$$

Note, that this is an indirect measurement effect as we consider an energy flow into the environment arising due to a projective measurement on the system, due to co-jumps.

[2] There, we have assumed implicitly that the measurement induced energy flow is to be considered as work

C.4. Split measurement effects

Despite the problems discussed in Sec. C.2, we try to split measurement induced energy into heat and work for general states, here. This is important as for weighted averages as encountered in the JR, e. g., we are interested in work and heat for trajectories[3]. As LEMBAS does provide us with heat and work up to the measurement only, it is necessary to have a means to distinguish between heat and work for measurement induced energy flow.

We start with the change of $\hat{H}_{\mathsf{sys}}^{\mathsf{eff},1}$. As a change in the effective Hamiltonian does not influence the state of the system its change should be interpreted as work. However, for instantaneous measurements it is not possible to decide how $\hat{\rho}_{\mathsf{sys}}$ changes while $\hat{H}_{\mathsf{sys}}^{\mathsf{eff},1}$ does. Also, it is not possible to distinguish between coherent and incoherent dynamics (in the sense of some time-evolution) of $\hat{\rho}_{\mathsf{sys}}$, rendering it hard to associate the change of the density operator with heat and work.

Therefore, the following considerations are to be understood as trial definitions. Only consistency checks may reveal whether these definitions may be useful or not.

We try the following ansatz: As the notions of time, evolution and simultaneity are ill-defined for instantaneous processes, assume that the changes of $\hat{H}_{\mathsf{sys}}^{\mathsf{eff},1}$ and $\hat{\rho}_{\mathsf{sys}}$ due to the measurement can be considered separately, as both cannot change *simultaneously*. The states before and after the measurement are given by $\hat{\rho}_{\mathsf{sys}}^{0}$ and $\hat{\rho}_{\mathsf{sys}}^{+}(n)$, respectively. The next step is based on the reasoning of Sec. C.3.1. If the system is in a pure state, then only work is being induced by the measurement. Therefore, the measured state should be compared to the original state where changes of the density operator without changing von Neumann entropy should be interpreted as work, also. To this end, we consider $\hat{\rho}_{\mathsf{sys}}^{0}$ in its eigenbasis, which is generally different from the energy eigenbasis,

$$\mathsf{diag}\left(\tilde{\hat{\rho}}_{\mathsf{sys}}^{0}\right) = \tilde{\hat{\rho}}_{\mathsf{sys}}^{0} = \mathcal{D}\hat{\rho}_{\mathsf{sys}}^{0}\mathcal{D}^{\dagger}, \tag{C.28}$$

where the unitary transformation $\mathcal{D}$ and its inverse, $\mathcal{D}^{\dagger}$, transform the density operator into a diagonal state in its eigenbasis representation[4]. The change of $\hat{\rho}_{\mathsf{sys}}$ in its eigenbasis still necessary to get to $\hat{\rho}_{\mathsf{sys}}^{+}(n)$ is then interpreted as

[3] In contrast to classical trajectories we think of two-time measurements, here.
[4] Note that $\tilde{\hat{\rho}}_{\mathsf{sys}}^{0} \neq \hat{\rho}_{\mathsf{sys}}^{D}$ defined in Eq. (C.6)

heat, thus

$$\begin{aligned}\Delta U^M_{\mathsf{sys}} =& \underbrace{\mathrm{Tr}\left\{\hat{H}^{\mathsf{eff},1^+}_{\mathsf{sys}}(n)\hat{\rho}^+_{\mathsf{sys}}(n) - \hat{H}'_{\mathsf{sys}}\mathcal{D}\hat{\rho}^+_{\mathsf{sys}}(n)\mathcal{D}^\dagger\right\}}_{đW^M_{\mathsf{sys}}(n)} + \dots \\ =& \dots + \underbrace{\mathrm{Tr}\left\{\hat{H}'_{\mathsf{sys}}\left[\mathcal{D}\hat{\rho}^+_{\mathsf{sys}}(n)\mathcal{D}^\dagger - \hat{\rho}^0_{\mathsf{sys}}\right]\right\}}_{đQ^M_{\mathsf{sys}}(n)}. \end{aligned} \tag{C.29}$$

Let us consider two simple examples: We consider cases where $\hat{H}^{\mathsf{eff},1}_{\mathsf{sys}} = 0$, thus $U_{\mathsf{sys}} = \mathrm{Tr}\left\{\hat{H}_{\mathsf{sys}}\hat{\rho}_{\mathsf{sys}}\right\}$.

First, the local density operator before the measurement is given by

$$\hat{\rho}^0_{\mathsf{sys}} = \frac{1}{2}\begin{pmatrix}1 & 1\\ 1 & 1\end{pmatrix}, \tag{C.30}$$

in the energy eigenbasis, which is a pure state. The two possible states after the measurements are

$$\hat{\rho}^+_{\mathsf{sys}}(0) = \begin{pmatrix}1 & 0\\ 0 & 0\end{pmatrix} \text{ and } \hat{\rho}^+_{\mathsf{sys}}(1) = \begin{pmatrix}0 & 0\\ 0 & 1\end{pmatrix}. \tag{C.31}$$

As we find

$$\tilde{\hat{\rho}}^+_{\mathsf{sys}}(0) = \mathcal{D}\hat{\rho}^+_{\mathsf{sys}}(0)\mathcal{D}^\dagger = \frac{1}{2}\begin{pmatrix}1 & -1\\ -1 & 1\end{pmatrix} \text{ and } \tilde{\hat{\rho}}^+_{\mathsf{sys}}(1) = \frac{1}{2}\begin{pmatrix}1 & 1\\ 1 & 1\end{pmatrix}, \tag{C.32}$$

we find according to Eq. (C.29) that

$$đQ^M_{\mathsf{sys}}(n) = \mathrm{Tr}\left\{\hat{H}'_{\mathsf{sys}}\left[\mathcal{D}\hat{\rho}^+_{\mathsf{sys}}(n)\mathcal{D}^\dagger - \hat{\rho}^0_{\mathsf{sys}}\right]\right\} = 0 \tag{C.33}$$

as $\mathrm{Tr}\left\{\hat{H}_{\mathsf{sys}}\hat{\rho}_{\mathsf{sys}}\right\} = \mathrm{Tr}\left\{\hat{H}_{\mathsf{sys}}\hat{\rho}^D_{\mathsf{sys}}\right\}$, which immediately gives

$$\Delta U^M_{\mathsf{sys}}(n) = \Delta W^M_{\mathsf{sys}}(n) \text{ for } n = 1, 2. \tag{C.34}$$

This is consistent with our discussion in Sec. C.3.1 as we find that measuring this pure state, here, induces only work. For further reference we will call this way of separating measurement induced heat and work flows method A.

The second example is concerned with a local state of maximal uncertainty,

$$\hat{\rho}^0_{\mathsf{sys}} = \frac{1}{2}\begin{pmatrix}1 & 0\\ 0 & 1\end{pmatrix}. \tag{C.35}$$

There, we would expect that the total measurement induced energy flow is attributed to heat as the state is already diagonal in the measurement basis. Indeed, from Eq. (C.29) we have

$$đW^M_{\mathsf{sys}}(n) = \mathrm{Tr}\left\{\hat{H}'_{\mathsf{sys}}\left[\hat{\rho}^+_{\mathsf{sys}}(n) - \mathcal{D}\hat{\rho}^+_{\mathsf{sys}}(n)\mathcal{D}^\dagger\right]\right\} = 0, \tag{C.36}$$

as $\mathcal{D}$ equals the identity, here.

However, what if the state with respect to the measurement basis was given by

$$\hat{\rho}^0_{\mathsf{sys}} = \begin{pmatrix} 1 & 0 \\ 0 & 0 \end{pmatrix}? \tag{C.37}$$

Then, the system is in a pure state and we expect that no heat flows during a measurement. According to our definition, however, measuring the system in the excited state would give rise to a massive heat flow. One may argue that the probability, thus the corresponding weight, for measuring the system in the excited state vanishes, but what about states with almost vanishing, but non-zero probability for the excited state? The von Neumann entropy would be close to zero, but one would have that measuring such a state would lead to tremendous heat flow into the measured system.

Also, consider the following state:

$$\hat{\rho}^0_{\mathsf{sys}} = \begin{pmatrix} 0.8475 & \Xi \\ \Xi^* & 0.1525 \end{pmatrix}, \tag{C.38}$$

with $\Xi \equiv -0.3585 + 0.025\mathrm{i}$ and Ξ^* being the complex conjugate of Ξ. This is a pure state as can be confirmed easily. For the respective measured states in the basis where $\hat{\rho}^0_{\mathsf{sys}}$ is diagonal we find

$$\tilde{\hat{\rho}}^+_{\mathsf{sys}}(0) = \mathcal{D}\hat{\rho}^+_{\mathsf{sys}}(0)\mathcal{D}^\dagger = \begin{pmatrix} 0.8475 & \mathsf{Re}(\Xi) \\ \mathsf{Re}(\Xi) & 0.1525 \end{pmatrix}, \tag{C.39}$$

$$\tilde{\hat{\rho}}^+_{\mathsf{sys}}(0) = \mathcal{D}\hat{\rho}^+_{\mathsf{sys}}(1)\mathcal{D}^\dagger = \begin{pmatrix} 0.1525 & -\mathsf{Re}(\Xi) \\ -\mathsf{Re}(\Xi) & 0.8475 \end{pmatrix}. \tag{C.40}$$

Assuming the effective Hamiltonian to have the eigenvalues ∓ 1, we find for the respective heat flows $\Delta Q^M_{\mathsf{sys}}(0) = 0$ and $\Delta Q^M_{\mathsf{sys}}(1) = 1.39$. Again, although we have a pure state, the measurement seems to induce heat. Note, that considering measurement dynamics, this could probably be explained (non-cancelling irreversible heat flows into and out of the system), however it is awkward to speak of measurement dynamics for instantaneous projective measurements, of course.

Therefore, we present a second definition of heat and work induced by measurements the following way: We restrict ourselves to spins, only (as we have already done in our examples). Then, the temperature of the spin is calculated, taking only the diagonal elements in the energy-basis representation into account: If it is positive, the state of the system is rotated for comparison with measuring the system in the excited state, if it is negative the state is rotated for comparison with the measurement of the ground state. The rotation naturally accounts for measurement induced work, as the rotation can be described by a unitary process,

$$\hat{U}(t) = \begin{pmatrix} 0 & 1 \\ 1 & 0 \end{pmatrix}. \tag{C.41}$$

This definition does not influence the first two examples. However, for a state given by Eq. (C.38), we now find that $\Delta Q^M_{\mathsf{sys}}(0) = \Delta Q^M_{\mathsf{sys}}(1) = 0$, as expected. For the measurement induced work we readily obtain $\Delta W^M_{\mathsf{sys}}(0) = -0.305$ and $\Delta W^M_{\mathsf{sys}}(1) = +1.695$. Weighting with the corresponding probabilities gives $\Delta W^M_{\mathsf{sys}}(\mathsf{ens}) = 0.8475 \cdot (-0.305) + 0.1525 \cdot (+1.695) = 0$, as expected for an ensemble measurement with $\mathrm{d}\hat{H}'_{\mathsf{sys}} = 0$. This is only one possible way to describe measurements, of course. We call this way of separating heat and work flows during measurements method B.

D. German summary - Deutsche Zusammenfassung

Die klassische Thermodynamik, ursprünglich phänomenologisch eingeführt und später im Zuge der statistischen Physik durch Plausibilitätsargumente aus den Grundgleichungen der Mechanik begründet, beschreibt unter anderem den stationären Gleichgewichtszustand, in den sich ein typischerweise makroskopisches System entwickelt. Darüber hinaus werden Prozesse, vermittelt durch Kontrolle äußerer Zwänge, die das System nur geringfügig aus solch einem Gleichgewichtszustand drängen, beschrieben. Ihren überwältigenden Erfolg verdankt die Thermodynamik Ihrer Einfachheit, mit der sie mikroskopisch extrem komplexe Vorgänge beschreibt. Daher ist es oft wünschenswert oder gar unumgänglich, das Verhalten eines großen Systems thermodynamisch zu beschreiben.

In der Natur wie auch in technischen Anwendungen hat man es jedoch häufig mit Prozessen zu tun, die - meist aufgrund der Geschwindigkeit, mit denen diese durchgeführt werden - das betrachtete System weit von einem Gleichgewichtszustand im Sinne der Thermodynamik entfernen. Möchte man beispielsweise die Leistung von Wärme-Kraft Maschinen optimieren, spielt die Geschwindigkeit der durchlaufenen Prozessschritte eine entscheidende Rolle. Daher war die Entdeckung mehrerer Fluktuationstheoreme in den neunziger Jahren ein entscheidender Schritt zur Beschreibung von Nicht-Gleichgewichts Phänomenen [19]. Ein herausragender Vertreter davon ist die Jarzynski Relation [6], welche die Arbeit, benötigt für einen Prozess welcher das System beliebig weit aus dem Gleichgewicht treiben möge, mit der Differenz der freien Energie zwischen zwei Gleichgewichtszuständen verknüpft.

Obwohl die Thermodynamik ursprünglich entwickelt wurde um makroskopische Systeme zu beschreiben, kann sie unter geeigneten Umständen auch auf kleinste Systeme bestehend aus wenigen Teilchen angewendet werden. Ein neuer quantenmechanischer Ansatz zur Erklärung thermodynamischen Verhaltens von kleinsten Systemen aufgrund geeigneter Einbettung in deren Umgebung [44] erlaubt die genaue Abschätzung der Anwendbarkeit thermodynamischer Prinzipien. Da die genaue Beschreibung des Verhaltens selbst nanoskopischer Systeme, die nicht-klassisches Verhalten zeigen und quantenmechanisch beschrieben werden müssen, aufgrund des starken Anwachsens des

Hilbertraumes schnell praktisch unmöglich werden kann, ist die Untersuchung von Fluktuationstheoremen in solchen Systemen interessant.

Unerlässlich für die Untersuchung von Nicht-Gleichgewichts Relationen in Quantensystemen ist, insbesondere für die Jarzynski Relation, eine konsistente verallgemeinerte Definition von Arbeit und Wärme. Da in der vorliegenden Arbeit ein Schwerpunkt auf abgeschlossenen Quantensystemen, welche nicht von außen getrieben werden, liegt, findet hier eine Verallgemeinerung für Arbeit und Wärme zwischen zwei Quantensystemen in beliebigen Zuständen Verwendung [33]. Mit Hilfe dieser Definition werden hier lokale Fluktuationstheoreme für die effektive Dynamik eines Teils eines modularen Quantensystems untersucht.

Darüber hinaus widmet sich diese Arbeit auch möglichen neuen Zugängen zur Beschreibung von Kreisprozessen, welche an Quantensystemen in endlicher Zeit und somit teilweise fernab vom thermischen Gleichgewicht durchgeführt werden. Hierbei findet die Effizienz dieser Prozesse besondere Beachtung.

D.1. Nichtunitäre Prozesse

Betrachtet man ein System, welches mit einer Umgebung in Wechselwirkung steht, so lässt sich die Zeitentwicklung dieses Systems alleine im Allgemeinen nicht mit einem unitären Zeitentwicklungsoperator beschreiben. Hier soll eine andere Ursache nichtunitärer Entwicklung betrachtet werden, die aufgrund von Änderungen von Randbedingungen auftritt. Dies soll am Beispiel eines typischen thermodynamischen Prozesses geschehen. Betrachten wir hierzu einen zweigeteilten Zylinder. In der einen Hälfte befinde sich ein ideales Gas in einem thermischen Zustand, in der anderen herrsche perfektes Vakuum. Die Trennwand soll nun so verschoben werden, dass dem Gas der ganze Zylinder zur Ausbreitung zur Verfügung steht. Ein klassisches Modell mit nur einem einzelnen Gasatom wird in [51] diskutiert und eine Verletzung der Jarzynski Relation gefunden.

Hier beschäftigen wir uns mit einem einfachen quantenmechanischen Analogon zu obigem Modell: Ein einzelnes Teilchen im eindimensionalen Potentialtopf (unendlich hohe Potentialstufen auf beiden Seiten). Das Verschieben der Trennwand wird durch eine zeitabhängige Breite des Topfes modelliert (BSP). Komplementär dazu betrachten wir eine in einem großen Potentialtopf befindliche Potentialstufe der Höhe V_h, deren Breite zeitlich variieren kann, siehe Abb. D.1 (QBSP). Wir betrachten dieses Modell als das realistischere im Hinblick auf die mikroskopische Begründung: Eine mikroskopische Modellierung des Zylinders, in dem sich das Gas befindet, sollte ein effektives, abstoßendes Potential, welches die Atome des Zylinders auf das Gas ausüben, beinhalten.

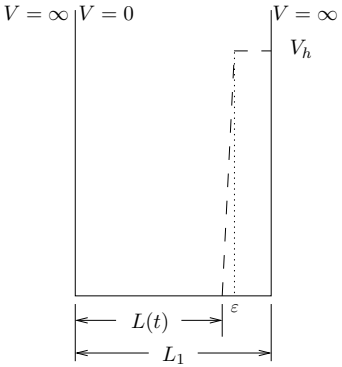

Abbildung D.1.: Potentialtopf variabler Breite zwischen L_0 und L_1, genähert durch einen Potentialtopf der Breite L_1 verwirklicht durch eine Potentialstufe der Höhe V_h. Diese Stufe wird bei $x = L(t)$ eingeführt und besitzt eine steile aber endliche Steigung zwischen L und $L+\varepsilon$. $L(t)$ wird extern kontrolliert, $L_0 \leq L(t) \leq L_1 - \varepsilon$.

Sicherlich erwartet man keine perfekte Potentialstufe aufgrund der möglichen Diffusion des Gases zumindest in die obersten Schichten der Zylinderwände. Auch erwartet man keine unendlich hohen Potentiale; tatsächlich sollte die Wahrscheinlichkeit, dass ein Gasatom durch die Zylinderwände hindurch in die Umgebung tunnelt für endlich dicke Wände nicht exakt verschwinden. Dass das zweite Modell auch eine unendlich hohe Stufe besitzt ist allein der Tatsache geschuldet, dass der numerische Aufwand für die folgenden Untersuchungen in erträglichen Grenzen bleibt. Desweiteren nimmt der unendlich hohe Teil des Potentials nicht an der Prozessdynamik Teil. Allerdings ist die mathematische Beschreibung durch BSP einfacher als durch QBSP.

Da wir hier ein abgeschlossenes System betrachten, verschwindet der Wärmefluss in das System und wir identifizieren die gesamte Energieänderung mit Arbeit, $\Delta E_{fi} = \Delta W_{fi}$. Numerische Untersuchungen zeigen, dass die JR für langsame, quasistatische Prozesse in beiden Modellen, BSP und QBSP, die Differenz der Freien Energie richtig abschätzt. Für quasistatische Prozesse, in denen die Idealisierung durch BSP hervorragende Ergebnisse im Bezug auf Experimente liefert, ergeben sich also keine Probleme. Da wir aber an Prozessen fernab des Gleichgewichts interessiert sind, betrachten wir nun den Fall, in dem die Trennwand (Potentialstufe) instantan verschoben wird. Hier zeigt sich, dass für BSP die JR die Freie Energieänderung falsch abschätzt, wobei der relative Fehler weit über 10% liegen kann. Für QBSP, hingegen, liefert

die JR das korrekte Ergebnis für die Freie Energie, unabhängig von der Höhe V_h der Potentialstufe, solange diese endlich bleibt. Daher ist mit der Idealisierung, die BSP darstellt, vorsichtig umzugehen wenn Prozesse betrachtet werden, welche das System weit aus dem Gleichgewicht treiben.

Ein anderer Aspekt der vorliegenden Untersuchungen beschäftigt sich mit der praktischen Anwendbarkeit der JR. Dabei zeigt sich, dass extrem unwahrscheinliche Ereignisse aufgrund deren starken Gewichtung durch die e-Funktion signifikant zum Mittelwert $\overline{\mathrm{e}^{-\beta\Delta W_{fi}}}$ beitragen können. Ist dies der Fall, so können unverhältnismäßig viele Messungen nötig sein, um eine gute Abschätzung der Freien Energie mittels der JR zu erhalten. Darüber hinaus kann sich ein Konvergenzverhalten des Mittelwerts einstellen, das sog. Plateaus aufweist, welche zur irreführenden Annahme verleiten können, dass der Mittelwert bereits konvergiert sei (vgl. Abb. 3.7). Ein möglicher Ausweg ist die gezielte Präparation von Anfangszuständen oder das Optimieren der verwendeten Arbeits-Protokolle [74].

D.2. Lokale Fluktuationstheoreme

Seither wurden Fluktuationstheoreme fast ausschließlich für extern getriebene Quantensysteme betrachtet. In dieser Arbeit liegt der Fokus jedoch hauptsächlich auf abgeschlossenen Quantensystemen ohne äußeren Einfluss, welche modular aufgebaut sind und ein Teil dieser lokal betrachtet werden soll. Die Einteilung des Energieflusses zwischen den Quantensystemen in Arbeit und Wärme erfolgt dabei nach LEMBAS (kurz für **L**ocal **E**ffective **M**easurement **Bas**is). Daher wird zunächst die zugrunde liegende Idee von LEMBAS kurz eingeführt, bevor verschiedene Möglichkeiten, lokale Fluktuationstheoreme zu definieren, nähers betrachtet werden.

D.2.1. LEMBAS

Wir gehen davon aus, dass per Messung die innere Energie eines Quantensystems ermittelt werden soll. Dabei definiere der Messoperator $\hat{H}^M$ und seine zugehörige Eigenbasis $\{\varphi_n^M\}$ die projektive Messung bzw. Messbasis. Für ein zweigeteiltes System, welches lokal gemessen werden soll, sei diese Messbasis vollständig im zugehörigen Teilraum des Gesamthilbertraumes. Der Einfachheit halber nennen wir im Folgenden das zu messende Teilsystem *System* (sys) und das andere Teilsystem *Umgebung* (env). Für den lokalen effektiven Hamiltonian $\hat{H}^{\mathsf{eff}}_{\mathsf{sys}}(t)$ des System (sys) gilt

$$\hat{H}^{\mathsf{eff}}_{\mathsf{sys}}(t) = \mathrm{Tr}_{\mathsf{env}}\Big\{\hat{H}_{\mathsf{se}}(\hat{1}_{\mathsf{sys}} \otimes \hat{\rho}^t_{\mathsf{env}})\Big\}. \tag{D.1}$$

Hierbei bezeichnen $\hat{H}_{\mathsf{se}}$ den Wechselwirkungsoperator zwischen System und Umgebung, $\hat{\rho}_{\mathsf{env}}$ den Dichteoperator sowie $\mathrm{Tr}_{\mathsf{env}}\{\ldots\}$ die Teilspur über die Umgebung. Zur inneren Energie trägt der Teil des Gesamtoperators $\hat{H}_{\mathsf{sys}} + \hat{H}^{\mathsf{eff}}_{\mathsf{sys}}(t)$ bei, welcher mit dem Messoperator kommutiert (für Details siehe [33]). Für unsere Zwecke setzen wir den Messoperator stets mit dem reinen, lokalen Hamiltonoperator des isolierten Systems gleich, $\hat{H}_{\mathsf{sys}}$. Damit erhalten wir

$$\hat{H}'_{\mathsf{sys}} \equiv \hat{H}_{\mathsf{sys}} + \hat{H}^{\mathsf{eff},1}_{\mathsf{sys}} \;\text{ mit }\; [\hat{H}^{\mathsf{eff},1}_{\mathsf{sys}}, \hat{H}_{\mathsf{sys}}] = 0 \;\text{ und }\; [\hat{H}^{\mathsf{eff},2}_{\mathsf{sys}}, \hat{H}_{\mathsf{sys}}] \neq 0, \quad \text{(D.2)}$$

sowie

$$\hat{H}^{\mathsf{eff}}_{\mathsf{sys}} = \hat{H}^{\mathsf{eff},1}_{\mathsf{sys}} + \hat{H}^{\mathsf{eff},2}_{\mathsf{sys}}. \quad \text{(D.3)}$$

Für die innere Energie ergibt sich somit $U \equiv \mathrm{Tr}\left\{\hat{H}'_{\mathsf{sys}}\hat{\rho}_{\mathsf{sys}}\right\}$. Die Einteilung in Arbeit und Wärme erfolgt über den ersten Hauptsatz der Thermodynamik; dabei wird ein Energiefluss, welcher zu einer Änderung der von Neumann Entropie führt, mit Wärme assoziiert und ein Energiefluss, der diese konstant lässt, mit Arbeit. Unter diesen Voraussetzungen ergeben sich dann für Arbeit- und Wärmefluss die Glgn. (5.7) und (5.8). Unter Verwendung dieser Grundideen werden zwei verschiedene Methoden vorgeschlagen, um Arbeit- und Wärmefluss auch für messinduzierte Änderungen der inneren Energie zu definieren, siehe Anhang C. Mit diesen Instrumenten werden nun vier verschiedene Methoden zur Abschätzung der Freien Energie untersucht.

D.2.2. Lokale effektive Fluktuationstheoreme

Hier werden die im Folgenden untersuchten Methoden zur Abschätzung der Freien Energie kurz vorgestellt. Dabei ist allen gemein, dass das untersuchte System vor der ersten Messung am Prozessbeginn in einem kanonischen Zustand vorliegen möge.

Energie-Fluktuationstheorem (EFT, $[\cdot E\cdot]$)

Die Idee ist, am Anfang und zu Ende des Prozesses jeweils die Energie des Systems (sys) lokal projektiv zu messen. Der Vorteil von EFT liegt ganz klar in seiner relativ einfachen Umsetzbarkeit. Man muss jedoch bedenken, dass EFT die Änderung der Freien Energie ganz allgemein nur dann richtig abschätzen wird, wenn sämtlicher Energiefluss in oder aus dem System (sys) heraus als Arbeit zu verstehen ist, da dann nach dem 1. HS $\Delta W_{fi} = \Delta E_{fi}$ gilt und EFT äquivalent zur JR ist. Sollte nach Lembas also - zumindest teilweise - ein Wärmefluss auftreten, erwarten wir eine Abweichung der EFT-Abschätzung zur Freien Energie vom richtigen Wert.

Bilokale Energie-Fluktuationstheoreme (bilokales EFT, $[\cdot EE]$)

Wenn wir eine Situation vorliegen haben, in der die Umgebung derart interpretiert werden kann, dass ein Teil dieser ausschließlich als effektiver Treiber auf das System fungiert, so nennen wir diesen Teil Treiber (dr). Hier ergibt sich dann die Möglichkeit, anstatt nur das System (sys) lokal zu messen, sowohl das System als auch die Umgebung (env) (nicht den Treiber) zu Beginn und am Ende des Prozesses jeweils projektiv zu messen (bilokales EFT). Sollte die effektive Freie Energie der Umgebung (env) zeitunabhängig sein, so erhalten wir auch mit dieser Methode die Änderung der effektiven Freien Energie des Systems allein.

Jarzynski Methode ($[\cdot W\cdot]$, $[W\cdot\cdot]$)

Konzeptionell ist die Abschätzung der Freien Energie über diese Methode direkt mit der ursprünglichen klassischen Methode verwandt: Die fluktuierende Größe ist die Arbeit, welche am (vom) System (sys) während des Prozesses verrichtet wird. Die Arbeit wird hierbei direkt aus LEMBAS bestimmt. Der Nachteil dieser Methode liegt darin, dass für allgemeine Betrachtungen unklar bleibt, wie die Arbeit, bestimmt nach LEMBAS, gemessen werden kann. Um hier Arbeit entlang von Trajektorien zu bestimmen, wird wieder wie bei EFT zu Beginn und am Ende des Prozesses das System gemessen. Dazu benötigen wir nicht nur die Arbeitsdefinition nach LEMBAS, sondern auch die Definition für messinduzierte Arbeit (vgl. Kap. C). Insgesamt erhalten wir dann

$$\Delta W_{fi} = \Delta W_i^{\mathsf{Lem}}(t) + \Delta W_{\mathsf{sys}}^{M}(f), \tag{D.4}$$

wobei der erste Summand den Arbeitsfluss nach LEMBAS während des Prozesses, der einer anfänglichen Messung des Systems im Energie-Eigenzustand $|i\rangle\langle i|$ folgt, angibt, und der zweite Summand die Arbeit, die durch die Messung und Projektion in den gemessenen Zustand $|f\rangle\langle f|$ an dem System verrichtet wird. Fließt während des gesamten Prozesses keine Wärme ins System, ist die Jarzynski Methode identisch mit EFT und der JR.

Crooks Methode ($[\cdot EQ]$)

Wir untersuchen hier eine Methode analog zu einer Idee von Crooks [22]. Hierbei bestimmt man die Arbeit, welche am System (sys) verrichtet wird dadurch, dass von der Gesamtenergieänderung des Systems (sys) der Wärmefluss in die Umgebung (env) abgezogen wird. So lässt sich dann die am System verrichtete Arbeit über den 1. Hauptsatz der Thermodynamik rekonstruieren. Der Zugang hier ist jedoch allgemeiner, da wir weder den schwach-Kopplungslimes

fordern, noch dass die Umgebung (env) ein perfektes Bad darstelle. Mittels LEMBAS bestimmen wir den Wärmefluss in die Umgebung. Dabei ist auch hier zu beachten, dass eine Messung am System zu einem Wärmefluss in die Umgebung mittels Korrelationen und auftretenden co-jumps führen kann. Wir messen hier also wie bei EFT das System am Anfang und Ende des Prozesses und zusätzlich noch den Wärmefluss in die Umgebung (env). Über den 1. HS erhält man dann

$$\Delta W_{fi} = \Delta E'_{fi} + \Delta Q^{\mathsf{Lem}}_{\mathsf{env},i}(t) + \Delta Q^{\mathsf{Lem}}_{\mathsf{env}}(f). \tag{D.5}$$

Dabei bezeichnet der zweite Summand den Wärmefluss in die Umgebung während des Prozesses (nach einer anfänglichen Messung und Projektion des Systems in den Energie-Eigenzustand $|i\rangle\langle i|$) und der dritte Summand den Wärmefluss hervorgerufen durch die Messung am System am Ende des Prozesses (Endzustand $|f\rangle\langle f|$). Hierbei ist zu beachten dass sich die Indizes immer auf Zustände des Systems beziehen.

D.3. Funktionalitäten modularer Quantensysteme

Bevor wir mit der Untersuchung obiger Methoden zur Abschätzung der lokalen effektiven Freien Energie beginnen, suchen wir zunächst nach Quantensystemen und geeigneten Kopplungen, die zu einer bestimmten Funktionalität zwischen den Quantensystemen führen. Insbesondere interessieren wir uns für effektive Treiber (dr) und Wärmequellen. Dazu untersuchen wir zuerst ein System genauer, von dem bereits bekannt ist, dass es als effektiver Treiber wirkt [31], mit Fokus auf der JR. Danach führen wir ein weiteres System, welches in der Lage ist effektiv zu treiben, ein, gefolgt von einem einfach Beispiel einer Wärmequelle.

D.3.1. Spin-Oszillator Modell (SOM): Arbeit

Ein Oszillator gekoppelt an einen Spin (System) kann, abhängig von der gewählten Wechselwirkung, als Treiber (dr) für das System (sys) gesehen werden. Der Hamiltonoperator für dieses Modell ist geben durch

$$\hat{H}_{\mathsf{SOM}} \equiv \frac{\omega_{\mathrm{sp}}}{2}\hat{\sigma}_z \otimes \hat{1}_{\mathsf{osc}} + \hat{1}_{\mathsf{sp}} \otimes \omega_{\mathrm{osc}}(\hat{a}^\dagger\hat{a} + \frac{1}{2}\hat{1}_{\mathsf{osc}}) + \Omega_{\mathrm{int}}\hat{\sigma}_z \otimes \hat{X}. \tag{D.6}$$

Der Wechselwirkungsoperator, $\hat{H}_{\mathsf{int}} = \Omega_{\mathsf{int}}\hat{\sigma}_z \otimes \hat{X}$, sorgt dabei für die gewünschte Funktionalität als Arbeitsquelle (Treiber). Analytische Berechnungen zeigen, dass nach LEMBAS keine Wärme ins System (sys) fließt. Für reine Anfangszustände des Spins (sys), die wir bei der Untersuchung der JR nach der

anfänglichen Messung vorliegen haben, kann gezeigt werden, dass auch der Oszillator (dr) keine Wärme aufnimmt oder abgibt[1]. Einziges Manko dieses Systems ist die Abhängigkeit des Arbeitsprotokolls, das dem Spin vom Oszillator aufgeprägt wird, von dem Anfangszustand des Spins (Zustandsabhängiges Treiben). Diese Zustandsabhängigkeit könnte als ein Problem der Reproduzierbarkeit von aufgeprägten Prozessprotokollen auch für klassische Systeme diskutiert werden. Das Zeitabhängige Treiben führt im Allgemeinen zu leichten Abweichungen der von der JR vorhergesagten Freien Energie von dem exakten Ergebnis[2]. Glücklicherweise wird diese Zustandsabhängigkeit aber auch in [31] diskutiert und Beeinflussungsmöglichkeiten über geeignete Parameterwahl genannt. Daher gelingt es mit nur geringen Abweichungen die verschiedenen Abschätzungsmethoden für die Freie Energie für diesen Treiber zu diskutieren.

D.3.2. Zweigeteiltes 3-Spin-Modell: Arbeit

Da die Untersuchung der JR in reinen Spinnetzwerken von Interesse ist, wird hier ein Modell bestehend aus drei Spins vorgestellt, bei dem zwei der Spins als effektiver Treiber (dr) auf den dritten Spin (im Folgenden System genannt) wirken (vgl. Abb. 7.1). Der Hamiltonoperator für dieses Modell ist gegeben durch

$$\hat{H} \equiv \underbrace{\frac{\omega}{2}\left(\hat{\sigma}_z \otimes \hat{1}_{23} + \hat{1}_1 \otimes \hat{\sigma}_z \otimes \hat{1}_3\right) + \frac{\lambda_{\mathsf{drint}}}{2}\hat{\sigma}_x \otimes \hat{\sigma}_x \otimes \hat{1}_3}_{\equiv \hat{H}_{\mathsf{dr}}\text{: Hamiltonoperator des Treibers}} + \underbrace{\frac{\omega}{2}\hat{1}_{23} \otimes \hat{\sigma}_z}_{\equiv \hat{H}_{\mathsf{sys}}\text{: getriebener Spin}} + \underbrace{\frac{\lambda_{\mathsf{dr}}}{2}\hat{1}_1 \otimes \hat{\sigma}_z \otimes \hat{\sigma}_z}_{\equiv \hat{H}_{\mathsf{drsys}}\text{: Kopplung Treiber}-\text{Spin}}. \tag{D.7}$$

Nebst des kleineren numerischen Aufwandes hat dieses Modell den Vorteil, dass wir für die interessierenden Anfangszustände analytische Lösungen für die Zeitentwicklung in geeigneter Operatorbasis sowie insbesondere der Arbeit nach Lembas finden können. Darüberhinaus ist der Effekt des Treibers auf das System im Hinblick auf die effektive Freie Energie des letzteren unabhängig vom anfänglich gemessenen Zustand des Systems.

[1] Aufgrund der unsymmetrischen Situation ist es durchaus möglich, dass sich weder Wärme- noch Arbeitsfluss ausgleichen (keine Extensivität). Insbesondere für kanonische Zustände des Spins (ohne Messung zu Beginn) haben wir einen nicht-verschwindenden Wärmefluss in den Oszillator, während der Spin weiterhin weder Wärme aufnimmt noch abgibt.

[2] Um genau zu sein lässt sich nicht sagen, was das exakte Ergebnis sein soll. Man muss sich darauf festlegen, für welchen Hamiltonian die effektive Freie Energie bestimmt werden soll.

D.3.3. 2-Spin-Modell: Wärme

Ein einfaches Modell für eine Wärmequelle stellen zwei Spins dar, welche geeignet miteinander gekoppelt sind,

$$\hat{H} \equiv \frac{\omega_{\mathsf{sys}}}{2}\hat{\sigma}_z \otimes \hat{1}_{\mathsf{env}} + \frac{\omega_{\mathsf{env}}}{2}\hat{1}_{\mathsf{sys}} \otimes \hat{\sigma}_z + \frac{\lambda_{\mathsf{env}}}{2}\hat{\sigma}_x \otimes \hat{\sigma}_x. \tag{D.8}$$

Eine Lembas-Studie zeigt, dass die beiden Spins nur Wärme miteinander austauschen, sofern beide in einem Diagonalzustand starten. Für eine detailliertere Lösung beschränken wir uns auf den resonanten Fall $\omega_{\mathsf{sys}} = \omega_{\mathsf{env}}$. Der Wärmeübertrag ist hierbei in dem Sinne nicht perfekt, da sich die Wärmeflüsse nicht zu jeder Zeit ausgleichen.

D.3.4. Thermalisierende Umgebung

Um die Studien über die lokale effektive JR abzurunden, muss noch das Zustandekommen des Anfangszustandes, der kanonisch sein soll, erklärt werden. Dies gelingt mit geeigneten Umgebungen (vgl. u. A. [44]). Es zeigt sich hierbei jedoch, dass manche Kopplungen dem System zwar den erwünschten kanonischen Zustand (näherungsweise) aufprägen, jedoch nach Lembas bei dieser Art der Thermalisierung auch ein nicht-verschwindender Anteil an Arbeit ausgetauscht wird.

D.4. Modulare Quantensysteme: Arbeit und Wärme

Aufgrund der engen Verknüpfung zwischen Freier Energie und Zustandssumme spielt es insbesondere bei der Betrachtung der JR keine prinzipielle Rolle, welche der beiden Größen man betrachtet,

$$\frac{Z^{\mathsf{eff}}_{\mathsf{sys}}(t)}{Z^{\mathsf{eff}}_{\mathsf{sys}}(0)} = \mathrm{e}^{-\beta^{\mathsf{eff}}_{\mathsf{sys}}\Delta F^{\mathsf{eff}}_{\mathsf{sys}}}. \tag{D.9}$$

Der Einfachheit halber betrachten wir daher im Folgenden die effektive Zustandssumme $Z^{\mathsf{eff}}_{\mathsf{sys}}(t)$ und setzten die Kenntnis der Zustandssumme zu Beginn, $Z^{\mathsf{eff}}_{\mathsf{sys}}(0)$, voraus. Wir definieren dann die relative Abweichung der Vorhersage der effektiven Zustandssumme einer bestimmten Methode m von dem exakten Wert über

$$\Delta^{Z}_{\mathsf{rel}}(m) \equiv \frac{Z^{m}_{\mathsf{sys}}(t) - Z^{\mathsf{eff}}_{\mathsf{sys}}(t)}{Z^{\mathsf{eff}}_{\mathsf{sys}}(t)}. \tag{D.10}$$

Im Folgenden werden nun die in Abschn. D.2.2 vorgestellten Methoden nähers untersucht.

D.4.1. Zweigeteilte Quantensysteme

Wir betrachten die oben diskutierten Fälle treibender Systeme, SOM und den Zwei-Spin Treiber. Da nach LEMBAS jeweils nur Arbeit am System verrichtet wird, erwarten wir dass EFT die Zustandssumme richtig abschätzt. Tatsächlich bestätigen unsere numerischen Ergebnisse, dass dies der Fall ist. Bei SOM ergibt sich eine winzige Abweichung wegen des Zustandsabhängigen Treibens. Ebenso liefert die Abschätzung über die Jarzynski Methode beste Ergebnisse innerhalb der numerischen Genauigkeit. Mithilfe der Arbeitsdefinition von LEMBAS sind wir also in der Lage die JR direkt für die lokale effektive Dynamik zu formulieren.

D.4.2. Zusätzlicher Umgebungsspin: Bilokale Messung

Hier betrachten wir die Situation, dass sich eine modular aufgebaute Umgebung des Systems (sys) in zwei Teile, welche nicht miteinander wechselwirken, trennen lässt, von denen einer als Treiber (dr) und der andere als Wärmequelle (env) fungiert, solange jeweils nur einer der Teile der Umgebung alleine mit dem System wechselwirkt. Durch das Zusammenschalten aller drei Teile können sich Abweichungen von oben beschriebenem Verhalten ergeben[3]. Es werden sowohl das System (sys) als auch die Wärmequelle (env) zu Beginn und Ende des Prozesses projektiv gemessen[4]. Es wird sowohl SOM (vgl. Abb. 11.1) als auch der Zwei-Spin Treiber (vgl. Abb. 11.11) mit zusätzlicher Kopplung einer Wärmequelle (siehe Abschn. D.3.3) untersucht. Da nach LEMBAS in diesen Modellen sowohl Arbeit am System verrichtet wird als auch ein Wärmefluss in dieses zu beobachten ist, erwarten wir, dass EFT, welches dann nicht äquivalent zur JR ist ($\Delta E'_{\mathsf{sys}} \neq \Delta W_{\mathsf{sys}}$), die effektive Zustandssumme falsch abschätzt. Dies wird durch unsere Numerik bestätigt. Da die Zustandssumme der Wärmequelle zeitunabhängig ist, liefert das bilokale EFT hingegen eine korrekte Abschätzung. Darüber hinaus ist auch die Jarzynski Methode in der Lage die Zustandssumme sehr gut abzuschätzen. Verwenden wir hier die Crooks Methode (im Prinzip betrachten wir einen Spezialfall, bei dem die Wärmequelle in einem reinen, statistisch verteilten Zustand startet), ist bei der Bestimmung des Wärmeflusses nach LEMBAS darauf zu achten, dass der

[3] Dies kann durch Korrelationen zwischen Treiber und Wärmequelle, vermittelt durch das System, geschehen auch wenn Treiber und Wärmequelle nicht direkt wechselwirken.

[4] Wir wählen hier die Messreihenfolge so, dass zuerst das System und dann die Wärmequelle gemessen wird.

Wärmefluss, welcher von der Messung induziert wird, unbedingt mit in Betrachtung gezogen wird (wie bereits in Abschn. D.2.2 diskutiert). Dann ist die Abschätzung der Zustandssumme über diese Methode exakt, während sich ohne Berücksichtigung dieses Wärmeflusses (hervorgerufen durch co-jumps und nach Abschn. C.3.2 als Wärme interpretiert) recht große Abweichungen ergeben.

D.4.3. Zusätzlicher Umgebungsspin: Lokale Messung

Hier betrachten wir eine Situation analog zu vorigem Abschnitt. Der einzige Unterschied besteht nun darin, dass wir nur das System (sys) lokal messen. Die Umgebung startet nun also für einen einzelnen Prozess in einem gemischten Zustand. Für diesen Fall liefert die Crooks Methode selbst bei der Berücksichtigung des durch die Messung verursachten Wärmeflusses im Allgemeinen keine brauchbare Abschätzung der Zustandssumme. Aufgrund der Tatsache, dass hier der einzige Unterschied zu oben darin besteht, dass die Wärmequelle für einzelne Prozesswiederholungen in einem gemischten Zustand startet, im vorigen Abschnitt jedoch in reinen Zuständen (nur im Ensemble-Sinne in gemischten Zuständen), nennen wir dies einen Quanteneffekt.

D.4.4. Nicht-adiabatisches Treiben

Bis hier wurden nur Situationen untersucht, in denen der Treiber zu einer reinen Spektrumsdeformation führte. Der Wechselwirkungsoperator zwischen Treiber und System war derart, dass $[\hat{H}^{\mathsf{int}}_{\mathsf{dr}-\mathsf{sys}}, \hat{H}_{\mathsf{sys}}] = 0$. Nun sollen Situationen untersucht werden, in denen der Kommutator nicht verschwindet. Zuerst verwenden wir hier einen externen Treiber, also einen explizit zeitabhängigen Hamiltonoperator. Für diesen Fall sagt LEMBAS voraus, dass nur Arbeit am System verrichtet wird und keine Wärme ins System fließt (unitäre Zeitentwicklung). Unsere Numerik bestätigt dass EFT, wie erwartet, die effektive Zustandssumme richtig abschätzt. Hierbei zeigt sich wieder, dass es für eine gute Abschätzung unabdingbar ist, den Einfluss der abschließenden Messung auf das System mit in Betrachtung zu ziehen. Die beiden hierfür vorgeschlagenen Methoden zur Bestimmung der messinduzierten Arbeit liefern unterschiedlich gute Ergebnisse. Das zusätzliche Ankoppeln einer Wärmequelle nach LEMBAS bestätigt die Befunde der vorangegangen Untersuchungen. Eine Betrachtung für ein abgeschlossenes Quantensystem ohne externen Treiber, in der ein SOM-ähnliches Modell mit leicht veränderter Wechselwirkung untersucht wird (Jaynes-Cummings Wechselwirkung, siehe Kap. 15), bestätigt vorstehende Ergebnisse.

D.5. Kreisprozesse

Der zweite Teil dieser Arbeit beschäftigt sich mit der Frage, inwieweit Erkenntisse aus vorstehenden Untersuchungen dabei helfen können, Kreisprozesse besser zu verstehen. Besonderes Augenmerk wurde hierbei auf die Effizienz von Kreisprozessen, welche das Arbeitssystem aus dem Gleichgewicht treiben, gelegt. Während die Bäder hier stets als perfekt im klassischen Sinne betrachtet werden, wurde das Arbeitssystem als Quantensystem behandelt. Die vorliegenden Untersuchungen drehen sich hauptsächlich um einen Quanten-Otto Kreisprozess, wobei die Bezeichnung als solche ihre Rechtfertigung in der Tatsache findet, dass Zustandsänderungen, welche die von Neumann Entropie konstant lassen (unitäre, adiabatische Schritte) mit solchen, in denen der Kontrollparameter des Hamiltonians unverändert bleibt (isochore Schritte) kombiniert werden. Über die Jarzynski Relation gelingt ein recht direkter Vergleich mit einem klassischen Stirling Prozess (Isotherme und Isochoren). Eine genauere Untersuchung unter Zuhilfenahme der Entropie und der strikten Forderung, dass dem (perfekten) Bad unter keinen Umständen Arbeit entnommen werden darf, gelingt es zu zeigen, dass der Wirkungsgrad des Quanten-Otto Prozesses kleiner als (oder höchstens gleich groß wie) der Carnot-Wirkungsgrad ist. Dabei zeigte sich, dass mögliche Kohärenzen im Arbeitssystem den Wirkungsgrad nicht zu verbessern vermögen. Um im Folgenden auch einen Vergleich zum Wirkungsgrad des klassischen Otto-Prozesses ziehen zu können, werden der Einfachheit halber nur Prozesse, die das Spektrum über den Kontrollparameter γ deformieren,

$$E_n(\gamma) = f(\gamma)E_n, \tag{D.11}$$

betrachtet. Für diese Prozessklasse gelingt es zu zeigen, dass der Wirkungsgrad dem des klassischen Otto-Prozesses entspricht für geeignete Zuordnung zwischen $f(\gamma)$ und Volumen V, bzw. für geeignete verallgemeinerte Temperaturen.

D.6. Fazit

Zusammenfassend lässt sich sagen, dass es in dieser Arbeit gelungen ist, verschiedene Methoden zur Abschätzung der Änderung der Freien Energie fußend auf der Jarzynski Relation für lokale effektive Dynamik modularer Quantensysteme zu untersuchen. Dabei zeigt sich, dass die Einteilung nach Lembas in Arbeit und Wärme im Einklang mit den Erwartungen bezüglich des Energie-Fluktuationstheorems steht, was eine solche Einteilung auch für kleinste Quantensysteme sinnhaft erscheinen lässt. Darüberhinaus kann die Arbeit gegeben

nach Lembas und hier erweitert durch messinduzierten Arbeitseintrag in das System direkt als fluktuierende Größe für ein Jarzynski-analoges Fluktuationstheorem mit Erfolg verwendet werden. Die hier generalisierte Idee nach Crooks, die Arbeit am System über Energieänderung desselben korrigiert durch den Wärmefluss in die Umgebung zu bestimmen verdeutlicht besonders gut, dass der Einfluss der Messung im Allgemeinen nicht vernachlässigt werden sollte. Die Untersuchungen zu Nicht-Gleichgewichtsprozessen können auch ein neues Licht auf den Wirkungsgrad von Kreisprozessen werfen, die an Quantensystemen durchgeführt werden und helfen, diese besser zu verstehen. Insbesondere konnte hier gezeigt werden, dass für das untersuchte Setup Kohärenzen im Arbeitsmedium den Wirkungsgrad nicht verbessern. Es bleibt zu hoffen, dass diese Arbeit einen Beitrag zum Verständnis von lokalen Fluktuationstheoremen in modularen Quantensystemen leisten kann.

List of Symbols

Frequently used abbreviations:

BSP	Boundary Switching Process
EFT	Energy Fluctuation Theorem
JR	Jarzynski Relation
LEMBAS	Local Effective Measurement Basis
QBSP	Quasi Boundary Switching Process
qOC	Quantum Otto Cycle
SOM	Spin-Oscillator Model

$\hat{a}, \hat{a}^\dagger$	Annihilation, Creation operator
$\langle \hat{A} \rangle_{\hat{\rho}}$	expectation value of $\hat{A}$ with respect to $\hat{\rho}$
β	Inverse temperature
$\mathfrak{B}$	Basis operator of some operator basis
$\mathcal{D}_B$	Bures distance
$\|\alpha\rangle\langle\alpha\|$	coherent state
$\hat{C}$	Correlation/Entanglement operator
λ	Coupling strength/Eigenvalue
c	Ground state occupation probability for TLS
$c_{p/V}$	Specific heat at constant pressure/volume
ΔE_{fi}	Difference between two energy eigenvalues
$\dim(\ldots)$	Dimension of ...
$\mathcal{D}$	Unitary transformation diagonalizing a density operator
E	Energy
E_j	Energy eigenvalue corresponding to energy eigenstate $\|j\rangle$
η	Normalization constant/Efficiency
$\vec{e}_i$	i-th vector of an orthonormal bais set
F	Free energy
f	Number of degrees of freedom
F^{eff}	Effective free energy
$\mathcal{F}$	Fidelity
$\mathcal{G}$	Operator given in reciprocal basis set
$\dot{\cdot}$	
γ	Control parameter in Hamiltonian
h	Planck's constant
$\hat{H}$	Hamilton operator

$\hbar$	$\frac{h}{2\pi}$
$\mathcal{H}$	Hilbert space
id	Identity
J	Interval
κ	$\frac{c_P}{c_V}$
k_B	Boltzmann constant
K_{fi}	Conditional probability of transition $\|i\rangle \longrightarrow \|f\rangle$
δ_{ij}	Kronecker delta
L	Length/width of potential well
ε_{ijk}	Levi-Civita tensor
$\mathcal{L}_{\mathsf{inc}}$	Incoherent dynamics superoperator
m, M	Mass
Ω_{int}	Interaction energy
ω	Energy splitting/(transition) frequency
$P(x)$	Probability distribution of random variable X
$\hat{P}$	Projection operator
p	Probability
P	Purity
Q	Heat
q_n	Occupation probability of level n
R	Non-unitary transformation
r	Ratio of two different widths of potential well
$\mathcal{R}$	Elements of group $\mathbb{S}$
$\mathrm{Re}(z)$	Real part of a complex number z
$\hat{\rho}$	Density operator
S	von Neumann entropy
$\mathbb{S}$	Group of coefficients
$\hat{\sigma}_{x,y,z}$	Pauli operators
T	Temperature
$\hat{T}$	Dyson time-ordering operator
T, $\mathcal{T}$	Transformation matrix
U	Internal energy
$\downarrow, \uparrow$	Ground, Excited state of a TLS
$\hat{U}$	Unitary time-evolution operator
V	Volume
$\hat{V}$	Potential operator
W	Work
Z	Partition sum
Z^{eff}	Effective partition sum

Bibliography

[1] A. E. Allahverdyan, R. S. Johal, and G. Mahler. Work extremum principle: Structure and function of quantum heat engines. *Phys. Rev. E*, **77**, 041118, (2008).

[2] A. E. Allahverdyan and Th. M. Nieuwenhuizen. Fluctuations of work from quantum subensembles: The case against quantum work-fluctuation theorems. *Phys. Rev. E*, **71**, 066102, 2 June 2005.

[3] A. E. Allahverdyan and Th. M. Nieuwenhuizen. Minimal work principle: Proof and counterexamples. *Phys. Rev. E*, **71**, 046107, (2005).

[4] A. Imparato and L. Peliti. Fluctuation relations for a driven Brownian particle. *Phys. Rev. E*, **74(026106)**, 4 August 2006.

[5] A. Polkovnikov. Microscopic Expression for Heat in the Adiabatic Basis. *Phys. Rev. Lett.*, **101**, 220402, 24 November 2008.

[6] C. Jarzynski. Nonequilibrium Equality for Free Energy Differences. *Phys.Rev. Lett.*, **78(14)**, 2690, 7 April 1997.

[7] C. Jarzynski. Nonequilibrium work theorem for a system strongly coupled to a thermal environment. *J. Stat. Mech.: Theor. Exp.*, page P09005, (2004).

[8] C. Jarzynski. Reply to comments by D.H.E. Gross. *cond-mat/0509344*, (2005).

[9] C. Jarzynski. Rare events and the convergence of exponentially averaged work values. *Phys. Rev. E*, **73**, 046105, April 2006.

[10] C. Jarzynski and D. K. Wójcik. Classical and Quantum Fluctuation Theorems for Heat Exchange. *Phys. Rev. Lett.*, **92(23)**, 230602, 11 June 2004.

[11] Michele Campisi, Peter Talkner, and Peter Hanggi. Fluctuation theorem for arbitrary open quantum systems. *Phys. Rev. Lett.*, **102(21)**, 210401, (2009).

[12] D. Bures. An Extension of Kakutani's Theorem on Infinite Product Measures to the Tensor Product of Semifinite w*-Algebras. *Trans. Am. Math. Soc.*, **135**, 199, (1969).

[13] D. J. Evans and D. J. Searles. Equilibrium microstates which generate second law violating steady states. *Phys. Rev. E*, **50**, 1645, (1994).

[14] D. J. Evans, E. G. D. Cohen, and G. P. Morriss. Probability of Second Law Violations in Shearing Steady States. *Phys. Rev. Lett.*, **71**, 2401–2404, (1993).

[15] E. Geva and R. Kosloff. A quantum-mechanical heat engine operating in finite time. A model consisting of spin-1/2 systems as the working fluid. *J. Chem. Phys.*, **96**, 3054, (1992).

[16] E. Geva and R. Kosloff. The quantum heat engine and heat pump: An irreversible thermodynamic analysis of the three-level amplifier. *J. Chem. Phys.*, **104**, 7681, (1996).

[17] E. H. Lieb and M. B. Ruskai. Proof of the Strong Subadditivity of Quantum-Mechanical Entropy. *J. Math. Phys.*, **14**, 1938, (1973).

[18] F. L. Curzon and B. Ahlborn. Efficiency of a Carnot Engine at Maximum Power Output. *Am. J. Phys.*, **43**, 22, (1975).

[19] F. Ritort. Advances in Chemical Physics. In *Nonequilibrium fluctuations in small systems: From physics to biology*, volume 137. John Wiley & Sons, (2008).

[20] F. Schwabl. *Quantenmechanik*. Springer-Verlag, 3 edition, (1992).

[21] G. E. Crooks. Entropy production fluctuation theorem and the nonequilibrium work relation for free energy differences. *Phys. Rev. E*, **60(3)**, 2721, September 1999.

[22] G. E. Crooks. On the Jarzynski relation for dissipative quantum dynamics. *J. Stat. Mech.*, page P10023, (2008).

[23] G. Gallavotti and E. G. D. Cohen. Dynamical Ensembles in Nonequilibrium Statistical Mechanics. *Phys. Rev. Lett.*, **74**, 2694, (1994).

[24] G. J. Chaitin. On the Length of Programs for Computing Finite Binary Sequences: Statistical Considerations. *J. Assoc. Comput. Mach.*, **16**, 145, (1969).

[25] H. Araki and E. H. Lieb. Entropy Inequlities. *Comm. Math. Phys.*, **18**, 160–170, (1970).

[26] H. B. Callen. *Thermodynamics and an Introduction to Thermostatistics*. John Wiley & Sons, 2 edition, (1985).

[27] H. E. D. Scovil and E. O. Schulz-DuBois. Three-Level Masers as Heat Engines. *Phys. Rev. Lett.*, **2**, 262, (1959).

[28] H. Haken and H. C. Wolf. *Molekülphyisk und Quantenchemie*. Springer-Verlag Berlin Heidelberg New York, 4th edition, (2003).

[29] H. Heuser. *Gewöhnliche Differentialgleichungen*. B.G. Teubner Stuttgart, (1989).

[30] H. S. Leff. Thermal efficiency at maximum work output: New results for old heat engines. *Am. J. Phys.*, **55**, 602, (1987).

[31] H. Schröder and G. Mahler. Work exchange between quantum systems: The spin-oscillator model. *Phys. Rev. E*, **81**, 021118, (2010).

[32] H. Tasaki. Jarzynski Relations for Quantum Systems and Some Applications. cond-mat/0009244, Department of Physics, Gakushin University, 25 September 2000.

[33] H. Weimer, M. J. Henrich, F. Rempp, H. Schröder, and G. Mahler. Local effective dynamics of quantum systems: A generalized approach to heat and work. *Europhys. Lett.*, **83**, 30008, 18 July 2008.

[34] Gerhard Huber, Ferdinand Schmidt-Kaler, Sebastian Deffner, and Eric Lutz. Employing trapped cold ions to verify the quantum jarzynski equality. *Physical Review Letters*, **101(7)**, 070403, (2008).

[35] I. Junier, A. Mossa, M. Manosas, and F. Ritort. Recovery of Free Energy Branches in Single Molecule Experiments. *Phys. Rev. Lett.*, **102**, 070602, (2009).

[36] G. Musiol I. N. Bronstein, K. A. Semendjajew. *Taschenbuch der Mathematik*. Harri Deutsch, 5 edition, (2001).

[37] J. Berg. Out-of-Equilibrium Dynamics of Gene Expression and the Jarzynski Equality. *Phys. Rev. Lett.*, **100**, 188101, (2008).

[38] J. Birjukov, T. Jahnke, and G. Mahler. Quantum thermodynamic processes: a control theory for machine cycles. *Eur. Phys. J. B*, **64**, 105, (2008).

[39] J. C. Reid, E. M. Sevick, and D. J. Evans. A unified description of two theorems in non-equilibrium statistical mechanics: The fluctuation theorem and the work relation. *Europhys. Lett.*, **72**, 726, (2005).

[40] J. E. Geusic, E. O. Schulz-DuBois, and H. E. D. Scovil. Quantum Equivalent of the Carnot Cycle. *Phys. Rev.*, **156**, 343, (1966).

[41] J. Gemmer and G. Mahler. Entanglement and the factorization-approximation. *Eur. Phys. J. D*, **17**, 385–393, (2001).

[42] J. Gemmer and M. Michel. Thermalization of quantum systems by finite baths. *Eur. Phys. Lett.*, **73**, 1, November 2005.

[43] J. Gemmer and M. Michel. Finite quantum environments as thermostats: an analysis based on the Hilbert space average method. *Eur. Phys. J. B*, **53**, 517–528, (2006).

[44] J. Gemmer, M. Michel, and G. Mahler. *Quantum Thermodynamics - Emergence of Thermodynamic Behavior Within Composite Quantum Systems*. Springer Verlag, 1 edition, (2004).

[45] J. Horowitz and C. Jarzynski. Comment on "Failure of the Work-Hamiltonian Connection for Free-Energy Calculations". *Phys. Rev. Lett.*, **101**, 098901, (2008).

[46] J. Kurchan. A Quantum Fluctuation Theorem. *cond-mat/0007360*, 16 August 2001.

[47] J. L. W. V. Jensen. Sur les fonctions convexes et les inégalités entre les valeurs moyennes. *Acta Mathematica*, **30**, 175–193, (1905).

[48] J. Liphardt, S. Dumont, B. Smith, Jr. I. Tinoco, and C. Bustamante. Equilibrium Information from Nonequilibrium Measurements in an Experimental Test of Jarzynski's Equality. *Science*, **296**, 1832, (2006).

[49] J. M. G. Vilar and J. M. Rubi. Failure of the Work-Hamiltonian Connection for Free-Energy Calculations. *Phys. Rev. Lett.*, **100**, 020601, (2008).

[50] J. M. G. Vilar and J. M. Rubi. Vilar and Rubi Reply:. *Phys. Rev. Lett.*, **101**, 098904, (2008).

[51] J. Sung. Application range of Jarzynski's equation for boundary-switching processes. *Phys. Rev. E*, **77**, 042101, 2 April 2008.

[52] J. Teifel and G. Mahler. Model studies on the Quantum Jarzynski Relation. *Phys. Rev. E*, **76**, 051126, November 2007.

[53] J. Teifel and G. Mahler. Limitations of the quantum Jarzynski estimator: boundary switching processes. *Eur. Phys. J. B*, **75**, 275–283, (2010).

[54] K. Huang. *Statistical Mechanics*. John Wiley & Sons, Inc., 2 edition, (1987).

[55] L. I. Schiff. *Quantum mechanics*. Mc Graw Hill, (1955).

[56] L. Peliti. Comment on "Failure of the Work-Hamiltonian Connection for Free-Energy Calculations". *Phys. Rev. Lett.*, **101**, 098903, (2008).

[57] L. Peliti. On the work-Hamiltonian connection in manipulated systems. *J. Stat. Mech.*, **5**, 05002, (2008).

[58] M. A. Nielsen and I. L. Chuang. *Quantum Computation and Quantum Information*. Cambridge U. P., (2000). p. 355.

[59] M. Baiesi, T. Jacobs, C. Maes, and N. S. Skantzos. Fluctuation symmetries for work and heat. *Phys. Rev. E*, **74**, 021111, 10 August 2006.

[60] M. Esposito, K. Lindenberg, and C. Van den Broeck. Entropy production as correlation between system and reservoir. *New J. Phys.*, **12**, 013013, (2010).

[61] M. Esposito and S. Mukamel. Fluctuation Theorems for Quantum Master Equations. *Phys. Rev. E*, **73**, 046129, 24 April 2006.

[62] M. Esposito, U. Harbola, and S. Mukamel. Entropy fluctuation theorems in driven open systems: application to electron counting statistics. *Phys. Rev. E*, **76**, 031132, (2007).

[63] M. J. Henrich, G. Mahler, and M. Michel. Driven spin systems as quantum thermodynamic machines: Fundamental limits. *Phys. Rev. E*, **75**, 051118, (2007).

[64] P. T. Landsberg. Heat engines and heat pumps at positive and negative absolute temperatures. *J. Phys. A: Math. gen.*, **10**, 1773, (1977).

[65] P. Talkner and P. Hänggi. The Tasaki-Crooks quantum fluctuation theorem. *J. Phys. A: Math. Theor.*, **40**, F569–F571, (2007).

[66] P. Talkner, P. Hänggi, and M. Morillo. Microcanonical quantum fluctuation theorems. *Phys. Rev. E*, **77**, 051131, (2008).

[67] S. D. Deshpande and R. B. Pode. Matrix representation of vectors and operators in nonorthogonal basis vectors. *Am. J. Phys.*, **56**, 362, (1988).

[68] S. Mukamel. Quantum extension of the Jarzynksi Relation: Analogy with Stochastic Dephasing. *Phys. Rev. Lett.*, **90(17)**, 170604, 1 May 2003.

[69] S. Vaikuntanathan and C. Jarzynski. Escorted Free Energy Simulations: Improving Convergence by Reducing Dissipation. *Phys. Rev. Lett.*, **100**, 190601, May 2008.

[70] T. Feldmann and R. Kosloff. Performance of discrete heat engines and heat pumps in finite time. *Phys. Rev. E*, **61**, 4771, (2000).

[71] T. Gilbert and J. R. Dorfman. Fluctuation theorem for constrained equilibrium systems. *Phys. Rev. E*, **73(026121)**, 17 February 2006.

[72] T. Mai and A. Dhar. Nonequilibrium work fluctuations for oscillators in non-Markovian baths. *Phys. Rev. E*, **75**, 061101, 1 June 2007.

[73] T. Monnai. Unified treatment of the quantum fluctuation theorem and the Jarzynski equality in terms of microscopic reversibility. *Phys. Rev. E*, **72**, 027102, 9 August 2005.

[74] T. Schmiedl and U. Seifert. Optimal Finite-Time Processes In Stochastic Thermodynamics. *Phys. Rev. Lett.*, **98**, 108301, March 2007.

[75] T. Speck and U. Seifert. The Jarzynski relation, fluctuation theorems, and stochastic thermodynamics for non-Markovian processes. *J. Stat. Mech.*, page L09002, (2007).

[76] U. Fano. Description of States in Quantum Mechanics by Density Matrix and Operator Techniques. *Rev. Mod. Phys.*, **29(1)**, (1957).

[77] U. Seifert. Entropy Production along a Stochastic Trajectory and an Integral Fluctuation Theorem. *Phys. Rev. Lett.*, **95(04)**, 040602, 22 July 2005.

[78] V. Chernyak and S. Mukamel. Effect of Quantum Collapse on the Distribution of Work in Driven Single Molecules. *Phys. Rev. Lett.*, **93(4)**, 048302, (2004).

[79] W. Brenig. *Statistische Theorie der Wärme*. Springer, 4 edition, (1996).

[80] W. De Roeck and C. Maes. Quantum version of free-energy-irreversible-work relations. *Phys. Rev. E*, **69**, 026115, 26 February 2004.

[81] W. E. Thirring and E. M. Harrell. *Quantum mathematical physics: atoms, molecules and large systems*. Springer, 2 edition, (2002).

[82] W. Greiner, L. Neise, and H. Stöcker. *Thermodynamics and Statistical Mechanics*. Springer-Verlag, 1 edition, (1995).

[83] W. Nolting. *Grundkurs Theoretische Physik 4: Spezielle Relativitätstheorie, Thermodynamik*. Springer, 5 edition, (2003).